Alkaloidal constituents of *Crinum variabile* and *Crinum paludosum*, two southern African Amaryllidaceae species

Kim Henry Steyn

Supervisor: Prof. Willem A.L. van Otterlo; Co-supervisor: Prof. André J. de Villiers

With special mention of the contributions of Prof. Ivan R. Green

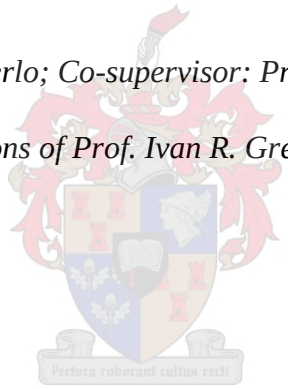

Thesis presented in partial fulfilment of the requirements for the degree of Master of Science in the Faculty of Science at Stellenbosch University.

The financial assistance of the National Research Foundation (NRF) towards this research is hereby acknowledged. Opinions expressed and conclusions arrived at, are those of the author and are not necessarily to be attributed to the NRF.

By submitting this thesis electronically, I declare that the entirety of the work contained therein is my own, original work, that I am the sole author thereof (save to the extent explicitly otherwise stated), that reproduction and publication thereof by Stellenbosch University will not infringe any third party rights and that I have not previously in its entirety or in part submitted it for obtaining any qualification.

1 Abstract

The extraction of dried bulbs of *Crinum variabile* and subsequent targeted fractionation led to the isolation of lycorine, 1,2-*O*,*O*-diacetyllycorine, 2-*O*-acetyllycorine, 1-*O*-acetyllycorine, a diastereomeric mixture of haemanthidine and 6-epihaemanthidine, bulbispermine and criwelline. HPLC-MS/MS analysis of the extract was carried out, providing information regarding other alkaloidal constituents of *C. variabile*. The isolation of lycorine, as well as a brief HPLC-MS/MS dereplication study was carried out on an extract of *Crinum paludosum*, allowing for the tentative identification of ten alkaloidal constituents therein, with five alkaloids remaining unidentified. A brief synthetic study was carried out on higginsianins A and B, resulting in the generation of some analogues thereof. These included acetylated analogues of both, as well as bromination products of higginsianin A, and reductive hydrogenation and epoxidation products of higginsianin B.

2 Opsomming

Ekstraksie van gedroogde *Crinum variabile* blombolle en die daaropvolgende fraksionering het likorien, 1,2-di-*O*-asetiellikorien, 2-*O*-asetiellikorien, 1-*O*-asetiellikorien, ‘n mengsel van haemantidien en 6-*epi*-haemantidien, bulbespermien en kriwelien opgelewer. HPLC-MS/MS analise van die *C. var.* ekstrak het adisionele informasie van ander alkaloïde tot gevolge gehad. Isolasie van likorien asook ‘n kort HPLC-MS/MS analise van ‘n ekstrak van *Crinum paludosum* het tot gevolg gehad dat tien alkaloïde tentatief geidentifiseer kon word met nog vyf wat nie geidentifiseer kon word nie.

‘n Kort sintetise studie op higginsiansins A en B was uitgevoer en het gelei tot die isolasie van die geasetileerde higggginsiansins A en B, die gebromeerde analoog van higginsiansin A, die hidrogeneerde higginsiansin B en die epoksineringsproduk van higginsiansin B.

3 Table of contents

4 List of figures

5 List of tables

6 Introduction

6.1 Background on plant-based medicines

6.1.1 Empirical use of plant-based treatments

Since before our collective recollection, human societies have been in close contact with their environments, and have utilized the inherent value present in the natural resources therein. A practice that has been indispensable in this regard is the use of living organisms, particularly plants, for the treatment of diseases, injuries and ailments.[1]

Determining the length of time for which humans have used plants as medicines is difficult, given that such practices predate written or illustrative records.[2] In fact, it seems that the use of plants for health benefits is not limited to humans, but has been seen in other animal species, including monkeys and apes. Furthermore, it has been shown that humans and chimpanzees choose some of the same plant species to use as combatants against similar symptoms.[3,4] This could suggest that such practices have evolutionary roots, and hints at a long history of close and intertwined interactions between our species and medicinally beneficial plants. Some archaeological evidence points towards the possibility that plants were cultivated for medicinal purposes over 60 000 years ago, as indicated by some discoveries in a Neanderthal burial site.[5] This evidence is based on the presence of pollen in a Neanderthal grave, from 28 species of flowers. Seven of these species were known to possess medicinal qualities at the time of this discovery (1975), leading to the postulation that they were possibly used as such.[5,6] There is also, however, the possibility that a rodent native to the area, known to store seeds and flowers, was responsible for their presence.[6] Regardless of the possibility of contamination, however, the presence of the flowers does not prove their function as medicines. They could have simply formed part of the diet, as ancient medicines often originated from foods with beneficial health effects.[6]

Regarding records of such plant uses; it seems as though medicines have been mentioned since the origin of written communications, in Mesopotamia and Egypt.[6] The oldest known records - from Mesopotamia, and written in cuneiform on clay tablets - date back to about 1700 BC.[6] Many, however were found to be copies of older texts, containing drug names dating back to 2000-3000 BC.[6,7] These refer to several plant species, including *Commiphora* species (myrrh), *Cupressus sempervirens* (cyprus) and *Papaver somniferum* (poppy) juice,[7] though Sneader warns that the identification of the plants in the texts is not reliable.[6] Drugs derived from the species, *vide supra*, are still in use today.

Ancient Egyptian medicine is also represented in written records, referred to as the papyri (sing. papyrus). These records range in date of origin from around 1820 BC to AD 250.[8] The most extensive

of the medical papyri is known as the Ebers papyrus, and dates back to about 1530 BC.[8] It lists over 800 prescriptions,[6] most of which concern plant-based treatments.[7] Like the cuneiform tablets, the Egyptian papyri contain elements dating back further than the document itself, as far as the fourth millennium BC.[6]

These early works intertwined the ideas of magic and/or religion with that of medicine, including rituals and incantations in treatment descriptions.[6,8] Many works compiling information regarding herbal remedies and medicines followed, of course, in the centuries proceeding such ancient civilizations. Over time, some cultures came to value approaches to medicine that excluded any superstitious nature. This is evidenced by the works of ancient Greek authors, such as Hippocrates, Aristotle and Dioscorides. The efforts of the ancient Greek physicians during this time period (460 BC to around AD 78) gave rise to works of great importance, such as the *Hippocratic corpus*, and *De Materia Medica*.[6] It should be noted that the use of medicinal herbs remained empirical, with little being known regarding the plant constituents causing the observed effects, and only some of the species in use being effective.

Towards the end of the 15th century (AD), exploratory voyages began to open new trade routes, and it became possible for European nations to access herbs from the Americas. Coupled with the development of the printing press in the mid-15th century, this lead to the publication of 'herbals', documenting investigations of herbs, medicinal and otherwise.[9] Herbals grew in popularity, leading to an increased focus on plants as medicines, and encouraging physicians to carry out and publish their own investigations.[6] This assisted in shifting the medicinal approach somewhat towards the logical, and away from the magical and ethereal.

Around the late 18th century, physicians finally began to carry out medical investigations that resembled the modern scientific approach.[6] James Lind famously developed a method for the first clinical trial, when he ran experiments testing the efficacy of various scurvy treatments on sailors and hospitalized scurvy patients[10] (though it has been proven that much earlier, others reached the conclusion that citrus fruits were a cure,[11] the trial itself reflected a scientific approach[10]). Soon after, during the mid- to late-18th century, other physicians began to conduct their own scientific studies on plant medications. Examples of such include Anton von Störck - who carried out dosage investigations on species of plants that were generally considered poisonous at the time - and William Withering, known for his reports on foxglove (*Digitalis purpurea* L.).[6] Such investigations as these indicate a shift towards a scientific approach, which eventually lead to investigations resulting in the isolation of the first active compounds from plants.

6.1.2 A brief history of natural products chemistry

As is outlined in the preceding section, crude plant remedies in many forms have been in use for thousands of years. However, as is well known, modern medicine is based almost entirely on the premise of utilising pure compounds and establishing their interactions within the human body. The use of pure bioactive organic compounds as drugs began when they were first isolated from plants.

Though several naturally isolated organic acids were first discovered by Carl Wilhelm Scheele in the late 18th century,[12] these substances did not exhibit high bioactivity by interaction with receptors in the human body, and thus (despite having many uses and health effects), are not of the same class of drugs as the compounds to follow.

The discovery of highly active drug compounds began, quite famously, with the isolation of morphine **1** from the opium poppy, *Papaver somniferum*, which was carried out by Friedrich Wilhelm Sertürner.[6,13,14] Sertürner published his first report on this in 1805,[13] and a year later, published a more detailed account of the isolation of this principal active of opium.[6,12,15,16] He called the substance - which he determined to be alkaline in nature - 'morphium',[6,17] after the Greek god of dreams.

"Morphium" was the first known plant substance that was basic in nature. The importance of this fact was noted by Joseph Gay-Lussac, when he noticed a report published by Sertürner in 1817, in which attention was drawn to the ability of "morphium" to form salts when reacted with acids.[6] Gay-Lussac was a highly respected French chemist, and the editor of the prestigious *Annales de Chemie*, in which he published Sertürner's work, bringing attention to the existence of plant alkalis, and sparking further investigation of such species by chemists.[6,16] Gay-Lussac suspected that more such compounds would be found, and suggested a convention in which their names end in the suffix '-ine'. It was in this way that the first isolated natural products drug was named 'morphine' **1** (Figure 6.1.1). To this day, morphine **1** (generally in a salt form) remains in common use as an analgesic for the treatment of moderate to severe pain.[16–18]

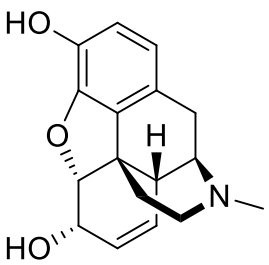

1

*Figure 6.1.1 - The chemical structure of morphine **1**.*

At this point, it may be necessary – as a disclaimer – to note that narcotine **2** (Figure 6.1.2) (or noscapine, also from the opium poppy) was arguably discovered before morphine **1** as the first plant

alkali. It was first isolated by Charles Louis Derosne in 1803.[6,12] Interestingly, it seems he noticed its basic nature, but ascribed it to the use of potash in the procedure during which it was obtained.[6] The reason this has been omitted is due to the lack of further investigation following its isolation, and the fact that it was only named and classified well after morphine **1** had set the stage for alkaloid discovery.[6,12]

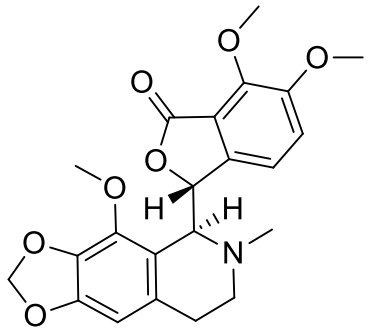

2

*Figure 6.1.2 - The chemical structure of narcotine **2**.*

Opium was of high interest for the isolation of active alkaloids, and several others were later discovered in this species. Thebaine **3** (Figure 6.1.3) was isolated in 1832 by Thibouméry, the manager of a factory built by Pelletier (see discussion of quinine **12** ahead) for alkaloid production.[6] Thebaine **3** did not exhibit great potential as a pharmaceutical agent, but has since proven very useful as a subject for synthetic studies on morphine-related opium alkaloids.[6,21] Also in 1832, Pierre-Jean Robiquet discovered a new alkaloid while exploring an alternative morphine **1** extraction process.[21] This was called codeine **4** (Figure 6.1.3) and it exhibited pharmacological action similar to – but less pronounced than – that of morphine **1**. Codeine **4** is still used as treatment for mild to moderate pain today. In 1848, George Merck isolated another alkaloid called papaverine **5** (Figure 6.1.3) from the mother liquor remaining after morphine **1** extraction in his father's factory.[21]

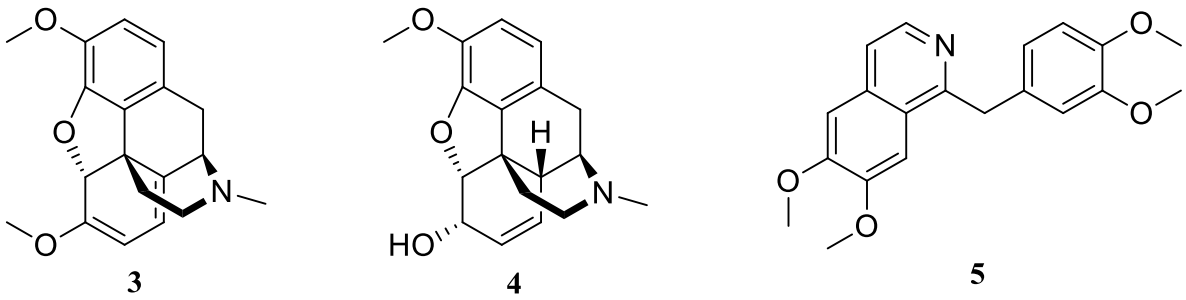

3 **4** **5**

*Figure 6.1.3 - The chemical structures of thebaine **3**, codeine **4** and papaverine **5**.*

The discovery of the first of the plant alkalis (later termed the 'alkaloids') was the frontrunner in a series of similar alkaloid isolations.[6,16] Nicotine **6** (Figure 6.1.4) was isolated in impure form in 1809, and as a pure crystal in 1828.[12] The isolation of impure emetine **7** (Figure 6.1.4) followed in

1817,[6,12,16] though the pure alkaloid was only isolated in 1887.[22] This alkaloid was used as a treatment for amoebic dysentery.[6,16] In 1819, impure colchicine **8** (Figure 6.1.4) was isolated for the first time, by the French chemists Pelletier and Caventou,[16,23] and was of interest for its application as a gout treatment. Currently it is used for the treatment of a variety of diseases and conditions.[23] Again, this alkaloid was only isolated in its pure form much later in, 1883.[23] Pelletier and Caventou isolated several other alkaloids in 1819, including strychnine **9** and brucine **10** (Figure 6.1.5).[12] Delphinine **11** (Figure 6.1.5) was also isolated that year, by J.-L. Lassaigne and H. Feneulle.[12]

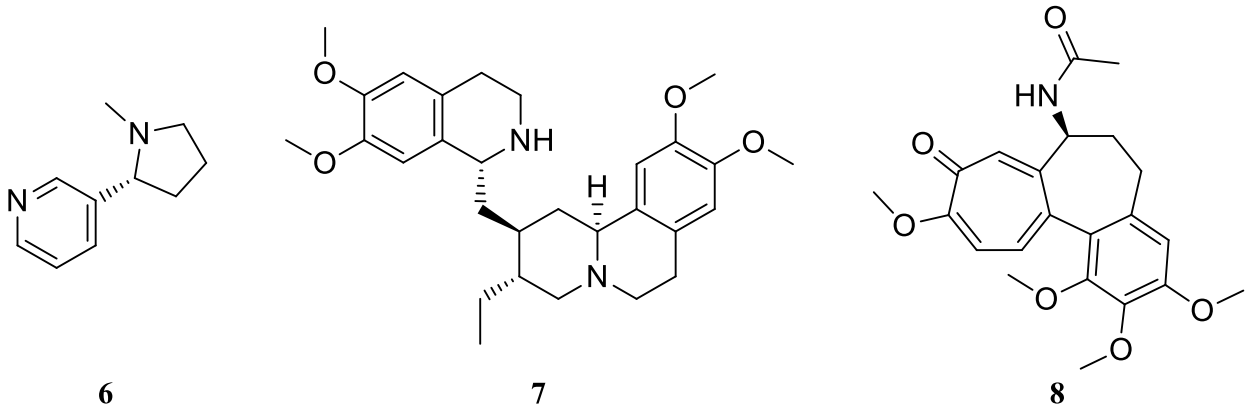

*Figure 6.1.4 – The chemical structures of nicotine **6**, emetine **7** and colchicine **8**.*

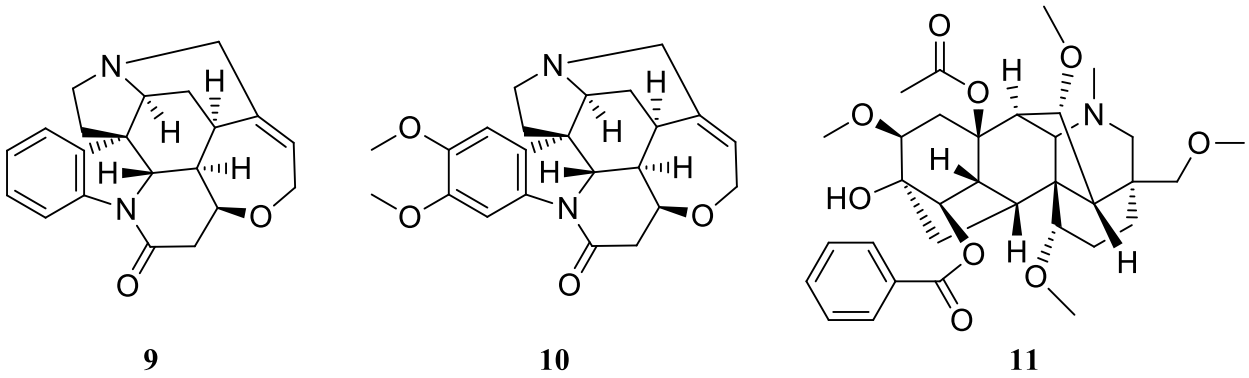

*Figure 6.1.5 – The chemical structures of strychnine **9**, brucine **10** and delphinine **11**.*

Quinine **12** (Figure 6.1.6), also isolated by Pelletier and Caventou, in 1820,[24] was the next significant alkaloid discovery, and proved to be a highly impactful one. It was isolated from the bark of *Cinchona cordifolia*, while the researchers were investigating the material based on work done by Bernardino Gomes, who isolated impure cinchonine from the bark around 1812.[6,12] During their investigation, Pelletier and Caventou isolated both cinchonine and quinine **12**. Quinine **12** was shown to be effective in the treatment of malaria, caused by the parasite *Plasmodium falciparum*. It remained the primary antimalarial drug for many years, and its bulk production in a factory in 1826 by Pelletier could be considered the birth of the pharmaceutical production industry.[6,16] Other alkaloids isolated in 1820 include piperine, veratrine and solanine.[12]

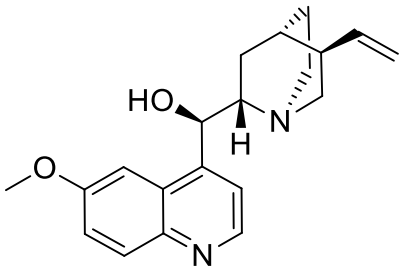

12

*Figure 6.1.6 - The chemical structure of quinine **12**.*

Caffeine **13** (Figure 6.1.7) was isolated from mocha beans by Ferdinand Friedlieb Runge in 1821.[6] The beans of *Coffea arabica* have continued to be used in brewing the popular stimulating beverage that is coffee to this day. Before the introduction of synthetic diuretics, caffeine **13** and other xanthine alkaloids were often prescribed as diurectics. Other xanthine alkaloids include theobromine **14**, isolated from *Theobroma cacao* seeds in 1878 and theophylline **15**, isolated from *Camellia sinensis* in 1888 (Figure 6.1.7).[6]

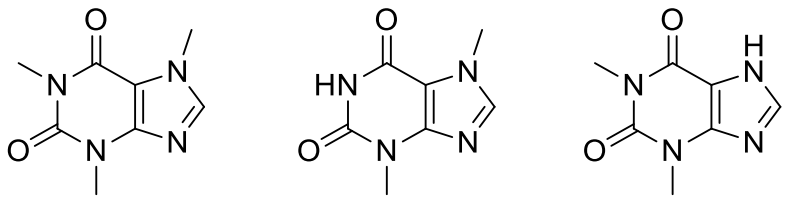

13 **14** **15**

*Figure 6.1.7 – The chemical structures of caffeine **13**, theobromine **14**, and theophylline **15**.*

Atropine **16** (Figure 6.1.8) is a tropane alkaloid, first isolated as a crude compound in 1822 by Rudolph Brandes. It was isolated in pure form in 1833.[6] Atropine **16** is an example of an artefact, which is a compound formed during the extraction or isolation processes, and is not present as such in the plant.[6,25] Atropine **16** is a racemate of hyoscyamine **17** (Figure 6.1.8), the source alkaloid, present as one stereoisomer, which forms a racemic mixture when in solution.[6,25] Artefacts produced during the isolation of alkaloids is something that must always be considered as a possibility by a natural products chemist undertaking such investigations.

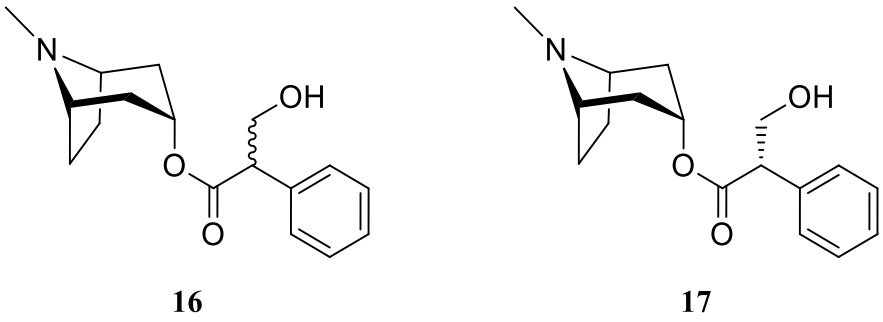

16 **17**

*Figure 6.1.8 - Chemical structures of atropine **16** and hyoscyamine **17**.*

An alkaloid which is well-known in modern society, though unfortunately not as a prescribed medicine, is cocaine **18** (Figure 6.1.9). Cocaine **18** is a stimulant, originating from the leaves of the coca plant, *Erythroxylum coca*. The leaves of the coca plant have been in use by indigenous inhabitants for centuries, with the first documented report of their use being published in 1565.[6] The popularity of the use of coca leaves sparked an intensive investigation of the plant by organic chemists, resulting in the isolation of the active alkaloid, cocaine **18**, in 1860 by Albert Niemann.[6,26] Interestingly, cocaine **18** was investigated by Sigmund Freud for its stimulating properties. Carl Koller, Freud's assistant at the time, noticed the ability of cocaine **18** to cause numbness when applied to an area, an application which ended up offering significant contribution in the field of ophthalmic surgery.[6,27] This discovery is considered the first instance of a local anaesthetic.[27]

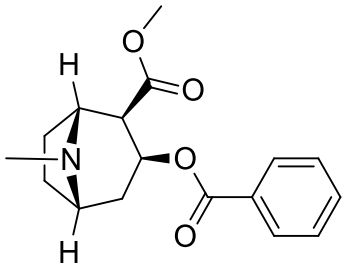

18

*Figure 6.1.9 - The chemical structure of cocaine **18**.*

The nineteenth century was thus the opening chapter for an ever-expanding archive of alkaloidal discoveries. Other alkaloids isolated in the 19th and 20th centuries include: physostigmine, obtained in 1864; pilocarpine in 1874 (a rare example of a natural product that has not had analogues made, as it was sufficiently active and was acceptable for its specific application); ephedrine in 1885; tubocurarine in 1935; reserpine in 1951; vinblastine in 1958; and vincristine in 1961 (this and vinblastine being of the vinca alkaloids, and of use in cancer therapy).[6]

As can be noted, up until this point, only alkaloidal isolations have been mentioned in this section. Though the use of alkaloids is stressed, due to the focus of this project, it must be noted that there were other impactful discoveries made during the 19th and 20th centuries.

As briefly mentioned above, there were several organic acids isolated by Carl Wilhelm Scheele, between 1770 and 1790.[12] These acids included: tartaric acid in 1770, benzoic acid in 1775, citric acid in 1784, oxalic acid in 1784, malic acid in 1785, glucuronic acid in 1785, and gallic acid in 1786.[12]

Inulin (though not a pure compound) was found in 1804 by Valentin Rose Jr., from the roots of elecampane (*Inula helenium*).[12] Inulin is a term applied to all β(1→2) fructans, a group of polysaccharides. Inulin has been shown to act as a prebiotic, promoting the growth of beneficial microbes in the gut, assisting in the formation of a healthy gut flora.[28]

Salicin was isolated in 1829 by Leroux, from meadowsweet, *Filipendula ulmaria*. Salicin was first used as an alternative to quinine **12**, as it assisted in abating the fevers that invariably accompany malaria. It was later found that salicin could be transformed into salicylic acid, and that this process occurred in the human body when salicin was ingested.[6,29] Salicylic acid was synthesised in 1860, and became a cheaper alternative to salicin, the use of which declined for this reason.[6,29] The common drug known as aspirin is derived from salicylic acid, being its acetic acid ester.[29] Methyl salicylate (the methyl ester of salicylic acid) was isolated by William Proctor in 1843, from wintergreen oil.[6]

Another noteworthy isolation was that of podophyllotoxin in 1880 by Podwyssotski,[30] from the rhizome of *Podophyllum peltatum*. Podophyllotoxin is very toxic, and has pronounced gastrointestinal side effects,[6] but exhibits potent cytotoxic biological activity.[6,31,32] The generation of analogues of podophyllotoxin has yielded several useful anticancer agents, such as etoposide and teniposide.[31,32] Derivatisation of podophyllotoxin in search of anticancer agents remains a subject of interest to this day.[33]

A screening programme established by the US National Cancer Institute resulted in the isolation of another useful anticancer drug in 1966,[6] called paclitaxel (taxol). Paclitaxel is active against a broad range of cancer types, and has approved applications in the treatment of ovarian and breast cancers.[6,34]

The information above provides only a very broad overview of just a few examples of some historical plant-based natural products and their medicinal contributions. The true contribution of natural products to modern medicine is immense, and in fact extends beyond the plant kingdom, with many notable contributions from animals, bacteria and fungi. The focus of this project is plant-oriented, and so the importance of plant-based medicinal chemistry is highlighted. As has hopefully been shown, even disregarding the contributions from other natural products sources, the potential of plants for medicinal applications is immense, and should be highly regarded for current and future investigations.

6.1.3 *What plants offer medicinal chemistry*

As the previous section demonstrates, there are numerous compounds that have been isolated from plants which have proven to be medicinally valuable. A concept that has added immense value to the field of medicinal chemistry is that of the generation of analogues of new molecular entities. Previously, morphine **1** was discussed as the first biologically active compound to be isolated from a plant. Perhaps as a result of this early development, morphine **1** was also the subject of studies resulting in the preparation of the first natural product analogues, by Henry How in 1853, who generated quaternary ammonium salts of morphine **1** by heating it with alkyl iodides.[6]

Such analogues were only tested pharmacologically when, 15 years later, Alexander Crum Brown sent the quaternary ammonium salts of several alkaloids to Thomas Fraser for testing. Despite the diverse actions of the original alkaloids, the quaternary ammonium salts all exhibited paralytic activity.[6] This suggested that the quaternary ammonium function conferred this particular property. Such was the result of the first known study correlating a structural feature to a specific activity.[6]

When the first structural modifications resulted in compounds that exhibited notably different pharmacological properties, the concept of structure-activity relationships (SARs) was encountered. The idea that the properties of a drug could be improved, in a directed fashion, by making changes to one or more of its functional groups has proven to be of immense value in the field of drug development. It thus transpired that natural products compounds were of use, not only as immediately marketable drugs, but as drug leads that could be structurally altered for improved activity. It is therefore important to include natural products analogues when discussing the contributions of natural compounds to modern treatment options.

Despite the fact that plants and other natural sources were the origin of the first pharmacologically active compounds, focus later shifted to synthetic approaches for drug discovery, due to the advent of high-throughput screening strategies.[1,6,35] However, it seems as though synthetic approaches have not provided as many viable drugs as hoped for in recent years, resulting in a renewed interest in natural products for drug lead discovery.[1,7,35–38] There seems to be an increasing interest in herbal medicines amongst the general public as well, which could be a contributing factor to the acceleration of natural products research.[39] Regardless, it is apparent that there is value to be found in biological compounds, and that research in this area is well-justified.

The contribution of natural products to the field of drug discovery is significantly dependent upon what one defines as a natural products contribution. There are several sources outlining recent information on this topic, with definition-dependent statistics ranging from about one third to around two thirds of approved drugs being related in some way to natural products.[37,40,41]

According to a paper by Thomford *et al.* published in 2018,[36] of all drugs approved by the Food and Drug Administration (FDA) and/or the European Medical Agency (EMA), about a quarter have been plant-based. About a third of the drugs approved over the last two decades were said to have been natural products-related, with added contributions from bacteria, fungi, animals and other natural sources.

Thomford *et al.* refer to a paper published in 2016 by Patridge *et al.*[41] when stating that a quarter of the approved drugs have been plant-based. Considering the data presented by Patridge *et al*., it seems a misunderstanding occurred. Patridge *et al.* report that over a third (38%) of all approved drugs are natural products related, and that of this percentage, approximately one quarter are based on plant compounds and their derivatives. Interestingly, this paper reports that 44% of approved natural products related drugs were from mammalian sources.

Patridge *et al.*[41] considered fully synthetic compounds related to their original natural counterparts as derivatives of natural products. The reason this makes a notable difference may be because most (around 80%) of the approved mammalian related drugs are fully synthetic (yet natural product-inspired).[41] Thus, if these are considered as natural products contributions, the statistics concerning mammalian input increase drastically. The information regarding non-mammalian natural products showed a higher percentage of unmodified compounds and their derivatives versus fully synthetic analogues.[41] In this data, plants dominated the non-mammalian contributors, though bacteria are gaining increasing interest in more recent years.[41] Also highlighting plant contributions, Alan Harvey reported in 2008 that there were over 200 natural products undergoing preclinical and clinical trials, almost half of which were plant-related.[7]

Anticancer agents are a group of medicines with a particularly high contribution from natural products, with approximately 74% of anticancer drugs in 2006 being natural products or natural products derived.[42] A more recent report, published in 2019 by Jin and Yao,[43] states that over 75% of small molecule anticancer drugs are natural products or are directly related to them. This indicates that the trend in natural products contributions to cancer treatments still prevails, and has not diminished to date.

The purpose of this section is to outline the significance of plant contributions to the medical world today. The topic of natural products contributions can become fairly complicated when considering the variety of definitions, and so it may not be within efficiency's best interests to go into too much detail. The above information should be sufficient to convince the reader that natural products play a significant role in the drug discovery field, and that plant products are an important resource in natural products investigations.

Despite the inherent value of plant extracts as a resource for the discovery of new medicinal compounds, only an estimated 10-15% of the higher plant species on earth has been investigated for medicinal potential[44]. Thus, there remains a largely untapped resource in plant biodiversity.

South Africa is a region of notable plant biodiversity, being home to over 23000 plant species,[45] which is over 8% of the world's plant species, while covering less than 1% of earth's land surface.[45,46] The "fynbos" eco-region of the Cape Peninsula alone holds over 9000 plant species – a total of around 3.4% of the world's plant species.[45] This Cape Floral Kingdom represents more than 40% of the subcontinent's flora, in only 4% of its area. Of the plants found in this area, 6192 species are found nowhere else – a remarkable level of endemism.[45] It is therefore clear that southern African plants hold an immense and untapped value in terms of species to be investigated for medicinal advancement. Investigations focusing on exploring this resource are therefore of importance. Not only are such investigations of interest for adding value to the medicinal world, but proving the existence of such value in South African biodiversity may provide additional motivation for the conservation of these biomes. Such reasoning was a factor backing the decision to focus on a southern African plant as the subject of investigation for this project.

One possible outcome of this project was the isolation of active principles that were novel, in an attempt to provide new drug leads for further development. To increase the chances of success in this regard, choosing plant species that had not previously been thoroughly investigated was an obvious advantage. Additionally, plant species from families known to be rich in active compounds were of high interest. With such reasoning in mind, two species were selected, namely *Crinum paludosum*, and *Crinum variabile*. Members of the *Crinum* genus have a history of use in traditional medicine[47], also adding to the likelihood of active isolations. These species are of the Amaryllidaceae family, which has provided a plethora of novel alkaloid structures.[48–51]

The Amaryllidaceae alkaloids are a structurally diverse group, and have a broad range of pharmacological actions, with several possible areas of application.[49,51]

6.2 The Amaryllidaceae alkaloids

6.2.1 An introduction to the Amaryllidaceae

The Amaryllidaceae is a family of monocotyledonous plants containing 75 genera and around 1600 species.[52] Southern Africa is a region of pronounced diversity with regards to the Amaryllidaceae, containing 18 genera and around 250 species, all within the subfamily Amaryllidoideae[53] (the old Amaryllidaceae[54]). This diversity is bested only by the Neotropics from Mexico to Chile, which contains 26 genera and about 375 species. The Mediterranean basin is the third most speciose region,

containing 8 genera within the family. Of the 18 genera present in southern Africa, all but three (*Crinum*, *Pancratium* and *Scadoxus*) are endemic to Africa, and of those, all but four are endemic to southern Africa.[53] The 11 genera endemic to southern Africa contain over 200 endemic species, with local centres of diversity in the southwest Western Cape, the Eastern Cape and the escarpment between Kwa-Zulu Natal and Mpumalanga.[53]

In Africa, four tribes within the subfamily Amaryllidoideae are represented. Of these four tribes (Amaryllideae, Cyrantheae, Haemantheae, and Pancratieae), Amaryllideae contains the most genera, this being 10 – more than all three other tribes combined. Within the Amaryllideae tribe, *Crinum* is the largest genus, containing approximately 65 species in southern Africa,[53] and around 103 species in total.[48] *Crinum* has its origin and centre of diversity in southern Africa, though it has species present in several other regions, including Madagascar, Asia, Australia and America. The genus was first established in 1753, then containing only 4 species, three of which are still recognized as valid today. All species within the genus are summer-growing, with the exception of *C. variabile*, which is winter growing.[53]

There are many examples of Amaryllidaceae members, such as species of the *Crinum* genus (and several others), which have a history of use in traditional medicine. There are examples of some species being used for the treatment of ailments such as (among many more[47]) joint pain, backache, rheumatism, earache, colds, urinary tract infection, and even kidney and bladder disease.[47,53] The plant material of several southern African *Crinum* species, including *C. campanulatum*, *C. gramnicola*, *C. moorei*, and *C. variabile* (as well as many species of other Amaryllidaceae genera) have shown positive results for acetylcholinesterase (AChE) inhibition, and have potential for Alzheimer's disease treatment.[53,55–58]

It has been shown that this activity (and many other pharmacological activities) can be attributed to the alkaloids present in these species, and that such alkaloids are present in species belonging to genera across the whole family of the Amaryllidaceae.[50,59,60] It seems, in fact, that most genera in the family have been validated to produce Amaryllidaceae alkaloids.[54]

The alkaloids present in members of the Amaryllidaceae, referred to as the "Amaryllidaceae alkaloids", are structurally diverse, and numerous. According to Jin and Xu (2013),[54] up to 500 alkaloids had been isolated up until 2013. With more being isolated every year, this number has now increased to over 600, as reported by a review published by Jin and Yao in 2019.[43] The book chapter published by Jin and Xu in 2013 is an extensive review of the Amaryllidaceae alkaloids, with 169 references, and outlines the structures of well over 200 known Amaryllidaceae alkaloids.[54] Also included in the review is information concerning alkaloid biosynthesis of the main Amaryllidaceae

alkaloid types, and the biological activities of a number of these alkaloids. The review paper published in 2019 by Jin and Yao[43] in *Natural Product Reports* is the most recent in a series of review articles entitled "Amaryllidaceae and *Sceletium* Alkaloids". This article comprises a comprehensive analysis of alkaloids isolated from the Amaryllidaceae family, and the closely related alkaloids from the *Sceletium* genus, from mid-2015 until mid-2017. This review series frequently covers the topic, and contains a compilation of information that is challenged by few, if any, other sources.

The first known Amaryllidaceae alkaloid, lycorine **19** (Figure 6.2.1), was isolated in 1877, from the species *Narcissus pseudonarcissus*. Lycorine **19** has since been shown to exhibit a range of biological activities, including: apoptosis-inducing effect, antitumor, antiviral, anti-inflammatory, antifungal, antimicrobial, antimalarial, antiretroviral and AChE inhibitory activities.[54] Lycorine **19** has drawn much attention as a possible natural lead for anticancer drug design, showing activity against several cancer types, including drug-resistant variants, at low concentration and with high specificity.[61]

As has been established, since the discovery of lycorine **19**, the number of known Amaryllidaceae alkaloids has increased significantly, revealing diverse structures and pharmacological activities. Well known amongst these is galanthamine **20** (Figure 6.2.2) (also known by the drug name galantamine, Reminyl®), a potent AChE inhibitor that was approved as a prescription drug for the treatment of Alzheimer's disease in 2001.[43,54,62] Galanthamine **20** is produced on an industrial scale by extraction and isolation from daffodils, though total synthesis is also possible as a means of production.[43] The value of the galanthamine **20** industry as reported in 2013 by Nair *et al.*[62] was approximately 150 million US dollars per year.

Also according to Nair *et al.* (2013),[62] an anticancer drug target related to the Amaryllidaceae alkaloid pancratistatin was undergoing advanced clinical evaluation, and was expected to be commercially available by 2023. This is indicative of the value and potential present in the development of analogue libraries of Amaryllidaceae alkaloids for the discovery of new drugs.

6.2.2 Classification of Amaryllidaceae alkaloids

Despite the notable structural diversity of the Amaryllidaceae alkaloids, they share biosynthetic roots and are considered to be biogenetically related.[54] They are biosynthetically derived from the precursor norbelladine,[54,61,63] which is an alkaloid present in some Amaryllidaceae species. The nature of their biogenetic relation is such that their production in a plant is considered a fairly reliable indicator of that plant's classification in the family (since these alkaloids are almost entirely exclusively produced by plants in this family). Thus, should a genus or species produce only unrelated alkaloids, reclassification of said plant(s) could be considered.[54]

Initially, the Amaryllidaceae alkaloids were classified, based on skeletal structure, into 9 groups.[54] However, following the discovery of alkaloids with skeletons that challenged classification based on this convention, a new grouping system was suggested shortly prior to 2013.[54] The new convention classifies Amaryllidaceae alkaloids based on skeletal ring systems into 12 possible groups, as follows: [1] norbelladine-type, [2] lycorine-type, [3] homolycorine-type, [4] crinine- and haemanthamine-types, [5] tazettine-type, [6] montanine-type, [7] plicamine-type, [8] graciline-type, [9] galanthindole-type, [10] galanthamine-type, [11] phenanthridone- and phenanthridine-types, and [12] other minor species populations.[54] This convention is the currently accepted rubric for Amaryllidaceae alkaloid classification.[43]

Table 6.1 – Examples of skeletal structures for each Amaryllidaceae alkaloid type. Note that each type may have additional skeleton structures which are related to those shown. R_1-R_6 = various groups.

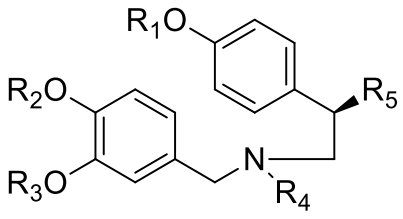 [1] Norbelladine-type	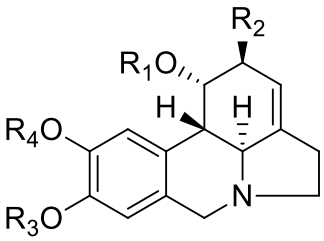 [2] Lycorine-type	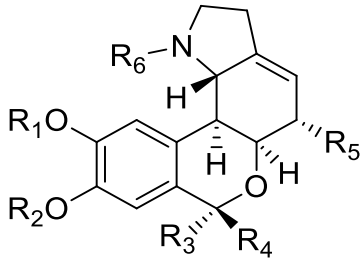 [3] Homolycorine-type
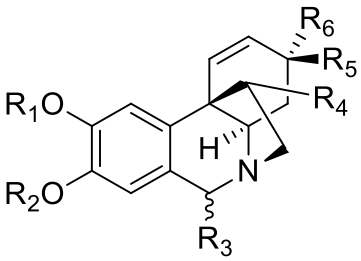 [4a] Crinine-type	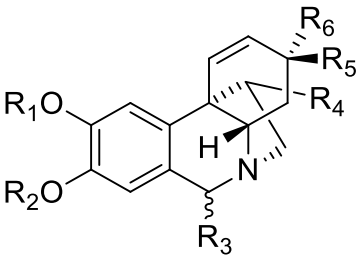 [4b] Haemanthamine-type	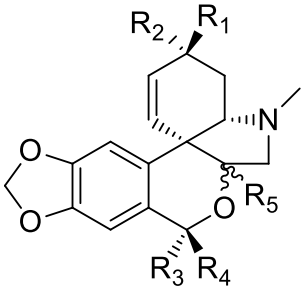 [5] Tazettine-type
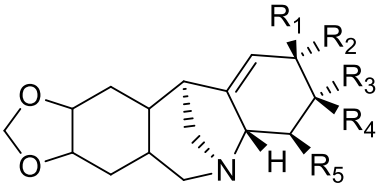 [6] Montanine-type	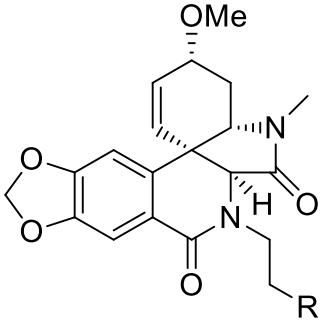 [7] R=*para*-phenol: Plicamine (plicamine-type)	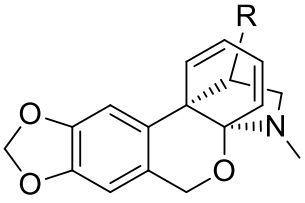 [8] Graciline-type

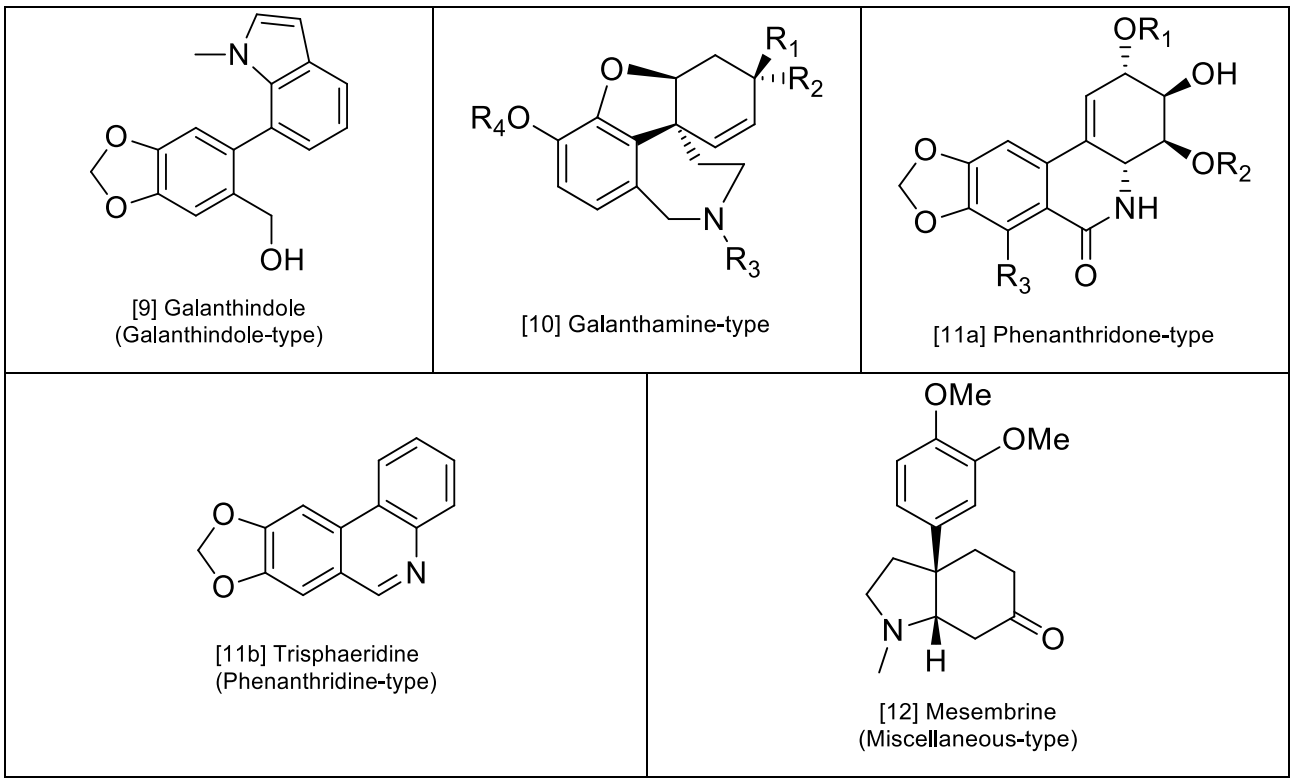

6.2.3 *Some Crinum alkaloids and their applications*

As mentioned in Section 3.2.2, members of the *Crinum* genus have a long history of use in traditional medicine for the treatment of numerous conditions and ailments. Extracts and isolates of *Crinum* species have been scientifically shown to exhibit a range of pharmacological properties.[47] Two important alkaloids commonly isolated from members of the *Crinum* genus, which have already been briefly discussed, are lycorine **19** and galanthamine **20**,[64] with lycorine **19** exhibiting promising potential as an anticancer drug lead, and galanthamine **20** already having found its place as a treatment for Alzheimer's disease.[54]

Lycorine **19** has been the subject of several studies reporting positive results regarding the anti-tumour activity of it and its derivatives.[61,63] Lycorine **19** itself has been shown to possess activity against many cancer types.[61] Zhang *et al.* (2019)[65] studied the activity of lycorine **19** against metastatic melanoma, a cancer type responsible for 60% of skin cancer deaths. They reported that the alkaloid significantly suppressed melanoma cell migration and invasion *in vitro*, and when tested on tumour-bearing mice, decreased the metastasis of melanoma cells to the lung tissue. This resulted in a significant increase in survival time of the treated mice, without obvious toxicity. Another study by Sun *et al.* (2018)[66] tested lycorine **19** against non-small cell lung carcinoma, reporting that treatment resulted in significant suppression of the growth and metastasis of the lung tumour.

Reports of the activity of lycorine **19** against other cancer types are extensive in the literature. The topic is outlined by Roy *et al.* (2018),[61] which reviews the alkaloid and its mechanisms of action for anticancer activities. Examples of cancer types against which lycorine **19** is active include leukaemia, multiple myeloma, prostate cancer, human breast cancer, human bladder cancer, ovarian cancer, large cell lung cancer, colon carcinoma and human heptatocellular carcinoma.[61] Against all of these, lycorine **19** exhibited IC_{50} values below 40 µM.

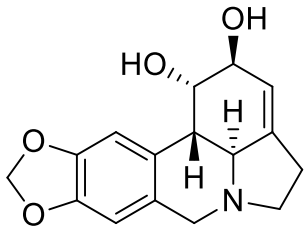

19

*Figure 6.2.1 - The chemical structure of lycorine **19**.*

Derivatives of lycorine **19** have also been shown to exhibit activity against a range of cancer types, some examples of which are outlined in an article by Lamoral-Theys *et al.* (2010).[63] This paper reviews the testing of 25 lycorine **19** derivatives on various cancer cell lines, reporting that 20 of these proved active against at least on cell line. Additionally, it is stated that there were approximately 300 molecules sharing lycorine's core ring structure in 2010 (this number has likely increased). That only 26 of these (including lycorine **19**) had been tested is testament to the work that has yet to be done on this topic.

Galanthamine **20** is an additional example of an Amaryllidaceae alkaloid of especial importance, and is, to the best of our knowledge, the only Amaryllidaceae alkaloid to be marketed as an approved drug in the developed world.[43,54] As briefly discussed previously, galanthamine **20** is approved for use in the treatment of Alzheimer's disease (approved by the FDA). Alzheimer's disease is the most common form of dementia among elderly individuals[67] and is also the most prevalent chronic neurodegenerative disease, affecting around 5.7 million people in the US alone.[68] Worldwide, it is estimated that there are 50 million people suffering from dementia, 30-35 million of which have Alzheimer's.[68]

One of the effects of the disease is the loss of cortical acetylcholine receptors, which are important for the passage of signals through synapses in the brain. Acetylcholine is a neurotransmitter which binds to these receptors as a means of transmitting signals between synapses. Thus the loss of these receptors weakens impulses passing between synapses, slowing cognitive function. Galanthamine **20** is a potent and reversible inhibitor of the enzyme acetylcholinesterase, which is responsible for the

catabolism of acetylcholine in the synaptic cleft. Inhibition of the enzyme that breaks down acetylcholine allows for an increase in the number of receptors being activated by the neurotransmitter, thus allowing for better inter-synaptic signalling despite decreased receptor density.[67]

Galanthamine **20** has also been used in anaesthesia to reverse neuromuscular paralysis caused by some muscle relaxants.[67] As mentioned previously, the alkaloid is produced industrially by extraction and isolation from daffodils, but can be generated synthetically.[54] Much of the recent literature concerning galanthamine **20** is dedicated towards options for its synthesis.

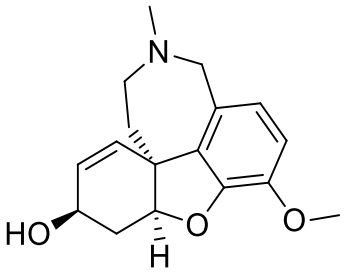

20

*Figure 6.2.2 - The chemical structure of galanthamine **20**.*

Lycorine **19** and galanthamine **20** are just two examples of alkaloids present in *Crinum* species that exhibit promising bioactivities. There are, of course, numerous other alkaloids present in members of the genus, with Refaat *et al.* (2012-2013)[48,69,70] producing a review series which presents around 180 different alkaloids reported from *Crinum* species. The fifth part in this review focuses on the biological profile of the genus and reports the pharmacological activities of extracts from some of these plants, and of some of the alkaloids found within them. Amongst the activities reported are: analgesic and anti-inflammatory effects, acetylcholinesterase inhibition, serotonin reuptake inhibition, hypotensive and hypertensive activities, muscle relaxant and reversal thereof, antiallergic and anti-anaphylactic activities, immunomodulatory properties, cytotoxic and anticancer, antimicrobial, antiparasitic and insecticidal activities.[71]

With such a diverse range of possible applications, and such a complex alkaloidal profile, investigations into the detection, isolation and characterisation of alkaloids from such plants has drawn much attention in the scientific community. Methods that can be applied to such investigations are thus of great interest.

6.3 A brief overview of some methods of natural product analysis

With the immense diversity presented by nature comes a diverse and multidisciplinary set of skills and techniques for the analysis of the compounds therein. Natural products chemistry thus

incorporates the use of many methods, often resulting in a number of possible approaches to a task. With the advancement of technology comes the development of new instrumentation and faster, more effective, techniques for the detection, isolation and characterisation of natural products compounds. It must, however, be acknowledged that the circumstances of the researcher play a determining role in the approaches taken during an investigation. Aspects such as available instrumentation, time restrictions, financial limitations, availability of trained collaborators and many other such resource and personnel limitations must be considered guiding forces in research projects.

When access to analytical instruments is limited by such restrictions, sometimes the most effective approach is the application of simple techniques such as solvent extraction, thin layer chromatography (TLC) and gravity column chromatography. The use of such techniques still holds a place in (even the most established) laboratories worldwide, and their efficacy cannot be challenged.

With this in mind, recent years have seen the development of some fascinating and effective techniques for natural products investigations. The use of high-performance liquid chromatography (HPLC) has established itself, and has proven to be of great use, with hyphenation to a number of detection methods further increasing its power. Ultraviolet/visible (UV/Vis) and infrared (IR) spectroscopies, and mass spectrometry (MS) are common examples of such detection methods, though even powerful structural elucidation tools such as nuclear magnetic resonance (NMR) spectroscopy can be hyphenated to such systems.[72]

When searching for natural compounds with a specific pharmacological action, bioassays can be employed as useful tests for the detection of compounds exhibiting the required action. In the book edited by Colegate and Molyneux (2008),[72] such a bioassay is defined as "…any *in vitro* or *in vivo* system used to detect the biological activity of an extract or a pure substance…". Bioassays are numerous and varied, ranging from general to very specific. A plethora of systems are used as tests, ranging from cell cultures to developed lab animals, and thus a range of properties and applications are exemplified in the field. Bioassay-guided fractionation is the process in which bioassays are used to determine the presence of bioactive substances in fractions throughout a series of separation steps, leading towards the isolation of a pure bioactive compound. Bioassays can, unfortunately, be time-consuming, and studies focused on increasing their speed continue.[72]

Important steps for the characterisation of natural compounds are, of course, separation and isolation. The first step in such processes is generally extraction of the original biological material. Sometimes this is done with sequentially low- to high-polarity solvents, but generally, polar alcoholic solvents are useful as they rupture cell membranes, and can thus extract more endocellular metabolites.[72] Thus, such extractions are often carried out first, leaving more selective processes for later separation steps.

Selective extraction processes can then be applied to the crude total extract achieved in this way, some examples being trituration with less polar solvents and acid/base extraction.

Isolation of a compound from a crude extract, or from fractions thereof, can be a demanding task, often requiring several separation steps and multiple chromatographic methods. There are many available methods of chromatographic separation, some of which will be outlined below.

Liquid-liquid chromatography involves the use of two immiscible liquid phases, and the mechanism relies on differing partition coefficients of the compounds in each of the solvents. Countercurrent chromatography (CCC) is an example of this, though HPLC and other solid support methods were preferred when it was developed, so it was largely overlooked.[72] Modern CCC, however, is much improved compared to the technique at its conception, and current advantages include: total recovery of loaded sample due to no irreversible adsorption, little risk of sample degradation, low solvent consumption, variability of both phases, and no need for expensive replaceable columns.[72]

A chromatographic type containing several popular techniques is that of planar chromatography. This covers chromatographic techniques in which the stationary phase is in a flat bed arrangement. Included in this are the widespread and indispensable TLC technique, preparative TLC (PTLC) – used for separation of larger sample quantities – and centrifugal TLC (CTLC). CTLC utilises a circular preparative plate, which is rotated while inclined, allowing for concentric circular bands to be collected as they reach the plate's edge. The sample is loaded at the centre of the plate, and can be eluted using a solvent gradient. Additional advantages include the ability to reuse plates, possible coupling of detectors, and the ability to carry out inert separations.[72]

Not to be forgotten in the separation of organic compounds is the concept of column chromatography. With a broad range of possible stationary phases, there are many techniques covered by the term. Gel filtration (also known as size exclusion chromatography) uses a gel stationary phase to separate compounds by molecular size. Conventional preparative column chromatography is gravity-driven with a silica, derivatised silica and ion exchange as stationary phase examples, and is used extensively in chemistry laboratories. Flash chromatography is similar, though solvent is forced through faster with pressure at the top of the column.[72]

Modern hyphenation methods (mentioned above), using separation systems such as HPLC and gas chromatography (GC) provide unchallenged resolution, and are imperative for dereplication processes. Dereplication is the process of identifying known compounds in extracts before searching for novel bioactive compounds, such that the search is more likely to provide previously uncharacterised drug leads. Dereplication of extracts containing known compounds can be carried out with access to standards and databases containing spectra of known compounds.[72] It must be

noted that the instrumentation for such systems can be exceedingly expensive, so numerous laboratories do not have access to many of these options.

As is well-known, and generally undisputed, nuclear magnetic resonance (NMR) spectroscopy is the most powerful structural elucidation tool currently available at most academic institutions, and the technique is improving as better instrumentation and experimental control are achieved. Both 1D- and 2D-NMR spectroscopy techniques are indispensable for natural products research, providing structural information that can rarely be matched. Some research groups are even using it as a first step in natural products investigations, obtaining the NMR spectra of a total extract to provide some information on the constituents, and to indicate any changes occurring during the fractionation process. Another interesting application is the development of quantitative NMR (qNMR) spectroscopy, which has the advantage of being non-destructive, which is particularly useful for natural products present in trace amounts.[72]

A hyphenation method of particular note and promise is that of HPLC-NMR. With NMR spectroscopy being such a powerful structural elucidation tool, and HPLC being a versatile method of separation with relatively simple sample preparation, the combination of the two could prove to be extremely valuable for natural products research. Current limitations of direct hyphenation include large solvent peaks, under which other peaks are hidden, chemical shift differences, and lack of sensitivity.[72] Such limitations reduce the possible application of the technique, though solutions to these could result in a particularly powerful analytical tool. Needless to say, the method is also a costly one.

The methods mentioned above are only a few examples, and many more exist, with varying specificity of application. The nature of the research being carried out thus dictates the methods that will be useful, and decisions must be made taking the strengths and weaknesses of such methods into consideration – a complex association of compromises is often at play.

7 Aims and objectives

As illustrated in the above sections, this project was focused on the investigation of the alkaloidal profiles of *Crinum variabile* and *Crinum paludosum*. These species were chosen because their alkaloid profiles had not previously been studied in depth, and because they belong to a family of plants with a history of use in traditional medicine. The family (Amaryllidaceae) also boasts a unique and promising record of alkaloid isolations. An additional advantage was the bulbous nature of the species, as bulbs act as storage organs for secondary metabolites and other plant products, and thus contain higher alkaloid concentrations.[47]

The aim of this project was to isolate and identify the major alkaloidal constituents of *Crinum variabile* and *Crinum paludosum*. These investigations add value to the field of natural products chemistry by identifying the major alkaloids present in the species, a task that has not previously been undertaken. This provides information to future researchers and contributes towards the body of knowledge on medicinal compounds available in the plant species in southern Africa. In the event of the isolation of a novel compound in sufficient quantities, a small library of semi-synthetic analogues could then be generated for a brief structure-activity relationship (SAR) study.

Also within the objectives of this project is a very brief synthetic study on two compounds, higginsianin A and higginsianin B. These two compounds are natural products isolated from the fungus *Colletotrichum higginsianum* by Cimmino *et al.*[73] Small quantities of these compounds were obtained from the original research group, with the intention of running small-scale test reactions for structural modification. All products obtained and characterized would be sent for biological activity evaluation.

8 *Crinum variabile*

8.1 Introduction

Crinum variabile is a winter-growing species, so named in reference to the variable colours of its flowers, which change from white to a deep pink as they age. The species is endemic to the north-western, western and southern areas of the Northern Cape of South Africa and grows near winter-flowing rivers in deep sand. It was originally classified as *Amaryllis variabilis* in 1804, with the first botanical illustration being drawn of a specimen obtained from the Cape of Good Hope. In 1873, it was transferred to the *Crinum* genus, but wild specimens were only rediscovered less than 60 years ago, in 1961. The species is easy to cultivate and micropropagation protocols have been established. However, flowering can be somewhat more difficult to achieve.[53]

Figure 8.1.1 – A botanical illustration of Crinum variabile, drawn by Barbara Jeppe, taken from "The Amaryllidaceae of Southern Africa" by Graham Duncan, Barbara Jeppe, and Leigh Voigt

Crinum variabile has been the subject of some limited phytochemical investigations, having been mentioned in a paper by Tanahashi *et al.* (1990), entitled "Radioimmunoassay for the Quantitative Determination of Galanthamine **20**".[74] In this paper, *C. variabile* was one of the species tested for galanthamine **20** content. The data presented shows that galanthamine **20** was found in small amounts, that being 0.006% of the dry weight of the plant material used.[74]

Another paper mentioning the species was published in 2004 by Jäger *et al.*, and was entitled "Acetylcholinesterase inhibition of *Crinum* sp.".[75] This paper did not focus on the isolation of active compounds from the species investigated, but rather tested the acetylcholinesterase inhibitory activities of extracts from the plants. Interestingly, the leaves of *C. variabile* exhibited the greatest activity in leaf extracts of the species tested. However, the *C. variabile* bulb and root extracts, while displaying significant activity, were not as active as those from some of the other species, with *C. macowanii* bulbs, and *C. macowanii* and *C. moorei* roots, exhibiting the greater activities.[75]

To the best of our knowledge, there have been no in-depth investigations regarding the alkaloidal constituents of *C. variabile*. Thus, this investigation provides new information on the species and adds value to the field.

8.2 Processing, results and discussion

Please note that there is a tree diagram present in Appendix A (Fig. A.1.1) which represents the processing of the plant material. It is recommended that this be referred to for context when reviewing the processes described below.

8.2.1 Preparation and extraction

The plant material was acquired as bulbs, purchased from a local nursery. This means of acquisition is preferable to removing natural specimens from their habitat, as it avoids depletion of wild populations. Two examples of live bulbs are thriving in the Botanical Gardens at the University of Stellenbosch (33°56'09.3"S 18°51'56.9"E) as reference material. A living specimen will be maintained in the Botanical Gardens, and in the case of its demise, this will be converted into a dried voucher specimen.

The bulbs were cut into slices, and air dried until constant mass was obtained (7 days at 25 °C). The dried bulb material was placed in a sealed bag and stored in a freezer (approximately -18 °C) until further processing. To prepare for extraction, the dried bulb material was frozen under liquid nitrogen in a large mortar and pestle and crushed to as fine a powder as possible. This method proved very useful, as the material was otherwise fibrous and difficult to crush without first making it brittle. Of course, the goal of this treatment was to increase the surface area of the material to maximise efficiency of extraction. All of the available dry bulb material (139 g) was prepared in this way.

The total mass of crushed, dry bulb was then covered with enough methanol to fully submerge it and allow for free movement during stirring, and the mixture was agitated with a mechanical stirrer for 2 hours. The plant material was then strained, and the methanol collected. The plant material was extracted in this way with four such portions of methanol, each extraction being left and stirred for 2 hours, except the fourth, which was left for 2 hours 40 minutes. All four portions of methanol extract were added together, and the solvent removed under reduced pressure. After drying for 3.5 hours under high vacuum, a total crude extract mass of 17.39 g was acquired. This crude extract was labelled **CVEXT001.**

8.2.2 Processing and isolations

To the dried **CVEXT001** was then added 300 mL of water, which had been acidified to pH3 using H_2SO_4. The reasoning behind this was that the alkaloids present in **CVEXT001** would be protonated, and transformed into their quaternary ammonium salt forms, which would have a higher affinity for aqueous solution. The acidified solution was found to have a pH of 6. This indicated that there were basic components in the extract which increased the pH of the acidified water, an indication

supporting the presence of alkaloids. The solution was then acidified further to a pH of about 4 using H_2SO_4 and was sonicated to evenly disperse the contents in solution.

The acidified aqueous **CVEXT001** was then extracted with hexane (3×100 mL). Because the alkaloids were in salt form, they would remain in the aqueous layer, and the hexane would remove compounds that were not of interest. The aqueous layer after extraction with hexane was labelled **CVAq1.**

CVAq1 was then exhaustively extracted with a more polar solvent, ethyl acetate (EtOAc) (7×100 mL), to further remove any unwanted compounds. The aqueous layer was then labelled **CVAq2**. The aqueous extract remained at a pH of 4 throughout the extractions with both organic solvents.

CVAq2 was then basified to pH 9 with aqueous sodium hydroxide (NaOH). This was done to deprotonate the alkaloids present, converting them to their free base forms, which have a higher affinity for organic solvents. Following this, a continuous liquid/liquid extraction apparatus (please see Appendix A for apparatus) was used to extract **CVAq2** with EtOAc for 24 hours, during which time, the alkaloids present in the aqueous layer should have moved into the organic layer. The EtOAc extract was labelled **CVAlk.EXT**, to infer that it was the extract containing alkaloids. The acquired mass after drying under high vacuum was 3.59 g.

*8.2.2.1 Isolation of lycorine **19***

Having obtained an extract containing the alkaloid content of the *Crinum variabile* plant material, a few solvent systems were tested using TLC in order to find one that effectively separated the components within the extract. The solvent system EtOAc:MeOH:H_2O (85:10:5) separated the constituents most effectively (Figure 8.2.2). An attempt was then made to dissolve **CVAlk.EXT** in MeOH with the intention of proceeding with chromatographic separation methods. It was noted that a light-coloured solid did not dissolve in the MeOH. This was filtered off, washed with MeOH, dried under high vacuum, and weighed. This solid, labelled **AlkEXT.S**, was an off-white powder-like substance, and had a mass of 0.934 g. It was decided that a crude NMR spectrum would be beneficial, so this was carried out using DMSO-d_6 as a solvent (the material was insufficiently soluble in MeOH, $CHCl_3$, and other organic solvents). The resulting spectrum corresponded to that of pure lycorine **19** (Figure 8.2.1). Table 8.1 and Table 8.2 illustrate the corresponding assignments based on literature values.

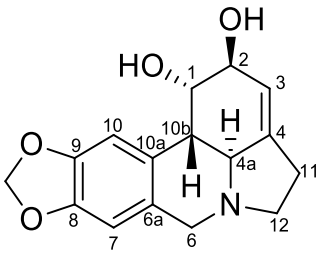

19

*Figure 8.2.1 – The numbered chemical structure of lycorine **19**.*

*Table 8.1 – ^{1}H NMR spectroscopy chemical shifts for lycorine **19**. Literature values cited from Likhitwitayawuid* et al. *(1993).*[76]

Proton	Lit.	Acquired
H-1	4.27 br s	4.25 br s
H-2	3.97 br s	3.95 br s
H-3	5.37 br s	5.34 br s
H-4a	2.60 d	2.58 d, J=10.3 Hz
H-6α	3.32 d	3.28 (overlap w/water signal)
H-6β	4.02 d	3.99 d, J=14.2 Hz
H-7	6.68 s	6.65 s
H-10	6.81 s	6.78 s
H-10b	2.50 m	Behind solvent peak (2.48)
H-11 (2H)	2.44 m	2.44 m (solvent peak overlap)
H-12α	2.19 ddd	2.18 ddd, J=8.6, 8.6, 8.6 Hz
H-12β	3.19 dd	3.17 m
O-CH_2-O	5.95 s	5.93 dd, J=5.6, 0.9 Hz
1-OH	4.79 br d	4.74 d, J=4.2 Hz
2-OH	4.90 br s	4.84 d, J=6.2 Hz
Solvent	DMSO-d_6	DMSO-d_6

*Table 8.2 - ^{13}C NMR spectroscopy chemical shifts of lycorine **19**. Literature values cited from Likhitwitayawuit* et al. *(1993).*[76]

Carbon	Lit.	Acquired	Δδ
1	70.21	70.20	-0.01
2	71.72	71.71	-0.01
3	118.48	118.46	-0.02
4	141.68	141.65	-0.03
4a	60.83	60.80	-0.03
6	56.73	56.71	-0.02
6a	129.75	129.74	-0.01
7	107.01	107.00	-0.01

8	145.20	145.18	-0.02
9	145.65	145.63	-0.02
10	105.06	105.04	-0.02
10a	129.57	129.57	0
10b	40.18	40.16	-0.02
11	28.13	28.11	-0.02
12	53.31	53.29	-0.02
OCH_2O	100.57	100.54	-0.03
Solvent	DMSO-d_6	DMSO-d_6	

The assignments shown were verified using two-dimensional NMR (2D NMR) spectroscopic experiments including COSY, HSQC and DEPT experiments (please see Appendix A for spectra), as well as by comparison to literature data. The ^{13}C NMR data presented in Table 8.2 show consistently minor chemical shift differences to those presented in the literature, though these differences are small enough to be inconsequential.

MS analysis showed a $[M+H]^+$ ion at 288.1241, correlating to the expected molecular formula of $C_{16}H_{17}NO_4$ (after removal of a proton to account for ESI +ve). The calculated mass for $[M+H]^+$ was 288.1236, with a difference between calculated and acquired masses of 1.7 ppm. Please see Table 8.17 for fragmentation information.

Optical rotation experiments resulted in an $[\alpha]_D^{20}$ of -61.5°, c=1, DMSO (lit. $[\alpha]_D^{22}$ of −63.2°, c=0.83, EtOH[77]; $[\alpha]_D^{20}$ of -62°, c=0.1, EtOH[76,78]). The acquired value is in good agreement with those reported in literature.

Thus, the isolation of 934 mg of lycorine **19** was carried out in a very straightforward manner. This mass of lycorine **19** correlates to 0.67% of the dry bulb mass (6.7 g/kg). Further on in this chapter, the isolation of additional lycorine **19** will be noted during the processing of **S1** (in the sample **PP1_2**), as well as in the sample **PP2_1**. Lycorine **19** was present in **PP1_2** with a mass of 42.4 mg. This mass of lycorine **19** was obtained from 100 mg of **S1**. Given that the total mass of **S1** was 297 mg, the total mass of lycorine present in **S1** was $42.4 \times \frac{297\ (\text{total mass of } \mathbf{S1})}{100} = 125.9$ mg. The lycorine **19** present in **PP2_1** had a mass of 53.2 mg. These masses can be added to the initially isolated mass of lycorine, resulting in a total mass of 1.113 g (0.80% of dry bulb mass – 8.0 g/kg)

An important point to note is that the isolated mass of lycorine **19** does not encompass the entirety of the lycorine **19** present in the original extract (**CVAlk.EXT**). Some lycorine **19** was also present in further fractions (such as in fractions of **C3.1**), based on TLC evidence. Unfortunately, time constraints did not allow for the exhaustive recovery of lycorine **19**, and thus, a total yield cannot be

reported. It can, however, be assumed that total recovery of lycorine **19** from *C. variabile* would likely result in a yield exceeding 0.80% of the dry bulbs mass. Though this is greater than the values reported for many species,[79,80] significantly greater yields have been reported for *Sternbergia lutea*, with one study reporting a yield of over 2% from dry bulb mass.[79,81]

*8.2.2.2 Isolation of 1,2-O,O-diacetyllycorine **21***

Having identified **AlkEXT.S**, the mother liquor from which it was acquired (**AlkEXT.F**) was subjected to further fractionation by chromatographic means. The first step in this regard was the implementation of a relatively short silica column (i.e. a silica plug), in order to crudely fractionate based on polarity. A consideration when deciding to use as little silica as possible for this initial separation was that compounds can bind irreversibly to silica.[72] Given that the entirety of the sample was being used, it was considered safer to avoid the large quantities of silica that would have been required for a column on this scale.

Before loading **AlkEXT.F** onto the silica plug (**P1)**, it had to be dissolved and loaded onto silica. MeOH was used for this, since the compounds present had previously dissolved in this solvent. The sample was then dry loaded and eluted from **P1**. Twenty-six fractions of 700 mL each were acquired (labelled **P1_1-26**), with eluents ranging from non-polar 100% hexane to highly polar EtOAc:MeOH:H_2O (70:20:10). For every solvent system applied to the plug, a single large fraction was collected. A final wash was carried out with EtOAc:MeOH:Et_3N (50:20:30), in the hopes that the basic Et_3N would bind to and deactivate the silica, helping to wash off any sample still on the plug.

In order to evaluate the results of **P1**, a large TLC plate was spotted with each of the 26 fractions on the baseline. It was then placed in a PLC chamber to develop, using EtOAc:MeOH:H_2O (85:10:5) (henceforth to be referred to as solvent system A) a photograph of this TLC plate is shown below (Figure 8.2.2):

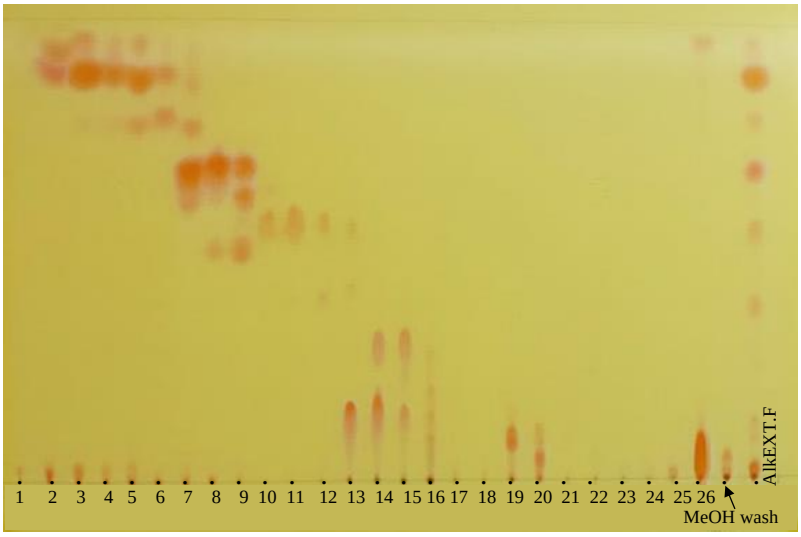

*Figure 8.2.2 - TLC plate representing the separation acquired from **P1**.*

The stain used to visualize the spots on this plate was Dragendorff's reagent, which is selective for alkaloids[82]. As can be seen in Fig. 6.3, **P1** provided a reasonable separation by polarity, and produced fractions which offered some level of grouping of the alkaloids present in **AlkEXT.F**. This allowed for the selection of fraction that could be grouped for further separation steps.

The first such group to be selected contained fractions 1-6 from **P1** (**P1_1-6**), which were recombined. This group contained a few relatively non-polar alkaloids, having eluted between 100% hexane and 1:1 hexane:EtOAc during **P1**. It was decided that a column would be the best way to obtain the major component of the group, and thus the sample (weighing 348 mg) was loaded onto a silica column (labelled **C1**), and a hexane/EtOAc gradient was applied for elution. The fractions (7 mL) of **C1** were monitored by TLC, and based on the results, were divided into ten fraction groups (**C1_1-10)**. The majority of the mass eluted was present in **C1_8**, which contained 221 mg of a white crystal after drying under high vacuum (grouped due to the presence of a single spot on TLC). This mass corresponds to 0.16% of the dry bulb mass. An aliquot of this sample was dissolved in chloroform-*d* and subjected to ^{1}H and ^{13}C NMR spectroscopic analysis, which resulted in spectra corresponding to those of pure 1,2-*O*,*O*-diacetyllycorine **21** (Figure 8.2.3). Table 8.3 and Table 8.4 illustrate the corresponding assignments based on literature values.

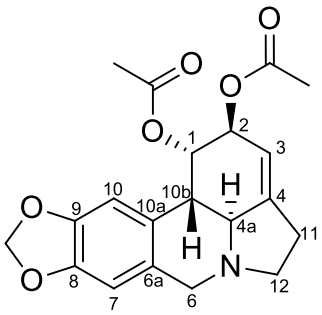

21

*Figure 8.2.3 – The numbered chemical structure of 1,2-*O,O*-diacetyllycorine **21**.*

*Table 8.3 - Proton chemical shifts of 1,2-*O,O*-diacetyllycorine **21**. Literature values cited from Lamoral-Theys* et al *(2009).*[83]

Proton	δ (ppm) Lit.	δ (ppm) Acquired
H-1	5.75 s	5.73 br s
H-2	5.27 s	5.24 br s
H-3	5.45 s	5.51 br s
H-4a	2.89 d	2.76 d, J=10.4 Hz
H-6α	3.55 d	3.52 d, J=14.3 Hz
H-6β	4.18 d	4.15 d, J=14.1 Hz
H-7	6.76 s	6.74 s
H-10	6.59 s	6.56 s
H-10b	2.79 d	2.87 d, J=10.4 Hz
H-11 (2H)	2.67 m	2.65 m
H-12α	2.42 m	2.39 ddd, J=8.8, 8.8, 8.8 Hz
H-12β	3.38 m	3.36 m
O-CH_2-O	5.94 s	5.93 s
1-*O*-Ac (**Me**)	1.97 s	1.94 s
2-*O*-Ac (**Me**)	2.09 s	2.07 s
Solvent	$CDCl_3$	$CDCl_3$

*Table 8.4 - Carbon chemical shifts of 1,2-*O,O*-diacetyllycorine **21**. Literature values cited from Lamoral-Theys* et al. *(2009).*[83]

Carbon	δ (ppm) Lit.	δ (ppm) Acquired	Δδ
1	69.3	69.40	0.1
2	71.0	71.05	0.05
3	113.9	113.95	0.05
4	146.5	146.57	0.07
4a	61.3	61.38	0.08
6	58.9	57.05	-1.85
6a	129.5	129.57	0.07
7	105.1	105.20	0.1
8	146.4	146.45	0.05

9	146.2	146.27	0.07
10	107.4	107.45	0.05
10a	126.6	126.71	0.11
10b	40.6	40.68	0.08
11	28.7	28.82	0.12
12	53.9	53.77	-0.13
OCH_2O	101.0	101.11	0.11
1-*O*-Ac (**Me**)	20.9	21.08	0.18
2-*O*-Ac (**Me**)	21.3	21.28	-0.02
1-*O*-Ac (**CO**)	172.3	170.12	-2.18
2-*O*-Ac (**CO**)	171.8	169.89	-1.91
Solvent	$CDCl_3$	$CDCl_3$	

These assignments were confirmed using 2D NMR spectroscopic experiments including COSY, HSQC, HMBC, and DEPT (please see Appendix A for spectra), in addition to comparison with literature data. Of the ^{13}C NMR peak shift differences (Δδ) presented in Table 8.4, some values are of note. C-6 and C-12, and both carbonyl signals, show lower values than those in the literature, while most other peaks are slightly higher when compared. Additionally, the shifts of C-6 and the carbonyl peaks differ by a greater margin than the majority of the other peaks. Reasons for these observations may include the possible presence of impurities in the NMR sample of **21** and differences in the water content of deuterated solvents used (water may interact with the carbonyl oxygens, affecting their corresponding carbons). Despite the observed differences, the evidence available is sufficient that the identity of **21** is assigned with relative confidence.

One additional difference with literature values can be noted in the ^1H NMR spectrum signals for protons H-4a and H-10b. The signal at 2.76 ppm was assigned as H-4a and that at 2.87 ppm was assigned as H-10b, while these assignments were reversed in the report by Lamoral-Theys *et al.* (2009)[83]. The reason the assignments were made this way was evident in the COSY spectrum, in which the signal at 2.87 ppm was coupled to that for H-1. This coupling would only be noted for H-10b, and not for H-4a, and so the signals reported here are more consistent with the structure of **21**.

MS analysis showed a $[M+H]^+$ ion at 372.1447, correlating to the expected molecular formula of $C_{20}H_{21}NO_6$ (after removal of a proton to account for ESI +ve). The calculated mass for $[M+H]^+$ was 372.1447, with no difference between calculated and acquired masses. Please see Table 8.17 for fragmentation information.

Optical rotation experiments resulted in an $[\alpha]_D^{20}$ of +23.6°, c=1, $CHCl_3$ (lit. $[\alpha]_D^{25}$ of +26.8°, c=1.22, $CHCl_3$[84]; $[\alpha]_D^{24}$ of +11.1°, c=0.84, MeOH[83]).

*8.2.2.3 Isolation of 2-O-acetyllycorine **22***

After the analysis of the **C1_8** fraction group, attention was drawn to the following fraction group of the same column (fraction group **C1_9**). The reason for this was the presence of a crystalline substance in **C1_9** which was visible in the sample vial. After ensuring that the sample responded to Dragendorff's reagent, and did not have the same R_f as 1,2-*O*,*O*-diacetyllycorine **21**, it was decided that a silica gel column should be utilised for this compound's purification. Based on the TLC performance of some test solvent systems, it was decided that this column (labelled **C1.1**) should be executed using a DCM/MeOH gradient. 20 mL fractions were collected, analysed by TLC, and combined, resulting in five groups of fractions (**C1.1_1–5**). The compound of interest was present in the third group (**C1.1_3**), with a mass of 45.2 mg. A portion of this sample was used for NMR spectroscopic analysis, which resulted in the spectra for 2-*O*-acetyllycorine **22** (Figure 8.2.4). Table 8.5 and Table 8.6 illustrate the corresponding assignments based on literature values.

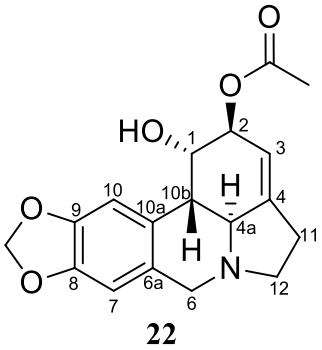

22

*Figure 8.2.4 - The numbered chemical structure of 2-O-acetyllycorine **22**.*

*Table 8.5 - Proton shifts of 2-O-acetyllycorine **22**. Literature values cited from Toriizuka* et al. *(2008).*[85]

Proton	δ (ppm) Lit.	δ (ppm) Acquired
H-1	4.52 s	4.37 br s
H-2	5.32 m	5.18 m
H-3	5.47 m	5.35 br s
H-4a	2.79 br d	2.67 d, J=10.4 Hz
H-6α	3.53 d	3.35 water peak overlap
H-6β	4.14 d	4.03 d, J=14.2 Hz
H-7	6.60 s	6.68 s
H-10	6.81 s	6.86 s
H-10b	2.71 br d	2.43 d, J=10.5 Hz
H-11 (2H)	2.65 m	2.51 m (solvent peak overlap)
H-12α	2.38 ddd	2.24 ddd, J=8.6, 8.6, 8.6 Hz
H-12β	3.37 ddd	3.21 dd, J=7.7, 7.7 Hz
O-CH_2-O	5.94, 5.92 two ds	5.94 dd, J=11.0, 0.8 Hz
2-*O*-Ac (**Me**)	2.09 s	2.02 s

Solvent	$CDCl_3$	DMSO-d_6

*Table 8.6 - Carbon shifts of 2-O-acetyllycorine **22**. Literature values cited from Toriizuka et al. (2008).*[85]

Carbon	**δ (ppm) Lit.**	**δ (ppm) Acquired**
1	69.4	67.57
2	73.7	73.80
3	113.6	113.81
4	146.0	145.85
4a	60.7	61.0
6	58.3	57.03
6a	127.0	128.88
7	107.7	107.50
8	146.4	146.14
9	146.6	146.65
10	104.6	105.79
10a	130.2	130.11
10b	41.8	41.69
11	29.4	28.69
12	57.0	53.60
O-CH_2-O	101.0	101.08
2-*O*-Ac (**Me**)	21.3	21.50
2-*O*-Ac (**CO**)	170.6	170.15
Solvent	$CDCl_3$	DMSO-d_6

The acquired assignments were verified using 2D NMR spectroscopic experiments including HSQC, HMBC, COSY and DEPT (please see Appendix A for spectra), as well as by comparison to spectra in the literature. It should be noted that the spectra were acquired using DMSO-d_6 as a solvent, which explains the difference in chemical shift noted for some of the protons when compared to literature values. Chemical shift differences for the ^{13}C NMR peaks are not presented for this compound, as a different solvent was used for NMR analysis of **22**. The reason for this was that solubility of **22** in $CHCl_3$ was somewhat problematic during this investigation.

MS analysis showed a $[M+H]^+$ ion of mass 330.1346, correlating to the expected molecular formula of $C_{18}H_{19}NO_5$ (after removal of a proton to account for ESI +ve). The calculated mass for $[M+H]^+$ was 330.1341, with a difference between calculated and acquired masses of 1.5 ppm. Please see Table 8.17 for fragmentation information.

Optical rotation experiments resulted in an $[\alpha]_D^{20}$ of +8.8°, c=0.77, MeOH (lit. $[\alpha]_D^{25}$ of +22.4, c=0.2, $CHCl_3$[83]).

*8.2.2.4 Isolation of 1-*O*-acetyllycorine **23***

Focus was then turned to the second fraction group of **P1**. This group consisted of fractions **P1_7-9** and contained a compound of moderate polarity as the major component, as can be seen in Figure 8.2.2 above. Given that the mass of **P1_7-9** was somewhat higher than would be adequate for a PLC plate, a silica gel column was chosen once again as the separation method for purification. After testing for optimal solvent elution systems, the 286.2 mg of sample was dry loaded, and the column (labelled **C2**) was eluted with an isocratic mobile phase of 100% EtOAc. The 20 mL fractions obtained were divided into four groups (**C2_1-4**), and it was noted that the third of these (**C2_3**) contained the major component, though it was still impure. Thus, a PLC plate was selected for further purification. Fraction **C2_3** was loaded in its entirety onto the plate (labelled **PP0**), which was placed in a chamber containing EtOAc to develop.

Allowing the solvent front to run up the plate a single time, however, proved insufficient for the effective separation of the sample's components. Thus, the process was repeated until satisfactory separation of bands on the plate was observed (a total of seven repetitions). The progress of this process was observed under UV light (254 nm). When complete, the plate contained three visible bands under UV, all of which were scraped off and collected. The compounds were removed from the silica by washing with organic solvents (namely DCM and EtOAc). These bands were labelled **PP0_1-3**, ordered by polarity such that **PP0_1** was the band with the highest R_f (this ordering convention was maintained for all separations).

It was found that the majority of the mass of the sample was present in the second band from this plate, **PP0_2**. This sample (178.5 mg) was dissolved in $CDCl_3$ and subjected to NMR spectroscopic analysis, providing spectra correlating to those of pure 1-*O*-acetyllycorine **23** (Figure 8.2.5). Table 8.7 and Table 8.8 illustrate the corresponding assignments based on literature values.

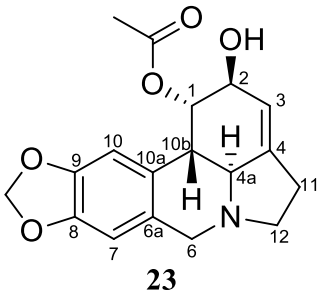

23

*Figure 8.2.5 - The numbered chemical structure of 1-*O*-acetyllycorine **23**.*

*Table 8.7 - Proton shifts of 1-O-acetyllycorine **23**. Literature values cited from Toriizuka et al. (2008).*[85]

Proton	δ (ppm) Lit.	δ (ppm) Acquired
H-1	5.64 br s	5.55 br s
H-2	4.24 m	4.13 (overlap w/H-6β)
H-3	5.56 s-like	5.52 m
H-4a	2.75 br d	2.73 d, J=10.5 Hz
H-6α	3.53 d	3.48 d, J=14.0 Hz
H-6β	4.15 d	4.13 (overlap w/H-2)
H-7	6.58 s	6.55 s
H-10	6.71 s	6.59 s
H-10b	2.87 br d	2.83 d, J=10.5 Hz
H-11 (2H)	2.65 m	2.59 m
H-12α	2.40 ddd	2.35 ddd, J=8.9, 8.9, 8.9 Hz
H-12β	3.37 m	3.33 ddd, J=4.7, 4.7, 9.2
O-CH_2-O	5.92 s-like	5.89 s
1-*O*-Ac (**Me**)	1.95 s	1.91 s
Solvent	$CDCl_3$	$CDCl_3$

*Table 8.8 - Carbon shifts of 1-O-acetyllycorine **23**. Literature values cited from Toriizuka et al. (2008).*[85]

Carbon	δ (ppm) Lit.	δ (ppm) Acquired	Δδ
1	72.6	72.66	0.06
2	69.6	69.35	-0.25
3	117.2	117.38	0.18
4	144.1	143.57	-0.53
4a	61.5	61.55	0.05
6	56.8	56.77	-0.03
6a	127.0	127.01	0.01
7	107.3	107.25	-0.05
8	146.2	146.18	-0.02
9	146.5	146.44	-0.06
10	104.9	104.84	-0.06
10a	129.3	129.19	-0.11
10b	39.3	39.12	-0.18
11	28.6	28.49	-0.11
12	53.6	53.65	0.05
OCH_2O	100.9	100.91	0.01
1-*O*-Ac (**Me**)	21.0	21.03	0.03
1-*O*-Ac (**CO**)	170.8	170.74	-0.06
Solvent	$CDCl_3$	$CDCl_3$	

Again, HSQC, HMBC, COSY and DEPT experiments were used to verify these assignments, in addition to comparison with literature data (please see Appendix A for spectra). The ^{13}C NMR peak shift differences presented in Table 8.8 show small differences when compared to literature values, with some being slightly higher and some slightly lower than those reported. The differences remain relatively minor despite the differing signs, and so are not of great concern, though the Δδ value for C-4 should be noted as a slight outlier. The possible presence of impurities in the NMR sample of **23** may explain the observed differences, or perhaps similar minor error in the literature value could be responsible. The differences observed are sufficiently small that the identity assigned is maintained with relative confidence.

MS analysis showed a $[M+H]^+$ peak at 330.1346, correlating to the expected molecular formula of $C_{18}H_{19}NO_5$ (after removal of a proton to account for ESI +ve). The calculated mass for $[M+H]^+$ was 330.1341, with a difference between calculated and acquired masses of 1.5 ppm. Please see Table 8.17 for fragmentation information.

Optical rotation experiments resulted in an $[\alpha]_D^{20}$ of -73.6°, c=1, $CHCl_3$ (lit. $[\alpha]_D^{25}$ of -64.8, c=0.9, $CHCl_3$[83]).

The $[\alpha]_D^{20}$ values acquired for 1-*O*-acetyllycorine **23** and 2-*O*-acetyllycorine **22** are evidence supporting the correct differentiation of the two compounds, as they rotate light in opposite directions, and the acquired values support their respective assignments.

Another telling virtue for the differentiation between 1-*O*-acetyllycorine **23** and 2-*O*-acetyllycorine **22** was evident in their H^1 NMR spectra. In 1-*O*-acetyllycorine **23**, H-1 of lycorine **19** (appearing as a broad single peak at δ 4.25) was strongly deshielded to a single peak at δ 5.55 while H-2 of lycorine **19** (originally a broad single peak at δ 3.95) underwent a shielding effect to a single peak at δ 4.13 due to the anisotropic shielding cone of the adjacent ester carbonyl. In the corresponding case of 2-*O*-acetyllycorine **22**, the broad single peak of H-2 of lycorine **19** at δ 3.95 was strongly deshielded to a single peak at δ 5.18, while H-1 of lycorine **19** – originally a broad single peak at δ 4.25 – was shielded in 2-*O*-acetyllycorine **22** to a single peak at δ 4.37, again by the shielding cone of the adjacent ester carbonyl functional group.

At this point, it had to be noted that the only compounds isolated had been lycorine **19** and acetylated versions thereof. This raised the concern that the extraction process (carried out at relatively high temperatures in EtOAc) could have been responsible for the formation of the acetylated analogues as artefacts.[86] Thus, an experiment was designed to test whether this was possibly the case. A small

amount of lycorine **19** was heated under reflux in EtOAc for 24 hours, to determine whether these conditions would be capable of acetylation of the -OH groups. After a period of 24 hours, TLC showed only one spot, with a R_f corresponding to that of lycorine **19**. This showed that reflux of lycorine in EtOAc under the same conditions as the extraction did not acetylate it, which is evidence that the acetates were produced in the plant itself, rather than having been generated as a result of the extraction process.

*8.2.2.5 Isolation of **CV3** – (6-epi)haemanthidine (**24**, **25**)*

Having confirmed the validity of the compounds isolated thus far, the process of purification of further compounds was continued. This recommenced with the third fraction group from **P1**, which was the combination of fractions 10, 11 and 12 (**P1_10-12**), and as can be seen in Figure 8.2.2, contained a Dragendorff-positive compound as the major component. Thus, these fractions were combined for further processing. Based on Figure 8.2.2, it may seem as though only one compound was present in these fractions. However, further TLC analysis showed the presence of two Dragendorff-positive compounds (amongst some other impurities visible under UV light), one of which had an R_f corresponding to that of lycorine **19**. The reason for the presence of the lycorine **19** spot not being immediately apparent in Figure 8.2.2 is that it does not respond strongly to Dragendorff's reagent, and takes some time to develop a darker colour in response to the stain.

During the process of recombining **P1_10-12**, a white solid did not dissolve when MeOH was added to the samples. The fractions were recombined regardless, and the solid that did not dissolve was filtered off and washed with cold MeOH. The mass of this white powder (labelled **S1**) was 297 mg. A 30 mg sample of this was dissolved in DMSO-d_6, and subjected to NMR spectroscopic analysis, resulting in spectra which clearly indicated a mixture of at least two compounds. Thus, further purification steps were necessary.

The white powder collected still showed two spots on TLC when stained with Dragendorff's reagent, one corresponding to lycorine **19**, and the other with a slightly higher R_f. The two spots were well resolved when solvent system A was used to develop the TLC. It was thus decided that a viable separation method would be the use of a PLC plate. Thus 100 mg of **S1** was dissolved in a minimum amount of MeOH (the addition of a small amount of H_2O and slightly heating the sample assisted in dissolving it) and streaked onto a PLC plate (labelled **PP1**), which was developed in solvent system A. A single development run was sufficient to resolve the bands, and they were scraped off and isolated by washing the silica with EtOAc:MeOH (8:2). The band above that corresponding to lycorine **19** (labelled **PP1_1**) had a mass of 44.8 mg after drying under high vacuum. **PP1_2** produced lycorine **19** (42.4 mg).

PP1_1, as the unknown substance, was naturally of higher interest and was thus the centre of focus. NMR spectroscopic analysis of this material still produced what appeared to be impure NMR spectra, despite only one spot being visible on TLC using Dragendorff's reagent. In order to address this challenge, the solvent system was optimised using test TLC experiments, and it was decided that a DCM/MeOH gradient would be ideal for purification. A column (**C3**) was wet loaded with **PP1_1** in DCM, and eluted using 5-10% MeOH in DCM. TLC was used to analyse each of the fractions eluting from **C3**, and only fractions which showed a single correlating spot under both UV light and Dragendorff's reagent were combined to generate the sample **CV3** (20.8 mg).

^{1}H and ^{13}C NMR spectroscopic analysis of **CV3** still provided spectra that indicated a mixture of compounds, suggesting the presence of two compounds with identical R_f values on silica. One note made while considering the ^{13}C NMR spectrum of the sample was that there appeared to be smaller "partner" peaks residing at nearby chemical shifts to those of many of the more intense peaks. This led to the suggestion that the sample may have been a mixture of two isomers, but further data was required before this assumption could be made. Separation of the components would, of course, be the most favourable outcome.

Several optimisation methods were attempted, including test TLCs using a number of solvent systems as well as TLCs with alumina (Al_2O_3) as a stationary phase, but all continued to show only a single spot, and thus failed to separate the coeluting compounds. An orthogonal separation method would be that of reversed phase (RP) chromatography, and HPLC analysis of the sample was selected as a possible means of separating the components present in **CV3**. This separation method can also be coupled to high-resolution mass spectrometry (HRMS), which could assist in providing some structural information on eluting compounds. Thus, **CV3** was subjected to HPLC-HRMS analysis using a RP C18 column.

The resulting total ion chromatograms (TICs) showed only one major peak, with some small minor peaks (one with a mass of 288, correlating to lycorine (**19**) $[M+H]^+$). Several optimisations of the HPLC method were attempted, but separation of the major peak into multiple components was not achieved. This showed that the compounds in **CV3** were of sufficiently similar chemical structure that even a high-performance separation technique was not capable of resolving them. The MS data provided by the HPLC-HRMS analysis of **CV3** provided some useful information, as data including fragmentation information (acquired using MS) was obtained.

The MS data showed a base peak ion (BPI) of *m/z* 318.1340. When using the MS analysis software Masslynx©, a tool is available which allows for the prediction of the elemental composition when provided with an accurate mass such as this. The program calculates the probability of each

composition using natural isotope abundances and reports a percentage which indicates the confidence with which each composition can be assigned. Elemental composition analysis of the peak of mass 318.1340 reports a molecular formula of $C_{17}H_{20}NO_5$ with a confidence of 99.76%, and a difference of 0.3 ppm between the calculated and acquired masses (calc. 318.1341, acq. 318.1340). Given that this data was acquired in positive ionisation mode, removal of a single proton gives the molecular formula of the major component of **CV3** as $C_{17}H_{19}NO_5$.

To gain further insight, the mass fragments acquired from this peak were also reviewed, a discussion of which will follow the presentation of NMR spectroscopic data.

With the information obtained from HPLC and HRMS analyses, the NMR spectra for **CV3** were revisited with a more informed perspective. Amaryllidaceae alkaloids with the molecular formula $C_{17}H_{19}NO_5$ were researched, and the ^1H NMR spectra reported for these were compared to that of **CV3**. Promising results were found when a mixture of haemanthidine **24** and 6-epihaemanthidine **25** (Figure 8.2.6) was proposed.

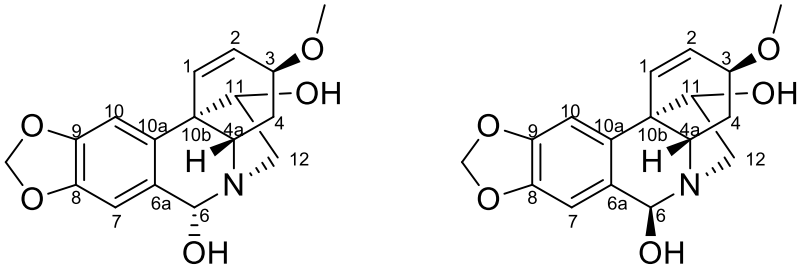

*Figure 8.2.6 - The chemical structures of haemanthidine **24** and 6-epihaemanthidine **25***

*Table 8.9 - The ^{1}H NMR spectroscopic peaks of CV3 and those reported for haemanthidine (**24**) and 6-epihaemainthidine (**25**). Literature values are cited from Bastida* et al. (2006),[87] *with an additional report from Nishimata and Mori (1998)*[88]*, which indicates peak integrals.*

	Bastida *et al.* [87]		**Nishimata & Mori**[88]		**CV3 peaks**	
Proton number	**Haemanthidine (24)**	**6-epihaemanthidine (25)**	**(−)-haemanthidine**	**"6-epihaemanthidine (25)"**	**Haemanthidine (24)**	**6-epihaemanthidine (25)**
1	6.33 d		6.37-6.40, 2H, m		6.16-6.31, 2H, m	
2	6.27 dd					
3	3.85 m		3.87-3.97, 2.55H, m		3.86-4.12, 2.5H, m	
4α	2.36 ddd	2.21 ddd	2.33, 0.45H, dt	2.18, 0.55H, dt	2.09-2.37, 2.5H, m	
4β	2.12 ddd	2.00 ddd	2.10, 0.45H, dd	2.03, 0.55H, dd		
4a	3.56 dd	3.20 m	3.59, 0.45H, dd		3.78, 0.5H, dd, J=12.2, 5.8 Hz	
6α	5.02 s		5.04, 0.55H, s		5.05, 0.5H, s	
6β	5.69 s		5.69, 0.45H, s		5.64, 0.5H, s	
7	6.94 s	6.79 s	6.98, 0.45H, s	6.83, 0.55H, s	7.00, 0.5H, s	6.84, 0.5H, s
10	6.70 s	6.73 s	6.77, 0.45H, s	6.80, 0.55H, s	6.76, 0.5H, s	6.78, 0.5H, s
11	3.92 m		3.87-3.97, 2.55H, m		3.86-4.12, 2.5H, m	
12 *endo*	4.20 dd	3.30 m	4.20, 0.45H, dd	3.34, 0.55H, m	4.24, 0.5H, dd, J=14.2, 6.7 Hz	3.26-3.52, 4.5H, m
12 *exo*	2.96 dd	3.20 m	2.94, 0.45H, dd	3.25, 0.55H, dd	3.04, 0.5H, br d, J=14.1 Hz	
OCH_2O	5.83 (2d)	5.86 (2d)	5.90-5.93, 2H, m		5.90-5.97, 2H, m	
OMe	3.32 s	3.28 s	3.38, 1.35H, s	3.35, 1.65H, s	3.26-3.52, 4.5H, m	
Solvent	$CDCl_3$		$CDCl_3$		$CDCl_3$	

Interestingly, Nishimata and Mori (1998)[88] report all their data in the above table as a single list of peaks, as the spectral data for (−)-haemanthidine. There are, of course, too many peaks to belong to just one isomer, and the spectral data shown correlates fairly well with a mixture of the two diastereomers, as can be seen upon comparison with the data from Bastida *et al*.,[87] which reports data based on a mixture of the diastereomers.[89] As is evident, the ^{1}H NMR spectrum of **CV3** shows evidence supporting the identification of the sample as a mixture of haemanthidine **24** and 6-epihaemanthidine **25**, though some differences in chemical shift values must be noted.

The presence of 6-epihaemanthidine **25** was substantiated by the presence of additional peaks which cannot be assigned to haemanthidine **24**. In particular, the four singlets at 6.76-7.00 ppm are strong evidence supporting a mixture, as a single epimer would only produce two singlets in this region corresponding to protons 7 and 10.

The spectra of **PP1_1** were reviewed at this point, and it was found that the sample was almost identical to **CV3**, with some very minor impurity peaks. Thus, it can be surmised that the mass of **CV3** present in 100 mg of **S1** was 44.8 mg, meaning that the total mass of **CV3** in **S1** (297 mg) was $44.8 \times \frac{297\ (\text{total mass of } \mathbf{S1})}{100} = 133.1$ mg.

As previously mentioned, the ^{13}C NMR spectrum of **CV3** was the first noted indicator that the sample may have been a mixture of isomers. With the additional information provided by the ^{1}H spectrum, as well as the HPLC-HRMS results, this notion is reinforced. The chemical shifts in the ^{13}C NMR spectrum of **CV3** also correlated with those reported in literature for (6-epi)haemanthidine.

*Table 8.10 - ^{13}C shifts acquired for both epimers of haemanthidine (**24** and **25**), reported with the shifts acquired for **CV3**. Literature values are cited from Bastida* et al.[87]

	^{13}C peaks of haemanthidine[87]		**^{13}C peaks of CV3**		**Δδ**	
Carbon number	**Haemanthidine 24**	**6-epihaemanthidine 25**				
1	126.7	126.3	123.12	122.93	-3.58	-3.37
2	132.3	132.8	134.6	135.85	2.3	3.05
3	72.5	72.5	75.95	75.64	3.45	3.14
4	27.8	27.6	29.69	29.41	1.89	1.81
4a	61.6	56.2	64.83	59.56	3.23	3.36
6	85.8	88.4	85.51	88.06	-0.29	-0.34
6a	129.2	127.8	128.78	127.34	-0.42	-0.46
7	108.2	109.5	108.31	109.54	0.11	0.04
8	146.5	146.4	146.73	146.56	0.23	0.16
9	147.4	147.7	147.6	147.83	0.2	0.13
10	102.7	102.9	102.68	102.81	-0.02	-0.09

10a	134.7	135.8	136.28	136.46	1.58	0.66
10b	50.7	50.3	50.45	50.84	-0.25	0.54
11	79.2	78.3	79.01	78.13	-0.19	-0.17
12	52	57.8	51.84	57.7	-0.16	-0.1
O-CH_2-O	101	101	101.12		0.12	
-OMe	56.8	56.5	55.95	56.01	-0.85	-0.49
Solvent	$CDCl_3$		$CDCl_3$			

The differences noted in the ^{13}C NMR chemical shifts are significant, especially for carbons C-1 to C-4a, as well as C-10a and the methoxy carbon. The differing signs of the Δδ values are also a cause for concern, as this indicates that the shift is not constant in nature (shielding/deshielding). These varying results may be due to differing ratios of the diastereomers, or perhaps due to the presence of some impurities in **CV3**. Despite the inconsistencies in the available data, (6-epi)haemanthidine (**24**, **25**) remains the most viable identification of **CV3** which can be suggested, to the best of our knowledge.

Having acquired data that indicated the identity of **CV3** as a mixture of haemanthidine epimers (**24** and **25**), the mass fragments acquired from the MS/MS analysis of the sample could be interpreted with some additional insight. Figure 8.2.7 below shows the obtained mass spectrum of the primary peak observed during HPLC-MS/MS analysis of **CV3**.

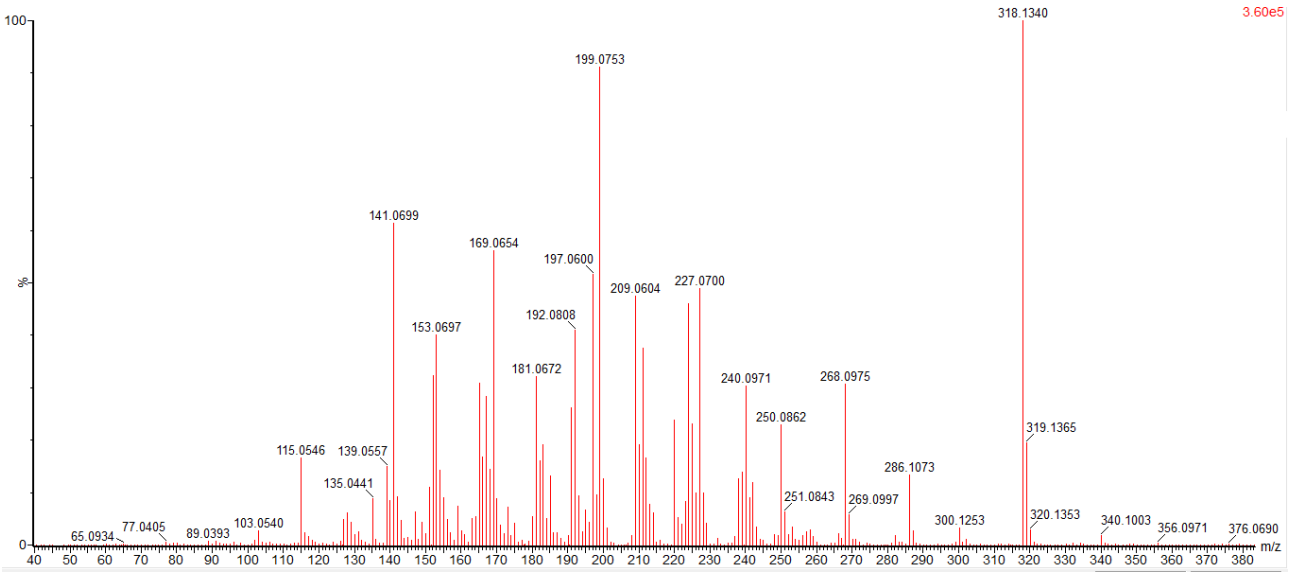

*Figure 8.2.7 – MS/MS spectrum of **CV3**, showing fragmentation information.*

In a book chapter by Bastida *et al*. (2006),[87] the fragmentation of haemanthamine-type alkaloids is discussed, and the information contained therein provided useful direction when attempting to explain some of the observed peaks. In fragmentation mechanisms shown by Bastida *et al.* (2006)[87] for haemanthamine, analogous peaks can be seen in the fragmentation pattern of **CV3** which are

applicable for corresponding mechanisms in haemanthidine **24**. For example, the peaks in the MS spectrum of haemanthamine indicate the loss of a CH_2=NMe fragment.[87] The analogous loss for haemanthidine **24** would be that of CH(OH)=NMe (due to the presence of the 6-hydroxy group in haemanthidine **24**). As can be seen in Table 8.11, some peaks present in the spectrum can be tentatively assigned to the loss of this fragment (amongst others).

*Table 8.11 - Tentative explanations for some observed fragment ions in the MS/MS spectrum of **CV3**.*

m/z	**Mass loss**	**Possible fragments lost**
318	0	None ($[M+H]^+$)
300	18	H_2O
286	32	MeOH, CHO, CH_2O
268	50	MeOH, H_2O
250	68	MeOH, H_2O, H_2O
227	91	CH(OH)=NMe, MeOH
224	94	CH(OH)=NMe,
220	98	MeOH, H_2O, H_2O, CH_2O
209	109	CH(OH)=NMe, MeOH, H_2O
199	119	MeOH, CHO, CH_2NH, CHO
169	149	MeOH, CHO, CH_2NH, CHO, CH_2O

Important to note is that no elucidation attempts regarding mechanisms for these suggested mass losses were made. Thus, the data presented in Table 8.11 is tentative and limited to only some of the peaks in the spectrum. Further investigations regarding this mass spectrum are necessary before conclusions can be drawn.

The mass fragments noted in Table 8.11 are in good agreement with those expected for haemanthidine **24**, and the fragments acquired for 6-epihaemanthidine **25** will likely be analogous to those of its epimer, which infers that this mass spectrum agrees with the notion that **CV3** is a mixture of the two epimers. Difficulty was faced in finding a literature source in which ESI+ve was utilised as an ionisation method when obtaining the fragmentation pattern of haemanthidine **24**. Thus, comparison of the acquired data with literature data could not occur. Given that this sample was a diasteriomeric mixture, optical rotation experiments were not carried out.

Further attempts to separate the two isomers were made, which included the acetylation of **CV3**, in the hopes that increasing the size of the moiety at the diastereomeric centre would generate sufficiently differing compound conformations to allow for separation. This attempt proved unsuccessful, unfortunately, with the resulting sample being a single spot on TLC which could not be resolved into multiple peaks on silica.

Unfortunately, the acetylation reaction was carried out before 2D NMR spectroscopic experiments had been done on **CV3**, and time constraints did not allow for the re-isolation of the compound in order to acquire these spectra. Despite this, the data acquired should be sufficient evidence for the identity of **CV3** as (6-epi)haemanthidine (**24**, **25**).

Only a portion of the available sample containing (6-epi)haemanthidine (**24**, **25**) was used in the isolation and characterisation of the sample. Thus, the yield of this component was not acquired. However, recovery of impure **CV3** from the remaining **P1_10-12** (the mother-liquor of **S1**) was achieved by gravity column (**C3.1**), resulting in a fraction group containing **CV3** as the major component. This impure **CV3** sample had a mass of 658 mg. Because the sample was impure, it cannot be assumed that this was the mass of **CV3** present in the filtrate of **P1_10-12**. However, given that **CV3** was the major component of the sample (based on TLC analysis, and selective recombination of fractions containing **CV3**), it can be assumed that the mass of **CV3** in the sample was relatively high. With the addition of the 133.1 mg of **CV3** present in **S1**, it seems that *C. variabile* produces (6-epi)haemanthidine (**24**, **25**) in relatively high concentrations. Unfortunately, despite the high concentration, time constraints did not allow for the exhaustive recovery of the alkaloid.

*8.2.2.6 Isolation of bulbispermine **26***

Following the characterisation of the major components in the first 12 fractions from **P1** (**P1_1-12**), the rest of the fractions (**P1_13-26**) were considered. Based on TLC analysis of these fractions, it was decided that there was little opportunity for the selection of further fraction groups, so all these fractions were combined, and a silica column (**C4**) was used for the fractionation of the resulting sample. Given the relatively high polarity of the components in the sample, a DCM/MeOH gradient was selected as an elution strategy. This column resulted in approximately 650 fractions, which were grouped by TLC profile into 23 fraction groups (**C4_1-23**).

Of these, **C4_12-16** displayed TLC profiles containing components of interest, and were combined, as the spots present suggested that these components were present across the fraction groups. The resulting sample was dried under high vacuum and its mass was recorded at 211.2 mg. It was decided that a PLC plate (**PP2**) would be preferable as a means of separation for this sample, as this technique had provided more reliable separation of polar compounds than silica columns during previous experiments. It must be noted that a sample of this mass required a PLC plate with a thicker stationary phase than those previously used, to avoid overloading the plate. Thus, the entirety of the sample was dissolved in a minimum amount of MeOH and streaked onto the baseline of a PLC plate with a 2 mm thick coating.

The plate was developed three times in solvent system A, resulting in 4 fairly resolved bands of interest (**PP2_1-4**) when viewed under UV light. These bands were all removed and washed off the silica. They were then analysed by TLC, to gain further insight regarding their compositions. **PP2_1** (53.2 mg) showed a spot corelating to that of lycorine **19**, and so was placed aside in the interest of finding a compound that had not previously been isolated from the plant. **PP2_2** (66.7 mg) showed promising results in this regard, displaying a spot with a R_f lower slightly lower than that of lycorine's, with relatively few, and visually less intense, additional spots (suggesting a relatively pure sample). The sample was subjected to ^{1}H NMR spectroscopic analysis, which showed the presence of impurities, and so further purification steps were taken before full characterisation.

PP2_2 was loaded onto an additional PLC plate (**PP3**) for this purpose. The plate was developed in solvent system A, and the band of interest (**PP3_3**) was removed and washed to recover the compound (this band was by far the most intense when viewed under UV light, with the other bands showing a very low response. Of course, the rest of the compound in the separation was not discarded, but also recovered and kept as a separate sample, though no components of interest were identified in these). The resulting major component (45.5 mg) was subjected to NMR spectroscopic analysis and found to be bulbispermine **26** (Figure 8.2.8), as shown in Table 8.12 and Table 8.13.

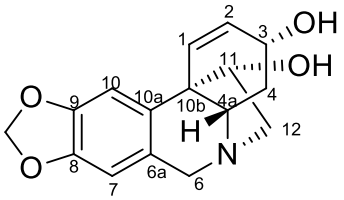

26

*Figure 8.2.8 - Numbered chemical structure of bulbispermine **26**.*

*Table 8.12 - The proton chemical shifts for bulbispermine **26**. Literature values are cited from Luchetti* et al. *(2012).*[90]

Proton	δ (ppm) Lit.	δ (ppm) Acquired
H-1	6.04 d	6.03 br d, J=10.3 Hz
H-2	6.23 dd	6.22 dd, J=10.3, 2.3 Hz
H-3	4.36-4.29 m	4.31 m
H-4α	2.15-2.03 m	2.10 m
H-4β	1.98-1.91 m	1.96 m
H-4a	3.44 dd	3.23 m
H-6α	3.73 d	3.74 d, J=16.7 Hz
H-6β	4.27 d	4.28 d, J=16.7 Hz
H-7	6.52 s	6.51 s
H-10	6.85 s	6.85 s
H-11	3.95 dd	3.95 dd, J=6.7, 3.3 Hz

H-12 *endo*	3.25-3.17 m	3.45 dd, J=13.8, 7.0
H-12 *exo*	3.25-3.17 m	3.23 m
O-CH_2-O	5.87 s	5.87 dd, J=3.1, 1.1 Hz
Solvent	CD_3OD	CD_3OD

*Table 8.13 - The carbon chemical shifts for bulbispermine **26**. Literature values are cited from Luchetti* et al. *(2012).*[90]

Carbon	**δ (ppm) Lit.**	**δ (ppm) Acquired**	**Δδ**
1	136.7	137.18	0.48
2	124.2	124.69	0.49
3	68.0	68.26	0.26
4	33.8	34.24	0.44
4a	67.7	67.45	-0.25
6	60.9	61.31	0.41
6a	125.2	126.40	1.2
7	104.4	107.80	3.4
8	148.0	147.69	-0.31
9	148.5	148.16	-0.34
10	107.9	104.23	-3.67
10a	137.4	137.23	-0.17
10b	51.6	51.42	-0.18
11	80.4	80.86	0.46
12	63.3	63.58	0.28
OCH_2O	102.4	102.23	-0.17
Solvent	CD_3OD	CD_3OD	

These assignments were verified with 2D NMR spectroscopic experiments, including HSQC, HMBC and COSY (please see Appendix A for spectra), as well as by comparison with literature data. The greatest differences from literature values (Δδ) noted for the ^{13}C NMR peak shifts were those of C-7 and C-10, though this is due to differing assignments, which will be explained below. Other inconsistencies which may be noted are the differing signs of the Δδ values, and the greater difference for C-6a. Though these are certainly significant factors, the only explanation which can be offered is the possibility of the presence of impurities in the NMR sample of **26**. Similar such errors in the literature values may also contribute to these inconsistencies. Despite the differences noted, the identification of **26** as bulbispermine is maintained with reasonable confidence, given the body of evidence in favour of this identity.

It may be noted that in comparing the ^{1}H spectra, assignments for H-4a and H-12 *endo* are switched for the acquired spectrum versus the literature spectrum. Evidence supporting this change in

assignments can be found in the HSQC spectrum, in which the peaks at 3.45 and 3.23 ppm both couple to the same carbon atom (that assigned as C-12), while the peak at 3.23 ppm also couples to the carbon assigned as C-4a. Another two assignments which have been interchanged from those reported in the literature are those for C-7 and C-10 in the ^{13}C NMR spectrum. The reason this was done was that the HSQC showed coupling between H-10 and the peak at 104.23 ppm in the ^{13}C NMR spectrum, as well as coupling between H-7 and the peak at 107.8 ppm in the ^{13}C spectrum. The reason H-10 and H-7 were not switched as assignments instead of their corresponding carbons was that the COSY spectrum showed stronger coupling between H-7 and H-6(α and β) than between H-10 and H-6(α and β), which is consistent with the proposed structure.

11-hydroxyvittatine **31a** (Figure 9.2.5) is a stereoisomer of bulbispermine **26**, with inverted stereochemistry of the 3-hydroxy group. The possibility that **26** was 11-hydroxyvittatine was ruled out by comparison with the literature data, in which the acquired ^{1}H NMR spectra were in better agreement with bulbispermine **26** than 11-hydroxyvittatine **31a**.[87,90] Optical rotation experiments for **26** resulted in an $[\alpha]_D^{20}$ of +87.5° (c=1, MeOH), which also compared more favourably to bulbispermine (lit. $[\alpha]_D^{20}$ of +107°, c=1.02, MeOH[91]) than to 11-hydroxyvittatine **31a** (lit. $[\alpha]_D^{25}$ of +11.3°, c=0.88, MeOH[92]). The presence of some minor impurities, as well as possible human error in terms of correct concentration values, may account for the difference between acquired values and those from literature.

Hamayne **31b** (Figure 9.2.5) is another such stereoisomer with inverted stereochemistry of the 11-hydroxy group. Unfortunately, this alkaloid does not have well-defined spectral data available in the literature, though the acquired $[\alpha]_D^{20}$ value still compares more favourably with bulbispermine **26** than with hamayne **31b** (lit. $[\alpha]_D^{12}$ of +43°, c=0.1, EtOH[93]).

MS analysis showed a peak for $[M+H]^+$ at 288.1238, correlating to the expected molecular formula of $C_{16}H_{17}NO_4$ (after removal of a proton to account for ESI +ve). The calculated mass for $[M+H]^+$ is 288.1236, with a mass difference between calculated and acquired masses of 0.7 ppm. Please see Table 8.17 for fragmentation information.

*8.2.2.7 Isolation of criwelline **27***

Having characterised the major component of **PP2_2**, attention was turned to the other bands from **PP2**. As has been established, four bands were removed from the plate, the first of which correlated with lycorine **19** when analysed with TLC, and the second of which was characterised as bulbispermine **26**. Thus, the third and fourth bands (**PP2_3-4**) were then focused on, and it was decided based on TLC analysis that they should be recombined and subjected to further separation (this was because they still shared components with R_f values below that of bulbispermine **26**, which

were of interest as they had not yet been isolated). Thus, the samples were recombined and subjected to further separation by PLC (this plate being labelled **PP4**).

PP4 was developed three times in $CHCl_3$:EtOAc:MeOH (2:2:1), resulting in three bands (**PP4_1-3**). When attempting to analyse these bands by TLC, difficulties were faced in lieu of the high polarity of the compounds. Defined profiles for the samples were difficult to achieve, as the components exhibited streaking on silica, making resolved spots impossible to achieve with conventional silica TLC plates. A few optimisation attempts were made in the hopes of solving this problem, including the use of alumina plates, as well as silica plates which had been pre-treated with triethylamine (NEt_3). The reason plates treated with NEt_3 were more likely to work is that the base could interact with the acidic sites on the silica, reducing the strong interactions with the alkaloid bases which were likely the cause of the streaking.

The most promising results were obtained when **PP4_1-3** were spotted on an alumina TLC plate and developed using 100% EtOAc. The result of this experiment was that a single spot moved up the plate, resolving itself from all the other components, which remained at the baseline. The component was present almost exclusively in **PP4_2**, with very light spots present in the other two bands. It was thus decided that **PP4_2** would be subjected to further separation using a small column (the mass of the sample was only 19.1 mg, so large stationary phase quantities were avoided) with alumina as a stationary phase. The sample was dry loaded in its entirety onto alumina, and the column (**C5**) was eluted with 100% EtOAc. Fractions were monitored using alumina TLC analysis, and the fractions containing the spot of interest (which was the first to elute) were combined until signs of additional spots were observed.

The sample showing only the spot of interest (**C5_1**) was dried under high vacuum, weighed (6.4 mg), and subjected to NMR spectroscopic analysis. The resulting spectra were those of criwelline **27** (Figure 8.2.9), as summarized in Table 8.14 and Table 8.15.

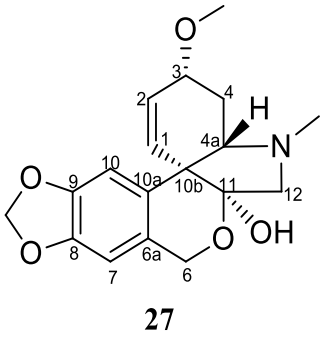

27

*Figure 8.2.9 - The numbered chemical structure of criwelline **27**.*

*Table 8.14 - The proton chemical shifts for criwelline **27**. Literature values are cited from Bastida et al. (2006).*[87]

Proton	δ (ppm) Lit.	δ (ppm) Acquired
H-1	5.78 d	5.79 d, J=10.1 Hz
H-2	6.20 dd	6.20 dd, J=10.2, 3.6 Hz
H-3	3.89 ddd	3.89 m
H-4α	1.93 ddd	1.94 ddd, J=15.0, 6.0, 3.6 Hz
H-4β	2.09 ddd	2.09 ddd, J=14.9, 4.4, 3.5 Hz
H-4a	2.95 t	2.97 t, J=4.2 Hz
H-6	4.68 d	4.67 d, J=14.7 Hz
H-6′	4.94 d	4.93 d, J=14.7 Hz
H-7	6.55 s	6.53 s
H-10	6.52 s	6.50 s
H-12	2.83 d	2.86 d, J=10.4 Hz
H-12′	3.30 d	3.33 d, J=10.4 Hz
O-CH_2-O	5.92 s	5.90 dd, J=4.2, 1.3 Hz
OMe	3.45 s	3.44 s
NMe	2.38 s	2.41 s
Solvent	$CDCl_3$	$CDCl_3$

*Table 8.15 - The carbon chemical shifts for criwelline **27**. Literature values are cited from Bastida* et al. *(2006).*[87]

Carbon	δ (ppm) Lit.	δ (ppm) Acquired	Δδ
1	130.1	130.29	0.19
2	128.9	129.08	0.18
3	72.1	72.20	0.1
4	25.4	25.62	0.22
4a	68.2	68.60	0.4
6	62.6	62.75	0.15
6a	126.2	126.43	0.23
7	108.5	108.68	0.18
8	146.6	146.82	0.22
9	146.2	146.49	0.29
10	104.2	104.37	0.17
10a	130.9	131.66	0.76
10b	50.0	50.25	0.25
11	102.6	102.71	0.11
12	64.5	64.61	0.11
OCH_2O	100.9	101.10	0.2
OMe	56.7	56.90	0.2
NMe	40.6	40.96	0.36

Solvent	$CDCl_3$	$CDCl_3$	

These assignments were verified using 2D NMR spectroscopic experiments including HMBC, HSQC and COSY (please see Appendix A for spectra), as well as by comparison with literature data. Regarding the Δδ values presented in Table 8.15 above, the acquired ^{13}C NMR peak shifts are in relatively good agreement with those reported in the literature. The values all share the same sign, indicating a constant shift in one direction (deshielded). One possible outlying value is that for C-10a, though this may be explained by the presence of some impurities in the NMR sample of **27**, for which there is evidence in the ^{1}H NMR spectrum.

MS analysis showed a $[M+H]^+$ peak at 332.1499, correlating to the expected molecular formula of $C_{18}H_{21}NO_5$ (after removal of a proton to account for ESI +ve), which adds credence to the identification as criwelline **27**. The calculated mass for $[M+H]^+$ of this formula is 332. 1498, with a difference between calculated and acquired masses of only 0.3 ppm. Please see Table 8.17 for fragmentation information. Optical rotation experiments provided an $[\alpha]_D^{20}$ of +163.1, c=0.325, $CHCl_3$ (lit. $[\alpha]_D^{20}$ of +278°, c=0.213, $CHCl_3$[94]).

It was verified that compound **27** was criwelline and not tazettine **36** (Figure 9.2.10) (a stereoisomer with inverted stereochemistry of the 3-methoxy group) by comparison of ^{1}H NMR spectra. The ^{1}H NMR spectrum of tazettine did not correlate with the acquired spectrum[87,95], while that of criwelline **27** did.[87]

*8.2.3 HPLC-ESI-MS/MS analysis of **CVAlk.EXT***

Time constraints meant that the remaining fractions could not be investigated further, though there were undoubtedly alkaloidal constituents remaining in some of the fractions (such as the more polar fractions from **C4**, and the rest of the components from **PP4**). In an attempt to gain some information to assist in the tentative identification of the remaining alkaloidal constituents, a small amount of the original alkaloidal extract was analysed using HPLC-MS/MS. This resulted in a TIC (Figure 8.2.10) which could provide accurate masses and fragmentation patterns for each peak.

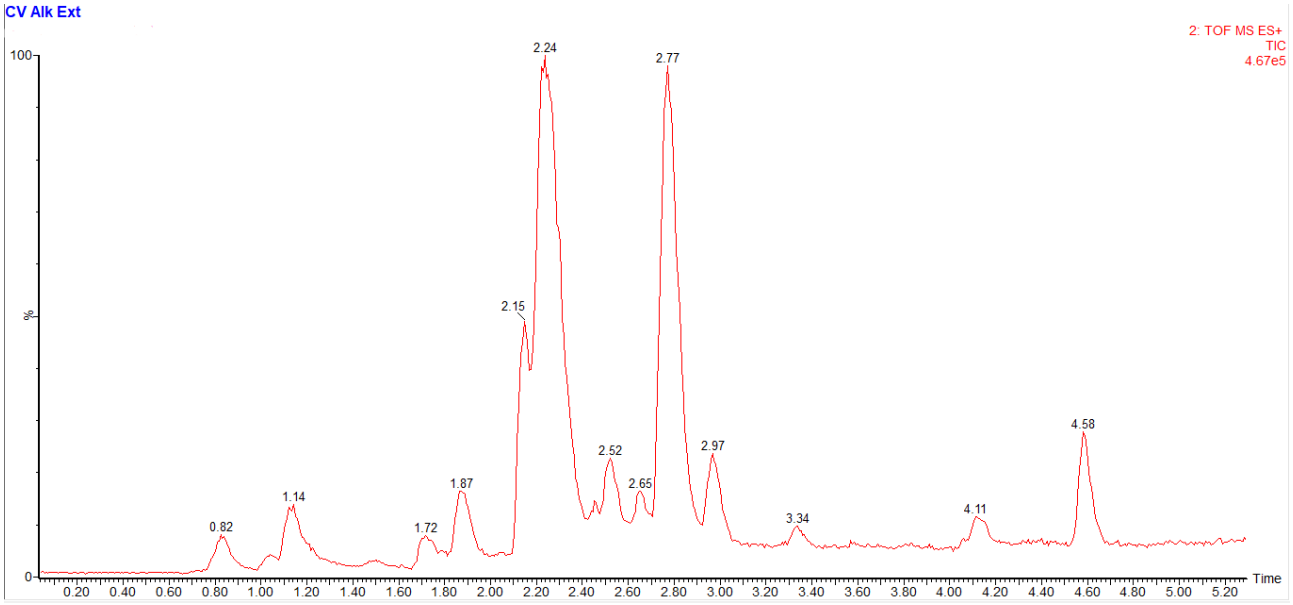

*Figure 8.2.10 - TIC of HPLC-ESI-HRMS analysis of **CVAlk.EXT**.*

*Table 8.16 - Table showing the HRMS and fragmentation (MS/MS) data for the peaks in the TIC of **CVAlk.EXT**.*

Retention Time/min	**Molecular Formula (Mass difference/ppm)***	**$[M+H]^+$ (*m/z*) (calc.)****	**Fragments (*m/z*)**	**Possible Identity**
0.82	$C_{16}H_{17}NO_4$ (1.4)	288.1232 (288.1236)	270, 252, 222, 177, 147, 119, 91	Lycorine **19**[96]
1.03	$C_{16}H_{17}NO_4$ (1.7)	288.1231 (288.1236)	266, 226, 199, 184, 147, **123**, 119	Unidentified
1.14	$C_{16}H_{17}NO_4$ (1.4)	288.1232 (288.1236)	270, 252, 222, 177, 147, 119, 91	Lycorine **19**[96]
1.50	$C_{16}H_{17}NO_5$ (1.3)	304.1181 (304.1185)	286, 268, 250, **226**	11-hydroxyvittatine-*N*-oxide **29**[97]
1.72	$C_{18}H_{21}NO_5$ (3.6)	332.1486 (332.1498)	**211**, 183, 140	Unidentified
1.87	$C_{16}H_{17}NO_4$ (1.7)	288.1232 (288.1236)	270, 244, 226, 224, 211, 196, 181, 153, 141, 115	Bulbispermine **26**
2.15	$C_{18}H_{19}NO_5$ (0.0)	330.1341 (330.1341)	270, 252, 222, 194, 177, 147, 134, 119	**1-*O*-acetyllycorine 23**, 2-*O*-acetyllycorine **22**
2.24	$C_{17}H_{19}NO_5$ (1.6)	318.1346 (318.1341)	300, 286, 268, 250, 240, 227, 224, 211, 209, 199, 192, 181, 169, 165, 153, 141, 115	Haemanthidine **24** (and 6-epihaemanthidine **25**)
	$C_{18}H_{21}NO_5$ (0.0)	332.1498 (332.1498)	Fragments are obstructed by haemanthidine peaks	Criwelline **27**
2.47	$C_{18}H_{19}NO_6$ (0.6)	346.1288 (346.1291)	328, 316, 268, 250, 226, 150	Candimine[98], **tazettamide**[99]

2.52	$C_{18}H_{19}NO_5$ (0.9)	330.1344 (330.1341)	270, 266, 252, 227, 226, 211, 196, 181, 168, 153	3-*O*-acetylhamayne[100], 3-*O*-acetyl-bulbispermine
2.65	$C_{18}H_{19}NO_4$ (1.0)	314.1395 (314.1392)	298, 254, 209, 141	**3-*O*-acetylvittatine**, 3-*O*-acetylcrinine. 1-*O*-acetylcaranine
2.77	$C_{20}H_{21}NO_6$ (0.8)	372.1450 (372.1447)	270, 252, 222, 194	1,2-*O*,*O*-diacetyllycorine **21**
2.97	$C_{18}H_{21}NO_5$ (1.2)	332.1494 (332.1498)	300, 268, 250, 227, **199**, 197, 169, 141, 115	Unidentified
3.34	$C_{22}H_{17}NO_3$ (1.2)	344.1291 (344.1287)	**224**, 166, 121, 103	Unidentified – structural similarities are noted
4.11	$C_{22}H_{17}NO_2$ (0.9)	328.1335 (328.1338)	367 (K adduct), 224, 166, **144**, 105	
4.58	$C_{15}H_{13}NO_2$ (2.9)	240.1032 (240.1025)	224, 210, 182,**167**, 166, 139	

The difference in calculated mass and that obtained for the molecular ion. **The calculated mass for $[M+H]^+$. Numbers in **bold represent base peak ions in cases where this is not the molecular ion.*

Table 6.16 (below) can be used as a means of comparison when identifying the peaks presented above.

The peak at 1.03 min could not be conclusively identified, though Amaryllidaceae alkaloids matching its molecular formula were researched. Pluviine was ruled out as a possibility, given that its ESI+ve fragmentation pattern did not match that of the peak.[101] Other possible compounds include nangustine, obesine and pancracine, though their ESI+ve fragmentation patterns were unavailable for comparison.

The peak at 1.50 min corresponds well with the ESI-MS/MS information of 11-hydroxyvittatine-*N*-oxide **29** (Figure 9.2.3)[97], showing good correlation with the fragments reported in the literature. An interesting possibility to consider would be that this compound may be an *N*-oxide of bulbispermine **26**, rather than one of 11-hydroxyvittatine **31a** (Figure 9.2.5), given the presence of **26** in the extract. However, no literature reports on bulbispermine-*N*-oxide are available, and so there is no evidence available to support this notion.

The peak at 1.72 min with a molecular formula of $C_{18}H_{21}NO_5$ could not be identified. This molecular formula is shared by many Amaryllidaceae alkaloids, though of those with reported ESI+ve MS fragmentation patterns, none were consistent with the fragments observed for this peak.

The peak at 2.15 min on the TIC is most likely that of 1-*O*-acetyllycorine **23**. The reasoning for this is as follows: the MS spectra of 1-*O*-acetyllycorine **23** and 2-*O*-acetyllycorine **22** differ in that 2-*O*-acetyllycorine **22** does not produce mass fragments at 177 and 134 *m/z*, and the fragment at 147 *m/z* produces a more intense peak than that from 1-*O*-acetyllycorine **23** (please see Table 8.17). The mass spectrum of the eluent at 2.15 min (taken from the early-eluting edge of the peak) matches that of 1-

O-acetyllycorine **23** well, showing peaks at 177 and 134 *m/z*, and a less intense 147 *m/z* peak than that from 2-*O*-acetyllycorine **22**.

Interestingly, it seems as though 2-*O*-acetyllycorine **22** co-eluted with 1-*O*-acetyllycorine **23**, though **22** eluted very slightly later, generating a peak for both compounds, which contained more of **22** at a later retention time and more of **23** at an earlier retention time. The reason this is suggested is that during the data analysis of this peak, the fragmentation spectrum of the later edge of the peak was subtracted from that of the earlier edge (a function which is possible using Masslynx® software). The result was a mass spectrum containing only a single fragment of *m/z* 134, which is a fragment present in 1-*O*-acetyllycorine **23**, but not in 2-*O*-acetyllycorine **22**. This information supports the postulation that **22** is present in the later edge and not the early edge. Additionally, a peak corresponding to 2-*O*-acetyllycorine **22** was not present anywhere else on the TIC.

Eluting under the peak for (6-epi)haemanthidine (**24**, **25**) at 2.24 min, was a peak with an $[M+H]^+$ mass of 332. This was identified as criweline **27**, as there were no other peaks matching the molecular formula and fragmentation pattern of **27** in the TIC (the peaks at 1.72 and 2.97 min did not have analogous fragmentation patterns). Unfortunately, the fragments could not be identified, as those of (6-epi)haemanthidine **24**, **25** were far more intense, and thus overshadowed those of the smaller peak of *m/z* 332.

The peak eluting at 2.47 min with a molecular formula of $C_{18}H_{19}NO_6$ corresponded to few Amaryllidaceae alkaloids reported in the literature. Only candimine[98] and tazettamide[99] were consistent with this molecular formula, based on literature searches. The fragment at *m/z* 316 represented the loss of CH_2O from the $[M+H]^+$ ion. This suggests the presence of a methylenedioxy-group, though this is consistent with both structures. The major peak in the fragmentation spectrum was that at *m/z* 226, This fragment is consistent with the loss of 120 mass units, corresponding to the loss of three fragments, those being MeOH (from a methoxy substituent), CH_2O (from a methylenedioxy substituent), and CH_3NCOH. The third of these is present as a substituent on tazettamide,[99] making it the more likely candidate.

The peak at 2.52 min had a molecular formula of $C_{18}H_{19}NO_5$ and showed many peaks in common with bulbispermine **26**, which indicated a similar structure to **26**, though with one acetylated hydroxy group. The peak shared several mass fragments with those reported for 3-*O*-acetylhamayne (yeminine A),[100,102] which is an acetylated analogue of hamayne **31b**, a stereoisomer of bulbispermine **26**. However, several mass fragments of the unknown compound were not present in the reported mass spectrum of 3-*O*-acetylhamayne.[100] The fragmentation pattern of the unknown compound was in better agreement with that of a reported isomer of 3-*O*-acetylhamayne, though still showed some

peaks (*m/z* 196, 168) which were not reported for the aforementioned isomer.[100] Given the presence of bulbispermine **26** in the extract, it was suspected that the unknown compound was the 3-*O*-acetyl-analogue thereof (theoretically 3-*O*-acetyl-bulbispermine).

The peak eluting at 2.65 min with a molecular formula of $C_{18}H_{19}NO_4$ corresponded to three compounds in the literature, namely 3-*O*-acetylvittatine, 3-*O*-acetylcrinine and 1-*O*-acetylcaranine. 3-*O*-acetylvittatine and 3-*O*-acetylcrinine were more likely, sharing structural skeletons with bulbispermine **26**. Fragmentation patterns for these compounds using electrospray ionisation were unavailable, and so this unknown compound could not be confidently identified. However, some fragments were shared with the EI-MS/MS fragments of 3-*O*-acetylvittatine[103], adding further credence to the possibility that this was the identity of the unknown compound. An interesting consideration would be the possibility that this unknown is the theoretical 3-*O*-acetyl-epivittatine (simply inverted stereochemistry of the 3-acetyl group of 3-*O*-acetylvittatine). The stereochemistry of 3-*O*-acetyl-epivittatine would correspond more favourably with that of bulbispermine **26**, which has been shown to be present. However, 3-*O*-acetyl-epivittatine has not been previously reported in the literature, and so there is no evidence available to support this notion.

The peak eluting at 2.97 min with a molecular formula of $C_{18}H_{21}NO_5$ could not be matched with any compounds for which the ESI-MS fragmentation information has been reported. However, the presence of fragments at *m/z* 300 and 268 suggest the losses of MeOH and 2×MeOH respectively, which may indicate the presence of two methoxy groups. The peak at 250 may represent the loss of water thereafter, which could be an indication of a hydroxy group as well.

The peaks eluting at 3.34, 4.11 and 4.58 had unusual molecular formulae and fragmentation patterns, and could not be matched to any known Amaryllidaceae alkaloids. The compounds in these peaks appeared to be structurally similar, all producing abundant fragments at *m/z* 224 and 166, which are rarely observed for ESI-MS/MS analyses of Amaryllidaceae alkaloids.[96,97,100,101,104,105] These results may indicate the presence of novel alkaloids, which could be of interest for future investigations.

The presence of two peaks corresponding perfectly in both molecular formula and fragmentation pattern with lycorine was noted. A possible reason for this observation is the conversion of an acetylated lycorine analogue into lycorine during the separation. The HPLC analysis was carried out using a mobile phase containing formic acid, and the acidic conditions on the column may have resulted in the hydrolysis of an acetate of lycorine. This may also be an alternative explanation for the absence of a clear peak corresponding to 2-*O*-acetyllycorine **22** in the TIC.

Table 8.17 - The HRMS data for all isolated compounds from C. variabile.

		Molecular Formula (Mass difference/ppm)	**$[M+H]^+$ (*m/z*) (calc.)**	**Fragments (*m/z*)**
1	Lycorine **19**	$C_{16}H_{17}NO_4$ (1.7)	288.1241 (288.1236)	270, 252, 177, 147, 119, 91
2	1,2-*O*,*O*-diacetyllycorine **21**	$C_{20}H_{21}NO_6$ (0.0)	372.1447 (372.1447)	270, 252, 222, 194
3	2-*O*-acetyllycorine **22**	$C_{18}H_{19}NO_5$ (1.5)	330.1346 (330.1341)	270, 252, 222, 194, 147, 119
4	1-*O*-acetyllycorine **23**	$C_{18}H_{19}NO_5$ (1.5)	330.1346 (330.1341)	270, 252, 222, 194, 177, 147, 134, 119
5	Haemanthidine **24** (and 6-epihaemanthidine **25**)	$C_{17}H_{19}NO_5$ (1.6)	318.1346 (318.1341)	300, 286, 268, 250, 240, 227, 224, 211, 209, 199, 192, 181, 169, 165, 153, 141, 115
6	Bulbispermine **26**	$C_{16}H_{17}NO_4$ (0.7)	288.1238 (288.1236)	270, 244, 226, 224, 211, 196, 181, 153, 141, 115
7	Criwelline **27**	$C_{18}H_{21}NO_5$ (0.3)	332.1499 (332.1498)	314, 230 202, **181**, 159, 153

8.3 General comments pertaining to the above processes

During the process of isolating components from **CVAlk_EXT**, the order of isolations was guided by the R_f of components on silica TLC. Essentially, the component represented by a spot at the top of the TLC profile was isolated first, followed by the spot directly below that, and so on and so forth.

As will have been noted in the introduction to this chapter, *C. variabile* has been the subject of only one phytochemical study prior to this project.[74] During the investigation, the presence of galanthamine (**20**) in *C. variabile* was verified. Despite this finding, it must be noted that galanthamine (**20**) was not isolated during this project. Tanahashi *et al.* (1990)[74] determined a yield of 0.006% from dried bulbs, which is a relatively low concentration of the alkaloid (6 mg per 100g dried bulb). This value is, of course, not constant across all specimens of *C. variabile*, with alkaloidal constituents of a single plant being dependant on a range of factors such as climatic conditions, time of harvest, and several others. Thus, it cannot be expected that exactly the same concentration of galanthamine **20** (or even any at all) would be present in the plant material used in this project.

The TIC acquired from LC-ESI-MS/MS analysis of **CVAlkEXT** showed no peaks containing the mass components expected for galanthamine. None of the peaks present in the TIC provided the molecular formula expected for galanthamine upon elemental composition analysis. The conclusion to be drawn from this is that galanthamine was not present in the specimen used for this project, despite the findings of Tanahashi *et al.* (1990)[74].

When carrying out a gravity column or washing compounds off silica, solvent systems with methanol composition higher than around 20% were generally avoided. The reason for this is that a white residue was noted in fraction collection vessels when working with higher methanol content in mobile phases. Thus, to avoid samples containing this residue (which would affect the masses acquired, and thus the yields reported), methanol content was kept at 20% or below, as a general procedural guideline.

Another precaution taken when working with PLC plates was exposure to air for long periods of time. Given that compounds bound to silica have high surface area, exposure to air increases the risk of oxidation. Thus, when plates were removed from the chamber after development, attempts were made to limit their exposure time to only as long as was required for drying. If further development runs were required, and could not be carried out immediately, plates were kept in a freezer at -18°C until they could be further processed.

When washing compounds from silica scraped off PLC plates, filtration through a packed bed of celite was useful as a means of ensuring no silica was washed into the filtrate. The celite was pre-washed with the solvents to be used, so as to ensure that no celite was washed into the filtrate.

When it is stated that a ^{1}H NMR spectrum showed impurities, the evidence for this in the spectrum was generally the presence of smaller peaks at unexpected shifts, with integrals that did not correlate. When an "impure" ^{1}H NMR spectrum was acquired, the sample was purified further before 2D NMR experiments were carried out, as these experiments were time consuming and thus expensive.

Observations such as "the sample showed a single spot under UV light and Dragendorff's reagent" were not taken as proof of a pure sample, but were used as a fairly reliable indicator, since the Amaryllidaceae alkaloids are generally UV active, and Dragendorff's reagent is selective for alkaloids. Of course, the presence of non-alkaloidal constituents which were unresponsive to UV was always a possibility when only a single spot was noted, but the extraction method minimised the risk in this regard. Thus, a sample showing a single spot under both UV and Dragendorff's reagent could generally be taken as a tentative indicator that the sample contained an acceptably pure alkaloid.

8.4 Conclusions and future work

The isolation and complete characterisation of compounds **19**, **21**, **22**, **23**, **24**&**25**, **26** and **27** was successfully achieved. Unfortunately, all of these compounds have been previously reported, though lycorine **19** was present in remarkably high concentrations in the bulbs of *C. variabile*. This could prove useful as a production method for lycorine **19**, which is of high interest for its multi-faceted biological activity.

Of course, the exhaustive investigation of the compounds in a plant species is a tremendous task, and this investigation did not result in the isolation of even all the alkaloidal constituents (as can be seen by the HPLC-ESI-MS analysis of the extract). Thus, a task of interest for future research could be the isolation of those compounds which could not be isolated or identified in this extract of *C. variabile* bulbs. Use of HPLC-ESI-MS could prove very effective in identifying fractions containing previously unknown compounds. The data acquired during this project could prove to be valuable for comparison during such investigations.

Time constraints did not allow for the in-depth investigation of all the samples acquired during the separation steps of this project. Some fractions which may have been of interest for further investigation are as follows: **C1_1-7** (though these fractions would contain relatively non-polar compounds, and did not show much promise upon TLC analysis); the remaining **C2** fractions, **C2_1,2** and **4** (these were not investigated as there were no obvious targets for isolation, though further investigation may reveal small quantities of additional alkaloids); **C3.1** fractions (these fractions contained a large portion of **P1_10-12**, and though **CV3** was the main target during this project, TLC analysis provided evidence of other components); **C4_1-11** and **17-23** (these fractions contained some of the more polar components of the extract, and despite the challenges faced while working with such samples, there are likely alkaloids present which this project did not reveal).

Separation of the epimers of haemanthidine (**24** and **25**) could be achieved by generating analogues which are more easily separated. A semi-synthetic investigation of this nature may reveal a simple method of separation that could prove useful in this regard.

Acquisition of a haemanthidine **24** standard would allow for the comparison of MS fragments with those of **CV3**, allowing for more conclusive results. Further investigations concerning the fragmentation pattern acquired for **CV3** may reveal fragmentation mechanisms which better explain the observed peaks.

Previous studies have shown that the alkaloidal composition of the bulbs of a plant is not the same as those of the leaves and roots.[106] Thus, perhaps investigation of the other parts of this plant species would be of interest.

9 *Crinum paludosum*

9.1 Introduction

Crinum paludosum produces white (sometimes light to deep pink) bell-shaped flowers and was first described fairly recently in 1968. It was illustrated using a specimen grown in Limpopo, from a plant originally found in Zululand.[53] The species name *paludosum* refers to the marshy habitat in which the species naturally occurs. It is found widely throughout southern Africa, with known areas of distribution in northern KwaZulu-Natal and Zululand, Gauteng, central Namibia, Botswana, eastern Zimbabwe and western Mozambique. *C. paludosum* is associated with seasonally flooded pans, marshes, etc., with clay soil that dries to be hard in the dry season. Due to the sparse and intermittent rainfall in some of these areas, it has evolved to become completely dormant in the dry season, sometimes remaining so for over a decade until favourable conditions are established.[53] Cultivation methods have been established, though susceptibility to fungal rot and invasive caterpillars makes it somewhat challenging.[53]

Figure 9.1.1 – A botanical illustration of Crinum paludosum*, drawn by Barbara Jeppe, taken from "The Amaryllidaceae of Southern Africa" by Graham Duncan, Barbara Jeppe, and Leigh Voigt*

To the best of our knowledge, there have been no investigations focused on the alkaloidal constituents of *C. paludosum*. Thus, this investigation will add some value to the field. The aim of the investigation carried out on this species was not the isolation of novel actives, but a time-efficient analysis of the alkaloidal constituents. It was also of interest, however, to determine the concentration of lycorine **19** in the dry bulbs of the species, given the relatively high concentration obtained from *C. variabile*, as discussed in the previous chapter.

9.2 Processing, results and discussion

9.2.1 Preparation and extraction

As with *C. variabile*, the bulbs of *C. paludosum* were obtained from a local nursery, and living specimens are present in the Botanical Gardens at the University of Stellenbosch (33°56'09.3"S 18°51'56.9"E) as reference material. These specimens will be maintained, and dried voucher specimens will be prepared from them in the case of their demise. The bulbs were sliced, dried in air until constant mass was achieved, and stored in a freezer (−18°C) before further processing. The resulting dried slices were crushed under liquid nitrogen to maximise the surface area for extraction.

The extraction of the *C. paludosum* bulb material began with acidic aqueous extraction of the prepared bulb material. 100 g of the material was submerged under 300 mL of 1% H_2SO_4 in H_2O. This was stirred for 2 hours (pH remained acidic, as tested using litmus paper), after which the material was strained and extracted once again in the same manner. A total of three extractions were carried out in this way, and the aqueous portions were combined. The reasoning behind this was that the acid present would protonate alkaloidal species, generating their sulphate salt forms, which would be more soluble in water, given their ionic nature.

Following this, the total aqueous extract was basified (checked using litmus paper) with NaOH. Theoretically, this will have generated the free-base forms of the alkaloids present, so that they could be extracted from the aqueous layer using an organic solvent. It may be noted that extraction of the acidic aqueous extract was not carried out before basification, as was done with *C. variabile*. This step was omitted in the interest of preserving any alkaloidal constituents which may move into the organic layer despite the acidic nature of the aqueous medium. Admittedly, the omission of this step somewhat decreases the selectivity of the extraction. However, despite this, all alkaloidal constituents would still be present in the extract, and the efficacy of the process remained robust.

Following basification, the aqueous solution was extracted with 250 mL of EtOAc. This was done three times using a separatory funnel, and the EtOAc extracts were dried using $MgSO_4$ and combined to obtain an alkaloidal extract (**CPAlk.EXT**, 0.4874 g after drying under high vacuum). In order to evaluate whether three EtOAc extractions was sufficient for the removal of the alkaloidal constituents, a continuous liquid/liquid extraction with EtOAc was then carried out on the aqueous layer (please see Appendix A for continuous liquid/liquid extraction apparatus). After 24 hours, an EtOAc extract was obtained which, after drying, had a mass of 0.2064 g. This mass is significant, suggesting that continuous liquid/liquid extraction is considerably more efficient than three extractions in a separatory funnel when extracting alkaloids.

*9.2.1.1 Isolation of lycorine **19***

TLC analysis of **CPAlk.EXT** and the continuous liquid/liquid extract showed analogous alkaloidal profiles, verifying the assumption that continuous extraction yielded more of the alkaloidal extract of interest. Thus, both samples could be considered **CPAlk.EXT** aliquots. Of these aliquots, the one of mass 0.4874 g was used for the isolation of lycorine, as was done with **CVAlk.EXT** in the previous chapter. After the addition of methanol to the sample, a light-coloured solid did not dissolve. This was filtered off and washed with cold MeOH to yield 112.5 mg of pure lycorine **19** (spectra were identical to those shown in Appendix A for lycorine **19**).

The total mass of lycorine **19** in **CPAlk.EXT** can be calculated using the total mass of **CPAlk.EXT** (0.6938 g): total mass of lycorine **19** $= 0.1125 \times \frac{0.6938}{0.4874} = 0.1601$ g, which is 160.1 mg. This mass is equivalent to a yield of 0.16% of the mass of dry bulbs used. This yield was not as high as that noted from *C. variabile*, although this is not surprising, given the notably high concentration of lycorine **19** present in the dried bulbs of *C. variabile*.

9.2.2 A brief LC-ESI-MS/MS dereplication study

Having isolated lycorine **19** in the interest of obtaining its yield from *C. paludosum*, a brief dereplication study was carried out by HPLC-ESI-HRMS analysis of a small amount of **CPAlk.EXT**. The sample was subjected to separation by HPLC under identical conditions to those used for **CVAlk.EXT**, to allow for comparison of elution times with the identified alkaloidal components of *C. variabile*. MS analysis was also carried out using identical parameters for trustworthy comparison of fragmentation patterns. Below is shown the TIC acquired for this analysis (Figure 9.2.1).

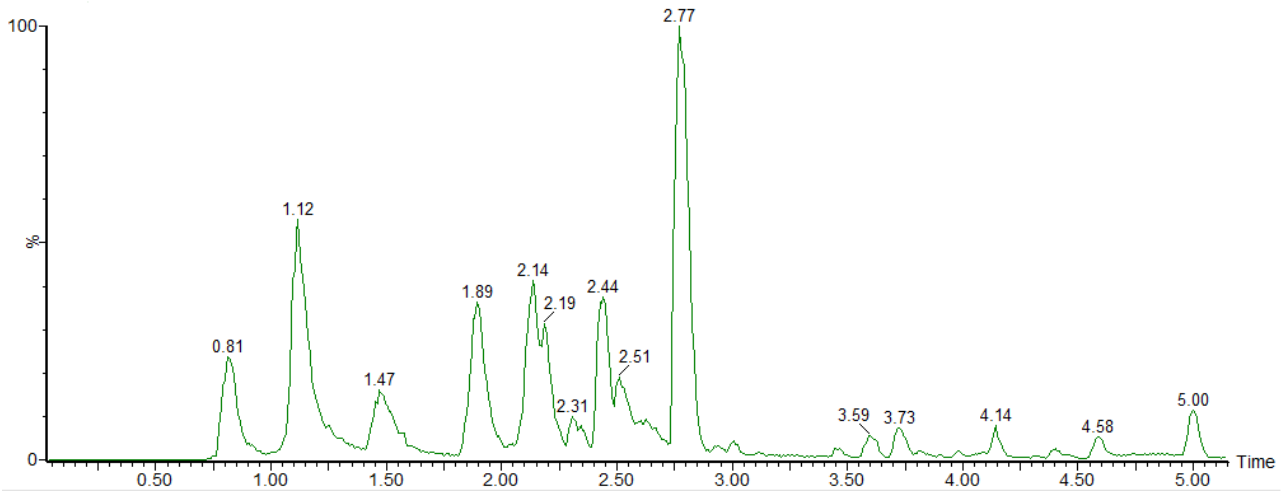

Figure 9.2.1 – Base peak ion (BPI) TIC of HPLC-ESI-HRMS analysis of CPAlk.EXT.

The table below (Table 9.1) contains the fragmentation patterns (as well as other information) that could be acquired for the peaks shown in Figure 9.2.1.

Table 9.1 - Peak data for TIC of CPAlk.EXT.

Retention Time/min	**Molecular Formula (Mass difference/ppm)***	**$[M+H]^+$ (*m/z*) (calc.)****	**Fragments (*m/z*)**	**Possible Identity**
0.81	$C_{16}H_{17}NO_4$ (2.4)	288.1229 (288.1236)	270, 226, 177, 147, 119, 91	Lycorine **19**
1.00	$C_{16}H_{19}NO_5$ (2.6)	306.1333 (306.1341)	290, 284, 266, 228, 213, 136	Unidentified
1.12	$C_{16}H_{17}NO_4$ (0.7)	288.1234 (288.1236)	270, 226, 177, 147, 119, 91	Lycorine **19**
1.47	$C_{16}H_{17}NO_5$ (0.0)	304.1185 (304.1185)	286, 268, 250, **226**	11-hydroxyvittatine-*N*-oxide **29**[97]
1.89	$C_{16}H_{17}NO_5$ (2.0)	304.1179 (304.1185)	288, 269, 242, 224, 181, 153	(2-epi)pancrassidine (**30a**, **30b**)[107]
	$C_{16}H_{17}NO_4$ (0.3)	288.1235 (288.1236)	270, 244, 226, 196, 168	11-hydroxyvittatine **31a**, hamayne **31b**, bulbispermine **26**
2.14	$C_{16}H_{17}NO_4$ (1.0)	288.1233 (288.1236)	270, 242, 224, 199, 185, 166, 153, 141, 129	Unidentified
2.19	$C_{16}H_{17}NO_3$ (0.4)	272.1288 (272.1287)	254, 226, 196, 168, 149, 136	Vittatine **32**[96]
2.31	$C_{17}H_{19}NO_5$ (0.6)	318.1343 (318.1341)	Overlapping peaks: 286, 274, 268, 238, 227, 226, 211, 209, 199, 197, 181, 169, 152, 141, 121	Crinamidine **33**[97]
	$C_{18}H_{21}NO_5$ (0.9)	332.1501 (332.1498)		Unidentified
2.44	$C_{17}H_{19}NO_5$ (0.6)	318.1339 (318.13410	300, 268, 256, 230, 224, 211, 202, **181**, 159, 153, 152	(iso)tazettinol (**34a**, **34b**)[54]
2.51	$C_{16}H_{12}NO_3^+$ (1.5)	266.0813 (266.0817)	236, 208, 178, 179, 180	Ungeremine **35**[96]
2.60	$C_{18}H_{19}NO_6$ (2.9)	346.1301 (346.1291)	288, 224, 197, 169	Unidentified
2.77	$C_{18}H_{21}NO_5$ (0.0)	332.1498 (332.1498)	314, 300, 282, 256, 238, 224, 230, 211, 202, **181**, 159, 153	Tazettine **36** (comparison with criwelline **27** and peak @ 2.44 min)

3.59	$C_{17}H_{17}NO_3$ (2.1)	284.1281 (284.1287)	147, 121, 119	3,4-anhydropowelline **37**[71] (low certainty)
3.73	$C_{18}H_{19}NO_4$ (2.5)	314.1384 (314.1392)	336 (Na adduct), **177**, 145, 117	Unidentified
4.14	$C_{18}H_{19}NO_6$ (0.3)	346.1292 (346.1291)	368, 328, 271, 241, 239, 211, 181, 153	(+)-3α-hydroxy-6β-acetylbulbispermine **38a**[104]
4.58	$C_{15}H_{14}NO_2$ (0.4)	240.1026 (240.1025)	224, 210, 182, **167**, 139	Unidentified
5.00	$C_{14}H_{10}O_2$ (0.9)	211.0761 (211.0759)	**181**, 153, 152	NON-ALKALOIDAL

The difference in calculated mass and that obtained for the molecular ion. **The calculated mass for $[M+H]^+$. Numbers in **bold represent base peak ions in cases where this is not the molecular ion.*

The peak eluting at 1.00 min was not identified with much confidence, though the molecular formula and the presence of the fragment at *m/z* 290 corresponded to lycoramine-*N*-oxide **28** (Figure 9.2.2).[96] Some analogous peaks with the EI-MS/MS spectrum of lycoramine-*N*-oxide **28** were also noted,[108] suggesting structural similarity.

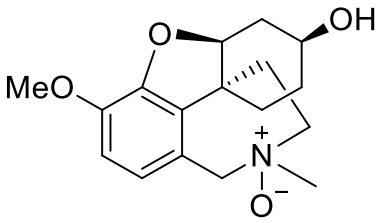

28

*Figure 9.2.2 - The chemical structure of lycoramine-*N*-oxide **28**.*

The peak at 1.47 min corresponds well with the known ESI-MS/MS information of 11-hydroxyvittatine-*N*-oxide **29** (Figure 9.2.3),[97] showing good correlation with the fragments and molecular formula reported in the literature. The elution time of this compound is also in agreement with that of a similarly identified peak in **CVAlk.EXT** (Table 8.16).

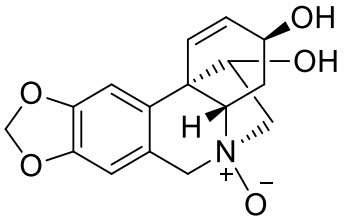

29

*Figure 9.2.3 - Chemical structure of 11-hydroxyvittatine-*N*-oxide **29**.*

At 1.89 min, a peak eluted which contained two compounds. One of these, with molecular formula $C_{16}H_{17}NO_5$, showed good correlation to analogous EI-MS fragments reported for 2-epipancrassidine **30a** (Figure 9.2.4) by Ghosal *et al.* (1989).[107] Of course, the possibility that this compound is pancrassidine **30b** should be considered.

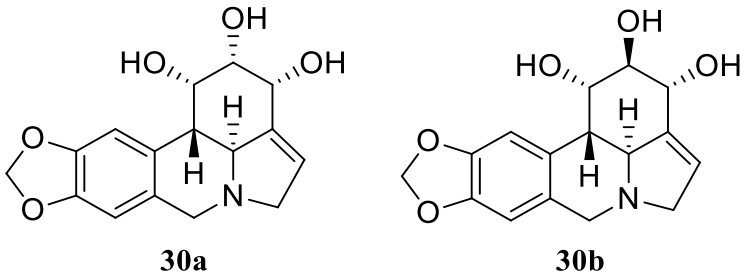

*Figure 9.2.4 - The chemical structures of 2-epipancrassidine **30a** and pancrassidine **30b**.*

The other peak at 1.89 min, with molecular formula $C_{16}H_{17}NO_4$, corresponded somewhat with both the fragmentation pattern and the elution time of bulbispermine **26**, as reported for **CVAlk.EXT**. However, some fragments observed for **26** were not seen for this peak, and the presence of a fragment at *m/z* 168 was not observed for **26** and were seen in the fragmentation pattern of this unknown. This suggests the possibility of an isomer, for which 11-hydroxyvittatine **31a** and hamayne **31b** (Figure 9.2.5) are strong candidates.

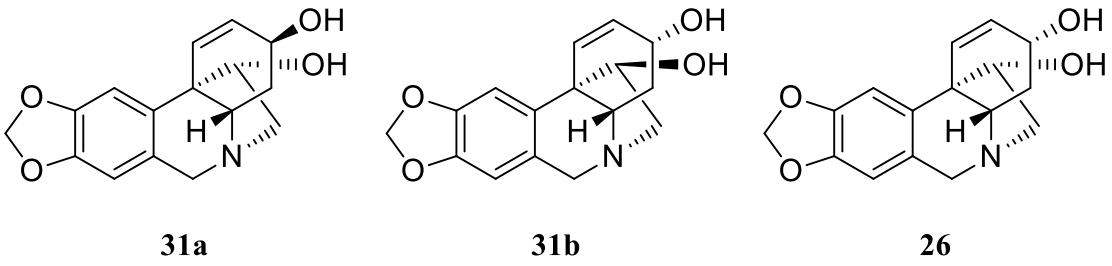

*Figure 9.2.5 - The chemical structures of 11-hydroxyvittatine **31a**, hamayne **31b** and bulbispermine **26**.*

The peak at 2.14 min with molecular formula $C_{16}H_{17}NO_4$ could not be identified, as its fragmentation pattern was not consistent with any reported in the literature. Fragment peaks at *m/z* 224, 199, 166 and 153 suggest structural similarities to (6-epi)haemanthidine (**24**, **25)**, which would indicate a haemanthamine-type alkaloid.

The peak at 2.19 with molecular formula $C_{16}H_{17}NO_3$ showed good correlation with the reported ESI-MS/MS fragments for vittatine **32**.[96] The molecular formula, as well as the evidence of the presence of 11-hydroxyvittatine **31a** (peak @ 1.89 min), are further indications that this component was likely vittatine **32** (Figure 9.2.6).

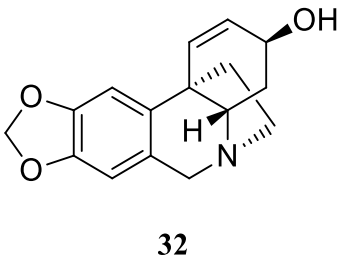

*Figure 9.2.6 - The chemical structure of vittatine **32**.*

At elution time 2.31 min, there is a peak which shows the masses for two components. The component with molecular formula $C_{17}H_{19}NO_5$ is most closely represented by crinamidine **33** (Figure 9.2.7), which has a correlating molecular formula, as well as matching fragments in its ESI-MS/MS spectrum.[97] The component with molecular formula $C_{18}H_{21}NO_5$ could not be matched with any alkaloids for which the ESI-MS/MS data was available in the literature. However, the component showed some analogous peaks to those of the EI-MS/MS fragments of tazettine **36** (Figure 9.2.10),[109] which may indicate a tazettine-type alkaloid. This may be an unknown alkaloid and may be of interest for further investigations.

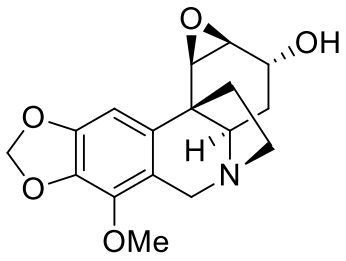

33

*Figure 9.2.7 - The chemical structure of crinamidine **33**.*

The peak at 2.44 min shows fragments remarkably similar to those of criwelline **27**, though the molecular formula suggests that instead of the 3-methoxy group, this compound has a 3-hydroxy group. This corresponds to isotazettinol **34a** (Figure 9.2.8).[54] Of course, tazettinol **34b** is also a strong candidate, especially given the identification of tazettine **36** in the extract (peak @ 2.77 min)

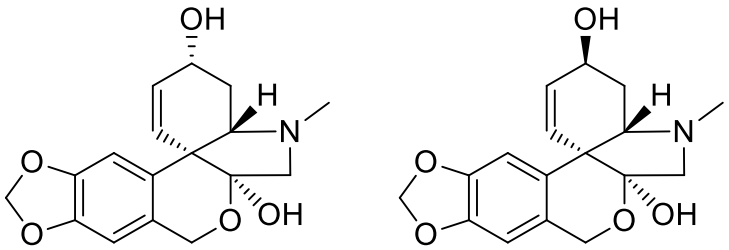

34a **34b**

*Figure 9.2.8 - The chemical structures of isotazettinol **34a** and tazettinol **34b**.*

Though perhaps not clearly visible in the TIC above (Figure 9.2.1), a component eluted at 2.51 min which had a molecular formula of $C_{16}H_{12}NO_3^+$. The fragmentation pattern of this component correlated with good agreement to that of ungeremine **35** (Figure 9.2.9) (This alkaloid appears to be stable in an ionic form, and so the removal of a proton was not necessary when considering its molecular formula), for which the ESI-MS fragmentation information is also reported.[96]

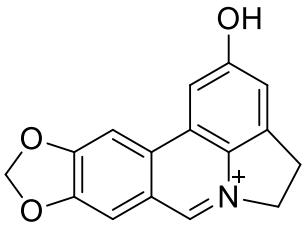

35

*Figure 9.2.9 - The chemical structure of ungeremine **35**.*

The peak eluting at 2.60 min had a molecular formula of $C_{18}H_{19}NO_6$, which is consistent with some Amaryllidaceae alkaloids, such as candimine and tazettamide. However, the mass fragments produced by this peak could not be correlated to any such compounds in the literature. Thus, the compound remained unidentified. This could therefore be an unknown alkaloid, and further investigation may be of interest for future research.

The peak at 2.77 min shared almost all of its mass fragments with the peak eluting at 2.44 min, and both showed base peaks at *m/z* 181. This suggests that these two compounds are likely structurally similar, though the molecular formula and the presence of a peak at *m/z* $[M+H]^+-32$ (loss of MeOH) suggests the presence of a 3-methoxy group instead of a 3-hydroxy. Given the tentative identification of the peak at 2.44 min as (iso)tazettanol (**34a**, **34b**), the peak at 2.77 min is likely tazettine **36**. The fragmentation pattern of this peak contains all the fragments of criwelline **27** (and some additional peaks), but the difference in elution time from **27** suggests an isomer thereof, with which tazettine **36** is consistent. Criwelline **27** is structurally very similar to tazettine **36**, with only an inversion of the 3-methoxy stereochemistry differentiating them. Thus, similar fragmentation patterns would not be surprising.

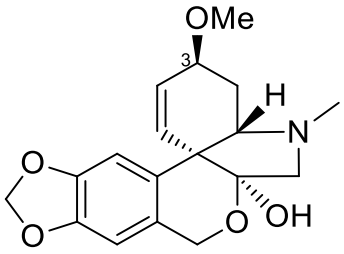

36

*Figure 9.2.10 - The chemical structure of tazettine **36**.*

The peak eluting at 3.59 min with molecular formula $C_{17}H_{17}NO_3$ was tentatively assigned as 3,4-anhydropowelline **37** (Figure 9.2.11) only because this was the only Amaryllidaceae alkaloid with a corresponding molecular formula in the literature.[71] The presence of the structurally similar crinamidine **33** in the extract may add some credence to this identity. Unfortunately, no fragmentation

information for 3,4-anhydropowelline **37** was available for comparison, and so the assignment as such is somewhat superficial.

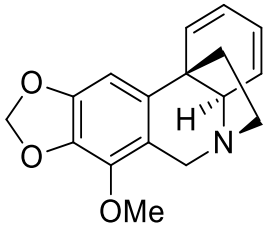

37

*Figure 9.2.11 - 3,4-anhydropowelline **37**.*

The peak eluting at 3.73 min had a molecular formula of $C_{18}H_{19}NO_4$. This molecular formula corresponded with O-acetylcaranine, and the presence of a peak at *m/z* 177 was shared with the fragmentation pattern of lycorine (O-acetylcaranine is a lycorine-type alkaloid). Though these observations may add some slight credence to the possibility that the peak was O-acetylcaranine, the fragmentation pattern showed no analogous peaks to those reported for the EI-MS fragmentation of O-acetylcaranine.[110] Thus, no definitive assignment could be made for this compound. This compound may be an unknown alkaloid and could be of interest for further investigation.

The peak eluting at 4.14 min contained a component which had the molecular formula $C_{18}H_{19}NO_6$ and showed a fragmentation pattern which corresponded well to the reported ESI-MS/MS fragments of (+)-3α-hydroxy-6β-acetylbulbispermine **38a** (Figure 9.2.12).[104] Given that there is evidence for the presence of 11-hydroxyvittatine **31a** in the extract (peak @ 1.89 min), the corresponding isomer (theoretically 6β-acetyoxy-11-hydroxyvittatine **38b**) should be considered as a possibility.

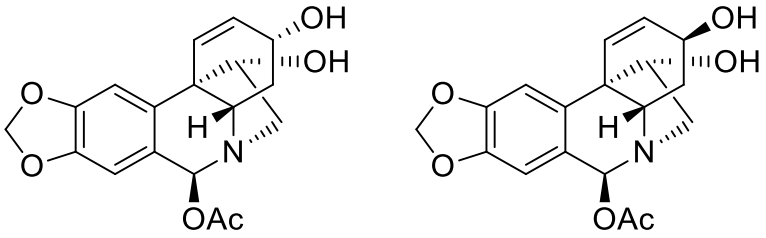

38a **38b**

*Figure 9.2.12 - The chemical structures of (+)-3α-hydroxy-6β-acetylbulbispermine **38a** and the theoretical 6β-acetoxy-11-hydroxyvittatine **38b**.*

The compound eluting at 4.58 min with a molecular formula of $C_{15}H_{14}NO_2$ was not identified, but was identical in both retention time and molecular formula to a peak observed in **CVAlk.EXT**.

The presence of a non-alkaloidal constituent (peak @ 5.00 min) can likely be explained by the extraction process described at the beginning of this chapter. The omission of an organic extraction of the acidic aqueous extract would mean that some non-alkaloidal constituents were not removed,

resulting in the presence of some non-alkaloidal compounds in the extract. Little can be said regarding the structure of this compound, as the trends seen in the structures of Amaryllidaceae alkaloids cannot be used as guidelines for non-alkaloidal constituents.

Finally, the presence of two peaks corresponding to the molecular formula and fragmentation pattern of lycorine **19** was noted (peaks @ 0.81 and 1.12 min). As was suggested in the discussion of the HPLC-ESI-MS/MS analysis of **CVAlkEXT**, this may be due to the conversion of a lycorine **19** derivative into **19** itself while on the column. The presence of formic acid in the mobile phase may have resulted in the hydrolysis of an acetyl group, thus generating lycorine **19** from a closely related compound, which could have then eluted at a different time to the lycorine **19** which was originally present in the sample (due to the time taken for this conversion to occur. It must be noted that this explanation is tentative, and further investigation would be required to confidently explain this result.

9.3 Conclusions and future work

The isolation of lycorine **19** was carried out, resulting in a yield of 0.16% from the mass of dried bulbs used. The data acquired from the LC-ESI-MS/MS analysis of the alkaloidal extract of *C. paludosum* (**CPAlk.EXT**) was used in a brief dereplication study to gain some insight regarding the alkaloidal constituents of the species.

This research allowed for the tentative or partial identification of eleven alkaloids present in *C. plaudosum* and offered some insight into structural aspects of four others. Five alkaloids could not be identified from previous reports in literature, and each of these has some promise as a possibly novel alkaloid. The pursuit of new compounds is beneficial to the field of medicinal chemistry, and so these unidentified compounds may be targets of interest for further research in this area.

Important to note is that, despite the usefulness of the data obtained from mass spectrometric analysis, the technique is not capable of unambiguous structural elucidation. It must therefore be kept in mind that the assignments suggested during this study were tentative and cannot be reported with absolute confidence. Despite this, the information provided is certainly sufficient to allow reasonable assumptions to be made, and in some cases, even for a compound to be identified with a fair level of certainty.

A clear possibility for future research endeavours would be the isolation of the alkaloids present in *C. paludosum*, in the interest of confirming or disproving the suggested identities noted in this chapter. Compounds which are previously undiscovered are of highest interest in this regard, and even those compounds for which an identity has been suggested may prove to be novel (since some identities were suggested based on close similarities with literature data, rather than identical results).

In conclusion, *C. paludosum* shows some promise for the discovery of novel compounds (including those which are not alkaloids), and further investigation would be beneficial.

10 A Brief synthetic study on higginsianins A and B

10.1 Introduction

In a study by Evidente and colleagues (2016),[73] two natural products compounds were isolated from the fungus *Colletotrichum higginsianum*, and were named higginsianins A and B (**39** and **40** respectively, Figure 10.1.1). The compounds both exhibited considerable antiproliferative activity against the human glioma cancer cell line Hs683. Higginsianin A exhibited an IC_{50} value of 1 µM, and higginsianin B one of 2 µM (these being concentrations required to inhibit cell growth by 50% after 72 hours of incubation). The compounds also showed promising results against some other cell lines, including a melanoma line (B16F10).[73]

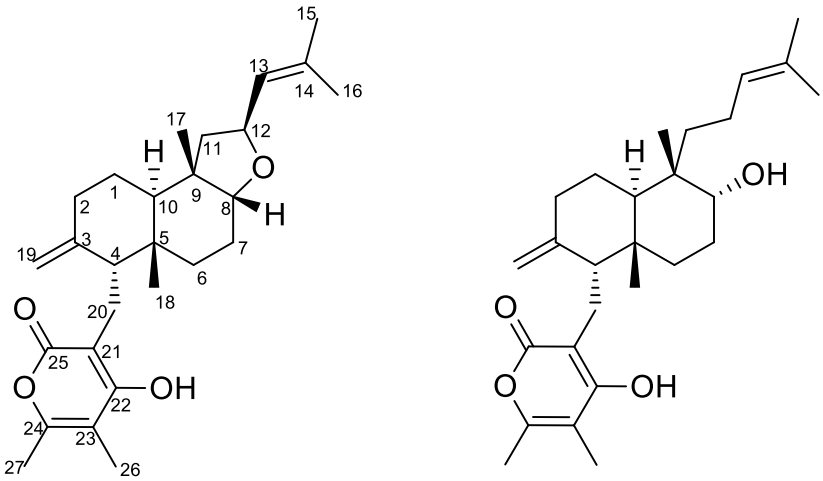

*Figure 10.1.1 - The chemical structures of higginsianin A **39** and higginsianin B **40**. The atom numbers for higginsianin B reflect those of higginsiainin A.*

As was discussed in the background chapter, derivatisation of natural products has proven invaluable in the field of drug discovery. Despite the inherent activity of the natural products compounds isolated, drug-like properties (as well as activity) can be greatly improved by structural alteration.[37,40,41] As reported by Newman and Cragg (2016), of all the new approved drugs from 1981 to 2014, 21% were natural products derivatives.[37] This highlights the importance of synthetic modifications to natural products compounds in the search for new drugs.

Thus, as a synthetic accompaniment to the current natural products-focused project, it was decided that a brief study would be done in which a few test reactions could be attempted on these two compounds. The purpose of this study was the synthesis of some analogues of **39** and **40**, with the intent that the resulting compounds be tested for their bioactivity.

Samples of these compounds were acquired from the research group of Antonio Evidente, University of Napoli, Italy. Reactions were generally carried out on a 20 mg scale, to ensure that the available starting material (*ca.* 250 mg of **39** and *ca.* 350 mg of **40**) could be subjected to a reasonable number of reaction attempts.

10.2 Reactions

*10.2.1 Higginsianin A **39***

As the first reaction for Higginsianin A, it was decided that an acetylation would be of interest, as the acetate could be of use as a starting material for other reactions. The acetate of Higginsianin A **39** had already been acquired, and so was not novel.[73]

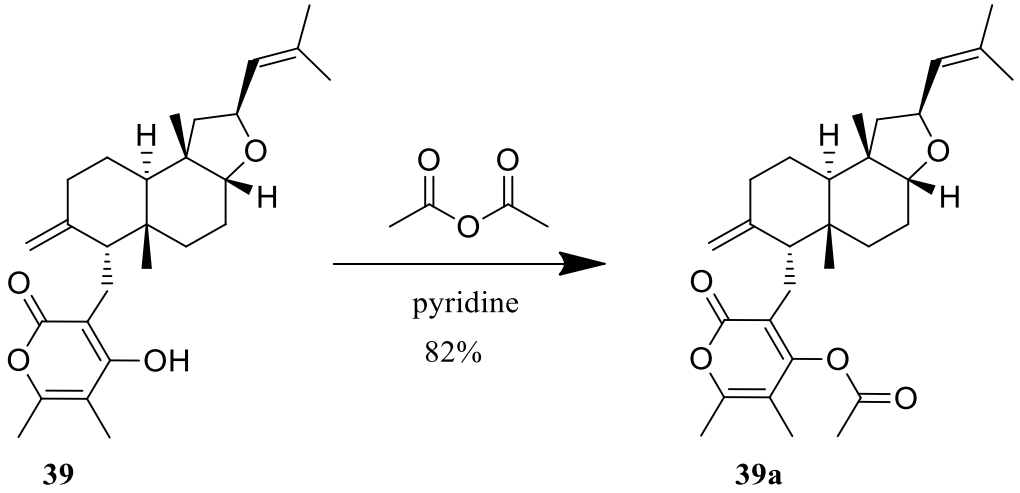

39 **39a**

*Figure 10.2.1 - The reaction scheme of Higginsianin A **39** acetylation. Pyridine was used as a solvent, and acetic anhydride was added in excess.*

The acetylation reaction was left to stir for 24 hours, after which complete conversion to the acetate was achieved, and the reaction was poured over ice to precipitate **39a** in 82% yield (45 mg). The proton NMR spectrum (Appendix B) was confirmed by comparison to the same product in the study by Evidente and colleagues (2016).[73]

Following this, it was decided that acetate **39a** would be a good starting material for an attempted Diels-Alder reaction. The intention was for the action of the lower pyrone ring as a diene, with previous evidence of analogous reactions.[111] Maleic anhydride (1.1 eq) was used as a dienophile, and the reaction solvent was benzene. Unfortunately, the reaction did not proceed, despite attempts to promote it, such as the addition of a Lewis acid ($AlCl_3$), and the addition of more maleic anhydride. The starting material was then recovered by gravity column (*ca.* 75% recovery – some may have been lost to binding on silica).

Acetate **39a** was also used as a starting material for an attempted epoxidation reaction using *meta*-chloroperbenzoic acid (*m*-CPBA) and DCM as a solvent. The reaction did not proceed, and heating to 30°C for *ca.* 48 hours still resulted in recovery of the starting material (*ca.* 90% recovery – recovered by extraction).

Following this, hydrogenation of the double bonds of higginsianin A **39** was attempted using 10% palladium on carbon under positive H_2 pressure. The reaction was attempted using dry MeOH as the solvent, and a balloon of H_2 gas to provide a positive pressure. Unfortunately, this reaction gave rise to a mixture of many products, and the small quantity of each did not allow for isolation and characterisation of any primary products.

A bromination reaction was then attempted using **39**, making use of *N*-bromosuccinimide (NBS) (1 eq.) and a catalytic amount of azobisisobutyronitrile (AIBN – a radical initiator) in DCM. The reaction was carried out under allylic bromination conditions, and resulted in full conversion of the starting material into two closely eluting compounds after 6 hours. Initially, an attempt was made to separate these two compounds by preparative TLC. However, the TLC resulted in a mixture of many compounds, suggesting degradation of the products on the silica plate. The reaction was then repeated, and the benzoic acid side product (from the *m*-CPBA starting material) removed by washing with sodium bicarbonate solution. A ^{1}H NMR spectrum was then acquired of the product mixture after drying of the organic layer. Another ^{1}H NMR spectrum was acquired two days later, having left the tube at room temperature (RT), and exposed to ambient light. The second spectrum showed that the compounds had once more degraded. These results led to the assumption that the products were either thermo- or photo-sensitive.

Thus, the reaction was repeated a third time, keeping tinfoil over the reaction vessel to avoid light exposure. The products were isolated by extraction once again, and the NMR spectroscopic sample prepared from the resulting dried organic layer was kept in the fridge, wrapped in tinfoil. Characterisation of the product mixture by ^{1}H, ^{13}C and 2D NMR spectroscopic experiments (HSQC, HMBC, COSY, DEPT) (Appendix B) led to the identification of the products shown in the scheme below:

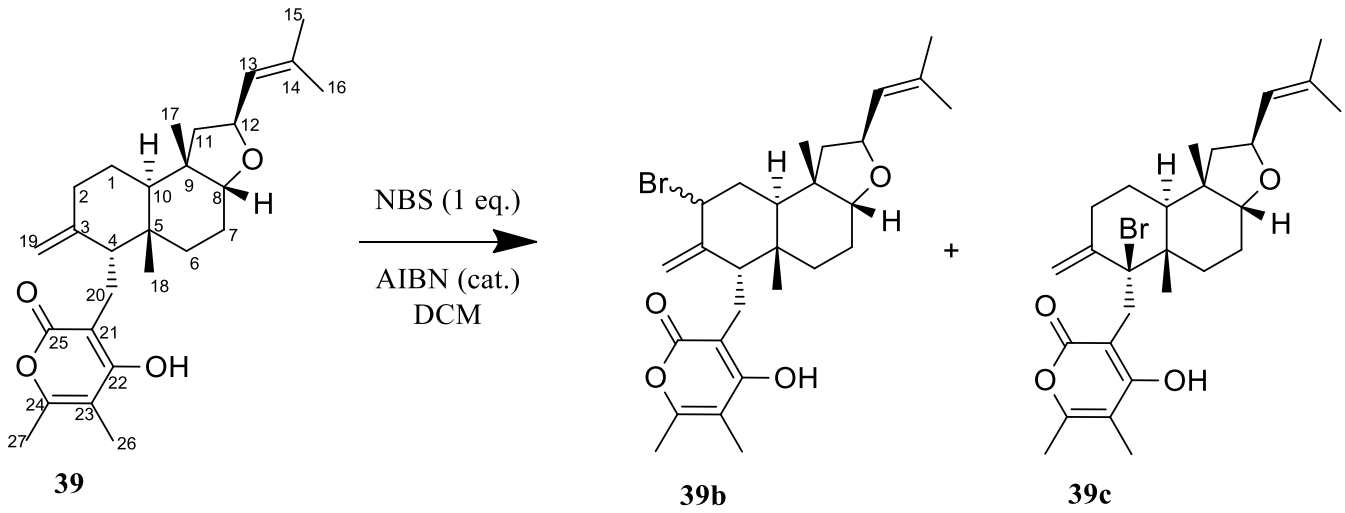

*Figure 10.2.2 - Reaction scheme of NBS bromination of higginsianin A **39**.*

The reasoning behind the identification of these products is as follows: Bromination does not occur at position 13, as the H-12 and H-13 peaks remain unaffected in the ^{1}H NMR spectrum for the product mixture. In the resulting ^{1}H NMR spectrum, the peak representing H-18 (3H) was split from a singlet in the starting material into two singlets in the product mixture. Bromination at the C-4 position of **39** would result in deshielding of the protons on C-18 (electron withdrawing nature of bromine). Thus, the more downfield of the two H-18 singlets represented that for **39c**. The relative integrals of these two singlets suggested that approximately 40% of the **39** had been brominated at the C-4 position, and 60% had been brominated at the C-2 position. Shifts of the H-19 peaks also suggested a mixture of two products, as the original two peaks were split into four. The relative integrals of these peaks suggested similar product ratios as those discussed above.

Separation of **39b-d** (brominated products) was not carried out, due to time constraints not allowing the navigation of the difficulties associated with separating sensitive compounds. Both products are, however, novel compounds (though their medicinal promise may be challenged by their proclivity to degradation).

*10.2.2 Higginsianin B **40***

As with higginsianin A **39**, the first reaction carried out for this compound was an acetylation reaction. This reaction was carried out in reagent grade chloroform, with excess pyridine and acetic anhydride. The reaction was monitored by TLC analysis, and the reaction was stopped once all the starting material had been consumed. At this point, two product spots were visible, and were isolated by washing the organic layer with 1M HCl, followed by brine. After drying of the organic layer, the two products were separated on by PLC and isolated for NMR spectroscopic analysis. The two compounds acquired (**40a**, 49.3%, 29.5 mg and **40b**, 35.2%, 19.3 mg) were subjected to ^{1}H and ^{13}C NMR spectroscopic and HRMS analyses (Appendix B), and were identified as 8,22-*O*,*O*-diacetylhigginsianin B **40a** and 22-*O*-acetylhigginsianin B **40b**. The scheme below shows the resulting compounds (HRMS analysis supports the identification of the products as those shown).

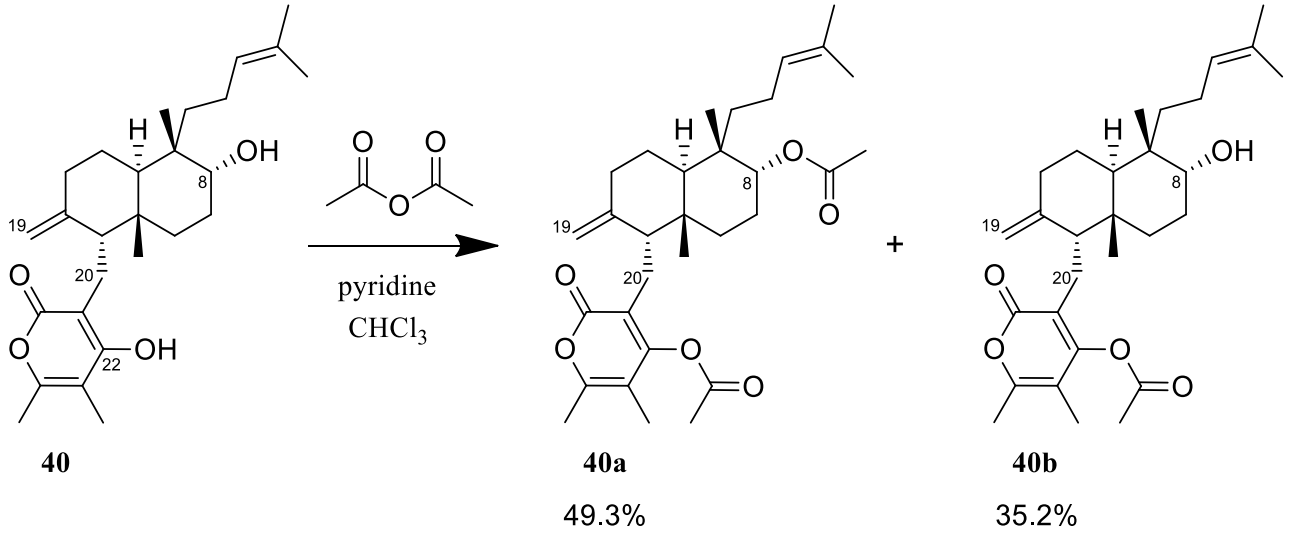

*Figure 10.2.3 - Reaction scheme of the acetylation of Higginsianin B **40**.*

Comparing the ^{1}H NMR spectra of the starting material **40** and the products **40a** and **40b** (Figure 10.2.4), a shift of proton 8 only occurs in the spectrum of the diacetylated product **40a**. This suggests that acetylation occurs preferentially on the hydroxy of the lower ring. A shift of one of the protons at the 19- position occurs in the spectra of both products, further supporting this hypothesis. Additionally, the peaks corresponding to H-20 were also affected in both products (which adds credence to the notion that acetylation occurred at the 22-hydroxy in both products). Furthermore, the appearance of additional methyl peaks in the product spectra are further evidence of the formation of the suggested products. Neither of these acetates were synthesised in the original study by Evidente and co-workers (2016),[73] and so both are novel compounds.

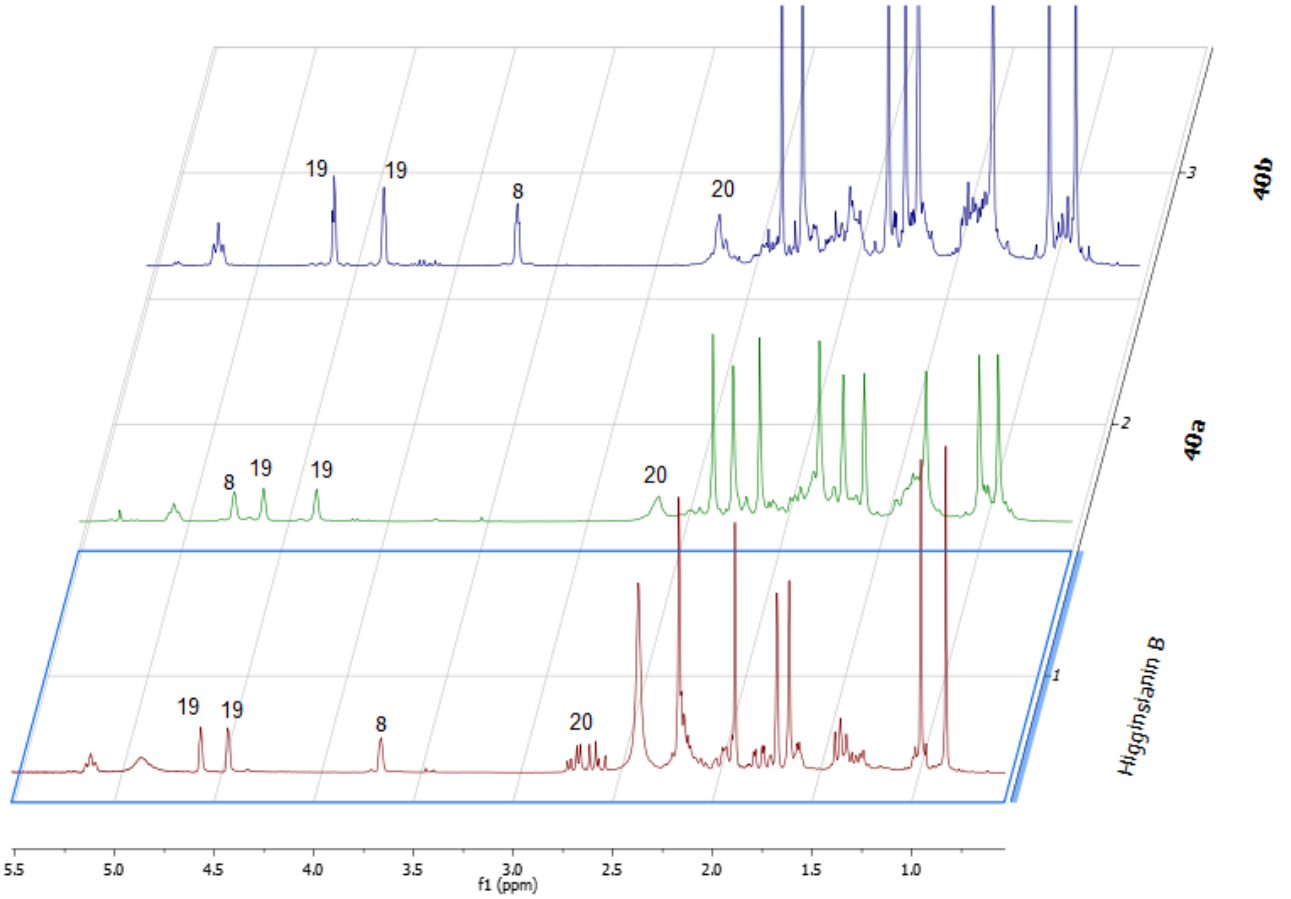

*Figure 10.2.4 – Comparison of ^{1}H proton spectra for **40**, **40a**, and **40b**.*

Following this, an oxidation of higginsianin B **40** was attempted using pyridinium chlorochromate (PCC). A common problem faced when using PCC is that the by-products form "clumps", which can trap solid reagents, reducing surface area and slowing the reaction, as well as making the workup challenging.[112] In order to solve this, the PCC was ground with a small amount of silica before using it in the reaction. The resulting fine yellow powder dispersed effectively in the reaction solvent. The expected product was one in which the secondary alcohol of higginsianin B **40** was transformed to a ketone. Unfortunately, the result of this reaction was a mixture of compounds that could not be identified due to the small quantities present.

An ozonolysis of higginsianin B **40** was also attempted, using MeOH and DCM as solvents, and an acetone/dry ice slurry to maintain a cold temperature (−78°C) during ozone saturation. Me_2S (4 eq.) was used to reductively work up. The reaction mixture was kept under oxygen or ozone throughout the length of the reaction, and so following the reaction progress with TLC analysis was not possible. TLC analysis of the resulting product mixture revealed a complex mixture. Attempts were made to gain further insight using HRMS, but this provided no useful information, as only species of significantly lower molecular weight than the starting material were observed, suggesting

degradation. (*m/z* 335, 345, 361 were acquired as masses of resulting components, suggesting degradation to smaller compounds, as the mass of the starting material was 428.6 u).

As with higginsianin A **39**, a reductive hydrogenation using palladium on carbon (Pd/C – 10%) was attempted on higginsianin B **40**. This reaction produced a promising TLC profile after reaction in dry MeOH for 72 hours. The reaction mixture was prepared as a crude NMR spectroscopy sample, which unfortunately degraded (supposedly due to the acidic nature of $CDCl_3$) before separation or characterisation were attempted. Time constraints did not allow for the repetition of this reaction, but given that the reaction proceeded, producing what appeared to be two spots on TLC (Figure 10.2.5), this reaction is promising for future investigation.

*Figure 10.2.5 - TLC profile of reaction with **40** and Pd/C at 72 hours.*

The crude ^{1}H NMR spectrum (Appendix B) of the hydrogenation product mixture shows large shifts of peaks for H-19 and H-13, which supports the reaction scheme shown in Figure 10.2.6, as hydrogenation of the double bonds at these positions would result in protection of these protons, causing upfield shifts into the aliphatic range. The presence of two spots on TLC suggests two products, and the appearance of a quartet at δ4.13 ppm in the ^{1}H NMR spectrum of the product mixture suggests the possibility of hydrogenation of the double bond at C-23 on the lower ring (Figure 10.2.6). This would indicate **40d** as a product, in which case H-24 may produce the aforementioned quartet (deshielding by the adjacent electron withdrawing oxygen atom may be the reason for the higher chemical shift value).

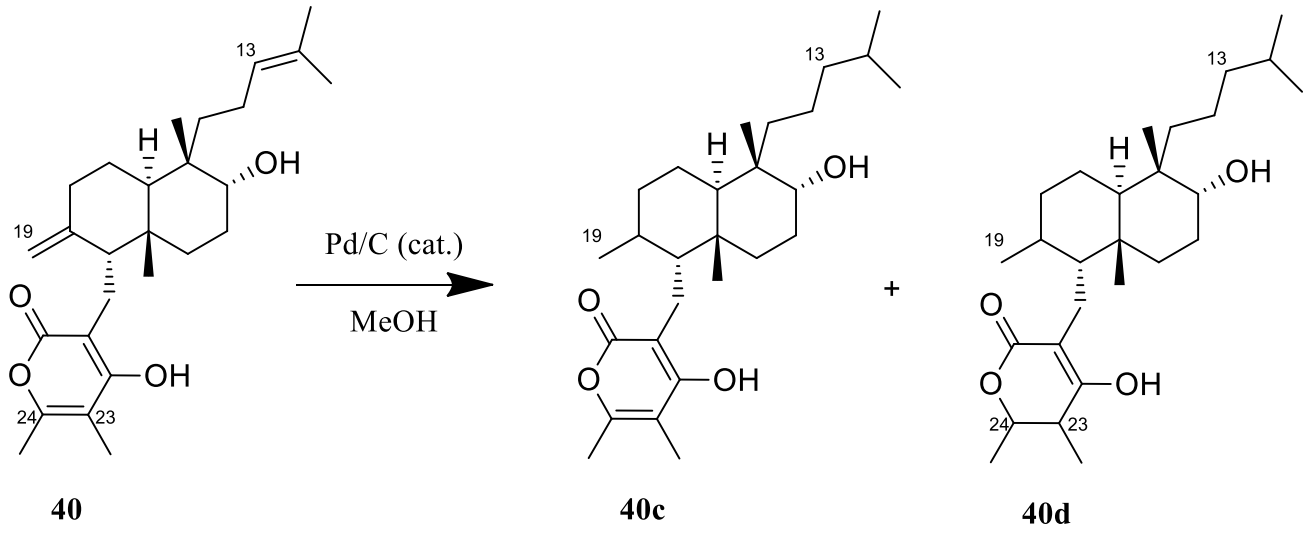

*Figure 10.2.6 - Reaction of higginsianin B **40** with Pd/C.*

Epoxidation of higginsianin B **40** using *m*-CPBA was then attempted in DCM. The reaction proceeded slowly, and solubility of the starting material in DCM was sparing. However, after approximately 50 hours of stirring at room temperature, all the solid material had dissolved, and full conversion to a single spot on TLC was noted after 72 hours. Crude ^{1}H NMR spectroscopic analysis (Appendix B) showed shifts of protons at position 19, which would support the scheme shown below (Figure 10.2.7). No shift was observed for H-13, suggesting that epoxidation did not occur at this position. Unfortunately, time constraints (and other circumstances) did not allow for purification of the product and full characterisation, though this would be an obvious step for further investigations.

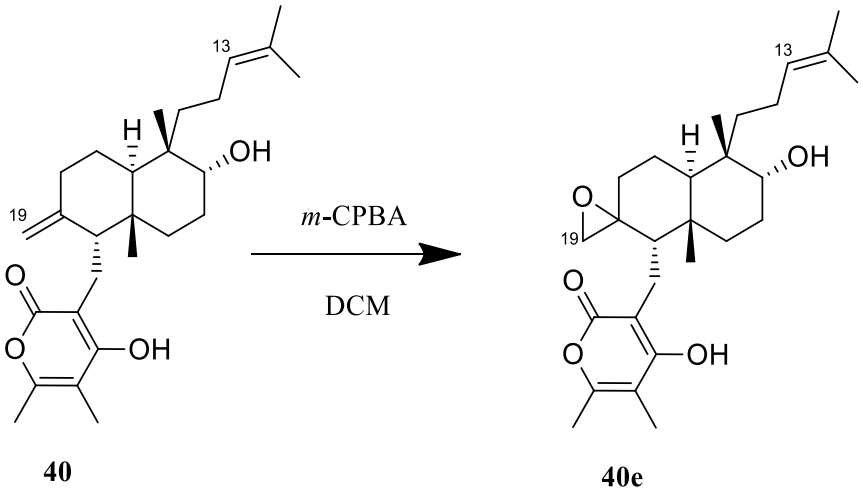

*Figure 10.2.7 - Reaction of higginsianin B **40** with m-CPBA.*

10.3 Conclusions and future work

This study resulted in the generation of 22-*O*-acetylhigginsianin A **39a**, though this analogue had been previously reported.[73] Also produced was a mixture of bromination products of **39**, though full characterisation of these was not achieved. Other reactions attempted on **39** included: PCC oxidation,

epoxidation with m-CPBA, diels alder with maleic anhydride, and hydrogenation of double bonds with Pd/C. However, these reactions proved unsuccessful, either yielding starting material, or a mixture of products which could not be characterised.

From Higginsianin B **40** was produced 8,22-*O*,*O*-diacetylhigginsianin B **40**a and 22-*O*-acetylhigginsianin B **40b**, both novel analogues. Oxidation with PCC and ozonolysis of **40** were attempted, though these reactions were unsuccessful, producing mixtures of compounds which could not be characterised. Reductive hydrogenation of **40** using Pd/C produced promising results, though degradation of the product(s) in $CDCl_3$ meant that full characterisation could not be achieved. Lastly, epoxidation of **40** using *m*-CPBA resulted in a single apparent product when analysed by TLC. Some structural aspects could be inferred by crude NMR spectroscopic analysis, though time constraints did not allow for full characterisation. Of course, full characterisation of all products making use of 2D NMR spectroscopy should be carried out to complete these studies.

This study was only preliminary, providing only a small number of analogues. Thus, development of a more extensive library of derivatives is a key objective for future work. Additionally, biological testing of the acquired derivatives is imperative, in the interest of developing SARs for higginsianins A and B (**39** and **40**), as well as for the discovery of novel active compounds.

In conclusion, the work presented above provides some useful information for the investigation of **39** and **40** as drug leads, as well as some novel compounds for biological testing. However, far more extensive research in this area is needed for more meaningful conclusions to be drawn, and for SARs to be elucidated.

11 Methods and materials

All chemicals were purchased from Sigma Aldrich or Merck. All ^{1}H, ^{13}C and 2D nuclear magnetic resonance spectra were obtained using a 300 MHz (75.5 MHz for ^{13}C), 400 MHz (100 MHz for ^{13}C) or 600 MHz (150 MHz for ^{13}C) Varian VNMRS using deuterated solvents.

11.1 *Crinum variabile*

Optical rotations were obtained on a Perkin Elmer 343 Polarimeter at 20 °C.

All chromatographic columns were prepared with a cotton wool plug at the base to minimise elution of unwanted solids (though columns with glass frits were invariably used).

All PLC plates were of dimensions 20×20 cm and bands were visualised under UV light (254 nm wavelength). When isolating the compounds present in bands, silica was crushed to allow for effective washing.

Spots on TLC plates were visualised under UV light (254 nm wavelength), as well as using Dragendorff's reagent (prepared according to standard procedure). TLC plates used during the elution of a column were analytical grade aluminium-backed (Merck, high performance analytical TLC, 5 cm length, F_{254}). TLC plates used for profiling of extracts and solvent system optimisation were glass-backed (Merck, silica gel 60, 0.25 mm film thickness, 10 cm length, F_{254}).

11.1.1 Separation experiments

11.1.1.1 ***P1***

CVAlk.EXT.F (2.469 g) was dissolved in MeOH and loaded onto coarse silica (Merck, silica gel 60, 0.063-0.200 mm), and placed under high vacuum to dry. **P1** was prepared in a glass column (42 mm internal diameter (i.d.)), with a cotton plug at the base, followed by silica gel (25 g) (Merck, silica gel 60, 230-400 mesh). An additional layer of cotton wool was placed above this, followed by the dried and loaded **CVAlk.EXT.F**.

P1 was then eluted , in 700 mL volumes, with: 100% hexane, 10% EtOAc in hexane (EtOAc/hex), 20% EtOAc/hex, 30% EtOAc/hex, 40% EtOAc/hex, 50% EtOAc/hex, 60% EtOAc/hex, 70% EtOAc/hex, 80% EtOAc/hex, 90% EtOAc/hex, 100% EtOAc, 2.5% MeOH/EtOAc, 5% MeOH/EtOAc, 10% MeOH/EtOAc, 15% MeOH/EtOAc, 20% MeOH/EtOAc, 100%DCM, 2.5% MeOH/DCM, 10% MeOH/DCM, 20% MeOH/DCM, EtOAc:MeOH:H_2O (78.2:20:1.8), EtOAc:MeOH:H_2O (76.4:20:3.6), EtOAc:MeOH:H_2O (74.6:20:5.4), EtOAc:MeOH:H_2O (72.5:20:7.5), EtOAc:MeOH:H_2O (70:20:10), 100% MeOH.

Each of these eluents was collected as a single fraction of **P1**, resulting in 26 fractions (**P1_1-26**). TLC analysis of these fractions (Figure 8.2.2) was carried out using EtOAc:MeOH:H_2O (85:10:5) on a glass-backed TLC plate (Merck, silica gel 60, 0.25 mm film thickness, 20×20 cm, F_{254}). The plate was pre-dried in an 80°C oven.

11.1.1.2 ***C1***

50 g silica (Merck, silica 60, 230-400 mesh) was equilibrated in 100% hexane and poured into a 20 mm diameter glass column. **P1_1-6** (348 mg) was loaded onto 1.4 g silica gel (Merck, silica 60, 230-400 mesh), and dried under high vacuum before being added to the top of **C1**.

C1 was then eluted with: 100% hexane (70 mL), 1% EtOAc/hex (250 mL), 5% EtOAc/hex (250 mL), 10% EtOAc/hex (250 mL), 20% EtOAc/hex (250 mL), 30% EtOAc/hex (1250 mL), 50% EtOAc/hex (500 mL), 60% EtOAc/hex (250 mL), 70% EtOAc/hex (500 mL).

The eluent was collected in 15 mL fractions, which were analysed by TLC during elution, based on which fractions were combined into ten groups (**C1_1-10**). Compound **21** (221 mg) was isolated during elution of 30% EtOAc in hexane, which is the reason for the increased elution volume using this solvent (only once all of the compound had eluted was the solvent composition altered further).

11.1.1.3 ***C1.1***

50 g silica (Merck, silica 60, 230-400 mesh) was equilibrated in 100% DCM and poured into a 20 mm diameter glass column. **C1_9** (53.1 mg) was sonicated in DCM (*ca.* 10 mL) and wet loaded onto **C1.1**.

C1.1 was eluted in 250 mL volumes with: 100% DCM, 1% MeOH/DCM, 2% MeOH/DCM, 3% MeOH/DCM, 4% MeOH/DCM, 5% MeOH/DCM.

15 mL fractions were collected and grouped based on TLC profile into 5 groups (**C1.1_1-5**). Compound **22** (45.2 mg) was isolated as **C1.1_3**.

11.1.1.4 ***C2***

45 g silica (Merck, silica 60, 230-400 mesh) was equilibrated in 100% EtOAc and poured into a 20 mm diameter glass column. **P1_7-9** (286.2 mg) was loaded onto 1.2 g silica (Merck, silica 60, 230-400 mesh), and added to the top of **C2**.

C2 was eluted using a single isocratic mobile phase of 100% EtOAc. 15 mL fraction were collected and, based on TLC analysis, were grouped into four fraction groups **C2_1-4**. The component of interest was noted in the third of these fraction groups, which was further processed on **PP0**.

11.1.1.5 ***PP0***

C2_3 (224 mg) was dissolved in MeOH and streaked onto the baseline of two PLC plates (Merck, silica gel 60, 1 mm film thickness, F_{254}). These PLC plates were developed simultaneously in 100% EtOAc seven times, to yield three bands (**PP0_1-3**). The compound was removed from each of these bands by scraping off the silica and washing with 20% MeOH in EtOAc. The component of interest (compound **23**) was noted by TLC analysis to be the sole constituent of **PP0_2** (178.5 mg).

11.1.1.6 ***PP1***

S1 (297.7 mg) was acquired by trituration of **P1_10-12** with MeOH. 100 mg of **S1** was dissolved in a minimum amount of MeOH (some H_2O added to assist), and was streaked onto a PLC plate (Merck, silica gel 60, 1 mm film thickness, F_{254}). After drying, the plate was developed once in EtOAc:MeOH, H_2O (85:10:5), showing two clearly visible bands (**PP1_1-2**). The top band (**PP1_1**, 44.8 mg) produced a ^{1}H NMR spectrum correlating to that of **CV3** (Appendix A) and was further processed on **C3**. The lower band (**PP1_2**, 42.4 mg) correlated by TLC to lycorine, and was kept aside.

11.1.1.7 ***C3***

21 g silica (Merck, silica 60, 230-400 mesh) was equilibrated in 100% DCM and poured into a glass column (1 cm diameter). **PP1_1** was dissolved in DCM and wet loaded onto the surface of **C3**.

C3 was eluted using the following solvent systems: 5% MeOH/DCM (1000 mL), 10% MeOH/DCM (750 mL).

20 mL fractions were collected and grouped based on TLC analysis into three fraction groups (**C3_1-3**). Only fractions showing a single spot under both UV and Dragendorff's reagent were placed grouped together (**C3_2**, 20.8 mg), and the sample was labelled **CV3**.

11.1.1.8 ***C3.1***

This column was carried out with the aim of purifying the **CV3** present in the mother liquor of **S1** (**P1_10-12** remaining after trituration, *ca.* 800 mg).

100 g silica (Merck, silica 60, 230-400 mesh) was equilibrated in 100% EtOAc and poured into a glass column (4 cm diameter). The remaining **P1_10-12** was loaded onto silica, and **C3.1** was eluted with: 100% EtOAc (2500 mL), 1% MeOH/EtOAc (1500 mL), 2% MeOH/EtOAc (2250 mL), 4% MeOH/EtOAc (2000 mL), 10% MeOH/EtOAc (1750 mL), EtOAc:MeOH:H_2O (85:10:5), 100% MeOH (750 mL).

20 mL fractions were collected and combined into five fraction groups (**C3.1_1-5**) based on TLC profile. **C3.1_4** (658 mg) contained **CV3** as the major component (though this was impure – TLC analysis showed the presence of lycorine **19**).

11.1.1.9 ***C4***

180 g silica (Merck, silica 60, 230-400 mesh) was equilibrated in 100% DCM and poured into a glass column (4 cm diameter). **P1_13-26** (*ca.* 760 mg) was loaded onto silica and added to the top of **C4**.

C4 was eluted with: 100% DCM (500 mL), 0.5% MeOH/DCM (500 mL), 1% MeOH/DCM (500 mL), 1.5% MeOH/DCM (500 mL), 2% MeOH/DCM (500 mL), 2.5% MeOH/DCM (250 mL), 3% MeOH/DCM (250 mL), 4% MeOH/DCM (250 mL), 5% MeOH/DCM (250 mL), 6% MeOH/DCM (250 mL), 7% MeOH/DCM (250 mL), 8% MeOH/DCM (250 mL), 10% MeOH/DCM (250 mL), 12% MeOH/DCM (250 mL), 15% MeOH/DCM (1750 mL), 20% MeOH/DCM (1000 mL), 30% MeOH/DCM (1250 mL), 50% MeOH/DCM (1000 mL). 100% MeOH (750 mL), 10% acetic acid in MeOH (250 mL).

15 mL fractions were collected and, based on TLC analysis, were combined into 26 fraction groups (**C4_1-26**).

11.1.1.10 ***PP2***

C4_12-16 (211 mg) was dissolved in MeOH and streaked onto a PLC plate (Merck, silica gel 60, 2 mm film thickness, F_{254}). **PP2** was developed three times in EtOAc:MeOH:H_2O (85:10:5), resulting in the visualisation of four bands (**PP2_1-4**). These bands were scraped off and washed with 20% MeOH in EtOAc to isolate the compounds. **PP2_2** was processed further on **PP3**, and **PP2_3-4** was processed further on **PP4**.

11.1.1.11 ***PP3***

PP2_2 (66.7 mg) was dissolved in MeOH and streaked onto a PLC plate (Merck, silica gel 60, 1 mm film thickness, F_{254}). **PP3** was developed once in EtOAc:MeOH:H_2O (85:10:5), resulting in five bands (**PP3_1-5**). **PP3_3** (45.5 mg) was the most intense band, with the others showing little response to UV light (254 nm). **PP3_3** was identified as compound **26**. Masses of the other bands were not recorded.

11.1.1.12 ***PP4***

PP2_3-4 (53.4 mg) was dissolved in MeOH and streaked onto a PLC plate (Merck, silica gel 60, 1 mm film thickness, F_{254}). **PP4** was developed three times in $CHCl_3$:EtOAc:MeOH (2:2:1), resulting in three bands (**PP4_1-3**). **PP4_2** was processed further on **C5**.

11.1.1.13 ***C5***

10 g of alumina (Sigma Aldrich, active neutral, 150 mesh) was equilibrated in 100% EtOAc, and **PP4_2** (19.1 mg) loaded onto 0.5 g alumina (as above) was added on top of **C5**.

C5 was eluted with: 100% EtOAc (750 mL – until all of compound of interest had eluted), 1% MeOH/EtOAc (25 mL), 2%MeOH/EtOAc (25 mL), 4% MeOH/EtOAc (25 mL), 6% MeOH/EtOAc (25 mL), 8% MeOH/EtOAc (25mL), 10% MeOH/EtOAc (150 mL), 15% MeOH/EtOAc (125 mL), 20% MeOH/EtOAc (100 mL), 100% MeOH (350 mL).

7 mL fractions were collected and grouped according to TLC profile into two fraction groups. **C5_1** contained pure compound **27** (6.4 mg), and **C5_2** contained all compounds which eluted after that.

*11.1.2 HPLC-MS/MS of **CVAlk.EXT***

Sample preparation: A small quantity of the sample (*ca.* 2 mg) was dissolved in 1 mL of analytical grade MeOH and filtered through a 0.2 µm syringe filter. Any necessary concentration corrections were made by dilution before analysis.

UPLC conditions: The UPLC system consisted of ACQUITY Ultra High-Performance LC system (Waters, Milford, MA, USA) and software MassLynx v4.1. Separation of Amaryllidaceae alkaloids was carried out on a Waters HSS T3 column, 2.1x100mm. Solvent A: Water (0.1% formic acid), Solvent B: Acetonitrile (0.1% formic acid). Gradient (linear programme) as follows: 0.0-0.50 min, 90%; 2.00 min, 70%; 5.50 min, 40%; 6.60 min, 10%; 6.70-10.00 min, 90% of A. Flow rate was 0.380 mL/min and injection volume was 1 µL.

ESI-MS/MS conditions: MS/MS analysis was performed on a Synapt-G2 High Definition Mass Spectrometer equipped with an ESI source (Waters, Milford, MA, USA) and Masslynx v4.1. Parameters as follows: polarity ES+ , capillary voltage 2.5 kV, sampling cone 15 V, extraction cone 4V, source temp. 120 °C, cone gas flow 50 L/h, desolvation temp. 275 °C, desolvation gas flow 650 L/h, Helium call gas flow 180 mL/min, trap gas flow 0.4 mL/min, trap collision energy 15 eV, ion energy 1.8 eV.

11.2*Crinum paludosum*

*11.2.1 HPLC-MS/MS of **CPAlk.EXT***

Sample preparation: A small quantity of the sample (*ca.* 2 mg) was dissolved in 1 mL of analytical grade MeOH and filtered through a 0.2 µm syringe filter. Any necessary concentration corrections were made by dilution before analysis.

UPLC conditions: The UPLC system consisted of ACQUITY Ultra High-Performance LC system (Waters, Milford, MA, USA) and software MassLynx v4.1. Separation of Amaryllidaceae alkaloids was carried out on a Waters HSS T3 column, 2.1x100mm. Solvent A: Water (0.1% formic acid), Solvent B: Acetonitrile (0.1% formic acid). Gradient (linear programme) as follows: 0.0-0.50 min,

90%; 2.00 min, 70%; 5.50 min, 40%; 6.60 min, 10%; 6.70-10.00 min, 90% of A. Flow rate was 0.380 mL/min and injection volume was 1 µL.

ESI-MS/MS conditions: MS/MS analysis was performed on a Synapt-G2 High Definition Mass Spectrometer equipped with an ESI probe (Waters, Milford, MA, USA) and Masslynx v4.1. Parameters as follows: polarity ES+ , capillary voltage 2.5 kV, sampling cone 15 V, extraction cone 4V, source temp. 120 °C, cone gas flow 50 L/h, desolvation temp. 275 °C, desolvation gas flow 650 L/h, Helium call gas flow 180 mL/min, trap gas flow 0.4 mL/min, trap collision energy 15 eV, ion energy 1.8 eV.

11.3 Higginsianins A and B

*11.3.1 Higginsianin A **39***

*11.3.1.1 Acetylation of Higginsianin A **39***

To a solution of **39** (50 mg, 1.17×10^{-4} mols) in pyridine (5 mL) was added acetic anhydride (5 mL) while stirring. The reaction mixture was stirred for 24 hrs, then poured over ice to precipitate the acetate product (22-*O*-acetylhigginsianin A **39a**, 45 mg, 81.9%), which was removed by filtration. Purification by gravity column was carried out on silica gel (Merck, silica 60, 230-400 mesh) using a gradient of EtOAc in hexane. Comparison of the ^{1}H NMR spectrum to that reported in literature confirmed the identity.[73]

*11.3.1.2 Reaction of **39a** with maleic anhydride*

To a solution of **39a** (20 mg, 4.27×10^{-5} mols) in pre-distilled benzene (*ca.* 10 mL) was added maleic anhydride (1.1 eq.), and the reaction mixture was left under reflux for 5 hrs. TLC showed starting material, and so additional 5 mg of maleic anhydride was added. No change noted on TLC after an additional hour, and so a catalytic amount (*ca.* 1 mg) of $AlCl_3$ was added. After an additional hour, no change was noted, and the reaction was stopped and starting material recovered by gravity column.

*11.3.1.3 Reaction of **39a** with m-CPBA*

Solid reagents (**39a**, 20 mg, 4.27×10^{-5} mols; *m*-CPBA, 1 eq.) were added to DCM (*ca.* 10 mL) and stirred for 5 hrs at −10 °C. No reaction occurred based on TLC analysis, and the reaction mixture was concentrated under reduced pressure to *ca.* 2 mL, and stirred at room temperature (RT) for a further 72 hrs. No reaction occurred after this time, and the reaction was heated to 30 °C and stirred for a further 45 hrs, after which no reaction had occurred, and the reaction was stopped. Starting material was recovered by extraction with sodium bicarbonate, followed by drying of the organic layer and solvent removal.

*11.3.1.4 Reductive hydrogenation of **39** with Pd/C*

Solid reagents (**39**, 20 mg, 4.69×10^{-5} mols; Pd/C (10% Pd), cat.) were added to dry MeOH (3 mL), and stirred at RT under positive H_2 pressure for *ca.* 6 hrs, after which the reaction mixture was filtered and the solvent removed under reduced pressure. The result was a mixture of products which were not characterised.

*11.3.1.5 Reaction of **39** with NBS*

Solid reagents (**39**, 20 mg, 4.69×10^{-5} mols; NBS, 8.3 mg, 1 eq.; AIBN, cat.) were placed in the bottom of a reaction vessel, and 1 mL of dry DCM was added to this. The reaction mixture was kept in the dark and stirred for 7 hrs at RT. The reaction mixture was then washed with sodium bicarbonate solution, the organic layer dried with $MgSO_4$, and the solvent removed under reduced pressure (exposure to light was minimised where possible by covering vessels in tinfoil). NMR spectroscopic sample was wrapped in tinfoil and kept in the fridge (4 °C) before analysis. The result was a mixture of products as discussed above (see Appendix B for crude NMR spectra).

*11.3.2 Higginsianin B **40***

*11.3.2.1 Acetylation of Higginsianin B **40***

Higginsianin B **40** (50 mg, 1.17×10^{-4} mols) was dissolved in $CHCl_3$ (2 mL) and pyridine (0.5 mL) mixture ($CHCl_3$ did not adequately dissolve **40**). This was added to a reaction vessel which had been purged with N_2, followed by acetic anhydride (0.5 mL). The reaction mixture was stirred under N_2 atmosphere at RT for 40 hrs. The reaction mixture was then diluted with DCM, washed with water (3×20 mL), 1 M HCl (3×20 mL), and finally brine (1×20 mL), after which the organic layer was dried with $MgSO_4$ and the solvent removed under reduced pressure. The resulting products were separated by TLC (2 plates, Merck, silica gel 60, 0.25 mm film thickness, F_{254}, 20×20 cm), developed three times in 10% EtOAc/hexane. Please see Appendix B for ^{1}H NMR and ^{13}C NMR spectra of the two products. Though full characterisation of the products was not carried out, evidence in the ^{1}H NMR spectrum showed the production of the expected products, as discussed in chapter 8.2.2.

*11.3.2.2 Reaction of **40** with PCC*

PCC (15 mg, 6.96×10^{-5} mols) was crushed with a spatula tip of silica in a mortar and pestle. This, along with **40** (20 mg, 4.67×10^{-5} mols), was added to a reaction vessel, which was purged with N_2. Dry DCM (3 mL) was then added under positive N_2 pressure. The reaction vessel was then sealed and left to stir for 3.5 hrs at RT. Reaction was stopped by filtration through celite to remove all solid reagents, and the solvent was removed from the filtrate. The result was a mixture of compounds which were not characterised.

11.3.2.3 *Ozonolysis of **40***

40 (30 mg, 7.0×10^{-5} mols) was added to dry MeOH (5 mL) in a 100 mL round bottom flask. Dry DCM (20 mL) was then added, along with a stir bar. This mixture was placed in a slurry of acetone and dry ice (−78 °C) while stirring. Once the mixture had been left to cool to this temperature, oxygen was bubbled through the mixture, followed by ozone (charge on ozone generator turned on to initiate ozone flow). Ozone was bubbled through for 15 min, to allow saturation (solution went blue after *ca.* 5 min). Following this, oxygen was once more bubbled through until the solution was clear. Positive N_2 pressure was then quickly applied (upon removal of O_2 supply), and the cold bath was removed. Me_2S (4 eq.) was then added under positive N_2 pressure, and the reaction mixture was left to cool to RT while stirring. The solvent was then removed under reduced pressure. The result was a mixture of products which were not characterised.

11.3.2.4 *Reductive hydrogenation of **40** with Pd/C*

Solid reagents (**40**, 20 mg, 4.67×10^{-5} mols; Pd/C (10% Pd), cat.) were added to dry MeOH (3 mL), and stirred at RT under positive H_2 pressure for *ca.* 72 hrs, after which the reaction mixture was filtered and the solvent removed under reduced pressure. The result was a single spot on TLC, though crude ^{1}H NMR spectroscopy suggested two possible products, which degraded in $CDCl_3$ after crude NMR spectroscopic analysis (see Appendix B for crude NMR spectra).

11.3.2.5 *Reaction of **40** with m-CPBA*

Solid reagents (**40**, 20 mg, 4.67×10^{-5} mols; *m*-CPBA, 2.4 eq.) were added to a reaction vessel, which was then purged with N_2. Dry DCM (2 mL) was then added under positive N_2 pressure, the vessel was sealed, and the mixture was stirred at RT for 72 hrs. Work-up was carried out by addition of DCM (*ca.* 15 mL) to the reaction mixture, followed by washing with saturated sodium bicarbonate solution, drying of the organic layer with $MgSO_4$, and removal of the solvent under reduced pressure to obtain the crude product. This showed a single spot on TLC, and was subjected to ^{1}H NMR analysis (see Appendix B for crude NMR spectra), with the intention of purification and full characterisation, though circumstances did not allow for this.

12 Acknowledgements

Big thanks to Prof Green for his continued support and availability, both in the lab and out.

Prof. Willem van Otterlo for his efforts as supervisor.

Prof. André de Villiers for his assistance as co-supervisor.

Jaco and Elsa at NMR spectroscopy facilities for their assistance in acquiring NMR spectra.

Maritjie Stander and her colleagues at CAF for their assistance in acquiring HPLC-ESI-MS/MS data.

GOMOC (Group of Medicinal and Organic Chemists) research group.

Lab colleagues in lab 2020/2021.

Debbie, Nulunthu, Raymond and Max for their assistance as technical staff

The financial assistance of the National Research Foundation (NRF) towards this research is hereby acknowledged. Opinions expressed and conclusions arrived at, are those of the author and are not necessarily to be attributed to the NRF.

Stellenbosch University Faculty of Science, Department of Chemistry and Polymer Science for equipment, chemicals, and other facilities.

My parents, for the upbringing and the genes.

Moscos, Khaya, Chris, Trégen, James, Jaco, Lydia and all other friends and colleagues present throughout.

Loren

13 References

1 A. L. Harvey, *Drug Discovery Today*, 2008, **13**, 894–901.

2 R. A. Halberstein, *Ann. Epidemiol.*, 2005, **15**, 686–699.

3 M. A. Huffman, *Am. J. Phys. Anthropol.*, 1997, **40**, 171–200.

4 M. Baker, *Am. J. Primatol.*, 1996, **38**, 263–270.

5 R. S. Solecki, *Science*, 1975, **190**, 880–881.

6 W. Sneader, *Drug Discovery: A History*, John Wiley & Sons, Ltd, Chichester, West Sussex, 2005.

7 G. M. Cragg and D. J. Newman, *Pure Appl. Chem.*, 2005, **77**, 7–24.

8 J. F. Nunn, *Ancient Egyptian Medicine*, British Museum Press, London, 1996.

9 A. Arber, *Herbals: Their Origin and Evolution - a Chapter in the History of Botany*, Cambridge University Press, Cambridge, 1912.

10 I. Milne, *J. R. Soc. Med.*, 2012, **105**, 503–508.

11 J. H. Baron, *Nutr. Rev.*, 2009, **67**, 315–332.

12 J. Drobnik and E. Drobnik, *Fitoterapia*, 2016, **115**, 155–164.

13 F. W. Serturner, *Trommsdorffs J. der Pharm.*, 1805, **14**, 47–98.

14 G. Samuelsson, *Drugs of Natural Origin: a Textbook of Pharmacognosy*, Apotekarsocieteten, Stockholm, Sweden, 6th edn., 2004.

15 F. W. Serturner, *J. Pharm. fur Aerzte und Apotheker*, 1806, **14**, 47–93.

16 E. Ravina, *The Evolution of Drug Discovery : From Traditional Medicines to Modern Drugs*, Wiley-VCH, Weinheim, 2011.

17 A. P. Klockgether-Radke, *Anasthesiol. Intensivmed. Notfallmed. Schmerzther.*, 2002, **37**, 244–249.

18 F. Khosrow-Khavar, S. Kurteva, Y. Cui, K. B. Filion and A. Douros, *Expert Opin. Drug Metab. Toxicol.*, 2019, **15**, 565–575.

19 I. Badash, C. G. Lui, K. Hur, J. R. Acevedo, E. H. Ference and B. B. Wrobel, *Laryngoscope*, 2019, 1–6.

20 S. Nielsen, R. Crossin, M. Middleton, C. Martin, J. Wilson, T. Lam, D. Scott, K. Smith and D. Lubman, *BMJ Open*, 2019, **9**, 1–9.

21 C. C. Presley and C. W. Lindsley, *ACS Chem. Neurosci.*, 2018, **9**, 2503–2518.

22 H. Kunz, *Arch. Pharm.* , 1887, **225**, 461–479.

23 M. Karamanou, *Curr. Pharm. Des.*, 2018, **24**, 654–658.

24 J. Pelletier and B. Caventou, *J. Ann Chim*, 1820, **15**, 289.

25 P. Śramska, A. Maciejka, A. Topolewska, P. Stepnowski and Ł. P. Haliński, *J. Chromatogr. B*, 2017, **1043**, 202–208.

26 R. A. Goldstein, C. DesLauriers, A. Burda and K. Johnson-Arbor, *Semin. Diagn. Pathol.*, 2009, **26**, 10–17.

27 M. Goerig, D. Bacon and A. van Zundert, *Reg. Anesth. Pain Med.*, 2012, **37**, 318–324.

28 M. B. Roberfroid, *Br. J. Nutr.*, 2005, **93**, S13–S25.

29 H. Haas, *Am. J. Med.*, 1983, **75**, 1–3.

30 V. Podwyssotski, *Arch. Exp. Pathol. Pharmakol.*, 1880, **13**, 29–52.

31 M. Guerram, Z.-Z. Jiang and L.-Y. Zhang, *Chin. J. Nat. Med.*, 2012, **10**, 161–169.

32 C. Canel, R. M. Moraes, F. E. Dayan and D. Ferreira, *Phytochemistry*, 2000, **54**, 115–120.

33 X. Zhang, K. P. Rakesh, C. S. Shantharam, H. M. Manukumar, A. M. Asiri, H. M. Marwani and H.-L. Qin, *Bioorg. Med. Chem.*, 2018, **26**, 340–355.

34 E. K. Rowinsky and R. C. Donehower, *N. Engl. J. Med.*, 1995, **332**, 1004–1014.

35 A. G. Atanasov, B. Waltenberger, E.-M. Pferschy-Wenzig, T. Linder, C. Wawrosch, P. Uhrin, V. Temml, L. Wang, S. Schwaiger, E. H. Heiss, J. M. Rollinger, D. Schuster, J. M. Breuss, V. Bochkov, M. D. Mihovilovic, B. Kopp, R. Bauer, V. M. Dirsch and H. Stuppner, *Biotechnol. Adv.*, 2015, **33**, 1582–1614.

36 N. Thomford, D. Senthebane, A. Rowe, D. Munro, P. Seele, A. Maroyi and K. Dzobo, *Int. J. Mol. Sci.*, 2018, **19**, 1578.

37 D. J. Newman and G. M. Cragg, *J. Nat. Prod.*, 2016, **79**, 629–661.

38 B. David, J.-L. Wolfender and D. A. Dias, *Phytochem. Rev.*, 2015, **14**, 299–315.

39 C.-T. Che and H. Zhang, *Int. J. Mol. Sci.*, 2019, **20**, 830.

40 D. J. Newman, G. M. Cragg and D. G. I. Kingston, in *The Practice of Medicinal Chemistry*, Elsevier, Cambridge MA, 4th edn., 2015, pp. 101–139.

41 E. Patridge, P. Gareiss, M. S. Kinch and D. Hoyer, *Drug Discovery Today*, 2016, **21**, 204–207.

42 G. Tan, C. Gyllenhaal and D. Soejarto, *Curr. Drug Targets*, 2006, **7**, 265–277.

43 Z. Jin and G. Yao, *Nat. Prod. Rep.*, 2019, **36**, 1462–1488.

44 A. Alvin, K. I. Miller and B. A. Neilan, *Microbiol. Res.*, 2014, **169**, 483–495.

45 J. le Roux, *The Biodiversity of South Africa 2002 - Indicators, Trends and Human Impacts*, Struik Publishers, Cape Town, 2002.

46 M. Cherry, *PLoS Biol.*, 2005, **3**, e145.

47 C. W. Fennell and J. van Staden, *J. Ethnopharmacol.*, 2001, **78**, 15–26.

48 J. Refaat, M. S. Kamel, M. A. Ramadan and A. A. Ali, *Int. J. Pharm. Sci. Res.*, 2013, **4**, 1239–1252.

49 A. Cimmino, M. Masi, M. Evidente, S. Superchi and A. Evidente, *Chirality*, 2017, **29**, 486–499.

50 F. Viladomat, J. Bastida, C. Codina, J. J. Nair and W. E. Campbell, *Nat. Prod. Commun.*

51 Z. Jin, *Nat. Prod. Rep.*, 2016, **33**, 606–614.

52 Ç. Karakoyun, M. Masi, A. Cimmino, M. A. Önür, N. U. Somer, A. Kornienko and A. Evidente, *Nat. Prod. Commun.*, 2019, **14**, 1–6.

53 G. Duncan, B. Jeppe and L. Voigt, *The Amaryllidaceae of Southern Africa*, Umdaus Press, Pretoria, 2016.

54 Z. Jin and X.-H. Xu, in *Natural Products - Phytochemistry, Botany and Metabolism of Alkaloids, Phenolics and Terpenes*, eds. K. G. Ramawat and J. M. Merillon, Springer-Verlag Berlin Heidelberg, 1st edn., 2013, pp. 479–514.

55 R. Gotti, J. Fiori, M. Bartolini and V. Cavrini, *J. Pharm. Biomed. Anal.*, 2006, **42**, 17–24.

56 M. Šafratová, A. Hostalková, D. Hulcová, K. Breiterová, V. Hrabcová, M. Machado, D. Fontinha, M. Prudêncio, J. Kuneš, J. Chlebek, D. Jun, M. Hrabinová, L. Nováková, R. Havelek, M. Seifrtová, L. Opletal and L. Cahlíková, *Arch. Pharm. Res.*, 2018, **41**, 208–218.

57 N. Vaněčková, A. Hošťálková, M. Šafratová, J. Kuneš, D. Hulcová, M. Hrabinová, I. Doskočil, Š. Štěpánková, L. Opletal, L. Nováková, D. Jun, J. Chlebek and L. Cahlíková, *RSC Adv.*, 2016, **6**, 80114–80120.

58 N. Cortes, R. A. Posada-duque, R. Alvarez, F. Alzate, S. Berkov, G. P. Cardona-gómez and E. Osorio, *Life Sci.*, 2015, **122**, 42–50.

59 A. Evidente and A. Kornienko, *Phytochem. Rev.*, 2009, **8**, 449–459.

60 A. Evidente, A. S. Kireev, A. R. Jenkins, A. E. Romero, W. F. A. Steelant, S. Van Slambrouck and A. Kornienko, *Planta Med.*, 2009, **75**, 501–507.

61 M. Roy, L. Liang, X. Xiao, P. Feng, M. Ye and J. Liu, *Biomed. Pharmacother.*, 2018, **107**, 615–624.

62 J. J. Nair, J. Bastida, C. Codina, F. Viladomat and J. van Staden, *Nat. Prod. Commun.*, 2013, **8**, 1335–1350.

63 D. Lamoral-Theys, C. Decaestecker, V. Mathieu, J. Dubois, A. Kornienko, R. Kiss, A. Evidente and L. Pottier, *Mini-Reviews Med. Chem.*, 2010, **10**, 41–50.

64 S. G. Ghane, U. A. Attar, P. B. Yadav and M. M. Lekhak, *Ind. Crops Prod.*, 2018, **125**, 168–177.

65 P. Zhang, M. Zhang, D. Yu, W. Liu, L. Hu, B. Zhang, Q. Zhou and Z. Cao, *J. Cell. Physiol.*, 2019, **234**, 10566–10575.

66 Y. Sun, P. Wu, Y. Sun, F. S. Sharopov, Q. Yang, F. Chen, P. Wang and Z. Liang, *Biochem. Biophys. Res. Commun.*, 2018, **495**, 911–921.

67 J. J. Sramek, E. J. Frackiewicz and N. R. Cutler, *Expert Opin. Investig. Drugs*, 2000, **9**, 2393–2402.

68 P. V. Fish, D. Steadman, E. D. Bayle and P. Whiting, *Bioorg. Med. Chem. Lett.*, 2019, **29**, 125–133.

69 J. Refaat, M. S. Kamel, M. A. Ramadan and A. A. Ali, *Int. J. Pharm. Sci. Res.*, 2012, **3**, 1883–1890.

70 J. Refaat, M. S. Kamel, M. A. Ramadan and A. A. Ali, *Int. J. Pharm. Sci. Res.*, 2012, **3**, 3630–3638.

71 J. Refaat, M. S. Kamel, M. A. Ramadan and A. A. Ali, *Int. J. Pharm. Sci. Res.*, 2013, **4**, 1239–

1252.

72 S. M. Colegate and R. J. Molyneux, Eds., *Bioactive Natural Products: Detection, Isolation and Structural Determination*, CRC Press, Boca Raton, 2nd edn., 2008.

73 A. Cimmino, V. Mathieu, M. Masi, R. Baroncelli, A. Boari, G. Pescitelli, M. Ferderin, R. Lisy, M. Evidente, A. Tuzi, M. C. Zonno, A. Kornienko, R. Kiss and A. Evidente, *J. Nat. Prod.*, 2016, **79**, 116–125.

74 T. Tanahashi, A. Poulev and M. Zenk, *Planta Med.*, 1990, **56**, 77–81.

75 A. K. Jäger, A. Adsersen and C. W. Fennell, *S. Afr. J. Bot.*, 2004, **70**, 323–325.

76 K. Likhitwitayawuid, C. K. Angerhofer, H. Chai, J. M. Pezzuto, G. A. Cordell and N. Ruangrungsi, *J. Nat. Prod.*, 1993, **56**, 1331–1338.

77 W. E. Campbell, J. J. Nair, D. W. Gammon, J. Bastida, C. Codina, F. Viladomat, P. J. Smith and C. F. Albrecht, *Planta Med.*, 1998, **64**, 91–93.

78 J. Razafimbelo, M. Andriantsiferana, G. Baudouin and F. Tillequin, *Phytochemistry*, 1996, **41**, 323–326.

79 G. S. Citoglu, B. S. Yilmaz and O. Bahadir, *Chem. Nat. Compd.*, 2008, **44**, 826–828.

80 G. I. Kaya, D. Cicek, B. Sarıkaya, M. A. Onur and N. U. Somer, *Nat. Prod. Commun.*, 2010, **5**, 873–876.

81 A. Evidente, I. Iasiello and G. Randazzo, *J. Chromatogr. A*, 1983, **281**, 362–366.

82 O. B. Abdel-Halim, T. Morikawa, S. Ando, H. Matsuda and M. Yoshikawa, *J. Nat. Prod.*, 2004, **67**, 1119–1124.

83 D. Lamoral-Theys, A. Andolfi, G. Van Goietsenoven, A. Cimmino, B. Le Calvé, N. Wauthoz, V. Mégalizzi, T. Gras, C. Bruyère, J. Dubois, V. Mathieu, A. Kornienko, R. Kiss and A. Evidente, *J. Med. Chem.*, 2009, **52**, 6244–6256.

84 W. C. Wildman and C. J. Kaufman, *J. Am. Chem. Soc.*, 1954, **76**, 5815–5816.

85 Y. Toriizuka, E. Kinoshita, N. Kogure, M. Kitajima, A. Ishiyama, K. Otoguro, H. Yamada, S. Omura and H. Takayama, *Bioorg. Med. Chem.*, 2008, **16**, 10182–10189.

86 W. A. Ayer and G. C. Kasitu, *Can. J. Chem.*, 1989, **67**, 1077–1086.

87 J. Bastida, R. Lavilla and F. Viladomat, in *The Alkaloids: Chemistry and Biology*, ed. G. A. Cordell, Elsevier Academic Press, Cambridge MA, 2006, vol. 63, pp. 87–179.

88 T. Nishimata and M. Mori, *J. Org. Chem.*, 1998, **63**, 7586–7587.

89 V. Pabuççuoglu, P. Richomme, T. Gözler, B. Kivçak, A. Freyer and M. Shamma, *J. Nat. Prod.*, 1989, **52**, 785–791.

90 G. Luchetti, R. Johnston, V. Mathieu, F. Lefranc, K. Hayden, A. Andolfi, D. Lamoral-Theys, M. R. Reisenauer, C. Champion, S. C. Pelly, W. A. L. van Otterlo, I. V Magedov, R. Kiss, A. Evidente, S. Rogelj and A. Kornienko, *ChemMedChem*, 2012, **7**, 815–822.

91 A. Ali, M. Ramadan and A. Frahm, *Planta Med.*, 1984, **50**, 424–427.

92 A. Evidente, *J. Nat. Prod.*, 1986, **49**, 168–169.

93 M. Ochi, H. Otsuki and K. Nagao, *Bull. Chim. Soc. Japan*, 1976, **49**, 3363–3364.

94 H. Hauth and D. Stauffacher, *Helv. Chim. Acta*, 1964, **47**, 185–194.

95 J. H. Rigby, A. Cavezza and M. J. Heeg, *J. Am. Chem. Soc.*, 1998, **120**, 3664–3670.

96 D. Katoch, S. Kumar, N. Kumar and B. Singh, *J. Pharm. Biomed. Anal.*, 2012, **71**, 187–192.

97 Y. Tian, C. Zhang, M. Guo and M. Iriti, *Molecules*, 2015, **20**, 21854–21869.

98 R. B. Giordani, J. P. De Andrade, H. Verli, J. H. Dutilh, A. T. Henriques, S. Berkov, J. Bastida and J. A. S. Zuanazzi, *Magn. Reson. Chem.*, 2011, **49**, 668–672.

99 E. Shawky, A. H. Abou-Donia, F. A. Darwish, S. M. Toaima, S. S. Takla, N. B. Pigni and J. Bastida, *Chem. Biodivers.*, 2015, **12**, 1184–1199.

100 X. Zhang, H. Huang, X. Liang, H. Huang, W. Dai, Y. Shen, S. Yan and W. Zhang, *Rapid Commun. Mass Spectrom.*, 2009, **23**, 2903–2916.

101 A. Ptak, A. El Tahchy, F. Dupire, M. Boisbrun, M. Henry, Y. Chapleur, M. Mós and D. Laurain-Mattar, *J. Nat. Prod.*, 2009, **72**, 142–147.

102 Y. Endo, Y. Sugiura, M. Funasaki, H. Kagechika, M. Ishibashi and A. Ohsaki, *J. Nat. Med.*, 2019, **73**, 648–652.

103 L. R. Tallini, J. P. de Andrade, M. Kaiser, F. Viladomat, J. J. Nair, J. A. S. Zuanazzi and J. Bastida, *Molecules*, 2017, **22**, 1–12.

104 G. L. Chen, Y. Q. Tian, J. L. Wu, N. Li and M. Q. Guo, *Sci. Rep.*, 2016, **6**, 1–10.

105 G. Chen, Y. Tian and M. Guo, *Rapid Commun. Mass Spectrom.*, 2016, **30**, 95–99.

106 N. Thi Ngoc Tram, T. V. Titorenkova, V. S. Bankova, N. V. Handjieva and S. S. Popov,

Fitoterapia, 2002, 73, 183–208.

107 S. Ghosal, S. Unnikrishnan and S. K. Singh, *Phytochemistry*, 1989, **28**, 2535–2537.

108 S. Kobayashi, K. Satoh, A. Numata, T. Shingu and M. Kihara, *Phytochemistry*, 1991, **30**, 675–677.

109 F. M. Zhang, Y. Q. Tu, J. D. Liu, X. H. Fan, L. Shi, X. D. Hu, S. H. Wang and Y. Q. Zhang, *Tetrahedron*, 2006, **62**, 9446–9455.

110 S. Berkov, A. Pavlov, M. Ilieva, M. Burrus, S. Popov and M. Stanilova, *Phytochem. Anal.*, 2005, **16**, 98–103.

111 I. E. Mark, G. R. Evans and J. Declercq, *Tetrahedron*, 1994, **50**, 4557–4574.

112 S. V. Ley and A. Madin, in *Comprehensive Organic Synthesis: Second Edition*, eds. B. M. Trost and I. Flemming, Elsevier Science Ltd., London, 2nd edn., 1991, vol. 7, pp. 251–289.

Alkaloidal constituents of *Crinum variabile* and *Crinum paludosum*, two southern African Amaryllidaceae species

Kim Henry Steyn

Supplementary Information - Appendices

A Appendix – Crinum variabile

A.1 Tree Diagram – Crinum *variabile*

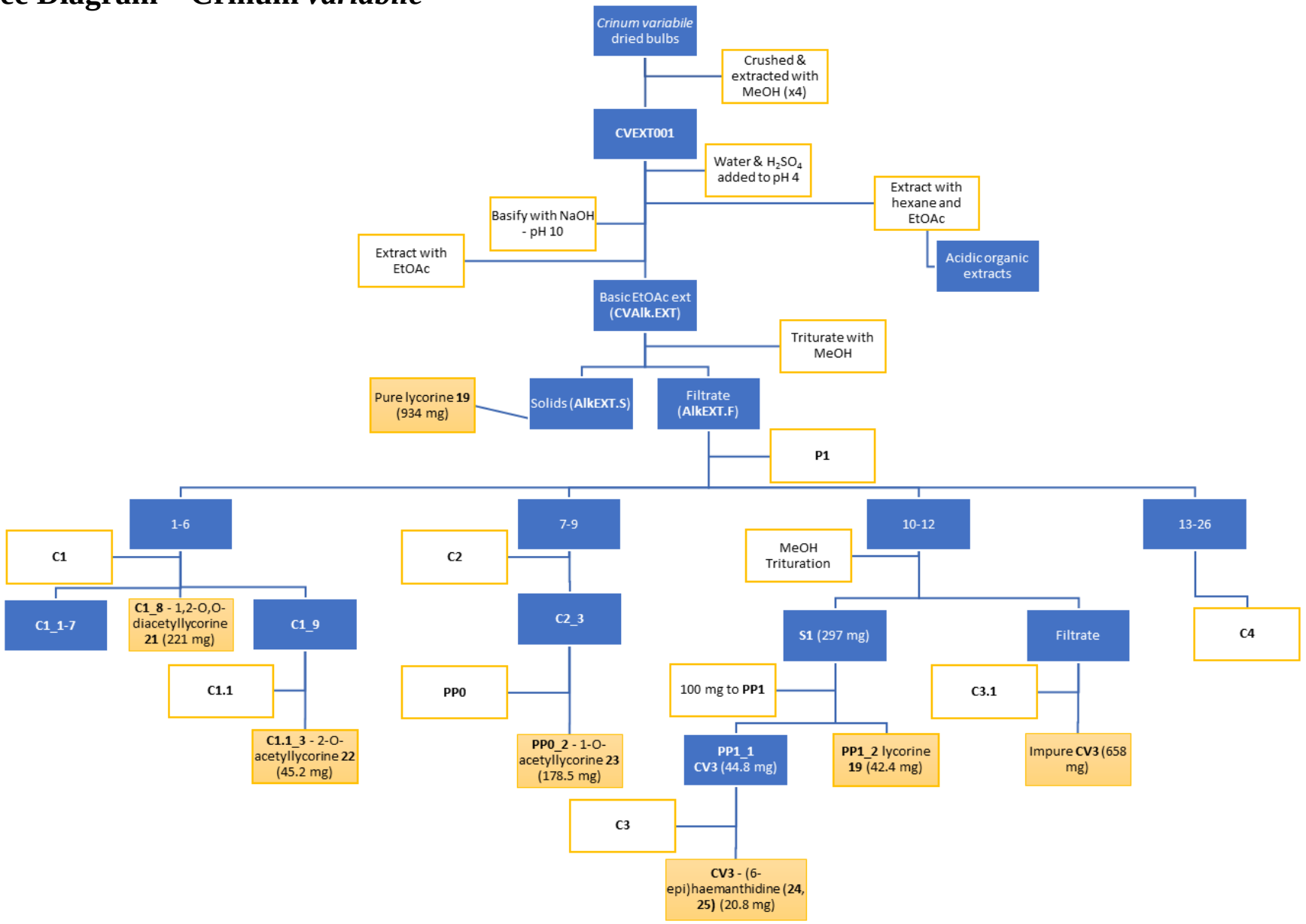

Figure A.1.1 - Tree diagram representing the processing of Crinum variabile *plant material. Continued in Fig A.1.2*

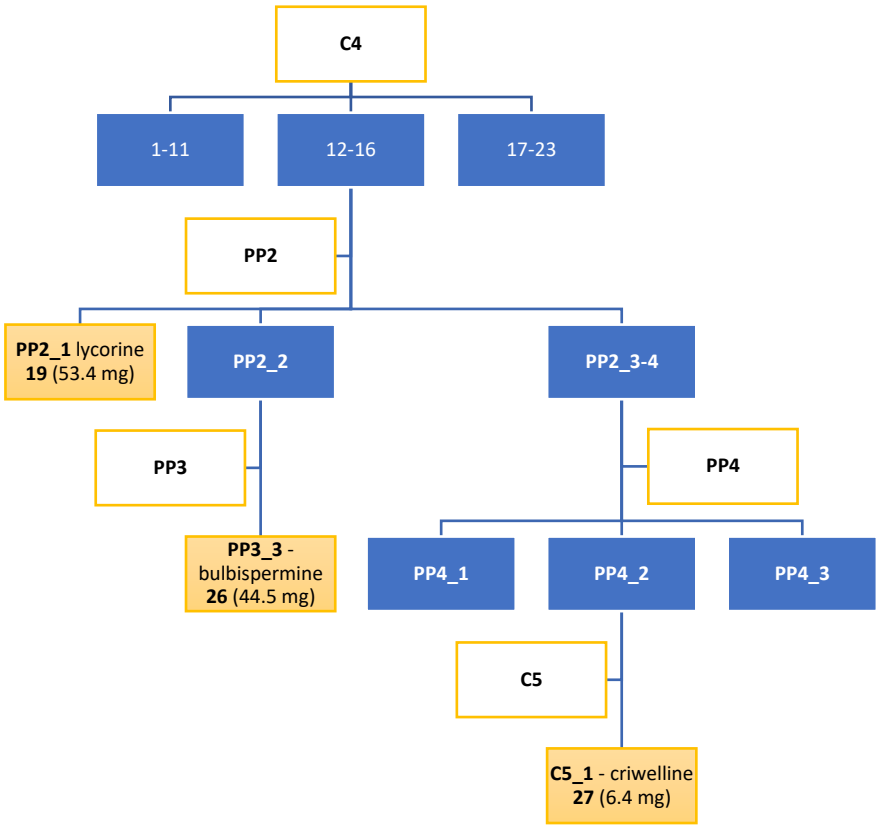

Figure A.1.2 - Tree diagram representing the processing of Crinum variabile *plant material – continued.*

A.2 **Lycorine 19**

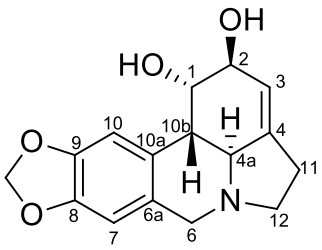

19

*Figure A.2.1 - The numbered chemical structure of lycorine **19**.*

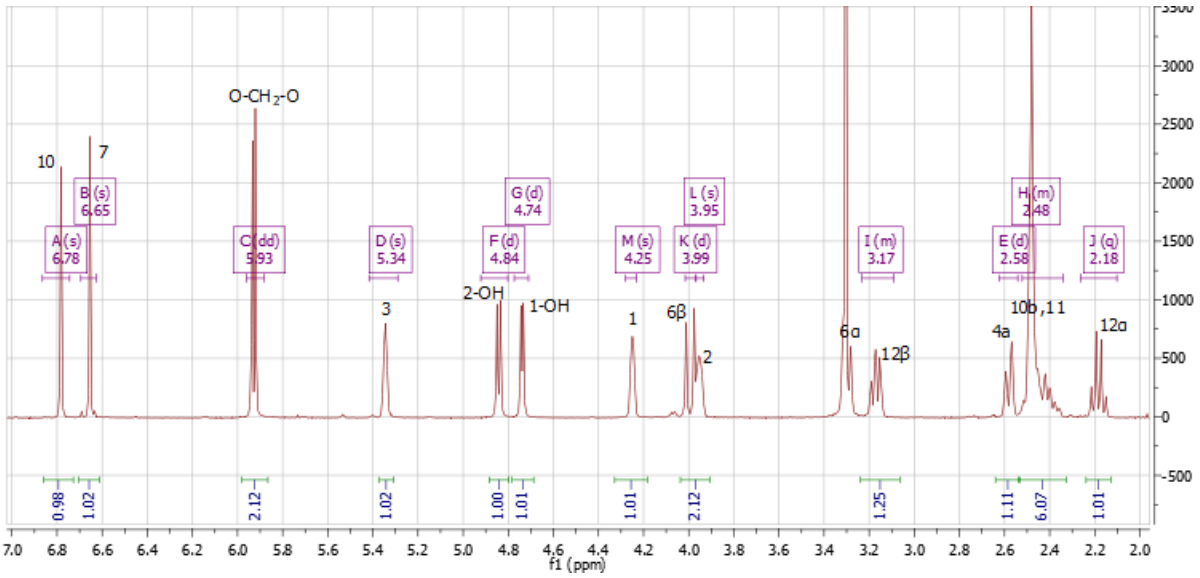

*Figure A.2.2 - ^{1}H spectrum of **19**.*

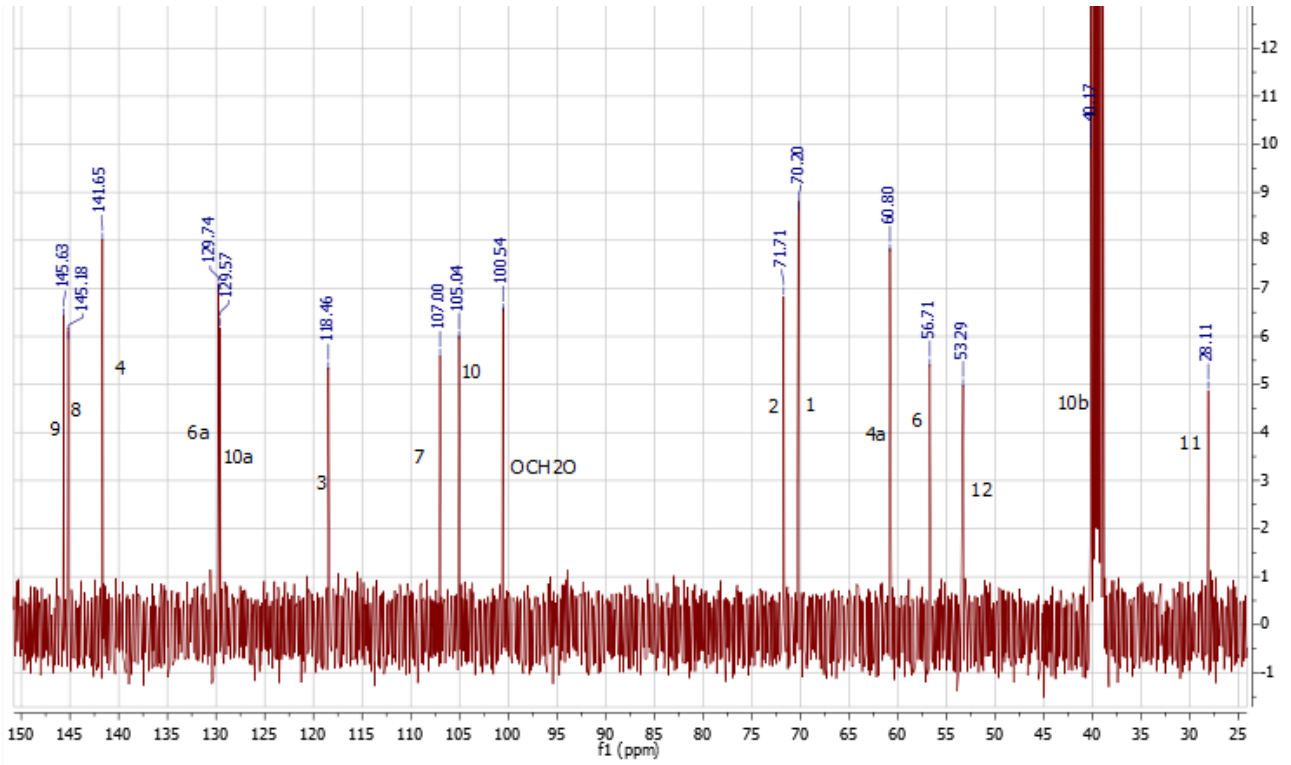

*Figure A.2.3 - ^{13}C spectrum of **19***

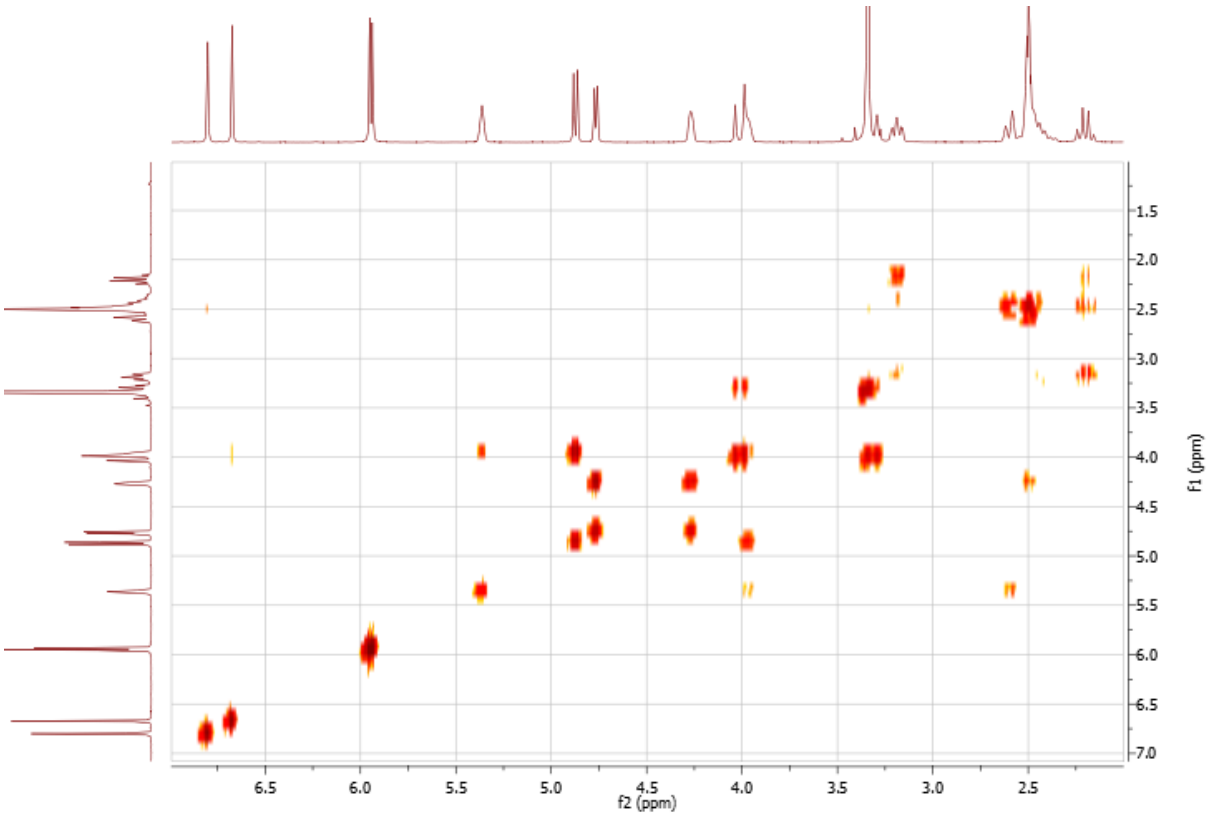

*Figure A.2.4 - COSY spectrum of **19**.*

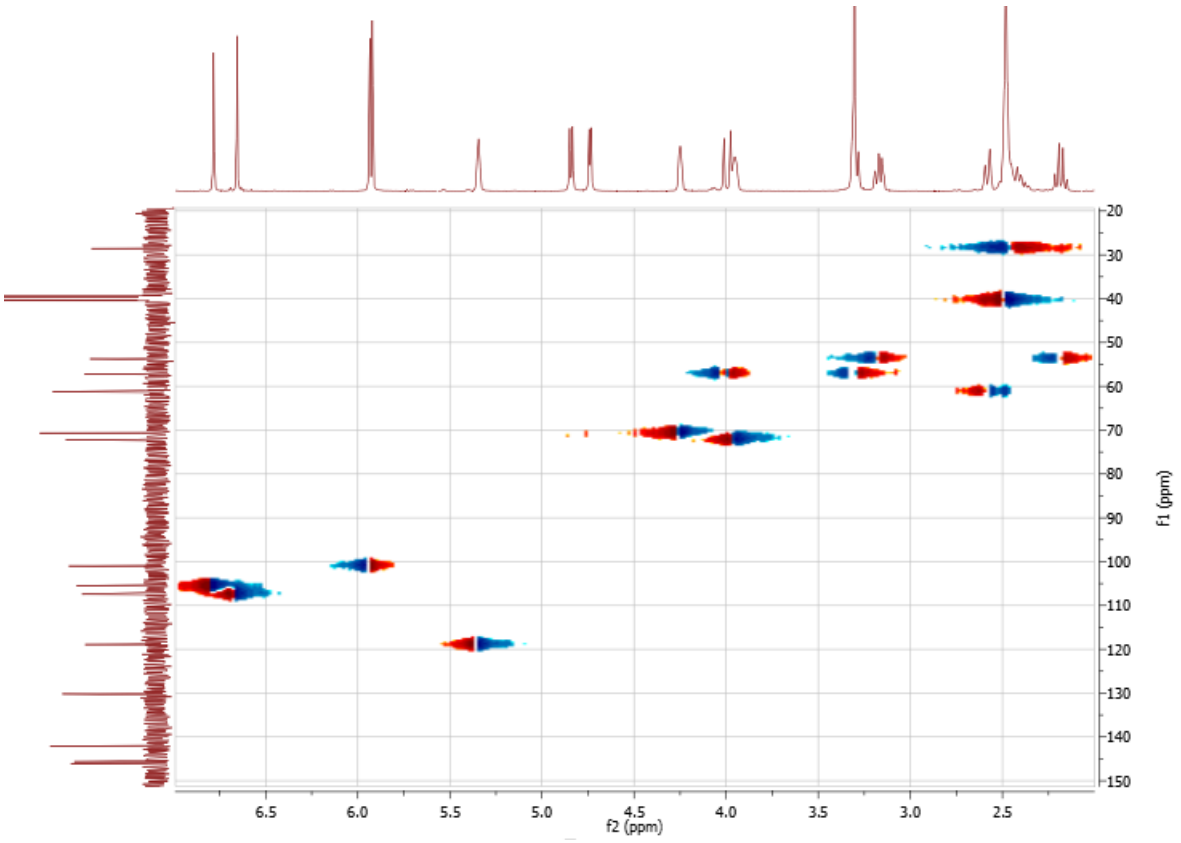

*Figure A.2.5 - HSQC spectrum of **19**.*

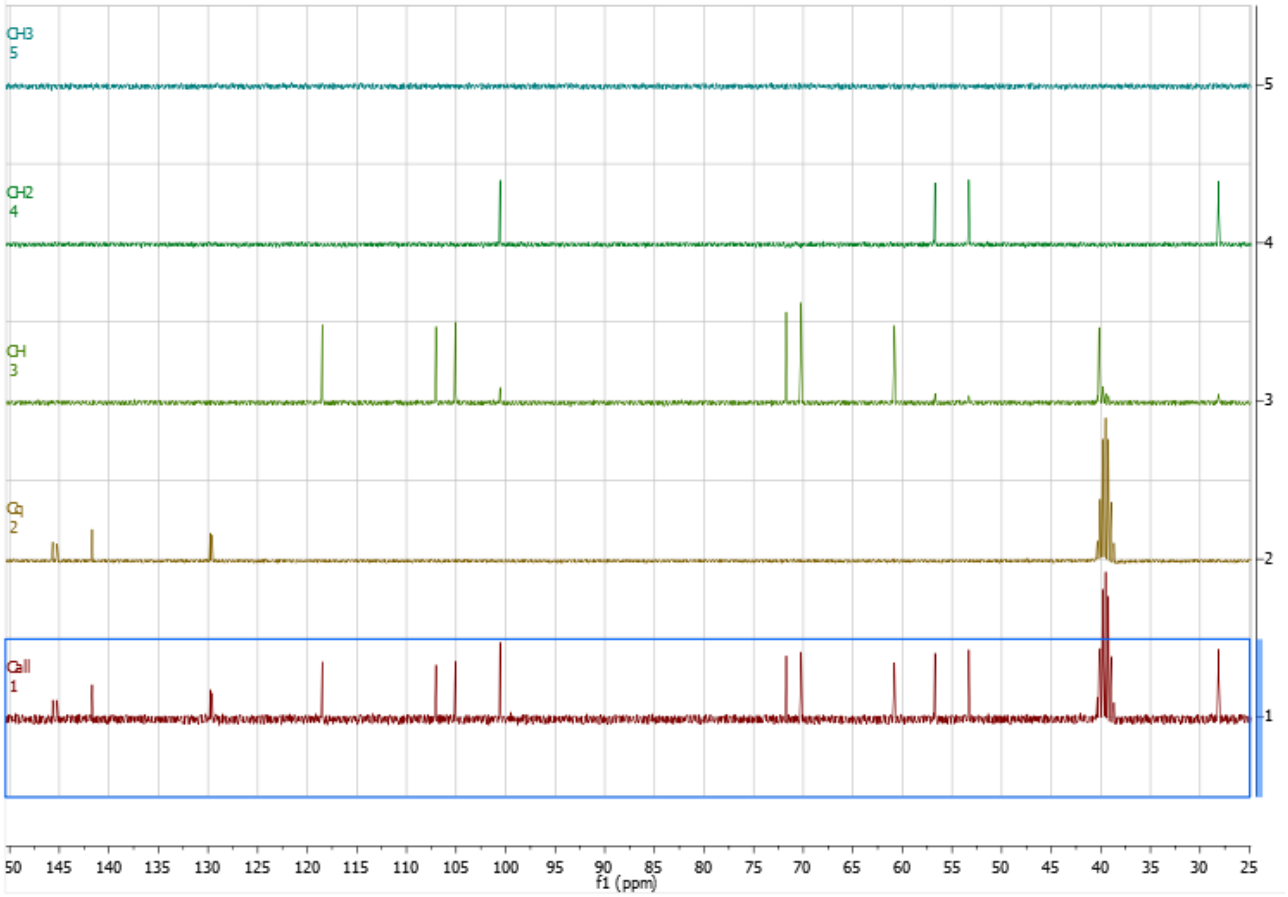

*Figure A.2.6 - DEPT spectrum of **19**.*

A.3 **1,2-O,O-diacetyllycorine 21**

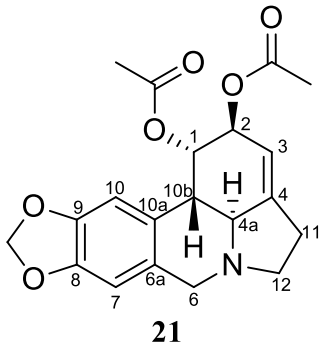

21

*Figure A.3.1 - The numbered chemical structure of **21**.*

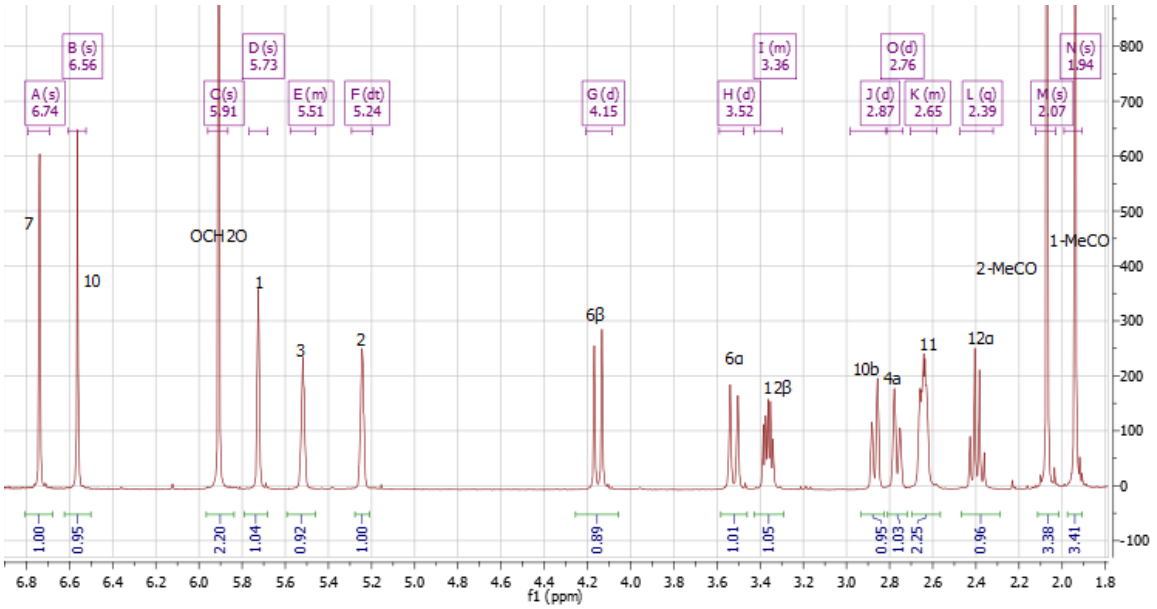

*Figure A.3.2 - [1]H spectrum of **21**.*

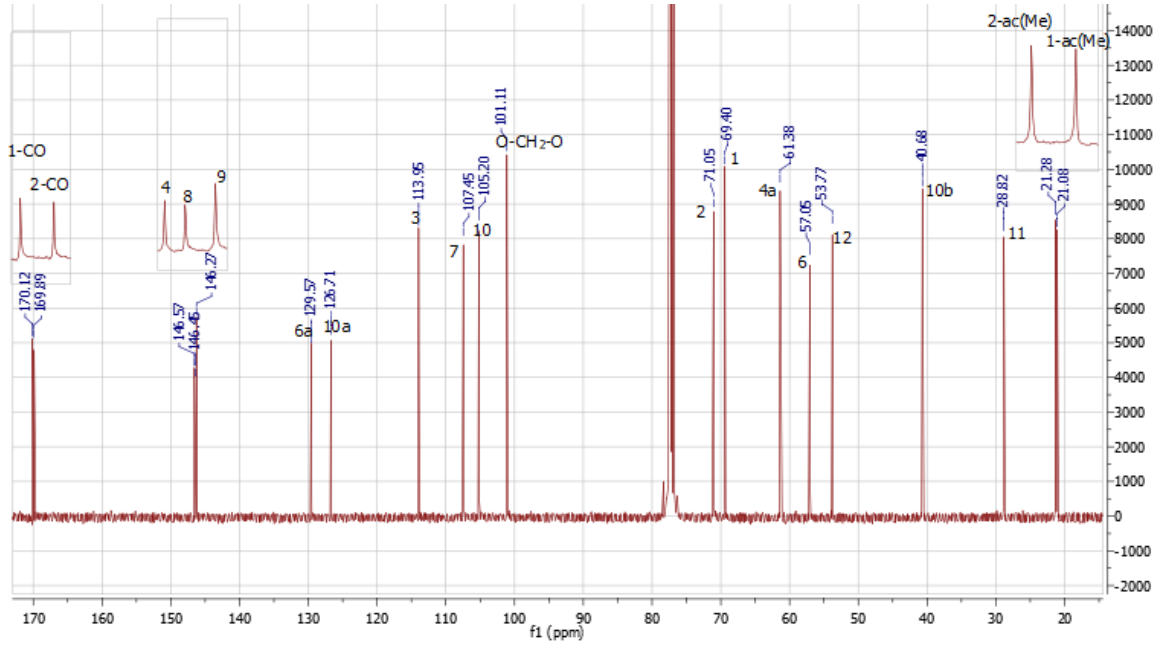

*Figure A.3.3 - [13]C spectrum of **21**.*

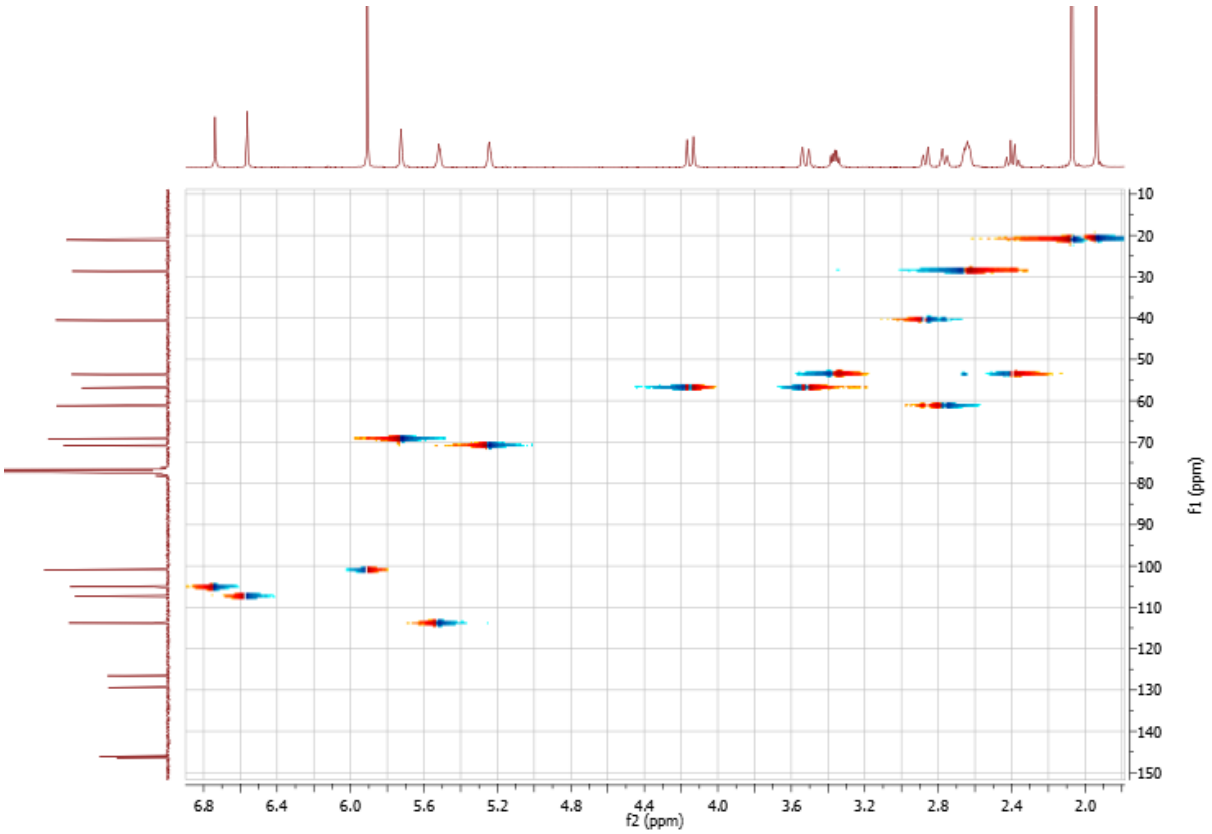

*Figure A.3.4 - HSQC spectrum of **21**.*

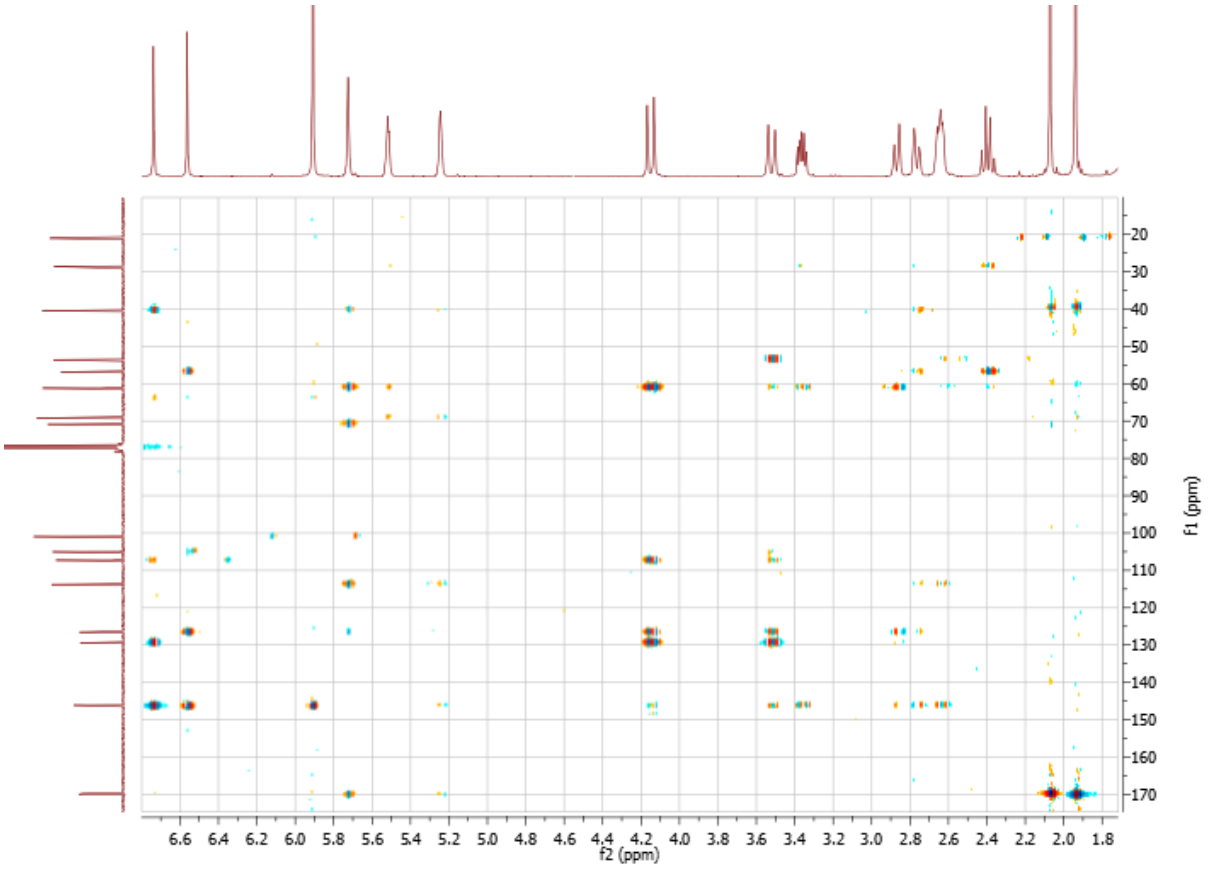

*Figure A.3.5 - HMBC spectrum of **21**.*

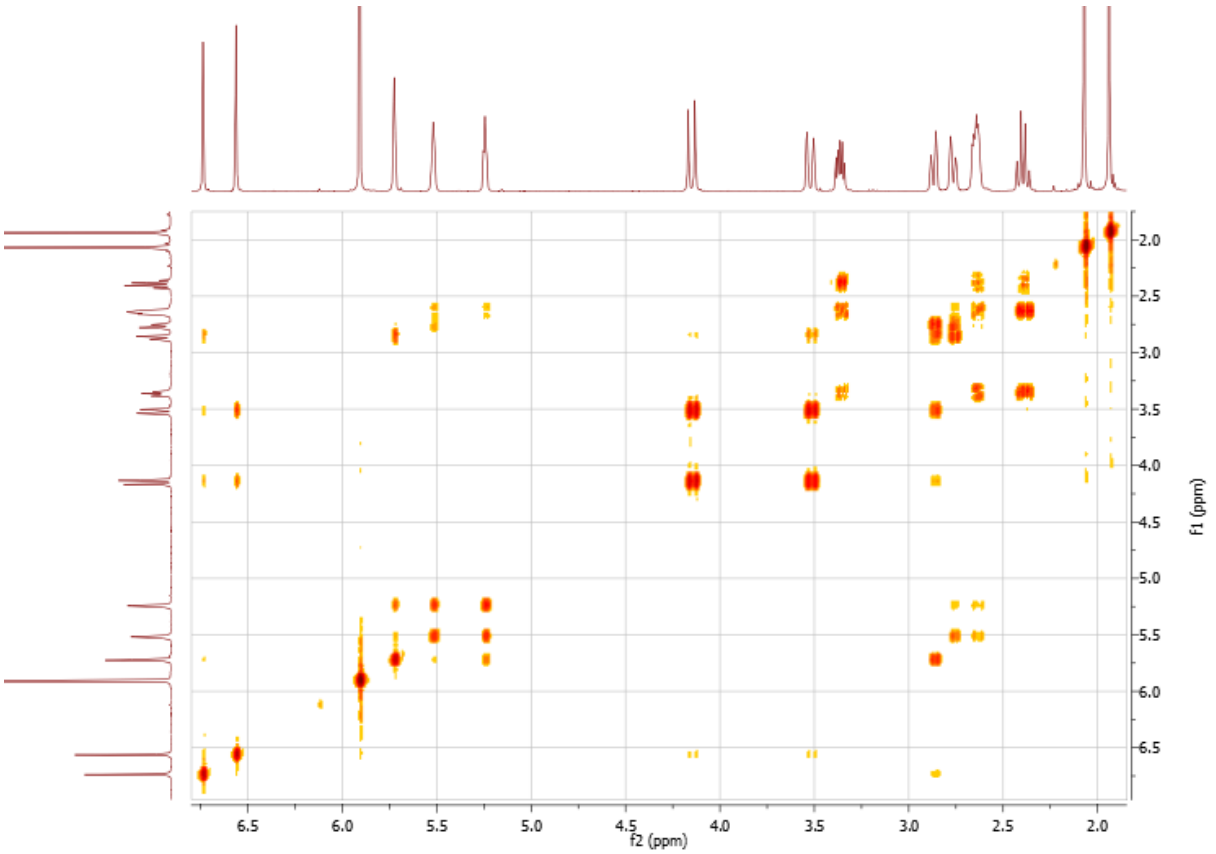

*Figure A.3.6 - COSY spectrum of **21**.*

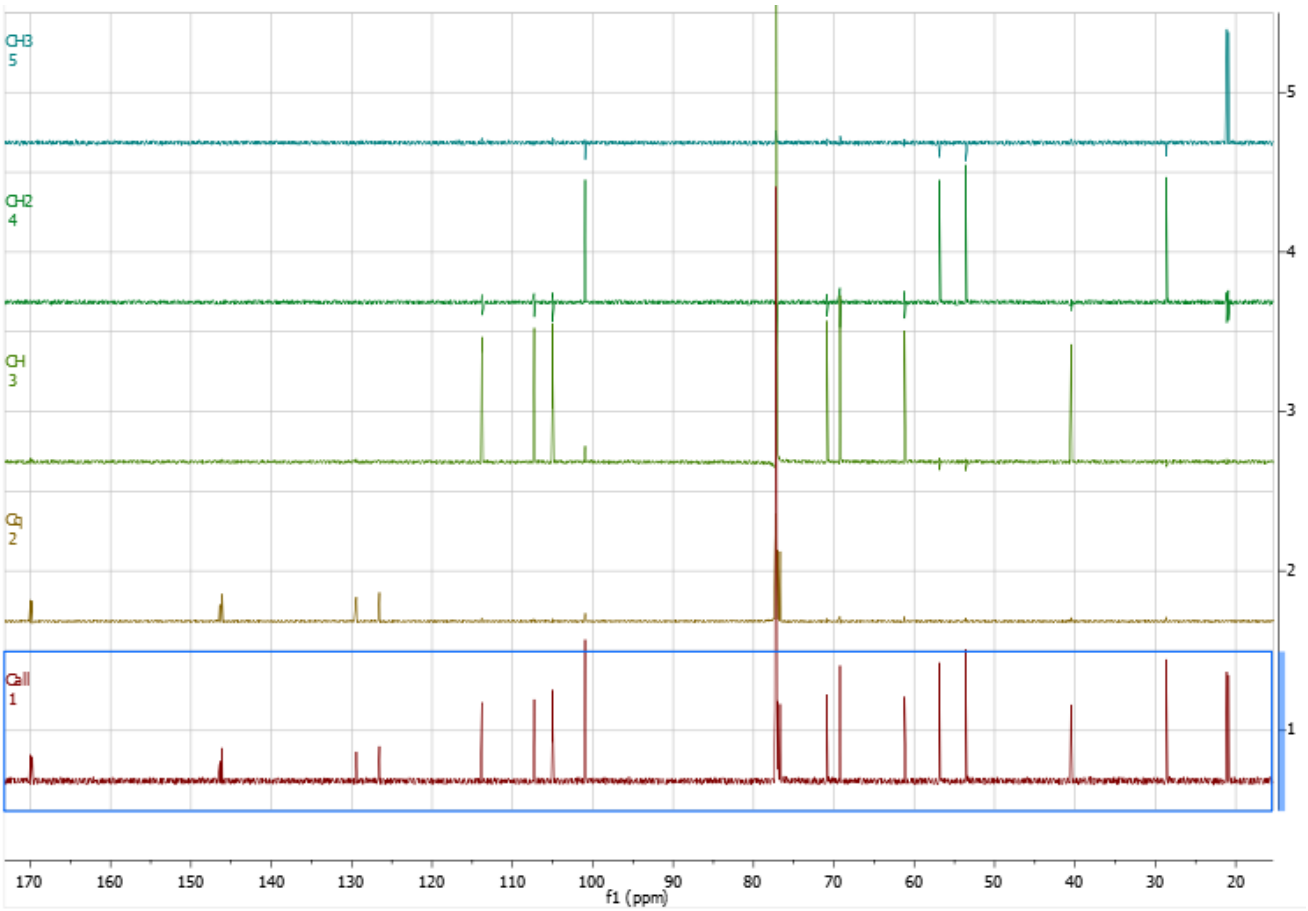

*Figure A.3.7 - DEPT spectrum of **21**.*

A.4 **2-O-acetyllycorine 22**

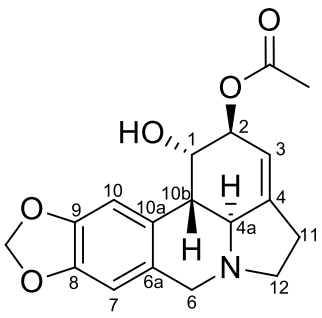

22

*Figure A.4.1 - The numbered structure of **22***

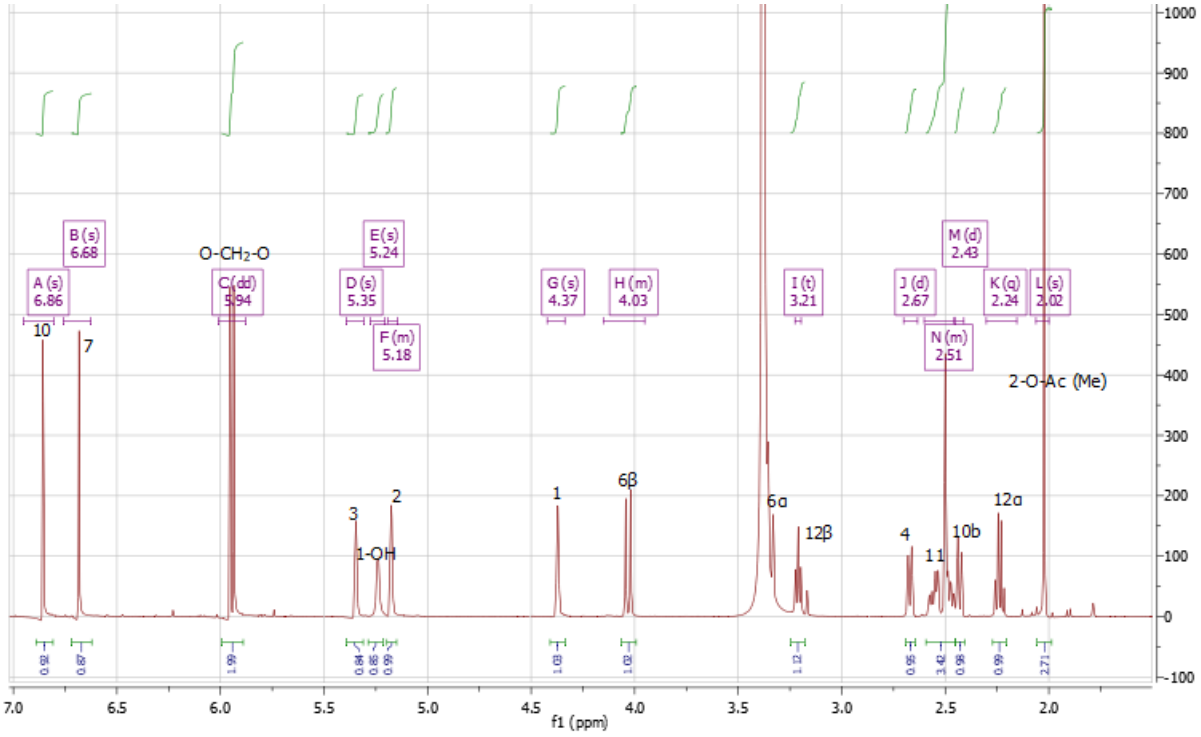

*Figure A.4.2 - The ^{1}H spectrum of **22***

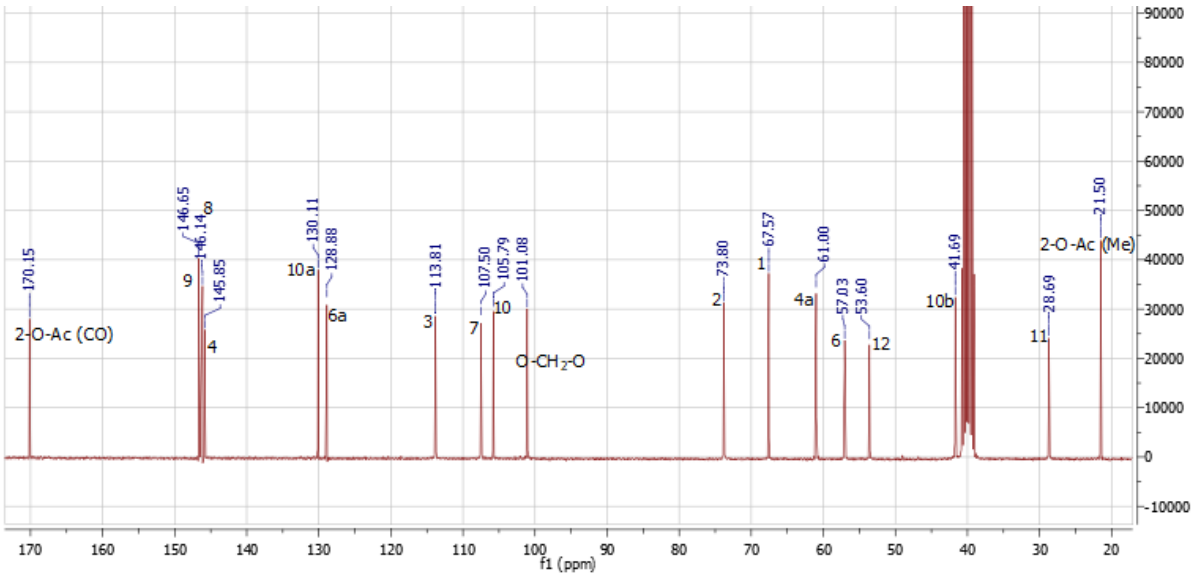

*Figure A.4.3 - ^{13}C spectrum of **22***

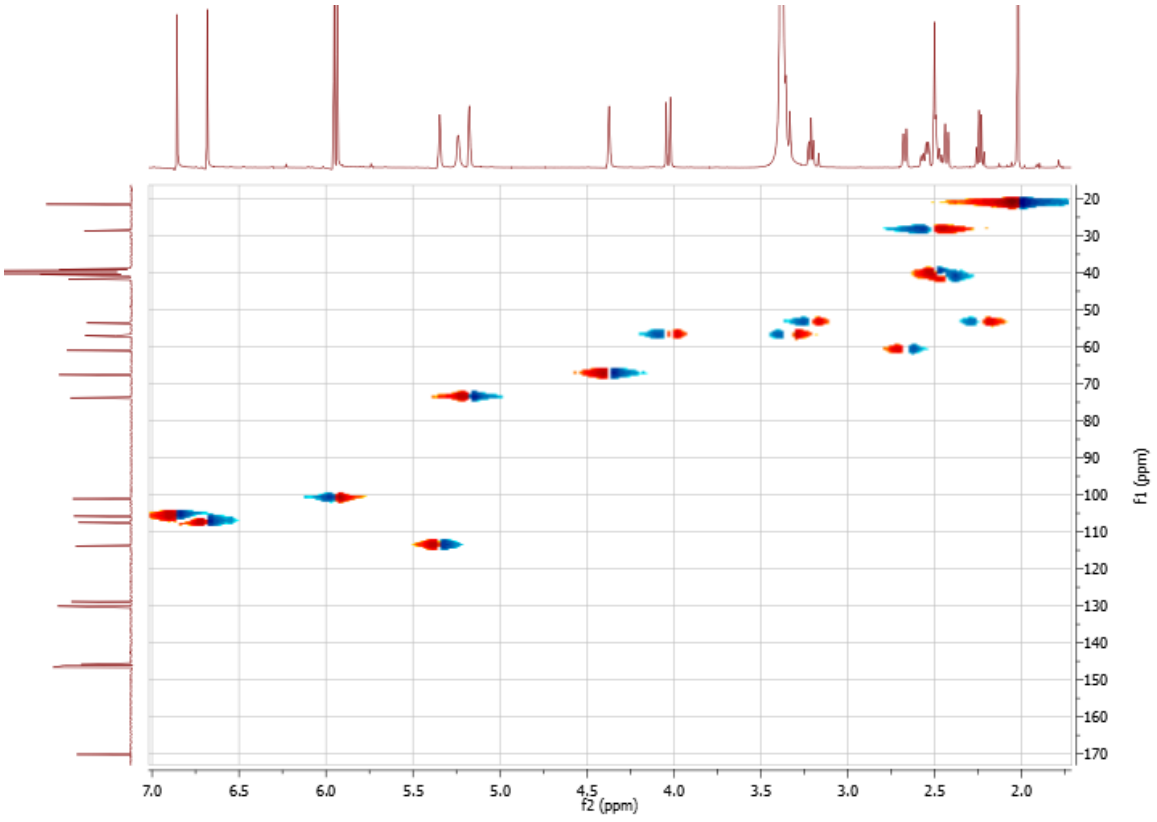

*Figure A.4.4 - HSQC spectrum of **22***

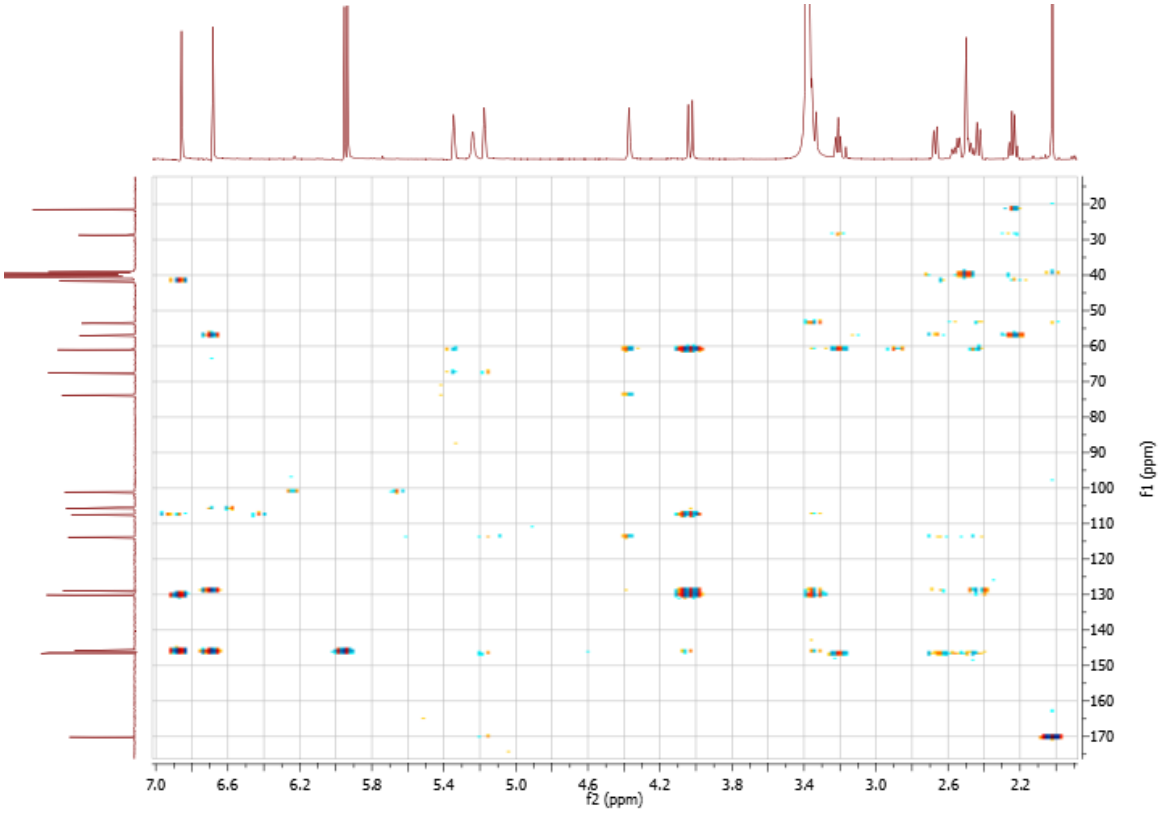

*Figure A.4.5 - HMBC spectrum of **22***

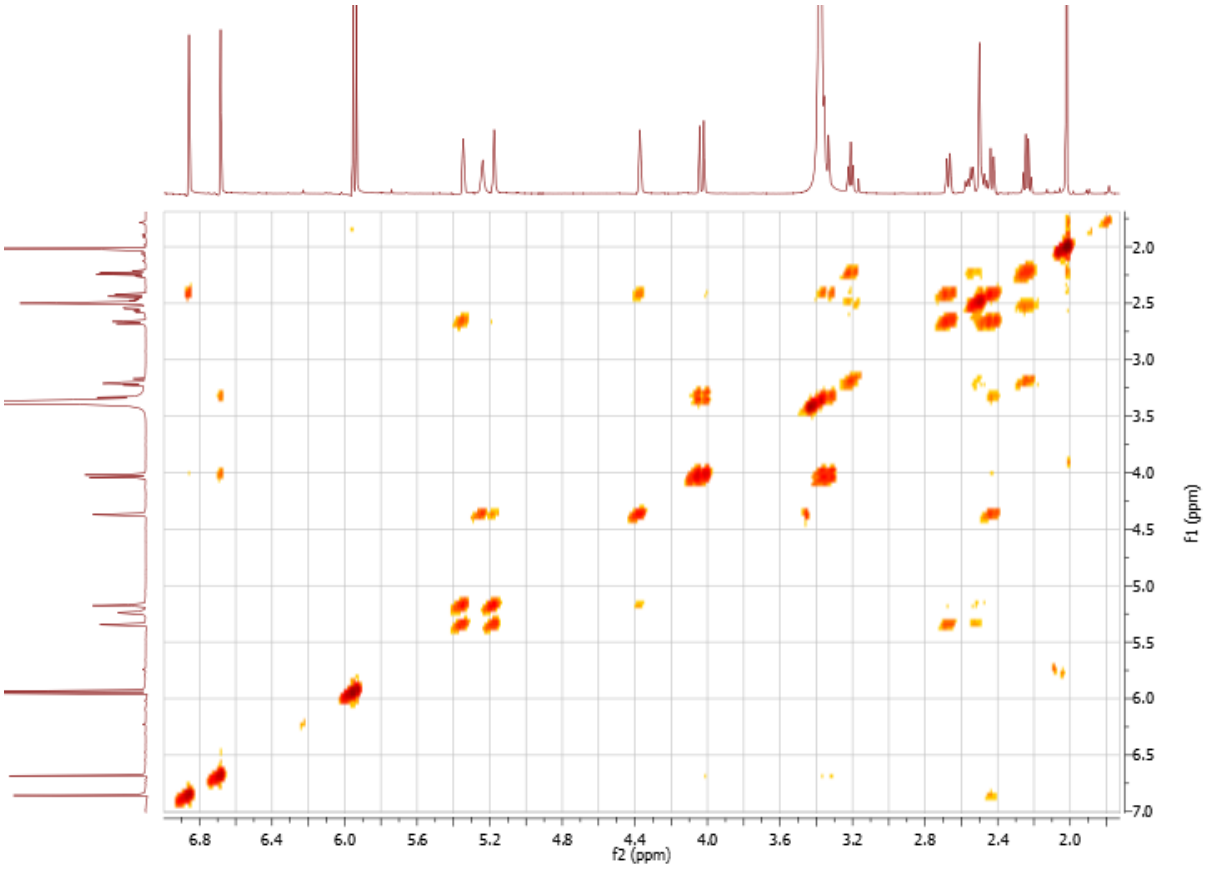

*Figure A.4.6 - COSY spectrum of **22**.*

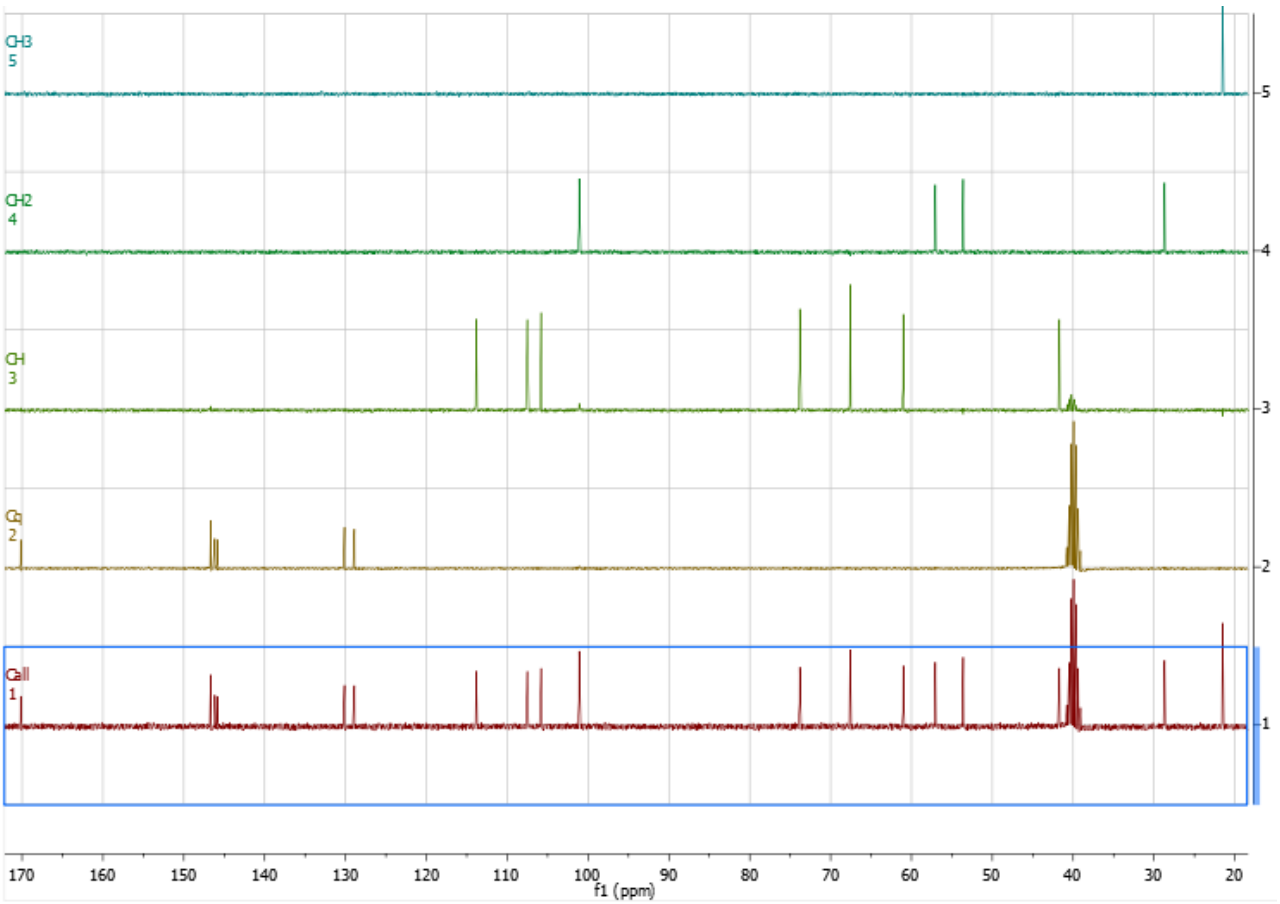

Figure A.4.7 - DEPT spectrum of ***22****.*

A.5 **1-O-acetyllycorine 23**

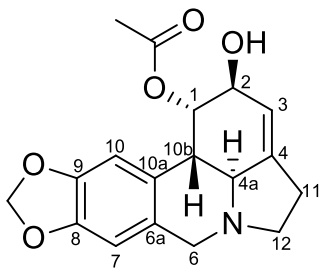

23

*Figure A.5.1 - Numbered chemical structure of **23**.*

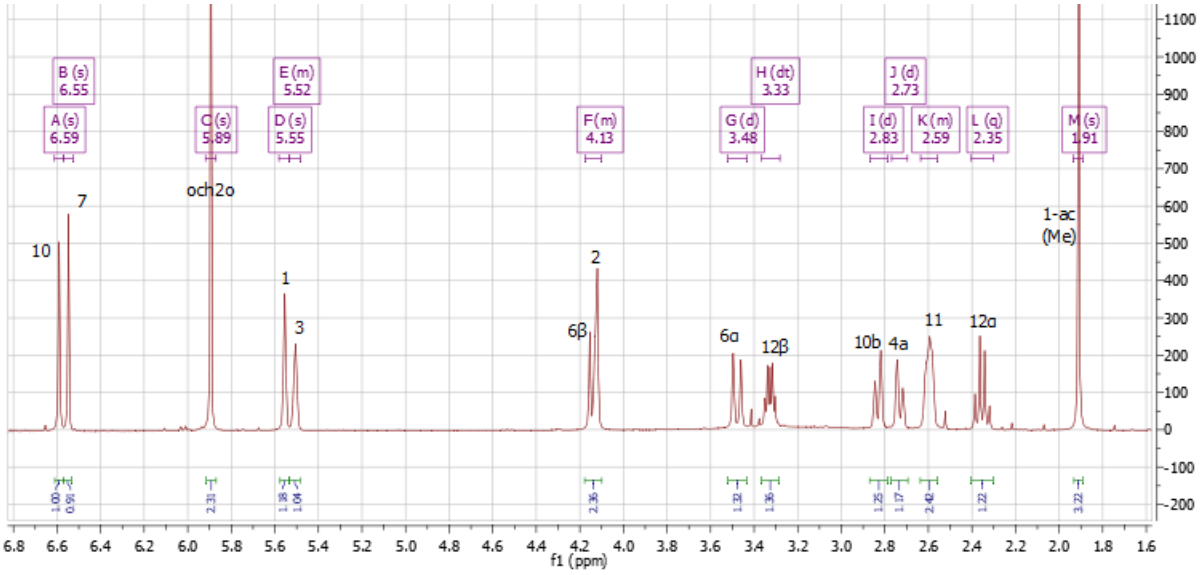

*Figure A.5.2 - ^{1}H spectrum of **23**.*

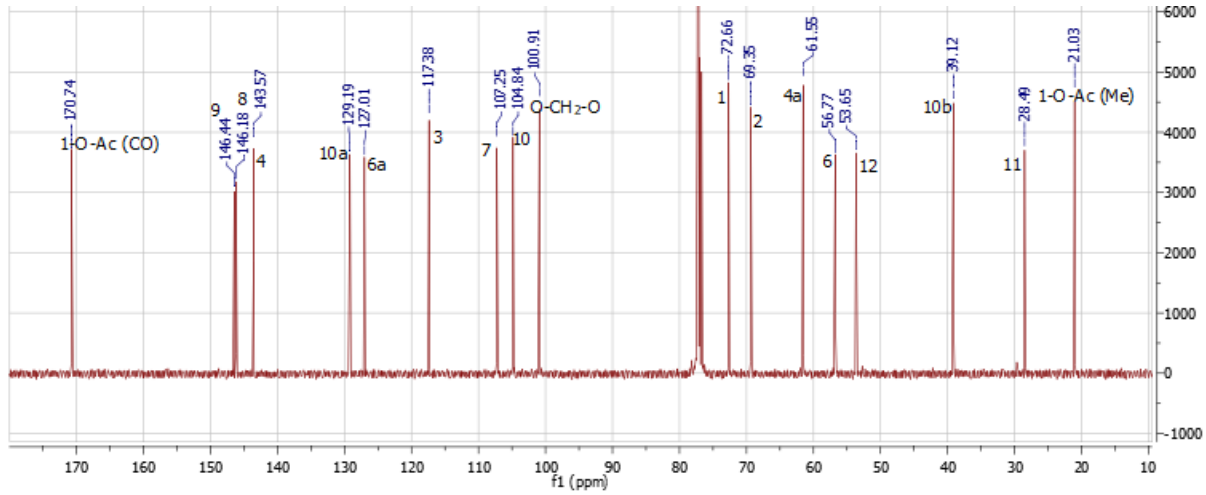

*Figure A.5.3 - ^{13}C spectrum of **23**.*

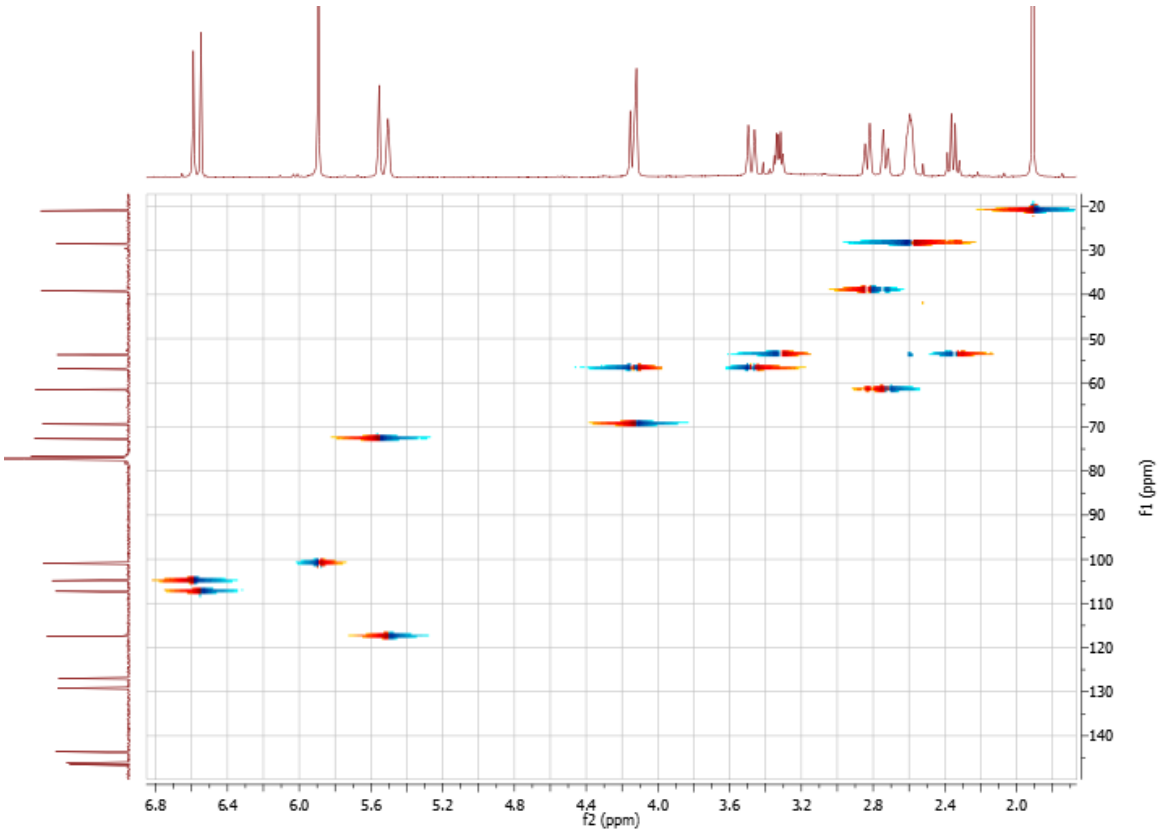

*Figure A.5.4 - HSQC spectrum of **23**.*

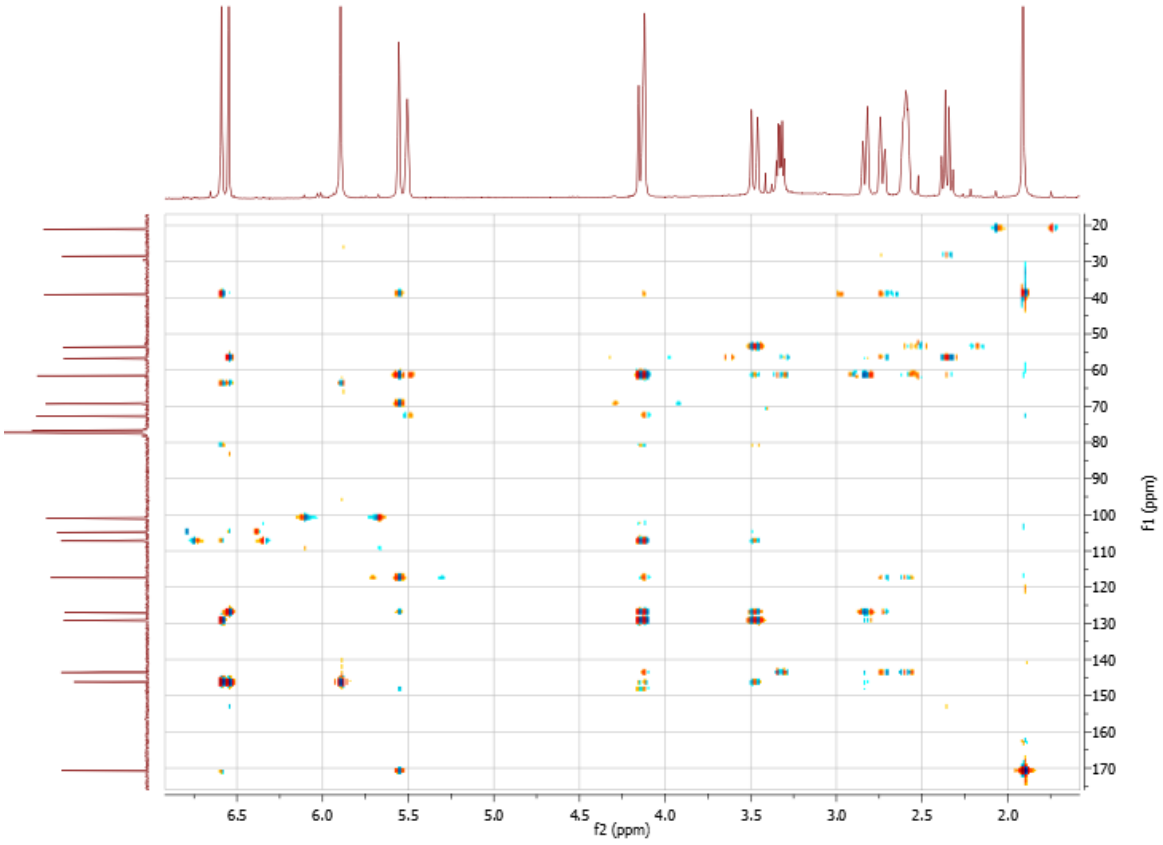

*Figure A.5.5 - HMBC spectrum of **23***

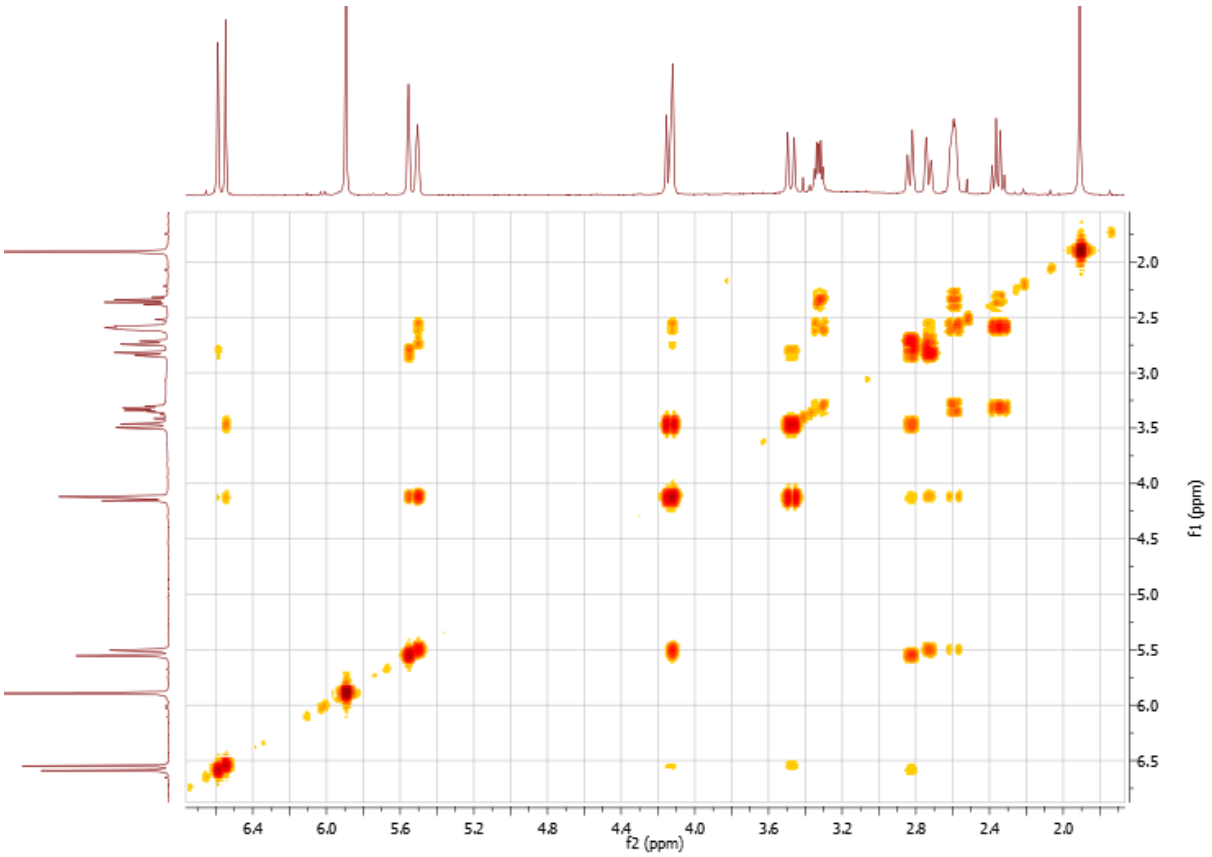

*Figure A.5.6 - COSY spectrum of **23**.*

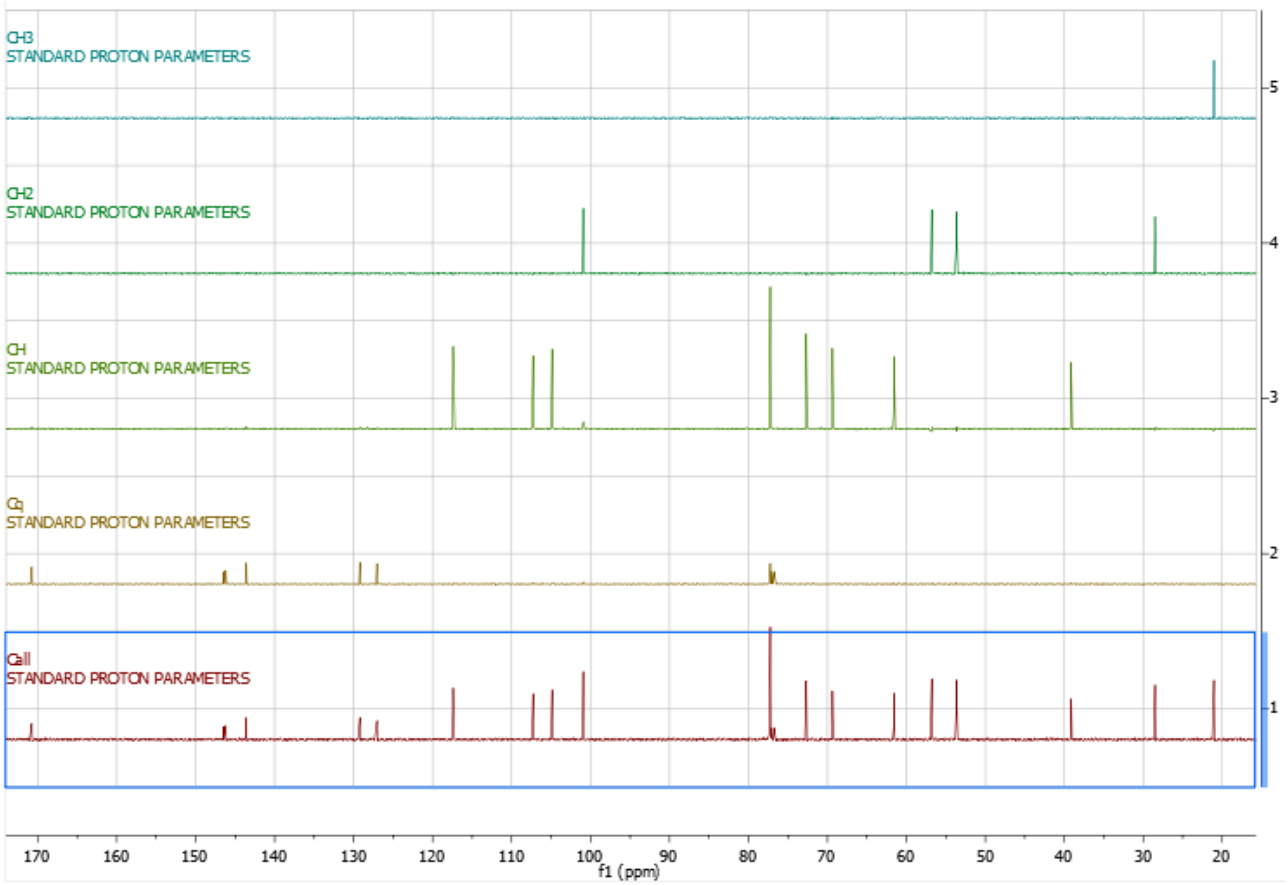

*Figure A.5.7 - DEPT spectrum of **23**.*

A.6 **Haemanthidine and 6-epihaemanthidine 24, 25**

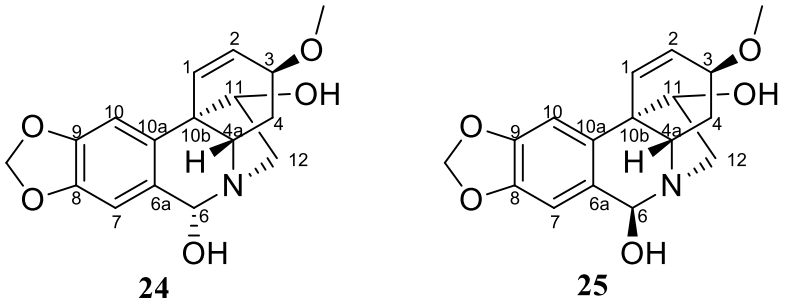

*Figure A.6.1 - Chemical structures of **24** and **25**.*

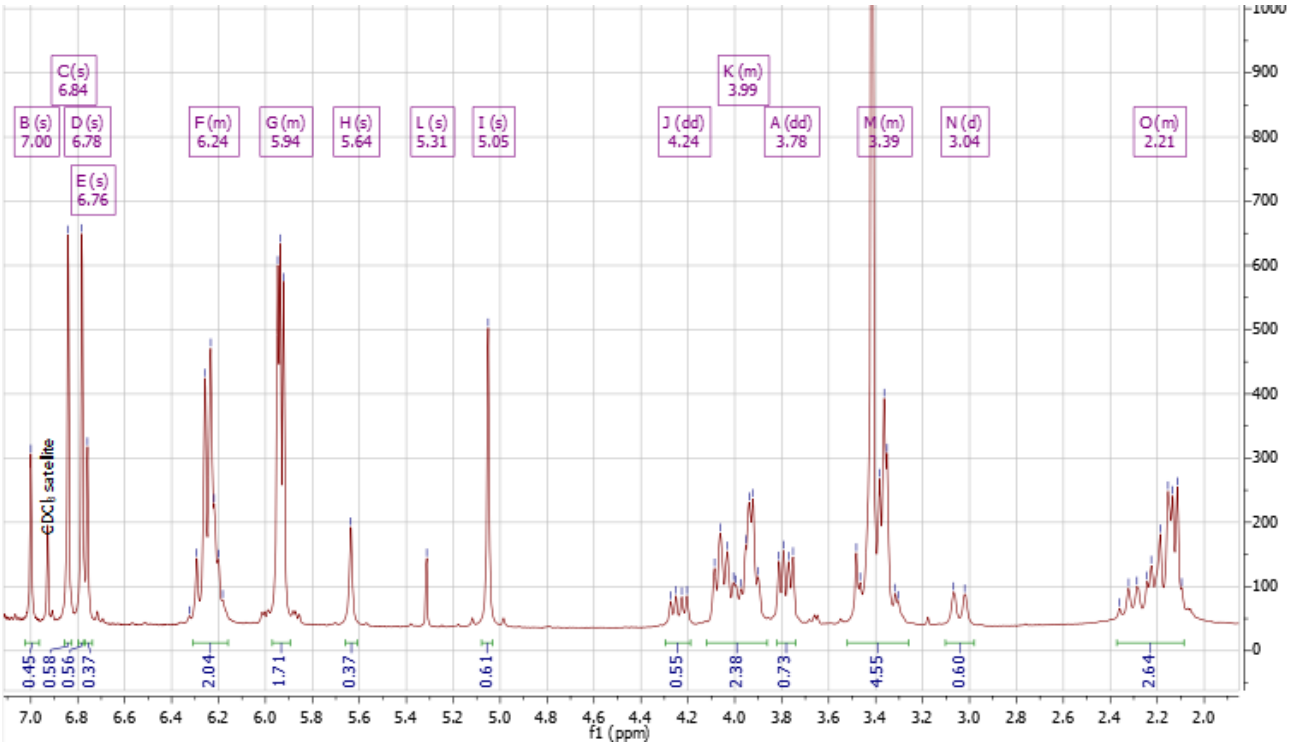

*Figure A.6.2 - ^{1}H NMR spectrum of **24** and **25**.*

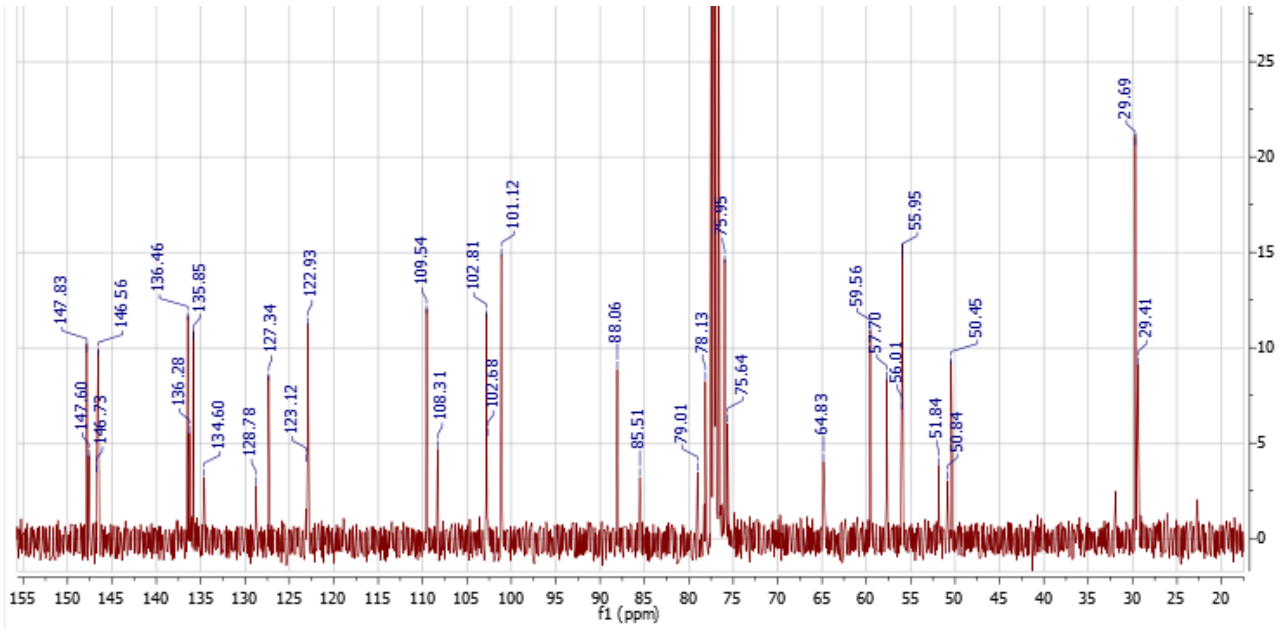

*Figure A.6.3 - ^{13}C NMR spectrum of **24** and **25**.*

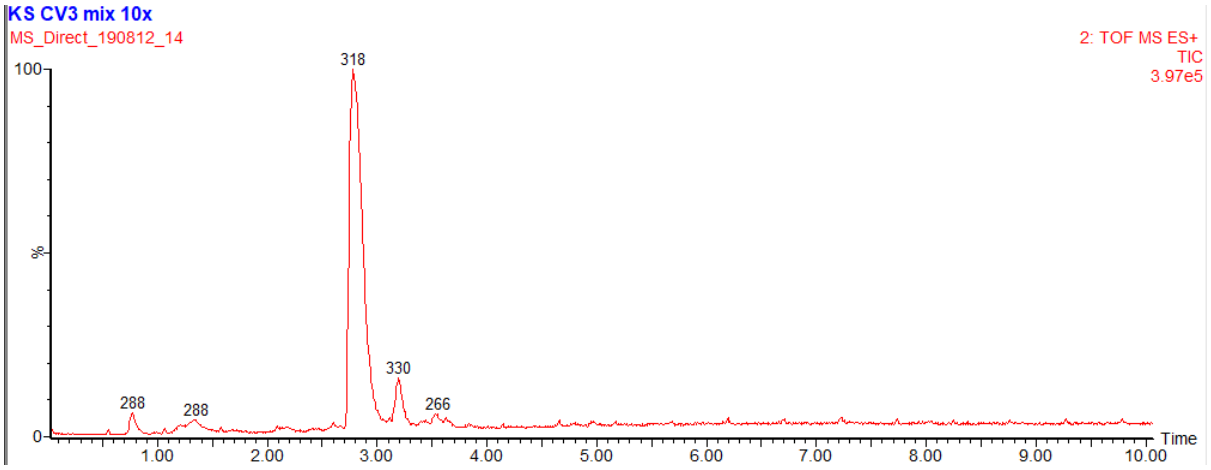

*Figure A.6.4 - TIC of **CV3** HPLC-MS analysis*

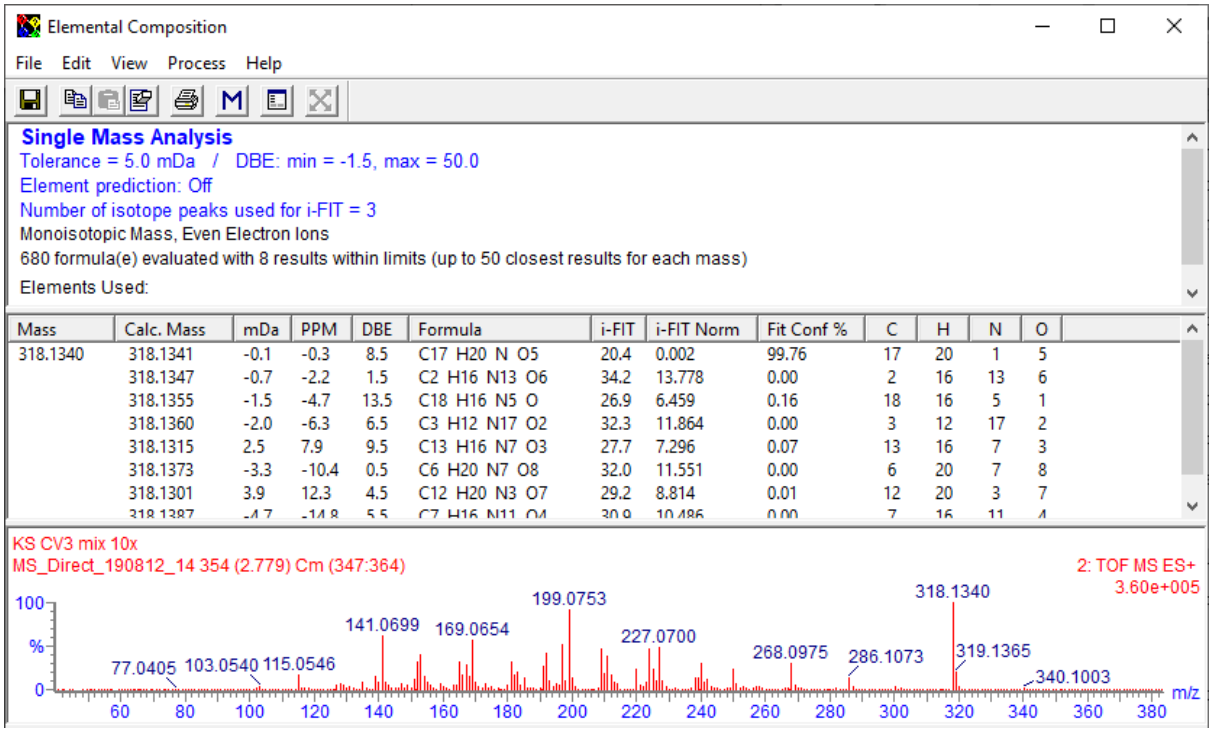

*Figure A.6.5 - Elemental composition analysis of **CV3** peak.*

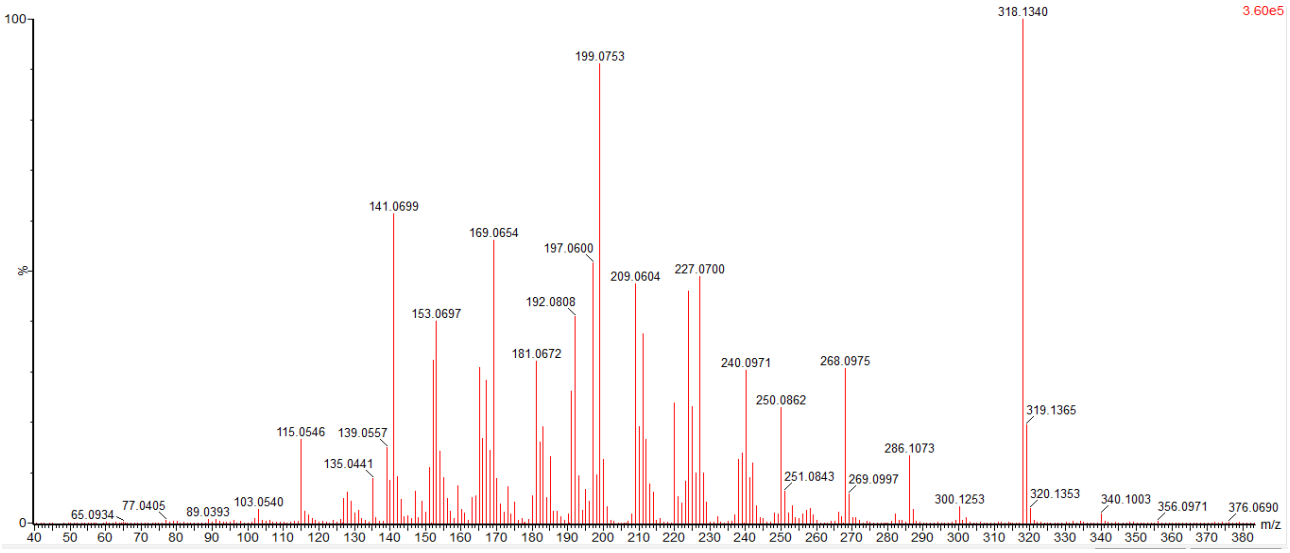

*Figure A.6.6 - Fragmentation pattern of **CV3**.*

A.7 **Bulbispermine 26**

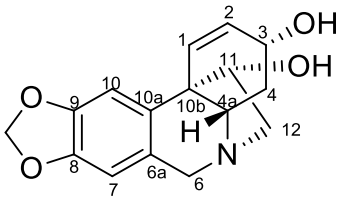

26

*Figure A.7.1 - The numbered chemical structure of bulbispermine **26**.*

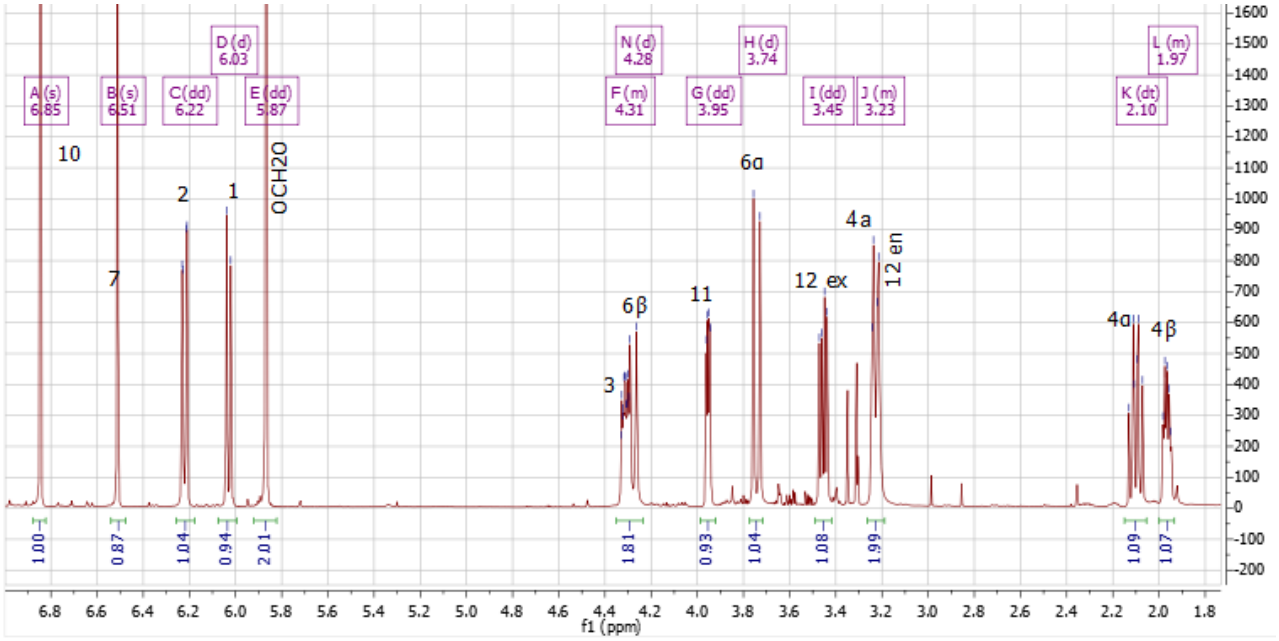

*Figure A.7.2 - ^{1}H NMR spectrum of **26**.*

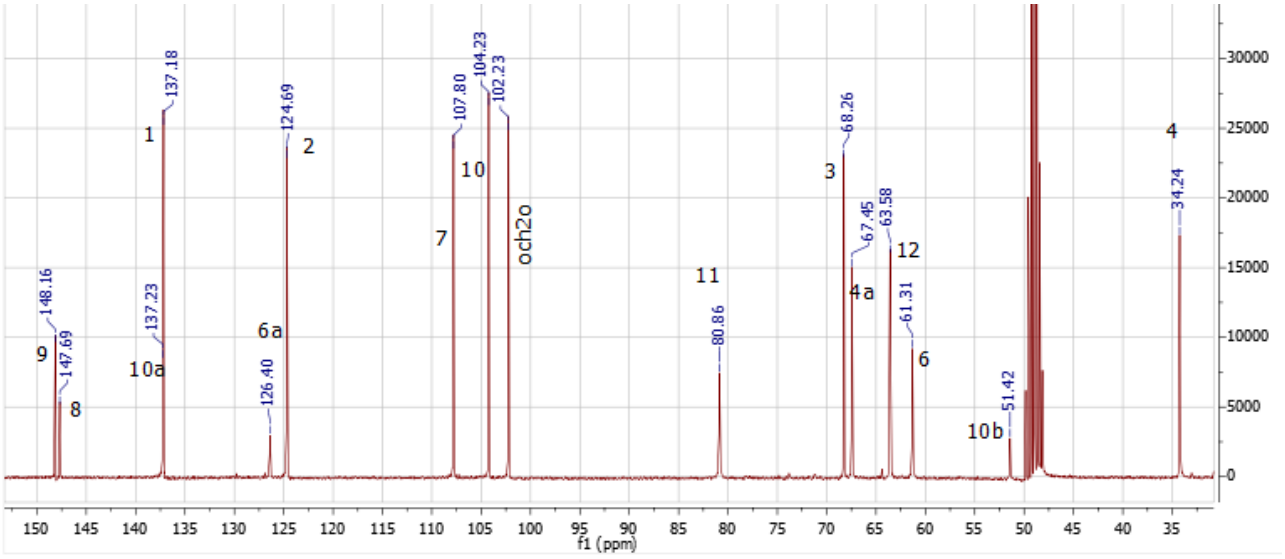

*Figure A.7.3 - ^{13}C spectrum of **26**.*

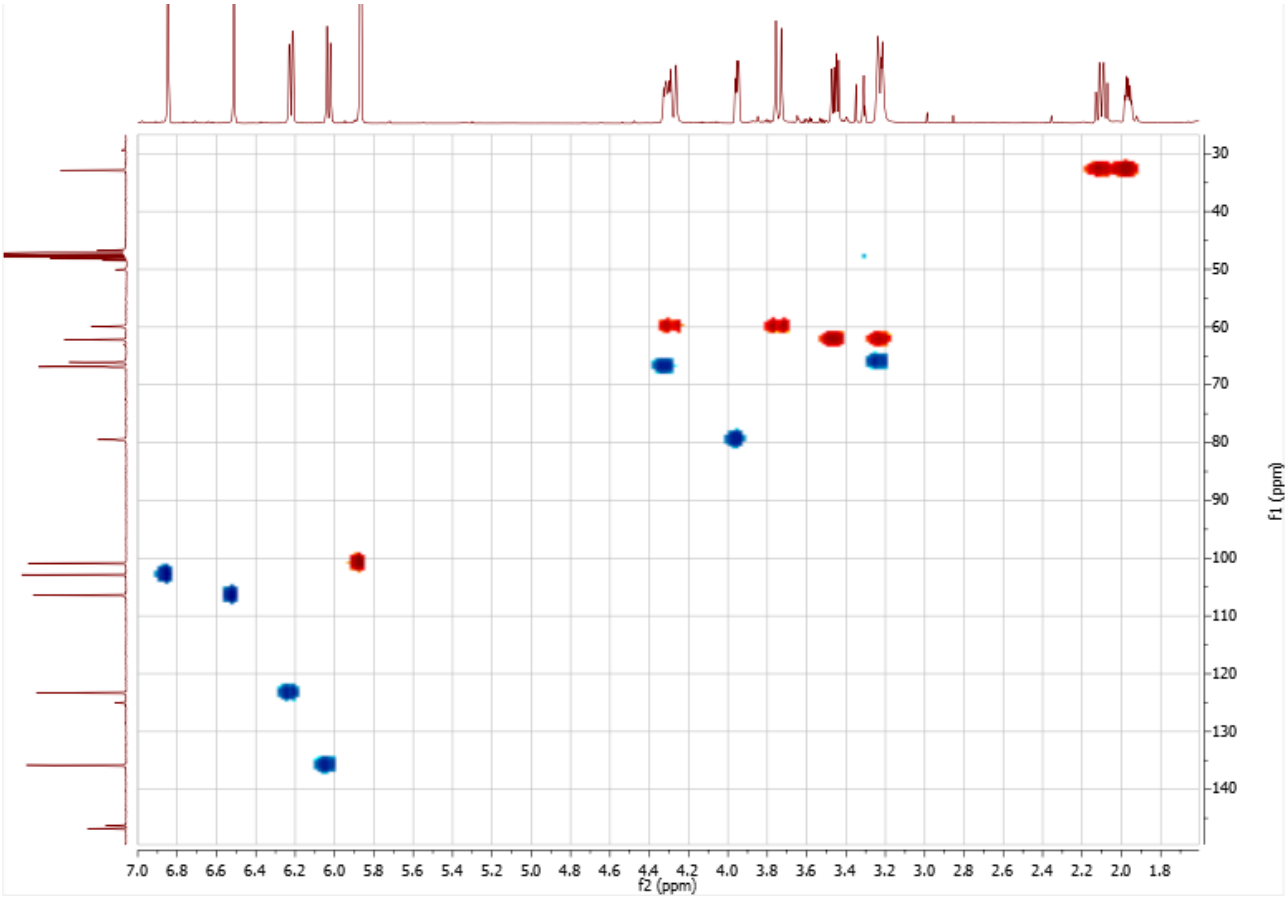

*Figure A.7.4 - HSQC spectrum of **26**. Using the appropriate phasing during processing, carbon atoms with 2 protons attached can be differentiated from others (shown by red coupling peaks).*

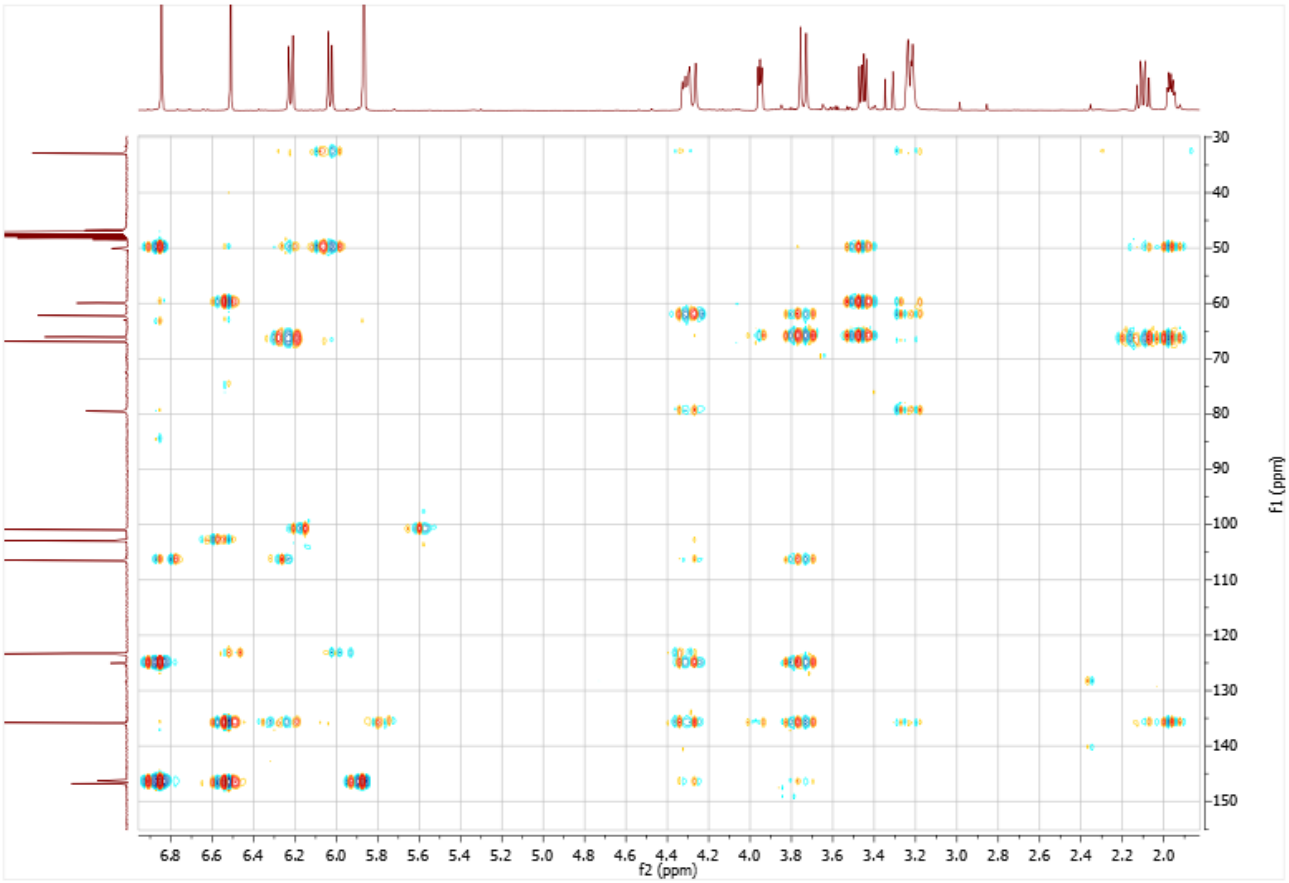

*Figure A.7.5 - HMBC spectrum of **26**.*

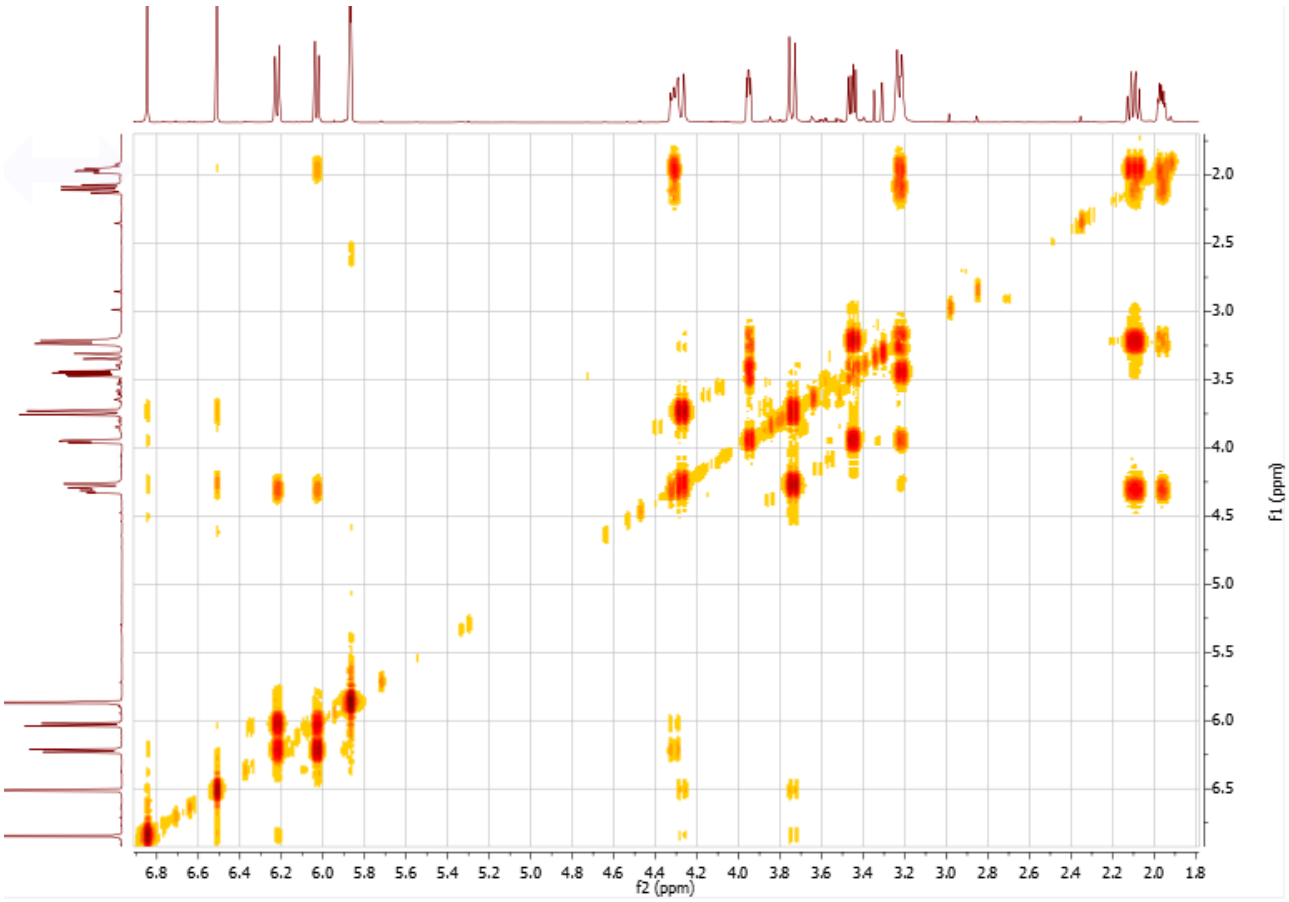

*Figure A.7.6 - COSY spectrum of **26***

A.8 **Criwelline 27**

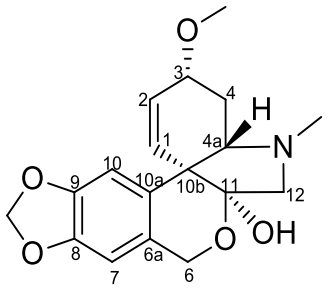

27

*Figure A.8.1 - The numbered chemical structure of **27**.*

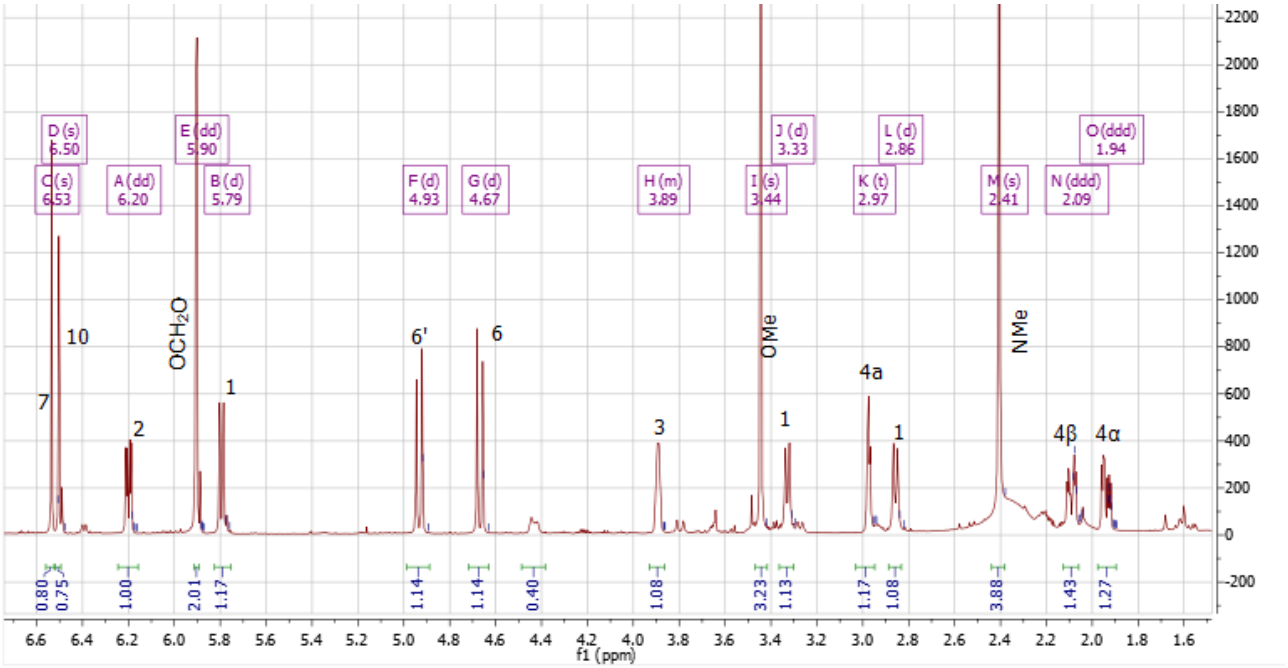

*Figure A.8.2 - ^{1}H NMR spectrum of **27**.*

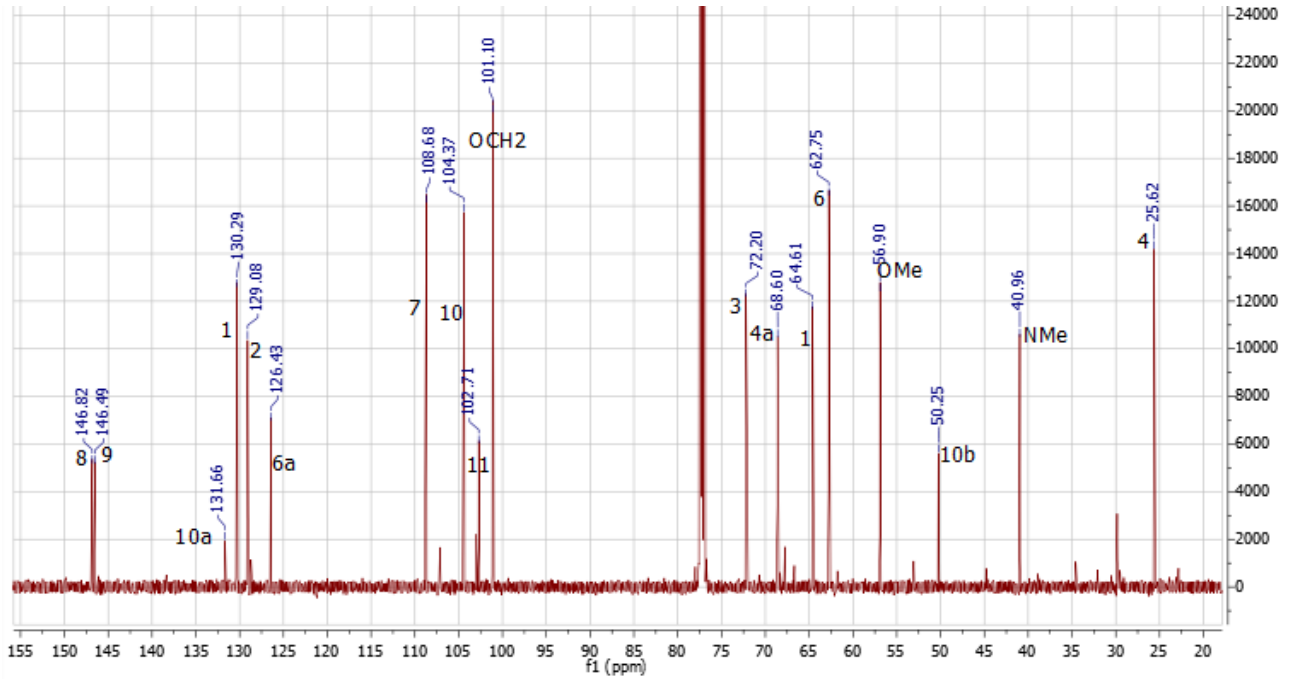

Figure A.8.3 - ^{13}C NMR spectrum of 27.

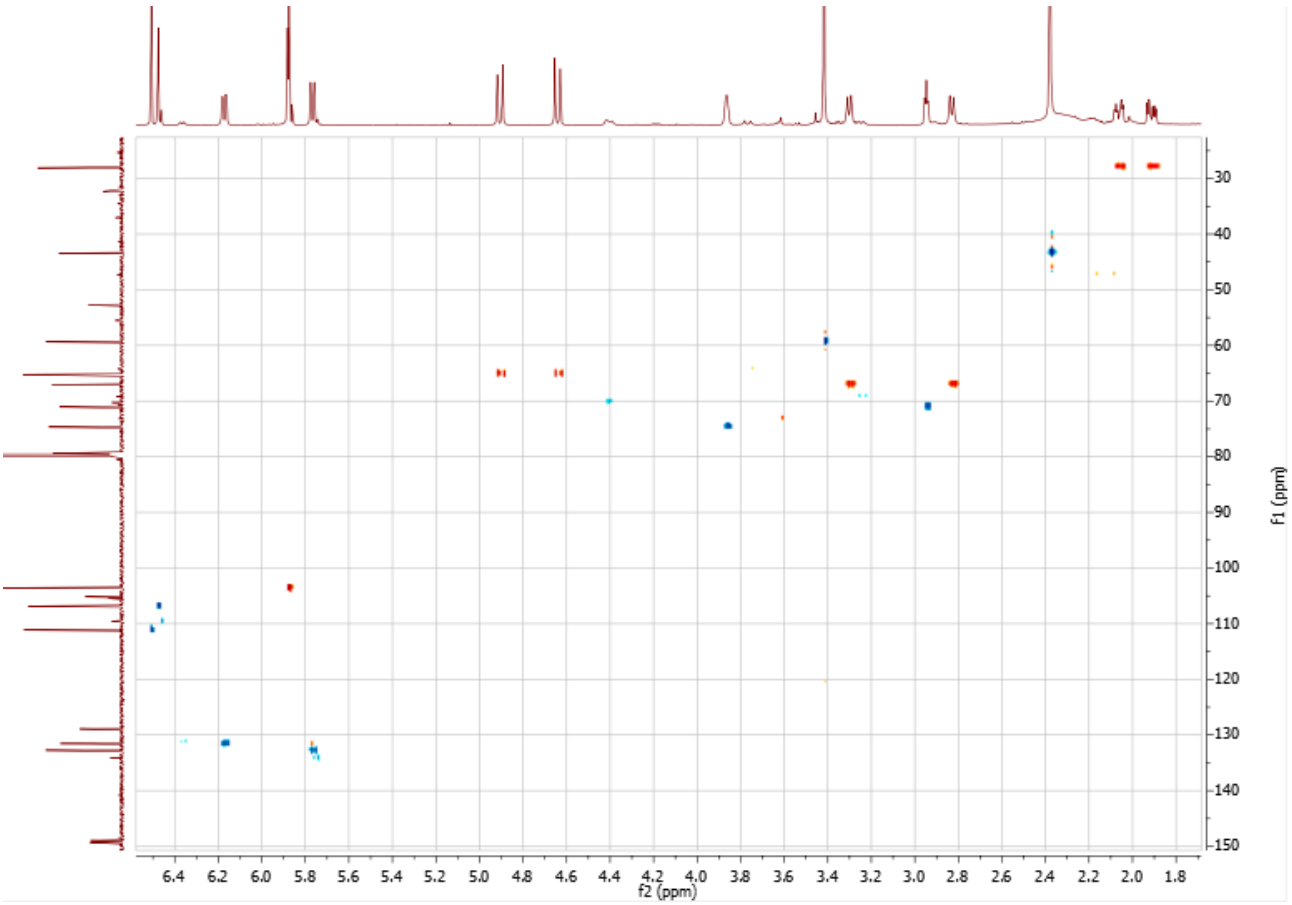

*Figure A.8.4 - HSQC spectrum of **27**. Using the appropriate phasing during processing, carbon atoms with 2 protons attached can be differentiated from others (shown by red coupling peaks).*

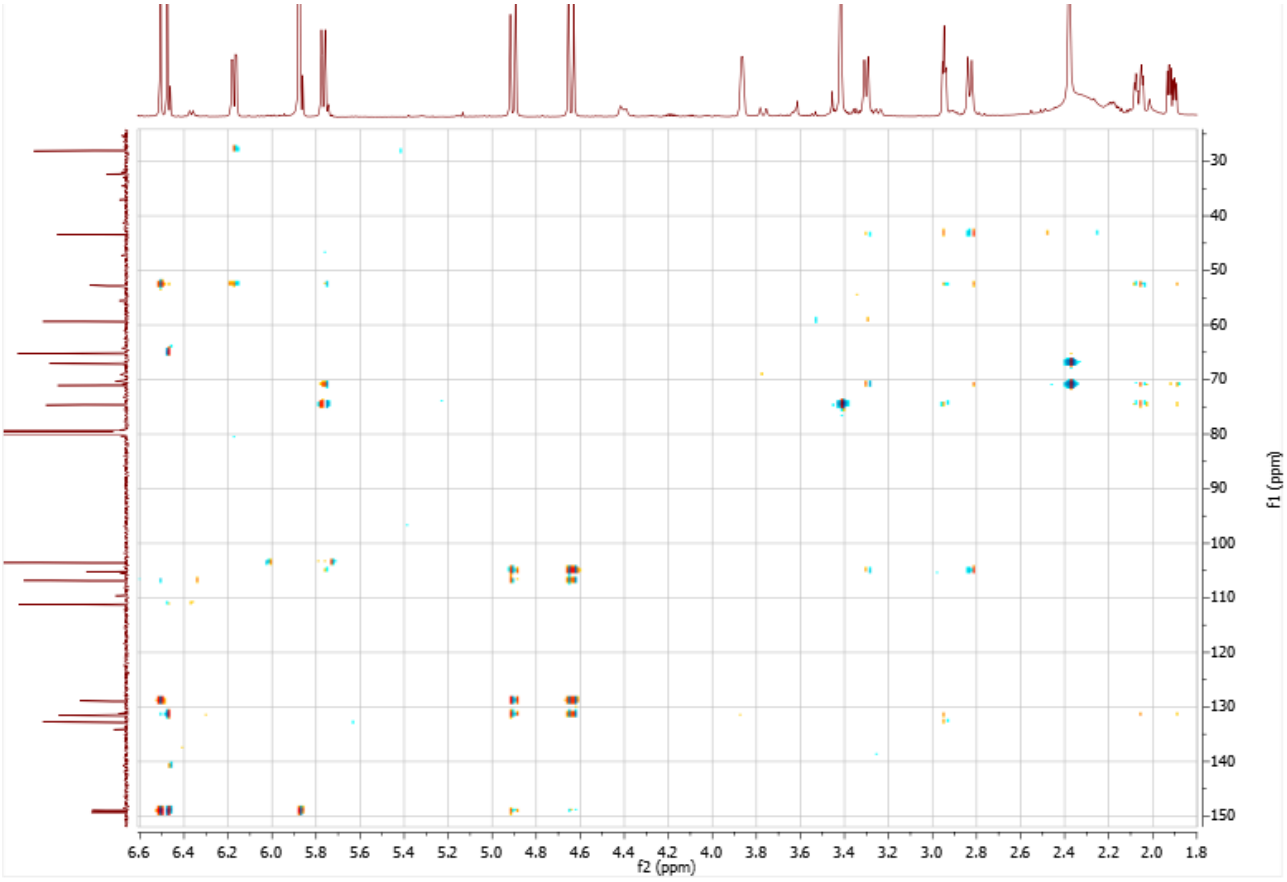

*Figure A.8.5 - HMBC spectrum of **27**.*

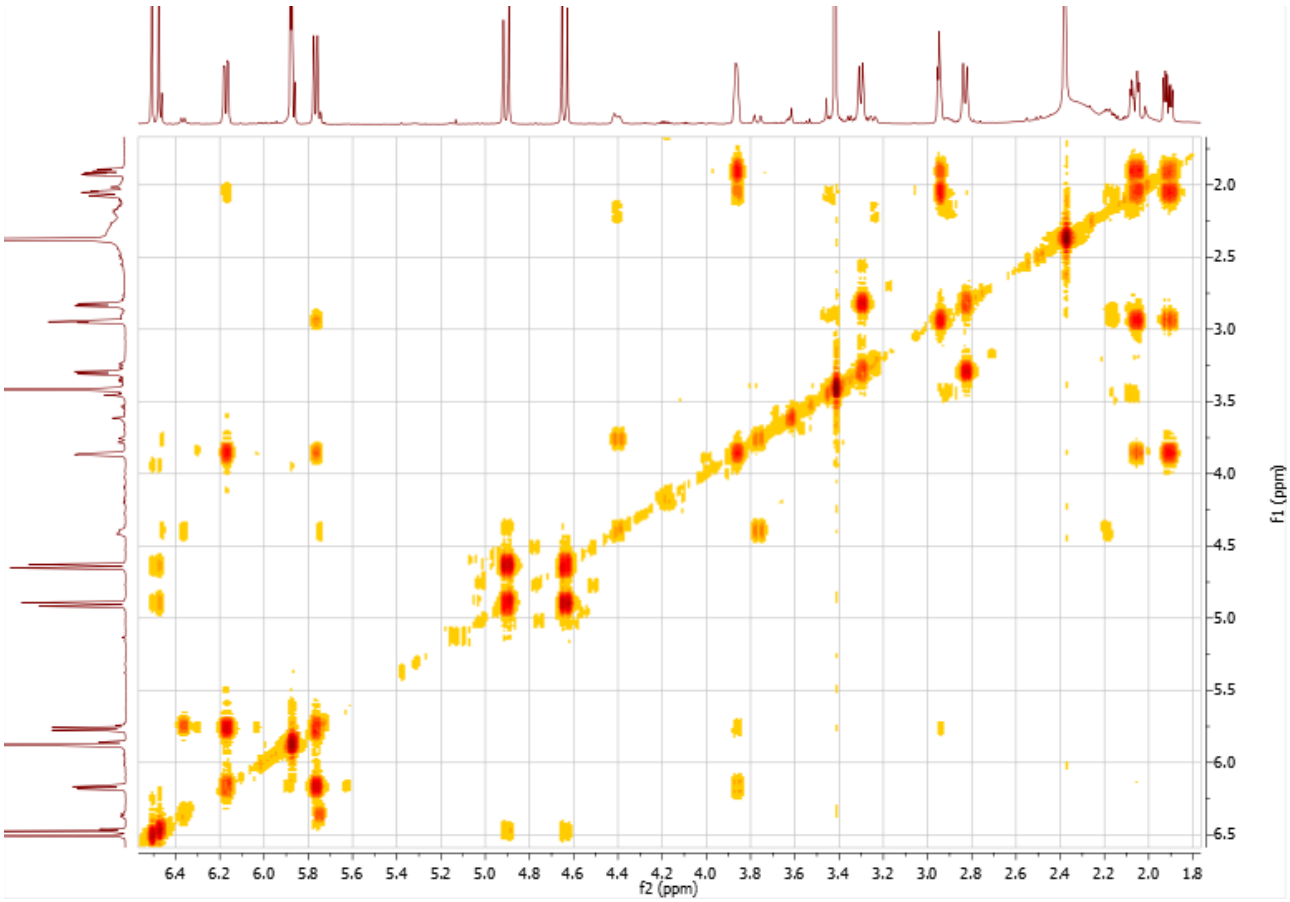

*Figure A.8.6 - COSY spectrum of **27***

A.9 **Continuous liquid/liquid extraction apparatus**

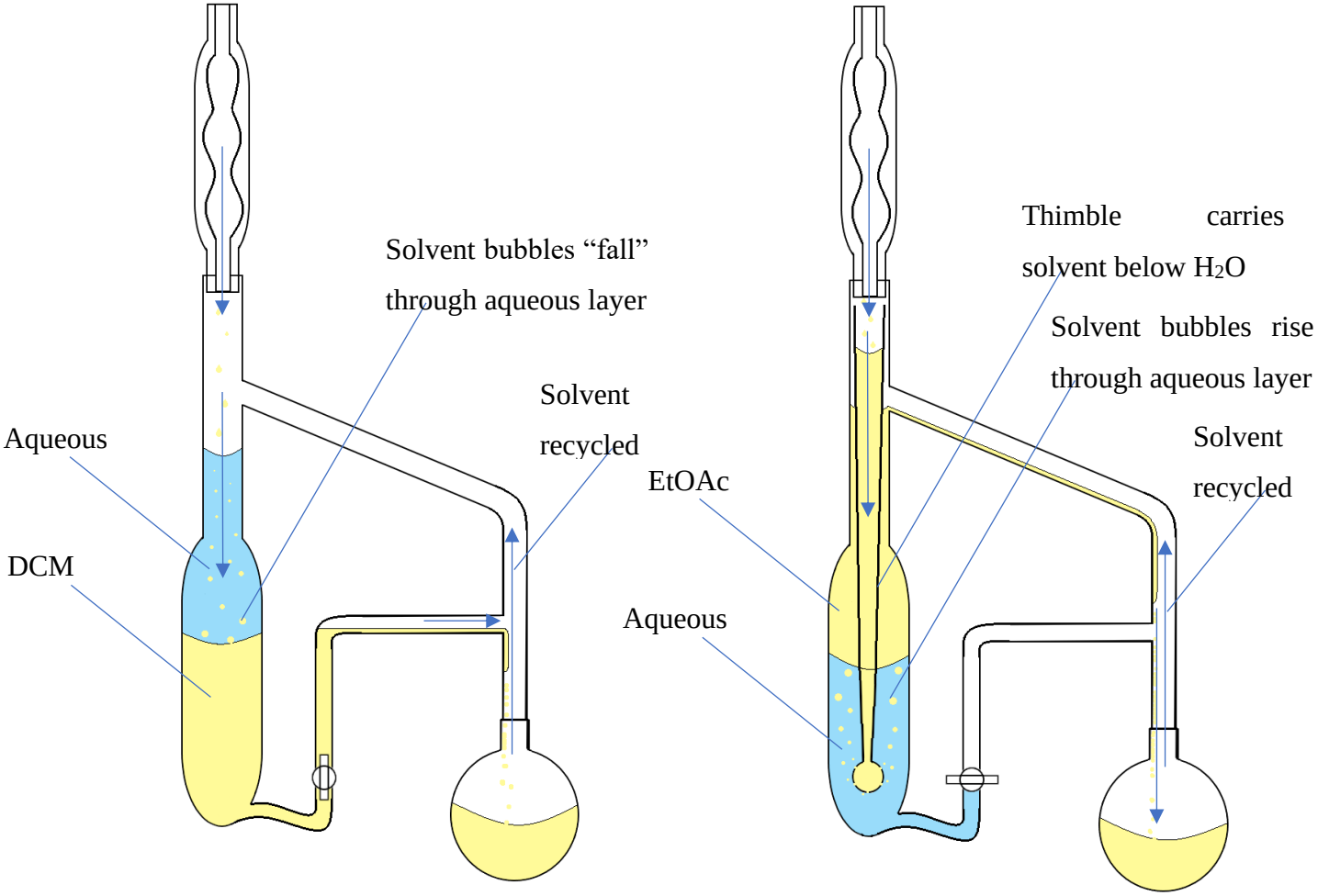

Figure A.9.1 - The operation of a continuous liquid/liquid extraction apparatus. Operation with more dense solvents such as DCM shown on the left, and operation with less dense solvents such as EtOAc shown on the right.

B Appendix – Higginsianins A and B

B.1 Higginsianin A 39

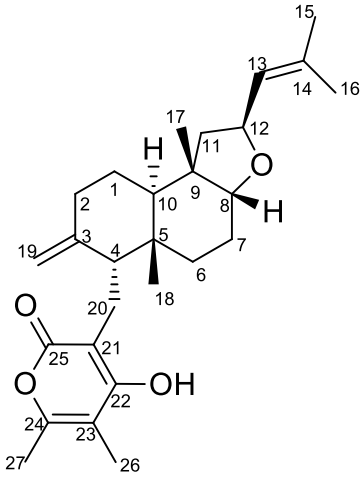

39

*Figure B.1.1 - Numbered chemical structure of higginsianin A **39**.*

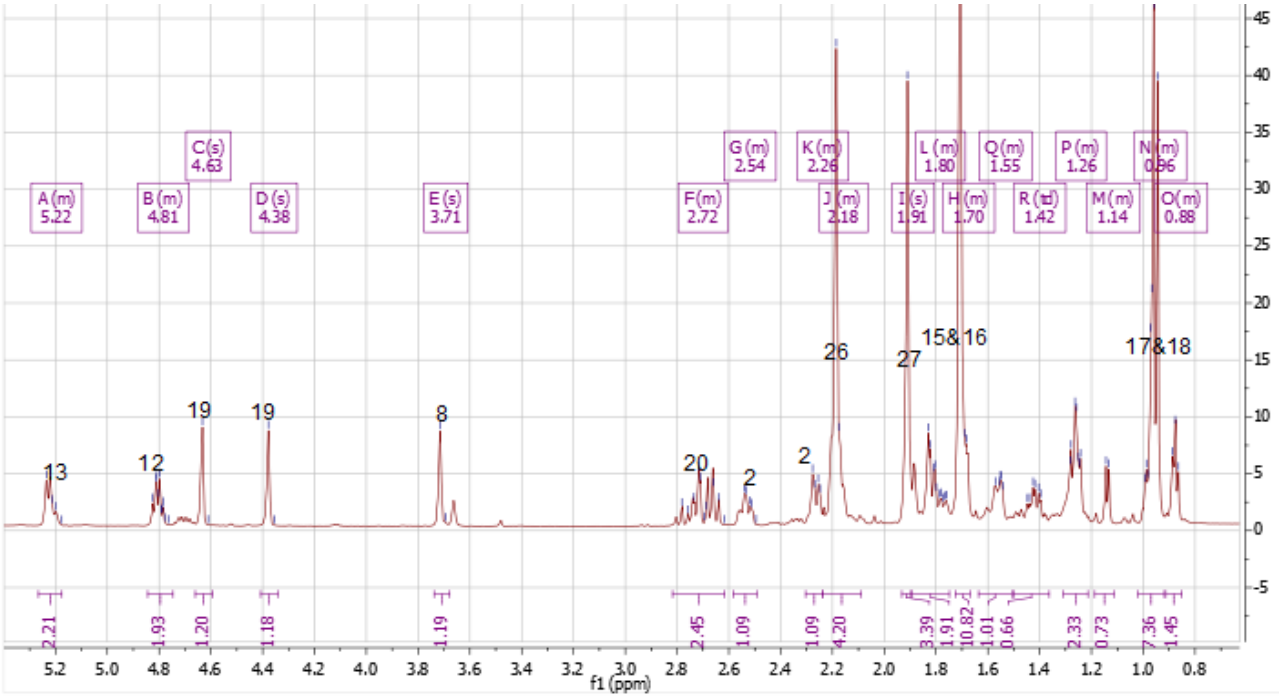

*Figure B.1.2- ^{1}H NMR spectrum of higginsianin A **39** acquired from corresponding research group.*

*B.1.1 22-O-acetylhigginsianin A **39a***

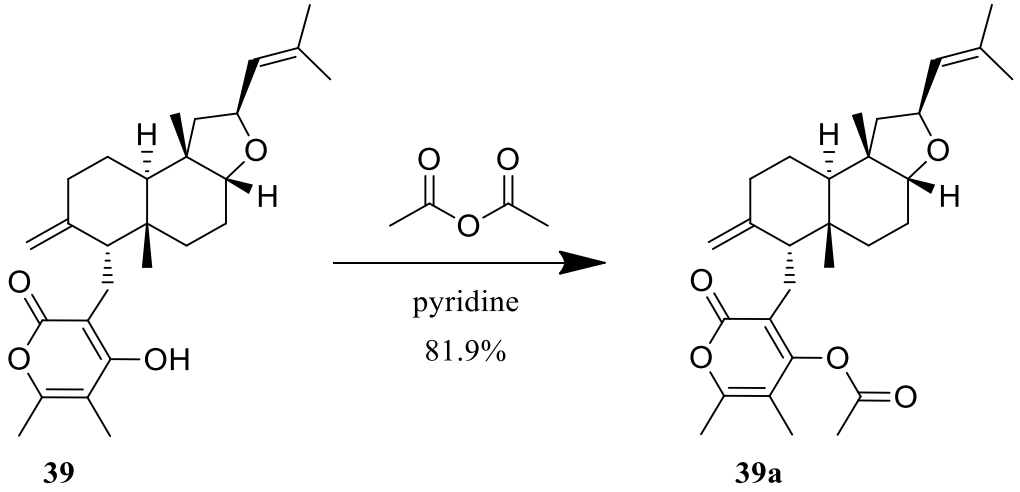

*Figure B.1.3 – Acetylation of **39** to 22-O-acetylhigginsianin A **39a**.*

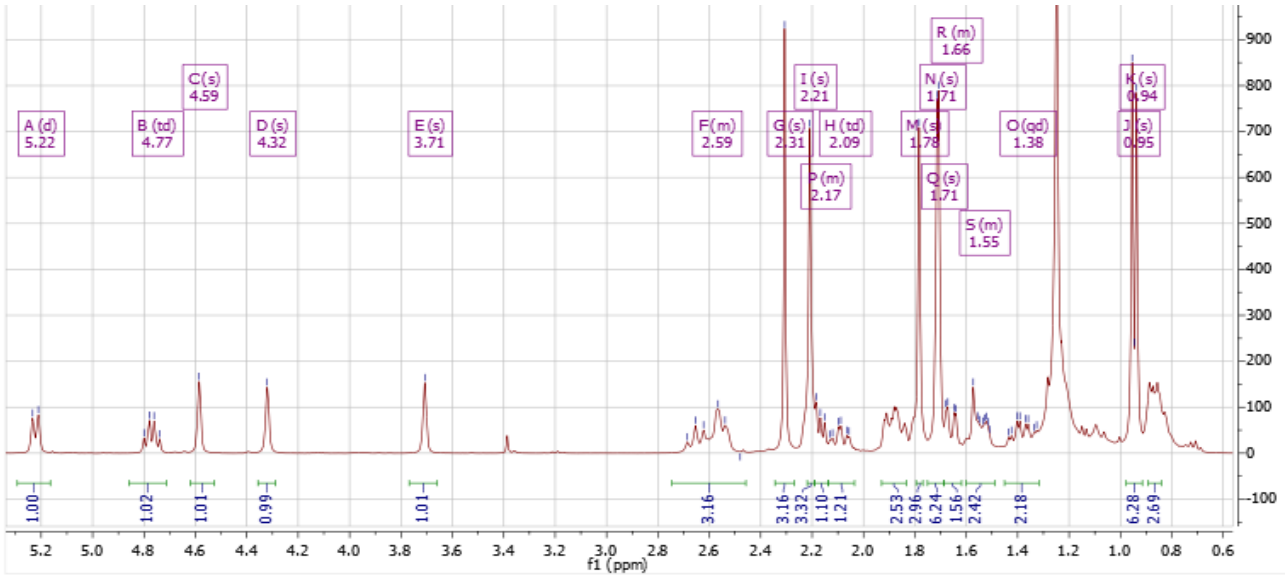

*Figure B.1.4 - ^{1}H NMR spectrum of **39a**.*

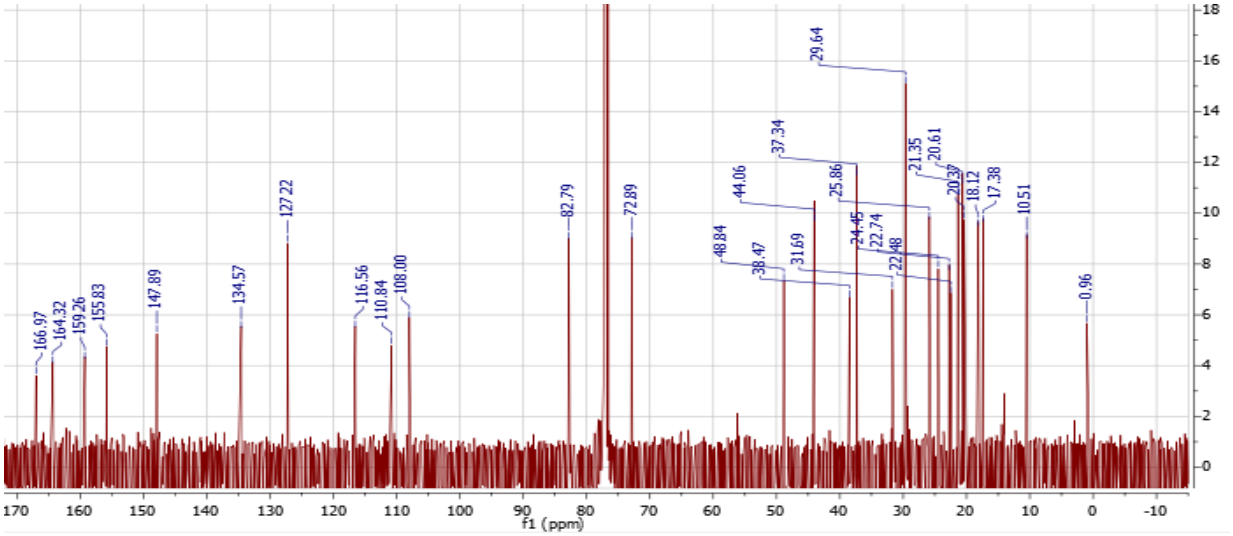

*Figure B.1.5 - ^{13}C spectrum of **39a**.*

B.1.2 *NBS bromination of **39***

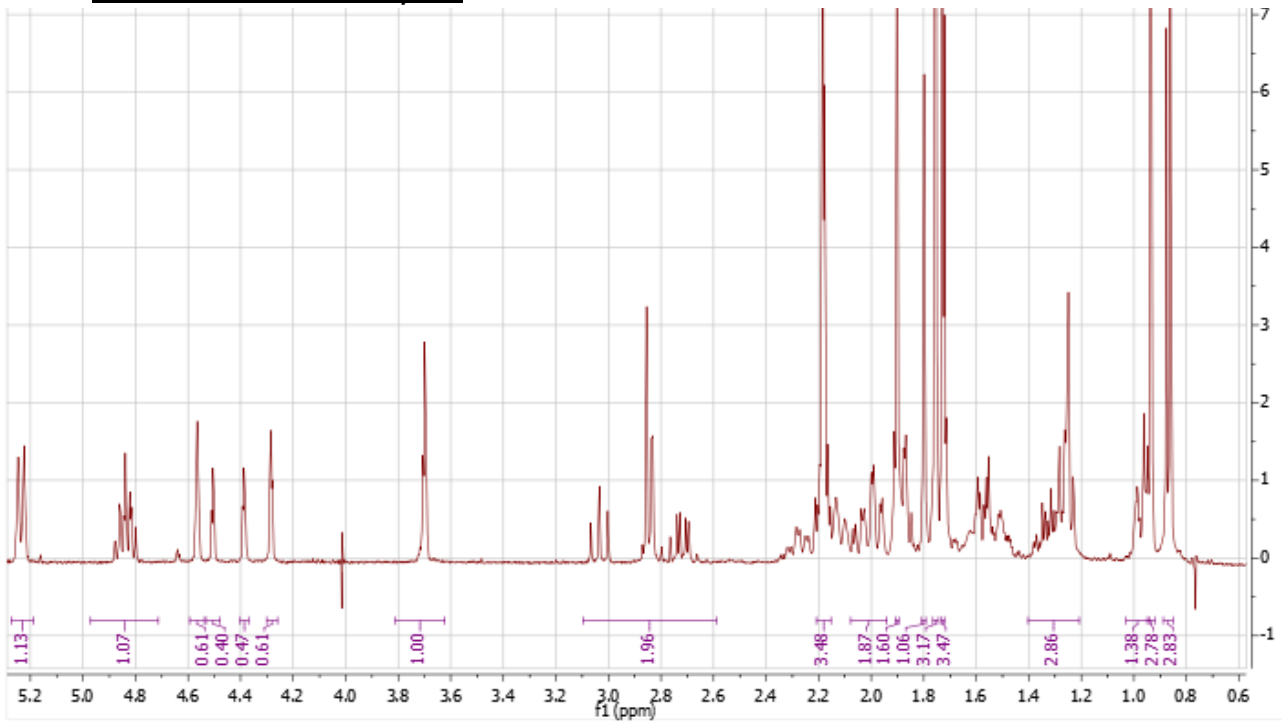

*Figure B.1.6 - ^{1}H NMR of product mixture from bromination of **39** with NBS.*

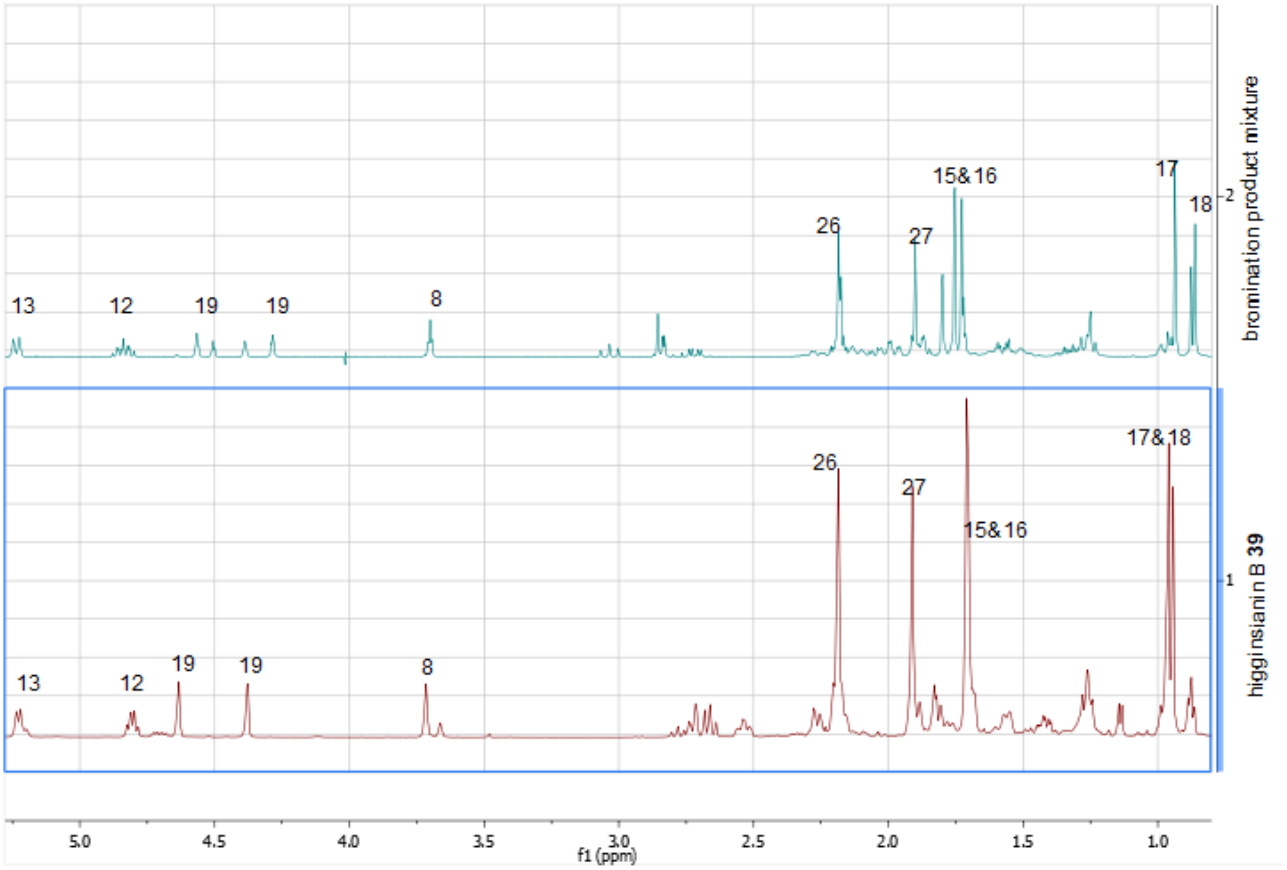

*Figure B.1.7 - Comparison of **39** ^{1}H NMR spectrum with that of bromination products.*

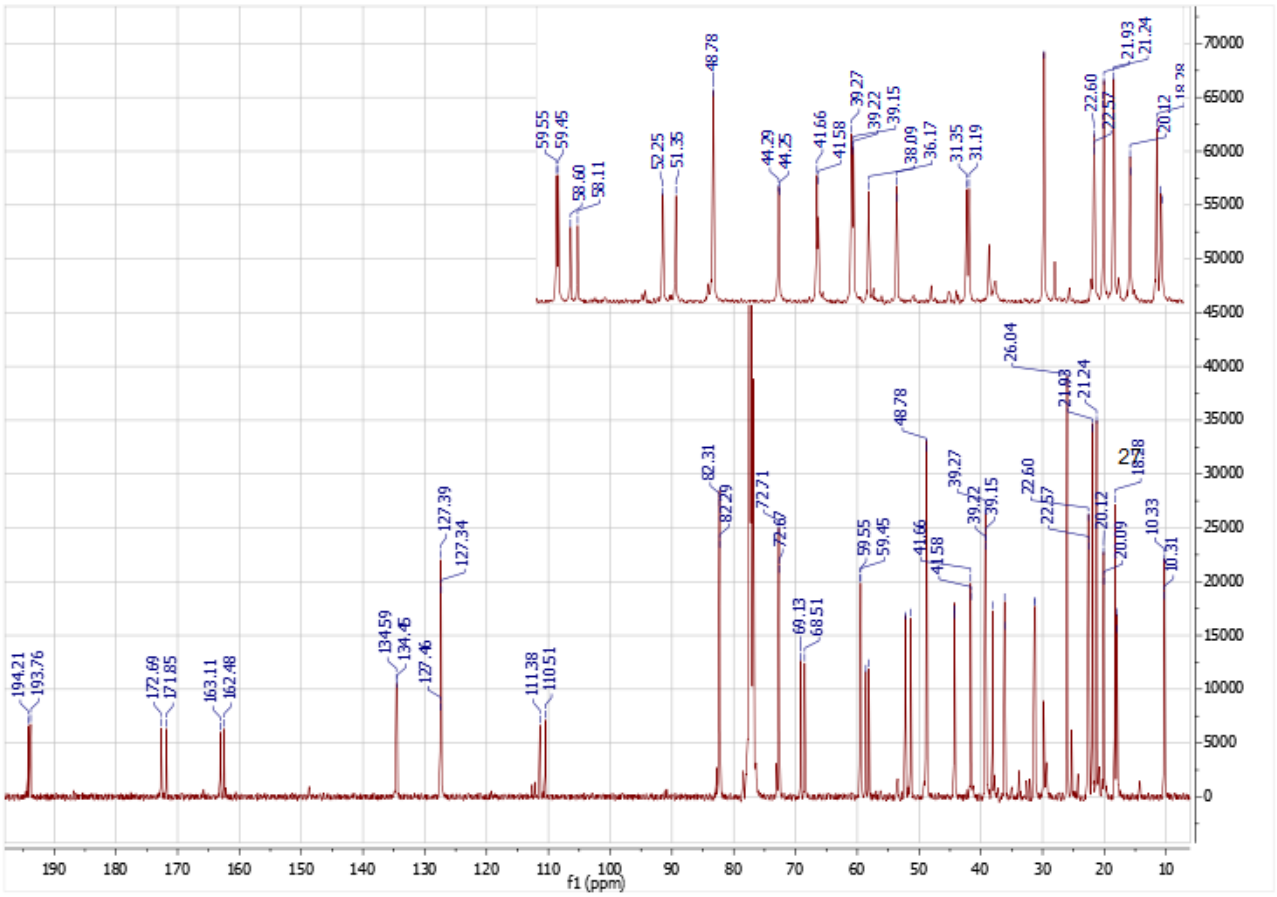

*Figure B.1.8 - ^{13}C NMR spectrum of products from bromination of **39**.*

B.2 **Higginsianin B 40**

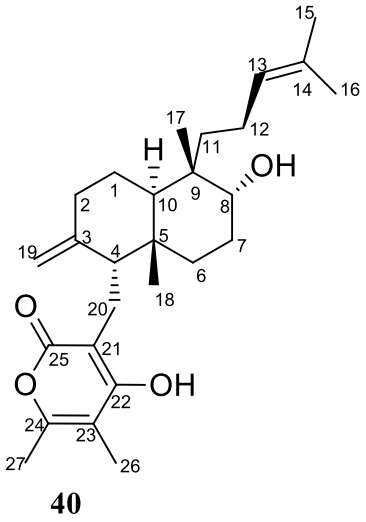

40

*Figure B.2.1 - Numbered chemical structure of higginsianin B **40**.*

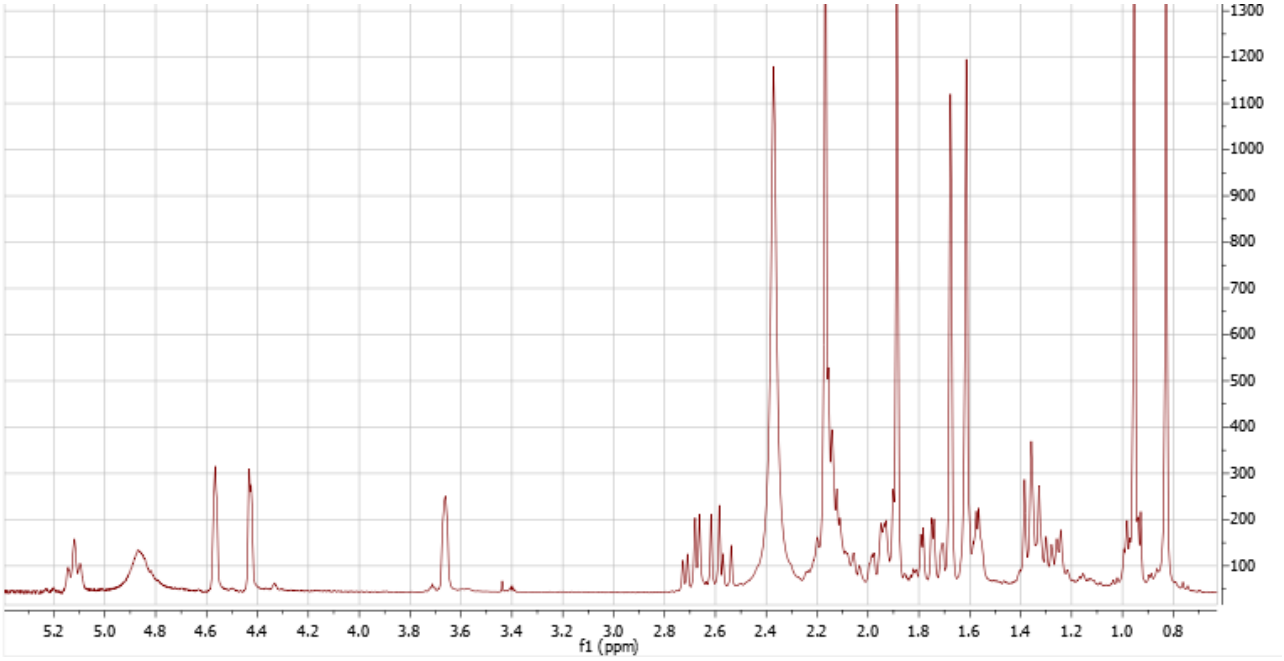

*Figure B.2.2 - ^{1}H NMR spectrum of higginsianin B **40** as acquired from corresponding research group.*

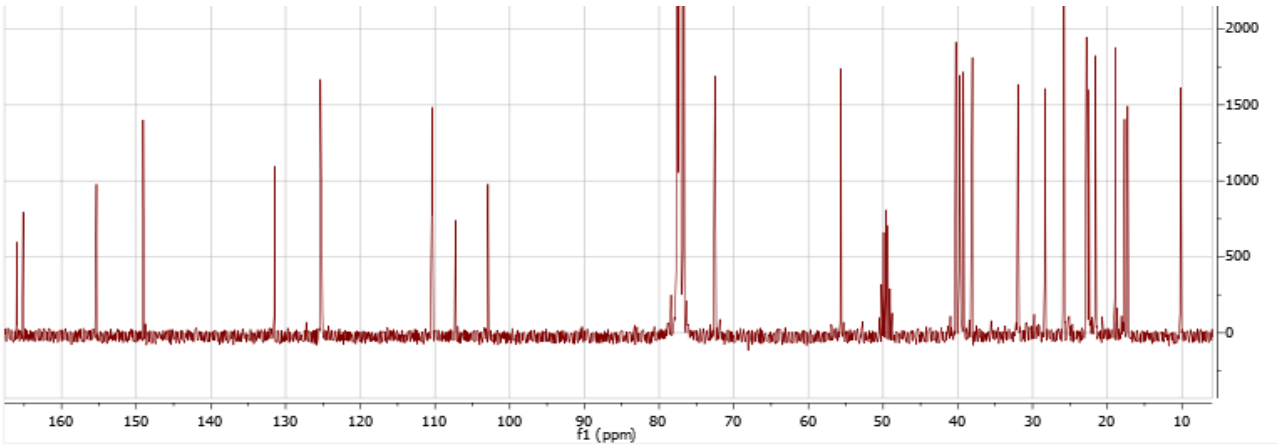

*Figure B.2.3 - ^{13}C NMR spectrum of **40** as acquired from corresponding research group.*

B.2.1 *Acetylation of **40***

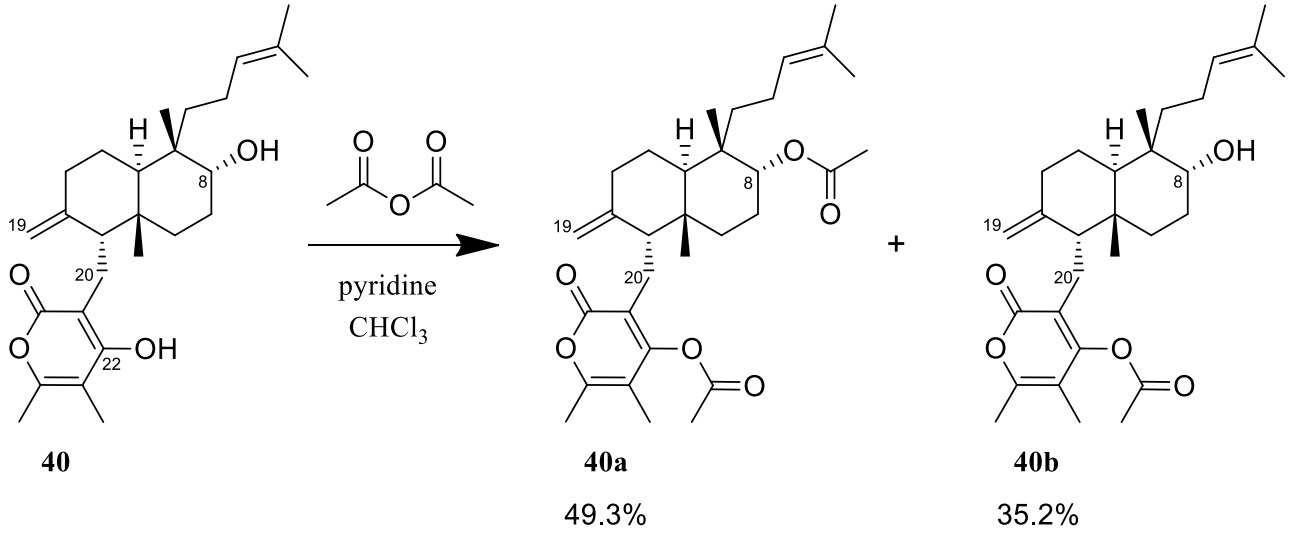

40 **40a** **40b**

49.3% 35.2%

*Figure B.2.4 - Scheme for the acetylation of higginsianin B **40**.*

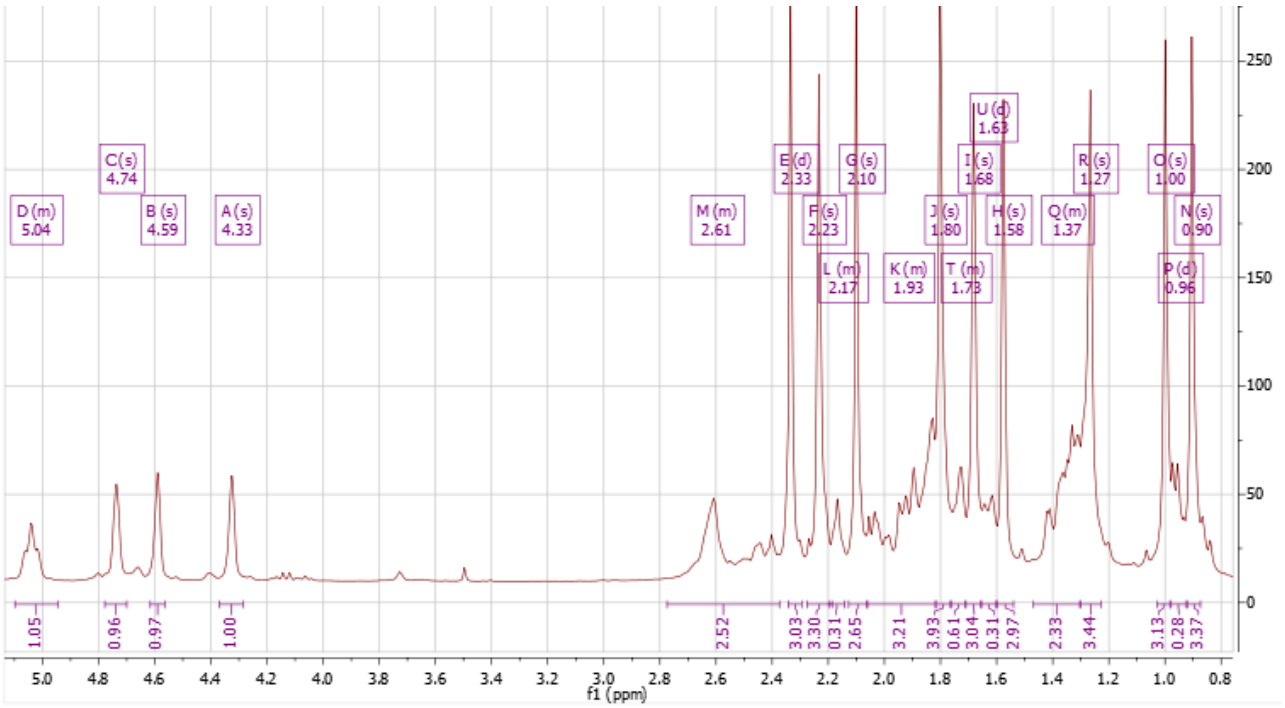

*Figure B.2.5 - [1]H NMR spectrum of **40a**.*

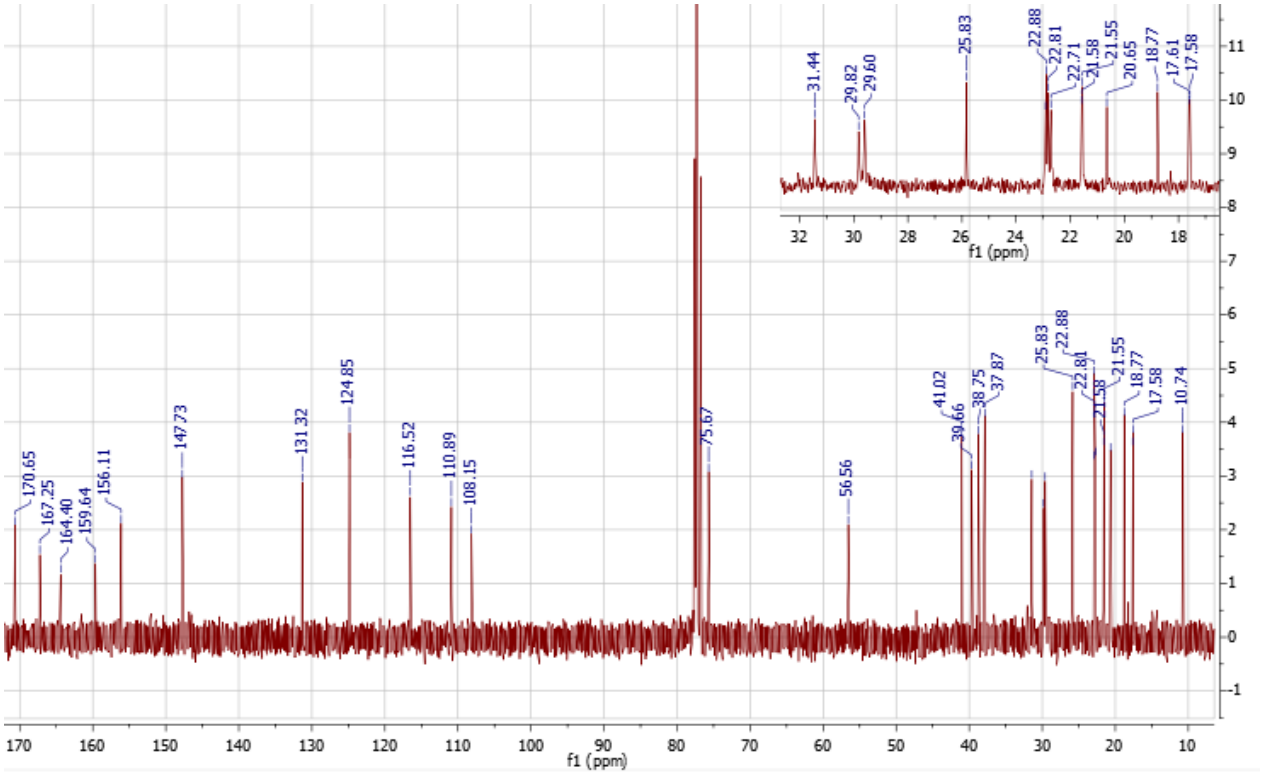

*Figure B.2.6 - [13]C NMR spectrum of **40a**.*

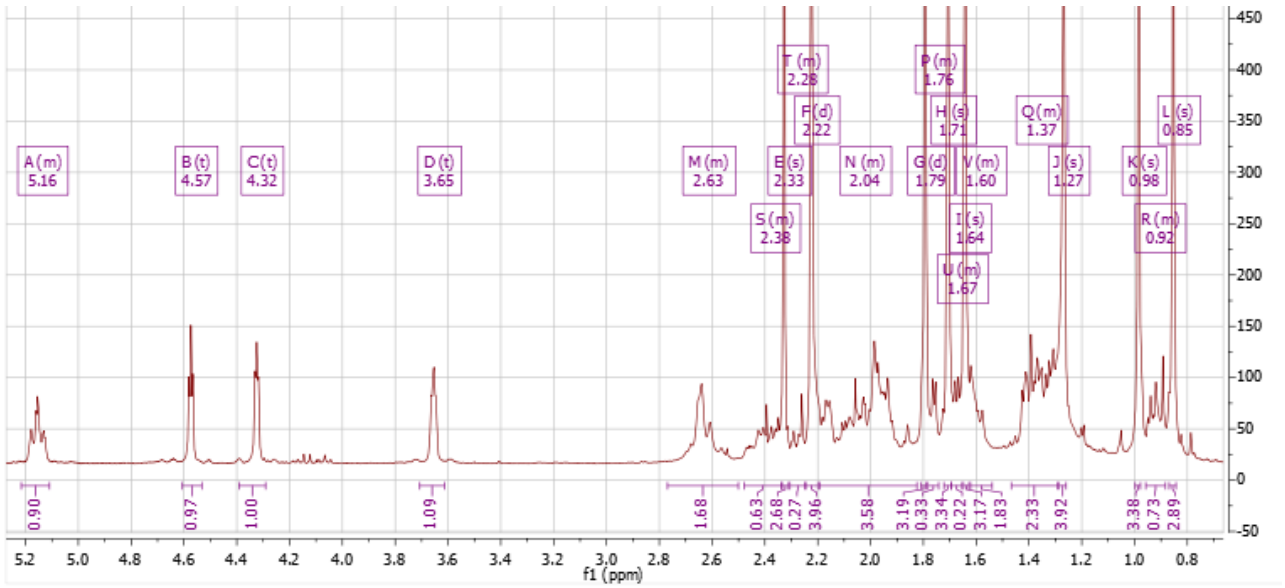

*Figure B.2.7 - ^{1}H NMR spectrum of **40b**.*

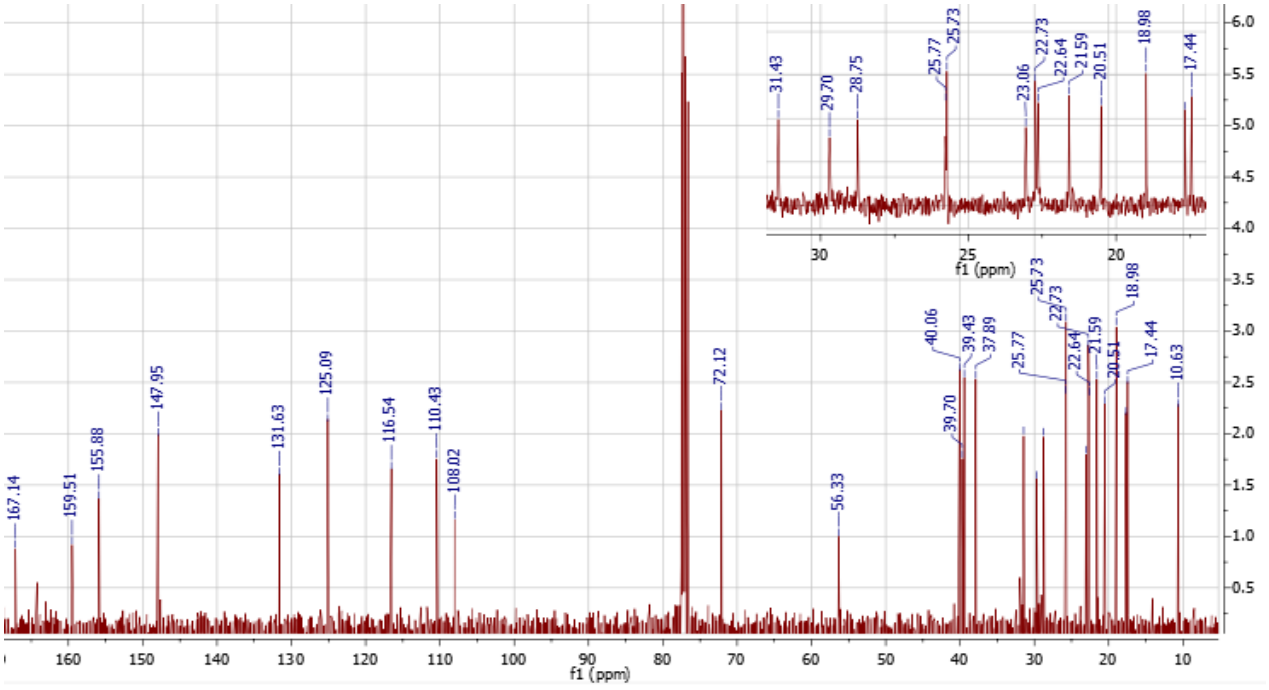

*Figure B.2.8 - ^{13}C NMR spectrum of **40b**.*

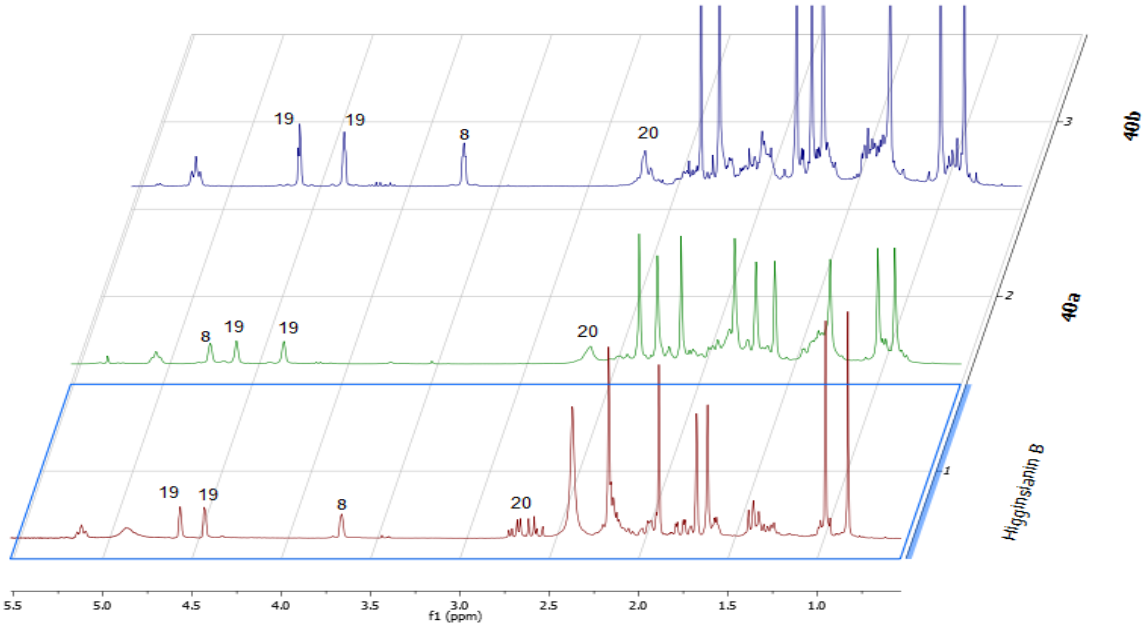

*Figure B.2.9 - ^{1}H NMR spectra of **40**, **40a** and **40b** stacked.*

Elemental Composition

File Edit View Process Help

Single Mass Analysis
Tolerance = 5.0 mDa / DBE: min = -1.5, max = 50.0
Element prediction: Off
Number of isotope peaks used for i-FIT = 3
Monoisotopic Mass, Even Electron Ions
2424 formula(e) evaluated with 16 results within limits (up to 50 closest results for each mass)

Mass	Calc. Mass	mDa	PPM	DBE	Formula	i-FIT	i-FIT Norm	Fit Conf %	C	H	N	O
513.3220	513.3221	-0.1	-0.2	2.5	C16 H41 N12 O7	28.1	6.743	0.12	16	41	12	7
	513.3216	0.4	0.8	9.5	C31 H45 O6	21.7	0.307	73.59	31	45		6
	513.3230	-1.0	-1.9	14.5	C32 H41 N4 O2	23.3	1.925	14.59	32	41	4	2
	513.3208	1.2	2.3	8.5	C13 H33 N22 O	29.3	7.844	0.04	13	33	22	1
	513.3235	-1.5	-2.9	7.5	C17 H37 N16 O3	27.7	6.278	0.19	17	37	16	3
	513.3203	1.7	3.3	15.5	C28 H37 N10	24.4	3.004	4.96	28	37	10	
	513.3240	-2.0	-3.9	0.5	C2 H33 N28 O4	33.6	12.178	0.00	2	33	28	4
	513.3194	2.6	5.1	3.5	C12 H37 N18 O5	29.7	8.326	0.02	12	37	18	5

*Figure B.2.10 - Elemental composition analysis window for **40a**.*

Elemental Composition

File Edit View Process Help

Single Mass Analysis
Tolerance = 5.0 mDa / DBE: min = -1.5, max = 50.0
Element prediction: Off
Number of isotope peaks used for i-FIT = 3
Monoisotopic Mass, Even Electron Ions
1933 formula(e) evaluated with 13 results within limits (up to 50 closest results for each mass)

Mass	Calc. Mass	mDa	PPM	DBE	Formula	i-FIT	i-FIT Norm	Fit Conf %	C	H	N	O
471.3122	471.3124	-0.2	-0.4	13.5	C30 H39 N4 O	155.8	3.172	4.19	30	39	4	1
	471.3116	0.6	1.3	1.5	C14 H39 N12 O6	165.1	12.471	0.00	14	39	12	6
	471.3129	-0.7	-1.5	6.5	C15 H35 N16 O2	165.3	12.618	0.00	15	35	16	2
	471.3134	-1.2	-2.5	-0.5	H31 N28 O3	172.3	19.621	0.00		31	28	3
	471.3110	1.2	2.5	8.5	C29 H43 O5	152.7	0.062	93.94	29	43		5
	471.3102	2.0	4.2	7.5	C11 H31 N22	168.5	15.810	0.00	11	31	22	
	471.3142	-2.0	-4.2	0.5	C18 H43 N6 O8	162.3	9.604	0.01	18	43	6	8
	471.3089	3.3	7.0	2.5	C10 H35 N18 O4	168.1	15.409	0.00	10	35	18	4

*Figure B.2.11 - Elemental composition analysis window for **40b**.*

*B.2.2 Reductive hydrogenation of **40** to **40c/40d.***

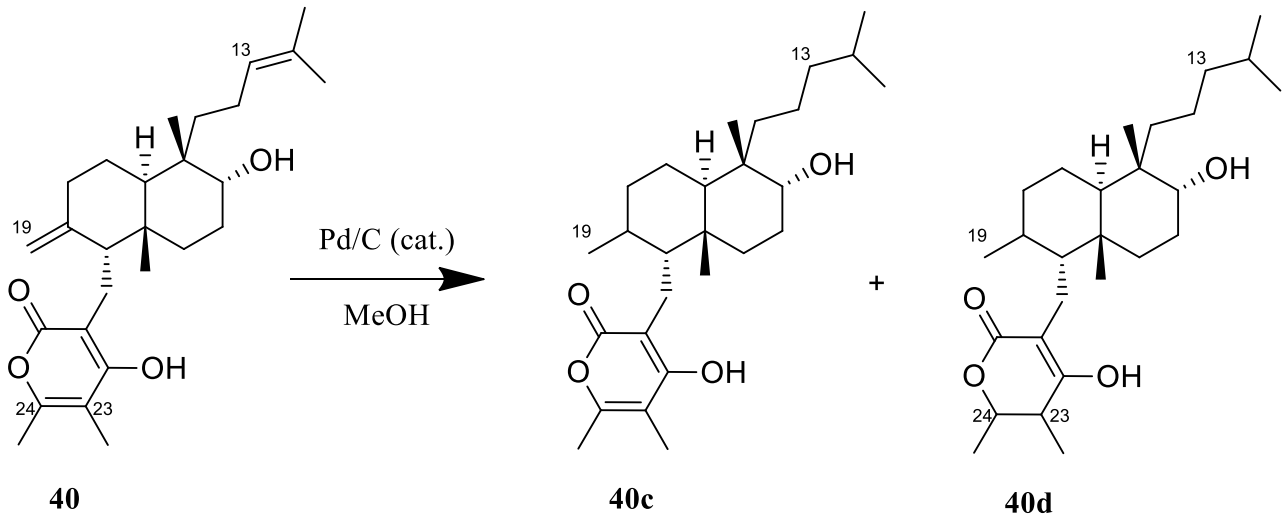

*Figure B.2.12 - Scheme for the reaction of **40** with Pd/C.*

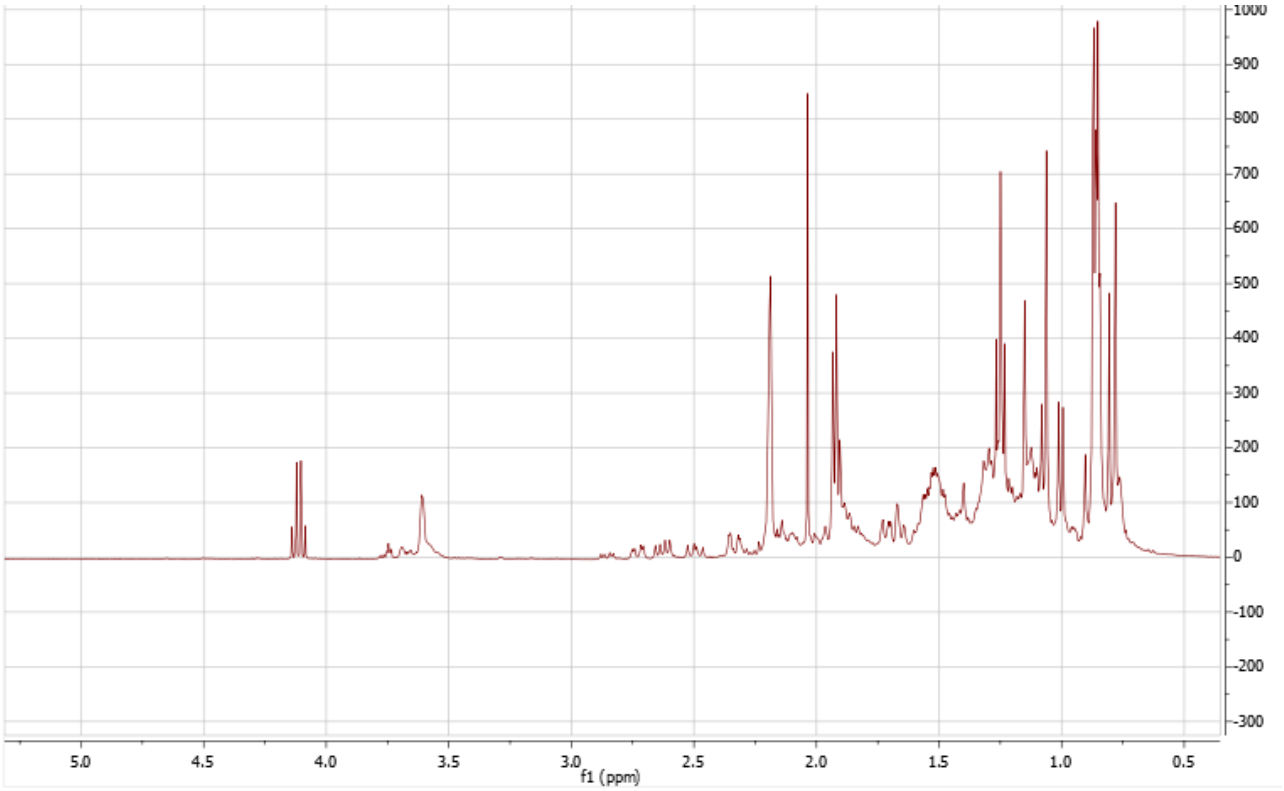

*Figure B.2.13 - ^{1}H NMR spectrum of crude **40c/40d**.*

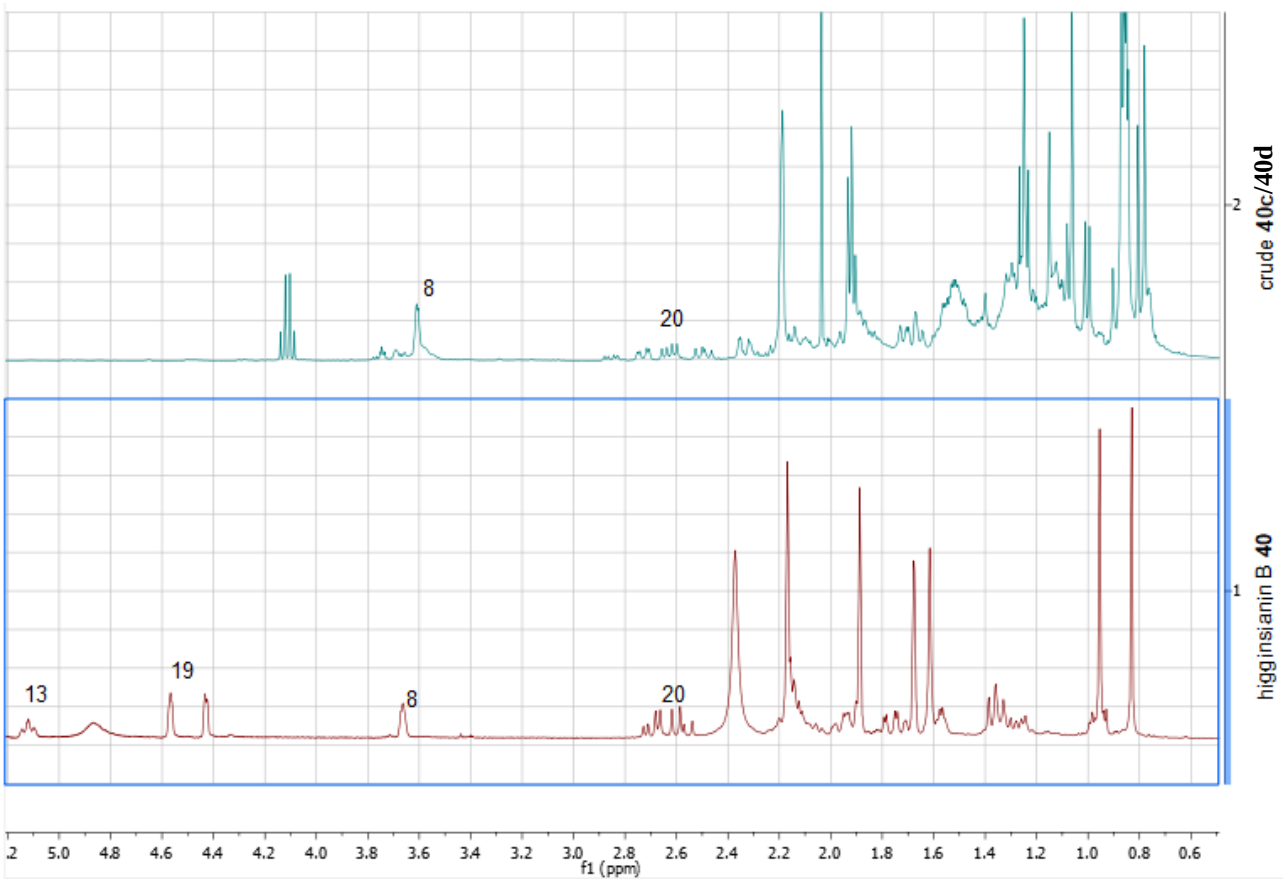

*Figure B.2.14 - Stacked spectra of **40** and crude **40c** and **40d**.*

B.2.3 *Epoxidation of **40** to **40e***

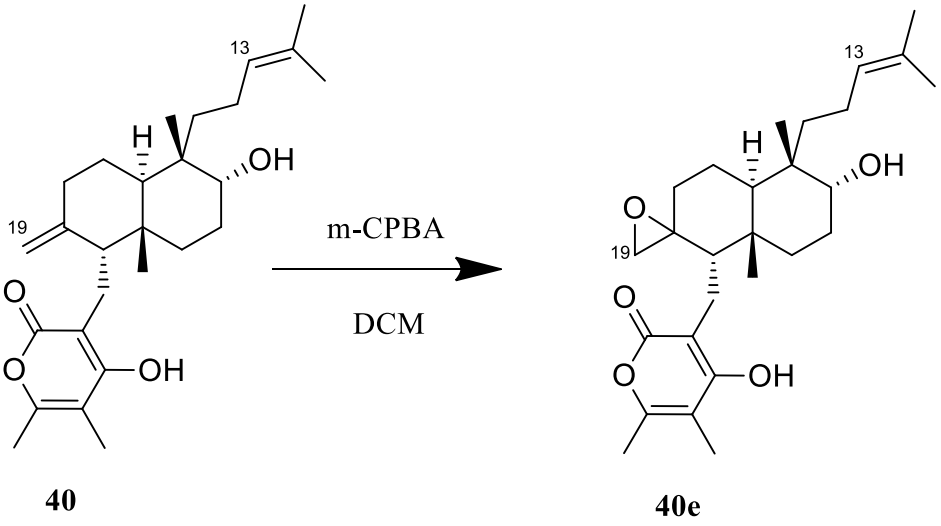

40 **40e**

*Figure B.2.15 - Scheme for the reaction of **40** with m-CPBA.*

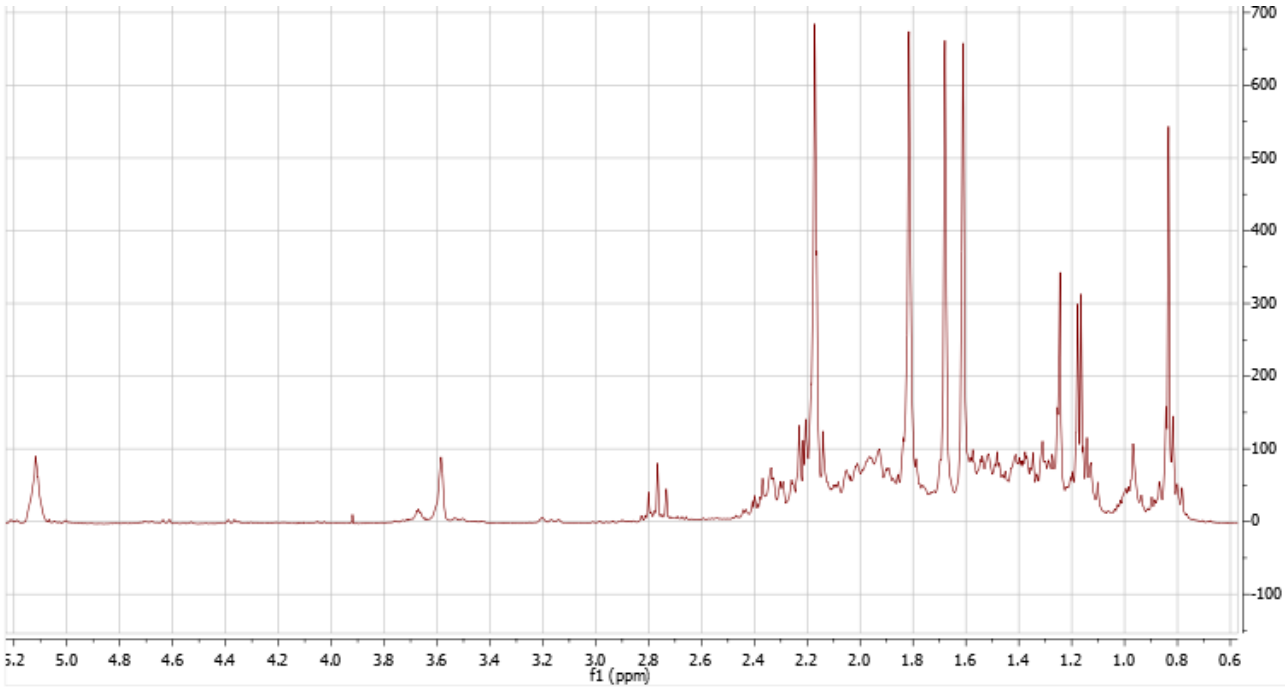

*Figure B.2.16 - ^{1}H NMR spectrum of crude **40e**.*

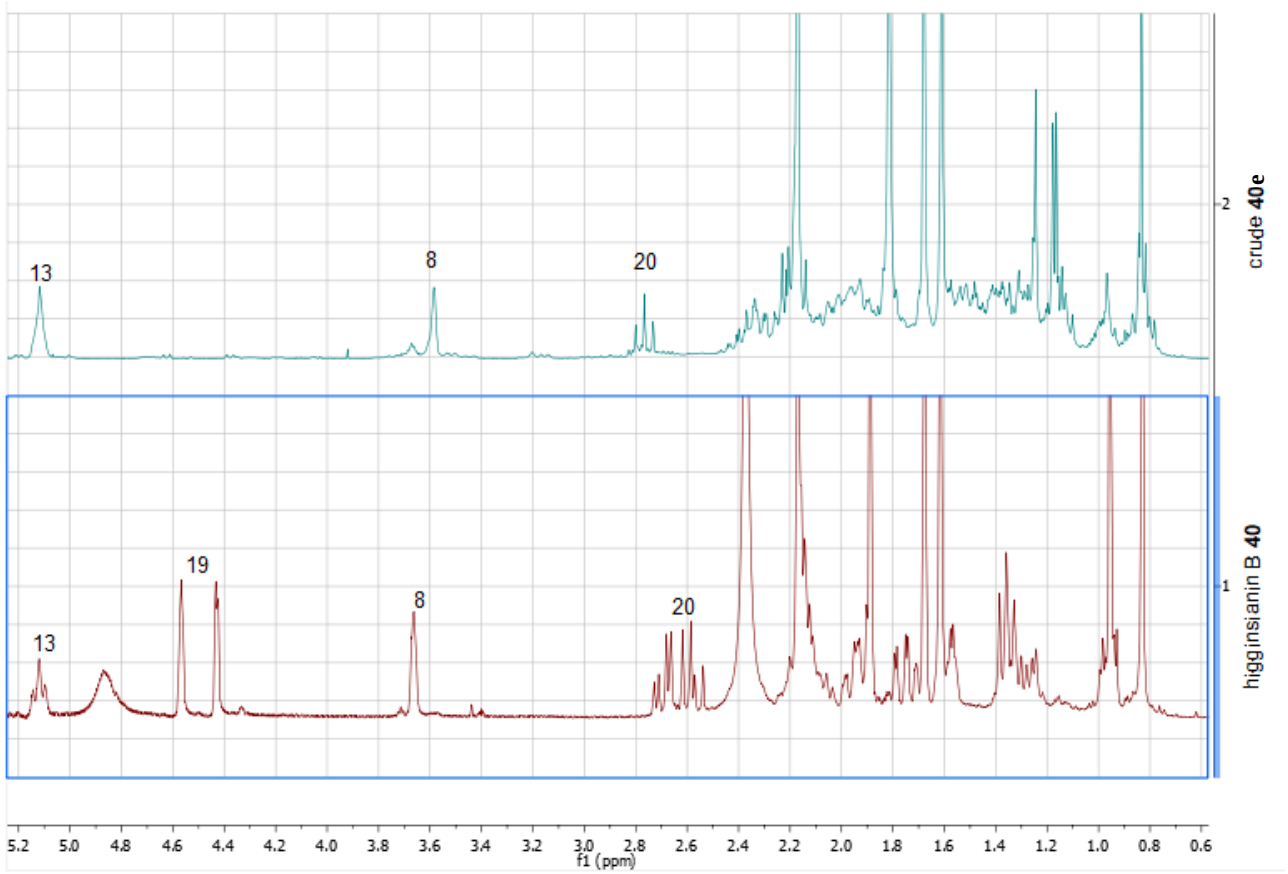

*Figure B.2.17 - Stacked ^{1}H NMR spectra of **40** and crude **40e**.*